

Electronic transport properties of materials: the memory function approach

A thesis submitted in partial fulfillment of
the requirements for the degree of

Doctor of Philosophy

by

Pankaj Bhalla

(Roll No. 11330026)

Under the supervision of

Dr. Navinder Singh

Associate Professor

Theoretical Physics Division

Physical Research Laboratory, Ahmedabad, India.



DISCIPLINE OF PHYSICS

INDIAN INSTITUTE OF TECHNOLOGY GANDHINAGAR

2017

To

my parents

*for your love, support and
encouragement...*

Declaration

I declare that this written submission represents my ideas in my own words and where others' ideas or words have been included, I have adequately cited and referenced the original sources. I also declare that I have adhered to all principles of academic honesty and integrity and have not misrepresented or fabricated or falsified any idea/data/fact/source in my submission. I understand that any violation of the above will be cause for disciplinary action by the Institute and can also evoke penal action from the sources which have thus not been properly cited or from whom proper permission has not been taken when needed.

Signature

Name: Pankaj Bhalla

(Roll No: 11330026)

Date:

CERTIFICATE

It is certified that the work contained in the thesis titled **“Electronic transport properties of materials: the memory function approach”** by **Mr. Pankaj Bhalla** (Roll No. 11330026), has been carried out under my supervision and that this work has not been submitted elsewhere for a degree.

Dr. Navinder Singh
(Thesis Supervisor)
Associate Professor,
Theoretical Physics Division
Physical Research Laboratory,
Ahmedabad, India.

Date:

Acknowledgments

This thesis is the end of my long journey in obtaining the doctoral degree. A journey is easier when you travel together. Interdependence is certainly more valuable than independence. This thesis is the result of five years of work whereby I have been accompanied and supported by many people. It is a pleasant aspect that I now have the opportunity to express my sincere gratitude for all of them.

First and foremost, I would like to express my thanks to my advisor Dr. Navinder Singh for his continuous support during my Ph.D. study. I would like to thank you for motivating and allowing me to grow as an independent researcher. Ever since, Navinder has supported me academically and non-academically through the rough roads to finish this thesis. Moreover, he gave the moral support and the freedom I needed to move on. It was a great experience working with him and I consider myself fortunate to have him as my thesis supervisor.

My heartfelt gratitude to Dr. Nabyendu Das for his encouragement and guidance in both the professional and personal life. I always like to have scientific discussions with him. His amicable nature has always made me feel at ease with him. For any support during my Ph.D. I always looked back on him. The work done with him has taught me how to achieve success which seems impossible to begin with.

I am also grateful to Prof. P. B. Allen (Stony Brook Univ.), Prof. J. P. Carbotte (McMaster Univ.), Prof. K. N. Pathak (Panjab Univ.), Prof. J. Hwang (Sungkyunkwan Univ.), Dr. S. G. Sharapov (Bogolyubov Institute), and Prof. E. Schachinger (Graz Univ.) for their scientific discussions and comments to improve the manuscripts.

I thank the PRL Director, Dean, Registrar, academic committee for their constant support and help. I am also thankful to Dr. Bhushit G. Vaishnav for his continual support. I am thankful to my committee members Prof. Angom Dilip Kumar Singh and Prof. Jitesh R. Bhatt for reviewing the work and motivating constantly during this period. Their comments and constructive criticisms at different stages of my research work were thought-provoking and I gained a lot from them.

I am grateful to Prof. K. P. Subramanian, Prof. A. D. K. Singh, Dr. V. K. Rai, Dr. N. Mahajan, Dr. N. Rastogi, Dr. D. Chakrabarty, Dr. L. K. Sahu, Prof. J. Banerji, Dr. J. Pabari, Dr. B. Bapat, Dr. R. Bhattacharyya, Prof. P. Venkatakrishnan, Prof. N. M. Ashok, Dr. R. D. Deshpande and Dr. A. B. Sarbadhikari for teaching the courses during my course work at PRL which turned out to be very useful in the tenure of research work. I also thankful to Prof. K.

S. Baliyan and Dr. B. Joshi for their guidance in the project as a part of course work. My special thanks to Prof. S. Goswami and Prof. S. Ramachandran for helping me in non-academic issues. I also thanks to all the members of Theoretical Physics division for their support.

I also thanks all the faculty members of the Department of Physics, Lyallpur Khalsa College, Jalandhar, who taught me during my Masters in physics. My special thanks to the head of the department Prof. B. S. Chahal for inspiring me towards higher studies in physics. I must thank to Fiziks Institute for encouraging me towards research, in particular Mr. Atul Gaurav who taught me how to think deeply.

I would like to thank Prof. S. K. Jain, Director; Prof. A. Prashant, Dean; Prof. N. George, associate Dean; and the academic section of Indian Institute of Technology, Gandhinagar for the support and help. Special thanks to Mr. Piyush, Mr. R. B. Bhagat and Mr. S. B. Menon for their prompt response and help during registration. I am grateful to all the staff members of PRL and IIT-GN library, computer center, dispensary and administration staff for their sincere support. I also thanks Dr. T. S. Kumbar (IIT-GN) for mailing many interesting articles. It is my duty to acknowledge Google scholar, Arxiv for keeping me updated.

I am grateful to Sudip Kumar Halder, Abhishek Atreya, Diganta Das, Arko Roy and Sampurn Anand for helping me with thesis editing.

Throughout the Ph.D. tenure, I used to share the office space with Newton Nath. Thank you for tolerating me, despite my gossipy nature and listen to my useless ideas. Let me take this moment to thank Mr. Razaahmed Maniar and Ms. Bhagyashree Jagirdar for the numerous help in official matters related to the Division. I thanks my Ph.D. batch mates, Asim, Bivin, Chandana, Deepak, Dipti, Jinia, Lalit, Mangla, Newton, Rahul, Rajat, Samiron, Venkatesh for their incredible support. My special thanks to Rukmani Bai and Pradeep Kumar Soam for their support. I am thankful to my seniors and juniors for making my stay comfortable and enjoyable at PRL.

I feel a deep gratitude for my grand parents, mother, father, who taught me good things that will help me a lot in life. Their priceless love and support has always been my strength. Their patience will remain my inspiration throughout my life. I thanks my brother, Deepak, for his love and affection. I also owe my deepest gratitude towards my better half, Rabia, for her eternal support and understanding of my goals and aspirations. I am thankful to my son Vivaan for

giving me happiness during the last year of my studies. I am also thankful to my mother-in-law, father-in-law and brother-in-law for their support. A special thanks to my all relatives for their love and affection.

Pankaj Bhalla

Abstract

The study of the transport properties is very important for understanding various interactions in electronic systems. These properties such as electrical conductivity, thermal conductivity and thermoelectric coefficients have been widely studied within the Bloch-Boltzmann approach. In this approach, the transport equations are generally solved analytically under the relaxation time approximation (RTA) and in the zero frequency limit. Success of this approach is mostly limited to the zero frequency behavior. It becomes very complicated while investigating the finite frequency behavior of these transport coefficients especially beyond RTA. Thus, one needs an alternative approach which goes beyond RTA and captures the finite frequency features of these coefficients with much ease. This approach is known as the memory function approach. By construction, this formalism is beyond RTA and using this formalism one can calculate the time dependent correlation functions upto any order. It has been used by Götze and Wölfle (GW) to calculate the dynamical electrical conductivity for metallic electrons. It is successfully applied to study the transport behavior in presence of weak electron-phonon, electron-impurity interactions in metals under the assumption of constant electronic density of states (EDOS). An attempt to extend the GW approach beyond its original assumption of constant EDOS is made here and also we have applied GW approach to a wide variety of transport coefficients (dynamical thermal conductivity, dynamical Seebeck coefficient, etc). Sharapov and Carbotte have also calculated the generalized Drude scattering (GDS) rate for systems with gapped density of states based on Kubo formalism. We reconsider that problem here using the memory function formalism. We show the suppression in GDS due to the presence of gap. We also compare the resulting GDS with that calculated by Sharapov and Carbotte (SC). We find discrepancy in the scattering rate using both approaches in the low frequency limit. This is due to the crucial assumption made by SC approach which is not assumed in the memory function approach. We then study the dynamical thermal conductivity of metals within the memory function formalism. Here we introduce the thermal memory functions for the first time and calculate them for the cases of the electron-impurity and electron-phonon interactions. Several new results have been obtained and discussed in various temperature and frequency regimes. In the

zero frequency limit, we find that the results are consistent with the results predicted by using the Bloch-Boltzmann approach and are also in accord with the experiments. Furthermore, we also investigate the dynamical behavior of the thermo-electric coefficient, namely Seebeck coefficient. This analysis is done to explore the possibility of obtaining large figure of merit in various materials so that the efficiency of thermo-electric devices can be enhanced. We first confirm that at the zero frequency and in the high temperature case, the results of the Seebeck coefficient are in qualitative agreement with the experimental findings. We further find that the Seebeck coefficient increases with increasing frequency. This enhancement hints towards a possibility of greater figure of merit if the device is operated at a certain non-zero frequency. We have also applied the memory function approach to other systems such as graphene, a two dimensional system and we investigate the electronic thermal conductivity. In that, we explore the roles of different acoustic phonons, characterized by different dispersion relations. It is found that at the high temperature, the thermal conductivity saturates for all type of phonons. But the longitudinal phonons gives larger contribution to the total thermal conductivity. While at the low temperature, it follows different temperature power law behavior for different type of phonons. We have also found the results at finite frequency regimes which are identical to the case of conventional metals. In the above studies, we performed analytical studies of various transport coefficients that have been done for the weak perturbative interactions by using the memory function approach. However, with the increase in the interaction strength, one needs to go beyond GW approach. In this context, we propose a high frequency expansion of the memory function in term of its various moments. Taking simple example of the electron-impurity interaction for the case of the metal, we calculate the memory function upto the second order moment. It is found that the higher moments contribute more in the low frequency regimes and in the case of large interaction strength. In a nutshell, we extend the GW memory function formalism to various physical situations of interest with encouraging new results in the dynamical regime. While in the dc limit, our results agree with the traditional approaches.

Contents

Acknowledgments	i
Abstract	v
Contents	vii
List of Figures	xi
List of Tables	xv
1 Introduction	1
1.1 Drude Theory	2
1.2 The Bloch-Boltzmann approach	5
1.2.1 Semi-classical treatment	5
1.2.2 Transport equation	6
1.3 Kubo approach	12
1.4 Memory Function approach	14
1.4.1 Projectors and Memory functions	16
1.4.2 Application to electronic transport	20
1.5 Objectives of the present study	21
1.6 Overview of chapters	22
2 Generalized Drude Scattering Rate: Memory Function approach	25
2.1 Model Hamiltonian	26
2.2 Electrical memory functions	27
2.2.1 For gapped density of states	31

2.3	Sharapov-Carbotte approach	35
2.4	Comparison of GW and SC approach	36
2.5	Conclusion	40
3	Dynamical Thermal Conductivity of metals	43
3.1	Thermal Conductivity	44
3.2	Thermal Memory functions	46
3.2.1	Electron-Impurity Interaction	46
3.2.2	Electron-Phonon Interaction	49
3.3	Results and Discussion	55
3.4	Conclusion	60
4	Dynamical Thermoelectric Coefficient of metals	63
4.1	Thermoelectric Coefficients	64
4.2	Thermoelectric Memory Functions	65
4.2.1	Electron-Impurity Interaction	66
4.2.2	Electron-Phonon Interaction	71
4.3	Results and Discussion	76
4.4	Conclusion	81
5	Dynamical Thermal Conductivity of Graphene	83
5.1	Theoretical Framework	85
5.1.1	Phonon Dispersion relations	86
5.1.2	Mathematical Calculations	88
5.2	Results	94
5.2.1	Thermal Conductivity in zero frequency limit	94
5.2.2	Thermal Conductivity in finite frequency regime	97
5.3	Conclusion	99
6	Moment Expansion to the Memory Function	101
6.1	Equation of motion method	103
6.2	Case of electron-impurity scattering	105
6.3	The MF with a higher order moment	107

6.4 Results and Comparison	109
6.5 Conclusion	112
7 Summary and Future directions	115
Appendices	119
A General formula of GDS for the case of non constant DOS	119
B Derivation of static correlation functions	120
B.1 Thermal-current thermal-current correlation function	120
B.2 Thermal-current electric-current correlation function	121
B.3 Thermal-current thermal-current correlation function for two dimensional system	121
C Derivation of Eq.(3.1.4) for thermal memory function	122
D Thermal conductivity using Boltzmann approach	123
D.1 For electron-impurity interaction	123
D.2 For electron-phonon interaction	124
E Calculation of inner product of the current with its time derivative	129
F Detailed calculation of the higher order contribution	130
G Integrals	132
Bibliography	135
List of Publications	145
Publications attached with thesis	147

List of Figures

1.1	In the left panel when the external particle of macroscopic size moves slowly, we see viscous drag with a streamline flow. In this case the time scales corresponding to the macroparticle and the fluid particles are nicely separable. In the right panel, due to the faster motion of a particle within fluid, a turbulence sets in and in such situation, separation of scales are not possible.	15
1.2	A schematic representation of the idea of projection in the memory function formalism. Here the full big circle is the total many body operator Hilbert Space. The Projection of full many body states defined by a few operators residing in the region P is represented by light blue circle. Rests are defined by I-Q.	16
2.1	Comparison plot of scattering rate $1/\tau(\omega, T)(=M''(\omega, T))$ calculated using Memory function approach (Mem, solid, green) and Sharapov-Carbotte approach (SC, solid, blue) at temperature $T= 10K$ and $200K$ and at gap $\Delta = 0.02eV$ and $0.20eV$. The agreement is excellent.	37
2.2	Temperature variation of scattering rate with two different approaches namely memory function (Mem, dotted) and Sharapov-Carbotte (SC, dashed) at gap $0.02eV$. (a) dc case (b) at $\omega = 0.05eV$ (c) at $\omega = 0.5eV$	38
2.3	Comparison of dc scattering rate $(1/\tau_{dc})$ as a function of Δ using Memory function approach (Mem, Purple) and Sharapov-Carbotte approach (SC, Red) at various temperatures $50K$ and $200K$	39
2.4	Variation of difference $= (1/\tau_{MF} - 1/\tau_{SC})$ of dc scattering rate with temperature calculated by two different approaches MF and SC at $\Delta = 0.02eV$. .	39

2.5	Plot of $ \Sigma(\epsilon + \omega) - \Sigma^*(\epsilon) $ with temperature at different frequencies such as (a) $\omega = 0.0001\text{eV}$, (b) $\omega = 0.001\text{eV}$ and (c) $\omega = 0.01\text{eV}$. Here $\Sigma(\omega)$ represents the self energy and * corresponds to the conjugate.	40
3.1	(a): The imaginary part of the thermal memory function for the case of electron-impurity interaction is plotted with frequency at different temperatures such as 200 (purple), 300 (brown) and 400K (blue) at fixed interaction strength U and impurity concentration N_{imp} . (b): The low frequency regime of Fig. 3.1(a) is elaborated.	57
3.2	(a): The imaginary part of the thermal memory function for electron-phonon interaction is plotted with frequency at different temperatures such as 200 (purple), 250 (red), 300 (brown) and 400K (blue) at fixed Debye temperature $\Theta_D = 300\text{K}$. (b): The low frequency regime of Fig. 3.2(a) is elaborated.	57
3.3	(a). The normalized frequency dependent thermal conductivity is plotted with the ratio ω/ω_0 for electron-phonon interaction at different temperatures such as 200 (purple), 250 (red), 300 (brown) and 400K (blue) and at Debye temperature $\Theta_D = 300\text{K}$. Here the dashed line corresponds to the scale for Debye frequency cutoff i.e. ω_D/ω_0 . (b). The low frequency regime of Fig. 3.3(a) is elaborated.	58
3.4	(a): Plot of temperature dependent normalized dc imaginary part of the thermal memory function for electron-phonon interaction at different Debye temperatures such as 200 (purple), 300 (brown) and 400K (blue). (b): The variation of the normalized thermal conductivity with T at same Debye temperatures.	59
4.1	(a): Plot of the imaginary part of the thermoelectric memory function for impurity case at different temperatures such as 200K (purple), 300K (brown) and 400K (blue). (b): The low frequency regime of $M_Q''(\omega, T)/M_0''$ of Fig. 4.1(a) is elaborated.	77
4.2	(a): Plot of the real part of the normalized Seebeck coefficient for impurity case at different temperatures such as 200K (purple), 300K (brown) and 400K (blue). (b): The low frequency regime of $\text{Re}[S(\omega, T)/S_0]$ of Fig. 4.2(a) is elaborated.	78

4.3	(a): Plot of imaginary thermoelectric memory function for phonon case at different temperatures such as 200K (purple), 250K (red), 300K (brown), 350K (blue). (b): The low frequency regime of Fig. 4.3(a).	78
4.4	Plot of imaginary part of the dc thermoelectric memory function for phonon case at different Debye temperatures such as 200(purple), 300(brown) and 400K(blue).	79
4.5	(a): Plot of finite frequency real part of the normalized Seebeck coefficient at different temperatures such as 200(purple), 250(red), 300(brown), 350(blue) and 375K(magenta) at fixed Debye temperature 300K. Here the dotted line corresponds to the Debye cutoff i.e. ω_D/ω_0 , where ω_0 is the constant scale parameter having dimensions of energy. (b): The low ω/ω_0 regime of Fig. 4.5(a) is elaborated. Here ω_0 is a normalizing parameter.	80
4.6	(a): Plot of the real part of the normalized Seebeck coefficient in zero frequency limit at different Debye temperatures such as 200 (purple), 300 (red) and 400K (brown). (b): The low temperature regime of $\text{Re}[S(\omega, T)]/S_0$ of Fig. 4.6(a) is elaborated.	80
5.1	Schematic representation of the displacement of acoustic in plane and out of plane phonon modes.	87
5.2	The imaginary part of the thermal memory function for the longitudinal and transverse acoustic phonons are plotted with temperature at different $\Theta_{BG} \propto \sqrt{n}$, where n is in the units of 10^{13} cm^{-2} . (a): for the longitudinal acoustic (LA) phonons, $\Theta_{BG} = 57\sqrt{n}\text{K}$ and (b): for the transverse acoustic (TA) phonons, $\Theta_{BG} = 38\sqrt{n}\text{K}$	94
5.3	The Thermal Conductivity for the (a): longitudinal (LA) and (b): transverse acoustic (TA) phonons are plotted with temperature at different $\Theta_{BG} \propto \sqrt{n}\text{K}$, where n is in the units of 10^{13} cm^{-2}	95
5.4	(a): The thermal memory function for the flexural acoustic phonons (ZA) is plotted with temperature at different $\Theta_{BG} = 0.1n\text{K}$, where n is in the units of 10^{13} cm^{-2} and (b): the corresponding thermal conductivity.	96

5.5	The frequency and temperature dependent thermal memory function or the thermal scattering rate for the (a): longitudinal and (b): transverse acoustic phonons are plotted with frequency at different T/Θ_{BG} ratio.	96
5.6	The frequency and temperature dependent thermal conductivity for the longitudinal acoustic phonons is plotted with frequency at different T/Θ_{BG} ratio.	97
5.7	The frequency and temperature dependent thermal conductivity for the transverse acoustic phonons is plotted with frequency at different T/Θ_{BG} ratio.	97
5.8	(a): The Thermal memory function for the flexural acoustic phonons (ZA) is plotted with frequency T/Θ_{BG} ratio. (b): The corresponding Thermal Conductivity variation of flexural phonons.	98
6.1	Plots of the imaginary part of normalized memory functions at different temperatures (a) at $T = 10K$ and (b) at $T = 200K$. Here the red curve corresponds to the case with first moment only and the brown curve corresponds to the case where second moment also considered within the present moment expansion of the memory function. In both cases, there is agreement between the results from the two different approaches at high frequency regimes. However they differ significantly in the low frequency regime.	110
6.2	Plots of the imaginary part of normalized memory functions at different impurity densities N_{imp} (a) 0.01 and (b) 0.04. Here the red curve corresponds to the case with first moment only and the brown curve corresponds to the case where the second moment is also considered in the moment expansion. Here also a deviation occurs at low frequency regime as in the previous case. The increase in the impurity density enhances the magnitude of the memory function.	110
6.3	Variation of the scattering rates with interaction strength U at different frequencies (a) $\omega = 0.02eV$ and (b) $0.2eV$. Here the red curve represents the scattering rate with the first moment only and the brown curve is with the inclusion of the second moment. It is observed that the deviation is more for higher interaction strength in the low frequency regime, as expected.	111

List of Tables

3.1	The results of thermal memory function and the real part of the thermal conductivity due to the electron-impurity interaction in different frequency and temperature domains.	50
3.2	The results of thermal memory function and the real part of the thermal conductivity due to the electron-phonon interaction in different frequency and temperature domains.	56
4.1	The thermoelectric and electrical scattering rates or memory functions due to the electron-impurity interaction in different frequency and temperature domains.	70
4.2	The thermoelectric and electrical scattering rates or memory functions due to the electron-phonon interaction in different frequency and temperature domains.	75
5.1	The results of thermal memory function and the thermal conductivity of graphene for the interaction of electrons with LA/TA and ZA phonons in different frequency and temperature domains.	92

Chapter 1

Introduction

The study of the transport properties of condensed matter systems provides a framework to understand or to determine the effects arising within the system when electrons under the influence of an external field, scatter among themselves or with other degrees of freedom like impurities or phonons. In general, these systems are considered to be in equilibrium in the absence of an external field. In this situation, the quantities such as charge and heat can not be transported over long distances. However, in the presence of an external field, the systems are driven out of equilibrium and the quantities transport over macroscopic length scales. In this situation, the flow of these quantities under the influence of an external field is determined by the transport properties. These properties include electrical conductivity, thermal conductivity, Seebeck coefficient, Hall coefficient, etc.

Experimentally, these transport properties are used as a tool to characterize a system. For example, the electrical conductivity is used to distinguish between the metals, semiconductors and insulators. On the other hand, theoretically these properties are used to test the models by comparing the predictions of the model with the experimental findings. But it is not straightforward to deal with the many body systems (with number of particles of the order of 10^{23} per cubic centimeter) and study the effects of different interactions within the system. Several theories like the Drude theory [1], the Bloch Boltzmann theory [2–5] and the memory function approach [6–13] have been proposed to study the transport properties. However, each has its own merits and demerits.

In addition to the experimental and theoretical interest, this study is also important in the applied field. For example, the behavior of the thermoelectric or Seebeck coefficient is important for the fabrication or design of the electrical circuits [14].

In this thesis, we investigate these transport properties using the memory function approach [6–13]. Before proceeding to the main calculations of the transport coefficients, first we review the preliminary theories such as Drude theory, Bloch-Boltzmann theory and the memory function approach with its pros and cons in this chapter. This will provide a conceptual background in order to discuss the theoretical study of these properties that we are presenting in this thesis.

1.1 Drude Theory

In 1900, Paul Drude, after the discovery of electron by J. J. Thompson, proposed the first model for the theory of metals [1]. It successfully reproduced the various features of the transport properties which were based on the classical kinetic theory of gases [15, 16]. In this model, Drude considered the free electrons of metal as conduction electrons which move under the influence of an external field and collide with positive ion cores which are taken to be immobile particles. To implement this idea, the basic assumptions are as follows [17, 18].

1. The collisions between electrons and ions (electron-ion collisions) are instantaneous.
2. The electrons are treated as noninteracting particles i.e. electron-electron collisions are neglected.
3. The probability of an electron to collide in small time interval dt is dt/τ , where τ is the relaxation time i.e. the time taken by the electrons to relax towards equilibrium and it is treated as a constant.
4. After each collision, electrons acquire random velocity.

Based on the above mentioned assumptions, the formulae of the transport properties such as electrical conductivity, thermal conductivity are derived. For general

idea of the Drude approach, we give derivation of one of the transport coefficient, the electrical conductivity as follows [17–19].

Consider a system i.e. metal in which electrons in the absence of an external field are moving randomly in all directions with random velocities \mathbf{v}_i . Thus the average over all velocities is zero and no current flows in the system. If an external field say an electric field \mathbf{E} is applied on the system, then electrons tend to move in a direction opposite to the electric field with a mean velocity \mathbf{v}_{av} or $\langle \mathbf{v} \rangle$. This oriented movement of electrons sets up an electrical current in the direction of an electric field. To elaborate this, assume that the electron (say 1) is moving with initial velocity \mathbf{v}_0^1 and accelerates for time t_1 after the last collision and adds additional velocity $-\frac{e\mathbf{E}t_1}{m}$, where m is the electron mass and e is the electron charge. Similarly, the electron (say 2) accelerates and adds velocity $-\frac{e\mathbf{E}t_2}{m}$ and so on. Thus, the average velocity acquired by all electrons is given by

$$\langle \mathbf{v} \rangle = \sum_{i=1}^N \mathbf{v}_0^i - \frac{e\mathbf{E}}{m} \sum_{i=1}^N t_i, \quad (1.1.1)$$

where N is the total number of electrons.

As the average of random velocities is zero i.e. $\sum_{i=1}^N \mathbf{v}_0^i = 0$ and the average time for accelerating the electrons is $\tau = \sum_{i=1}^N t_i$, substituting these in Eq. (1.1.1) the average velocity becomes

$$\langle \mathbf{v} \rangle = -\frac{e\mathbf{E}\tau}{m}. \quad (1.1.2)$$

Suppose that there are n electrons per unit volume moving with the average velocity $\langle \mathbf{v} \rangle$ and these electrons traverse the distance $\langle \mathbf{v} \rangle dt$. Then, the number of electrons crossing the area of cross section A in the direction of velocity will be $n\langle \mathbf{v} \rangle dt A$ and hence gives the current density as $\mathbf{J} = -ne\langle \mathbf{v} \rangle$. Using the above equation, the average current density proportional to the average velocity can be expressed as

$$\mathbf{J} = -ne\langle \mathbf{v} \rangle = \frac{ne^2\tau}{m}\mathbf{E}, \quad (1.1.3)$$

Also, from the Ohm's law: $\mathbf{J} = \sigma\mathbf{E}$, where σ is the electrical conductivity. Thus on comparing this expression with Eq. (1.1.3), the electrical conductivity becomes

$$\sigma = \frac{ne^2\tau}{m}. \quad (1.1.4)$$

This is the Drude formula for the electrical conductivity of a metal which is known as the Drude dc electrical conductivity [1, 17]. It states that for a fixed electron number density, the electrical conductivity is directly proportional to the average collision time or the relaxation time.

Further, for the time varying field i.e. when the electric field is time dependent but spatially uniform, the frequency dependent electrical conductivity can be obtained as below. In this case, the average electron velocity at any time t is represented as $\mathbf{v}(t)$. Hence, the equation of motion can be expressed as

$$m \frac{d\mathbf{v}(t)}{dt} + m \frac{\mathbf{v}(t)}{\tau} = -e\mathbf{E}(t). \quad (1.1.5)$$

Here the second term in the left hand side states the damping term to account for the effect of electron collisions. Now assuming $\mathbf{E}(t) = \text{Re}(\mathbf{E}(\omega)e^{-i\omega t})$ and $\mathbf{v}(t) = \text{Re}(\mathbf{v}(\omega)e^{-i\omega t})$ for time varying field and velocity respectively and substituting it in Eq. (1.1.5), we obtain

$$\mathbf{v}(\omega) = \frac{\mathbf{E}(\omega)}{1/\tau - i\omega}. \quad (1.1.6)$$

Since $\mathbf{J}(\omega) = -ne\mathbf{v}(\omega)$ and $\mathbf{J}(\omega) = \sigma(\omega)\mathbf{E}(\omega)$, the frequency dependent or AC electrical conductivity using Eq. (1.1.6) is given by

$$\sigma(\omega) = \frac{ne^2}{m} \frac{\tau}{1 - i\omega\tau}. \quad (1.1.7)$$

On separating the real and the imaginary parts, we have

$$\text{Re}[\sigma(\omega)] = \frac{ne^2}{m} \frac{\tau}{1 + \omega^2\tau^2}; \quad \text{Im}[\sigma(\omega)] = \frac{ne^2}{m} \frac{\omega\tau^2}{1 + \omega^2\tau^2} \quad (1.1.8)$$

These are the real and the imaginary part of the electrical conductivity for the case of metal within the Drude formalism where electron-phonon effects are neglected [17].

Based on the classical idea, the Drude theory successfully gives the expressions of the electrical and the thermal conductivity and explains the Wiedemann-Franz law [1, 20, 21]. The latter states that the ratio of the thermal conductivity to the electrical conductivity is directly proportional to the temperature. But, the Drude theory also suffers from important shortcomings. Particularly, it does not explain the temperature dependence of the electrical and thermal conductivity of a metal. Also, it does not consider the different mechanisms for collisions which may effect the relaxation time

for example electron-phonon interaction. The main reason of these shortcomings is the treatment of electrons as a classical electron gas [22].

To overcome these shortcomings and to capture the temperature dependent behavior of various transport properties, it is important to consider the quantum nature of the electron gas and describe the collision processes in detail. This is taken into account in semi-classical approach by Bloch [2, 3, 22] which is discussed in the next section.

1.2 The Bloch-Boltzmann approach

As discussed earlier, the study of the transport phenomenon depends on the two characteristic mechanisms such as the driving force i.e. the external field and the scattering of charge carriers i.e. scattering of electrons due to its interactions with impurities, phonons, etc. This interplay can be described by the Bloch-Boltzmann approach [2–5] which explains how the distribution of charge carriers in phase space evolve in the presence of an external field and with the electron scattering mechanisms. Also, it is studied in the framework of semi-classical treatment. Due to large number of electrons in many body interacting systems, it is futile to solve the problem for each electron to extract the transport properties. Hence, the statistical treatment (the Bloch-Boltzmann equation) is needed which consider the effect of average motion of electrons.

Before embarking on the main description of the Bloch-Boltzmann transport approach, we first discuss the important assumptions of this approach.

1.2.1 Semi-classical treatment

In semi-classical approximation, we consider electronic wave packet obtained from the superposition of plane wave states. This wave packet is assumed to be localized around a mean position \mathbf{r} and mean wave vector \mathbf{k} with an extent $d\mathbf{r}$ and $d\mathbf{k}$ such that $dr \ll l$, (l is the mean free path i.e. the distance travelled by an electron between two successive collisions) and $dk \ll k$ respectively. Also the phase space cell $d\mathbf{r}d\mathbf{h}\mathbf{k}$ is much bigger than the quantum limit \hbar to respect the Heisenberg uncertainty principle. Hence, the wave packet is to be constructed with the Bloch functions which consider the motion of electrons in a periodic potential [17, 19].

Within this picture, the motion of electrons subjected to an external electric field is described as

$$\dot{\mathbf{r}}(t) = \mathbf{v}_{\mathbf{k}} = \nabla_{\mathbf{k}}\epsilon_{\mathbf{k}}, \quad (1.2.1)$$

$$\dot{\mathbf{k}}(t) = e\mathbf{E}(\mathbf{r}, t). \quad (1.2.2)$$

Here $\epsilon_{\mathbf{k}}$ and $\mathbf{v}_{\mathbf{k}}$ are energy and velocity of electron in \mathbf{k}^{th} state respectively and $\mathbf{E}(\mathbf{r}, t)$ is the electric field. Also we set $\hbar = 1$ and $k_B = 1$ in throughout the calculations. This concludes that the dynamics of an electron in semi-classical approximation relies on the energy dispersion of an electron.

1.2.2 Transport equation

To discuss the motion of electrons, we introduce the electron distribution function $f_{\mathbf{k}}(\mathbf{r}, t)$ which is the occupation probability of an electron at position \mathbf{r} , at time t and having wave vector \mathbf{k} . This means that the number of electrons with in a phase space volume element $d\mathbf{r}d\mathbf{k}$ (a six dimensional space) about the point (\mathbf{r}, \mathbf{k}) are given as $d\mathbf{r}d\mathbf{k}f_{\mathbf{k}}(\mathbf{r}, t)$. Thus the total number of electrons becomes $\frac{2}{(2\pi)^3} \int d\mathbf{r}d\mathbf{k}f_{\mathbf{k}}(\mathbf{r}, t)$, where the factor 2 is introduced to account the two spin orientations of the electron.

According to the Liouville's theorem the time rate of change of the distribution function is zero i.e.

$$\frac{df_{\mathbf{k}}}{dt} = 0. \quad (1.2.3)$$

Now, the distribution function can evolve with time through the following mechanisms.

- 1 Diffusion: Due to the movement of carriers in and out of the region \mathbf{r} , the rate of change of the distribution becomes

$$\left(\frac{\partial f_{\mathbf{k}}}{\partial t}\right)_{\text{diffusion}} = -\mathbf{v}_{\mathbf{k}} \cdot \frac{\partial f_{\mathbf{k}}}{\partial \mathbf{r}} = -\mathbf{v}_{\mathbf{k}} \cdot \nabla_{\mathbf{r}}f_{\mathbf{k}}. \quad (1.2.4)$$

- 2 External Fields: As we have seen in Eq. (1.2.2), the presence of an external field gives the rate of change of wave vector \mathbf{k} . Thus, the change of distribution in such fields give rate as

$$\left(\frac{\partial f_{\mathbf{k}}}{\partial t}\right)_{\text{fields}} = -e\mathbf{E} \cdot \nabla_{\mathbf{k}}f_{\mathbf{k}}. \quad (1.2.5)$$

3 Scattering: Due to the interaction of electrons or collisions with lattice ions, the rate of change is represented as

$$\left(\frac{\partial f_{\mathbf{k}}}{\partial t}\right)_{\text{coll}}. \quad (1.2.6)$$

Using Eqs. (1.2.4) to (1.2.6), Eq. (1.2.3) becomes

$$\frac{df_{\mathbf{k}}}{dt} = \left(\frac{\partial f_{\mathbf{k}}}{\partial t}\right)_{\text{diffusion}} + \left(\frac{\partial f_{\mathbf{k}}}{\partial t}\right)_{\text{fields}} + \left(\frac{\partial f_{\mathbf{k}}}{\partial t}\right)_{\text{coll}} = 0. \quad (1.2.7)$$

$$-\mathbf{v}_{\mathbf{k}} \cdot \nabla_{\mathbf{r}} f_{\mathbf{k}} - e\mathbf{E} \cdot \nabla_{\mathbf{k}} f_{\mathbf{k}} = - \left(\frac{\partial f_{\mathbf{k}}}{\partial t}\right)_{\text{coll}}. \quad (1.2.8)$$

If there is a temperature gradient, then the above equation can be written as

$$-\mathbf{v}_{\mathbf{k}} \cdot \frac{\partial f_{\mathbf{k}}}{\partial T} \nabla_{\mathbf{r}} T - e\mathbf{E} \cdot \nabla_{\mathbf{k}} f_{\mathbf{k}} = - \left(\frac{\partial f_{\mathbf{k}}}{\partial t}\right)_{\text{coll}}. \quad (1.2.9)$$

This is the general form of the Bloch-Boltzmann transport equation (BTE) of the electron system.

To solve this, it is necessary to obtain the expression of the scattering term for different types of electronic collisions.

Scattering term

Consider that the electrons scatter from the state \mathbf{k} to \mathbf{k}' . In that case, the transition probability of electrons into the \mathbf{k}' state is $f_{\mathbf{k}}(1 - f_{\mathbf{k}'})W_{\mathbf{k} \rightarrow \mathbf{k}'}$, where $W_{\mathbf{k} \rightarrow \mathbf{k}'}$ is the scattering rate of electrons to go from \mathbf{k} to \mathbf{k}' state. Similarly, the probability of the electrons to scatter into \mathbf{k} state is $f_{\mathbf{k}'}(1 - f_{\mathbf{k}})W_{\mathbf{k}' \rightarrow \mathbf{k}}$. Here the occupation number $f_{\mathbf{k}}$ and $(1 - f_{\mathbf{k}})$ assure that electron is going from an occupied state to an empty state.

Thus

$$\left(\frac{\partial f_{\mathbf{k}}}{\partial t}\right)_{\text{coll}} = \sum_{\mathbf{k}'} [W_{\mathbf{k} \rightarrow \mathbf{k}'} f_{\mathbf{k}'} (1 - f_{\mathbf{k}}) - W_{\mathbf{k}' \rightarrow \mathbf{k}} f_{\mathbf{k}} (1 - f_{\mathbf{k}'})]. \quad (1.2.10)$$

According to the Fermi Golden rule [23, 24], for the scattering of electrons due to impurities, $W_{\mathbf{k} \rightarrow \mathbf{k}'}$ is written as [25, 26]

$$W_{\mathbf{k} \rightarrow \mathbf{k}'} = 2\pi |\langle \mathbf{k} | U | \mathbf{k}' \rangle|^2 \delta(\epsilon_{\mathbf{k}} - \epsilon_{\mathbf{k}'}). \quad (1.2.11)$$

Here U is the electron-impurity interaction strength. Similarly the expression for $W_{\mathbf{k}' \rightarrow \mathbf{k}}$ is same as Eq. (1.2.11) with the interchange of \mathbf{k} to \mathbf{k}' . Thus according to the principle of detailed balance [22],

$$W_{\mathbf{k}' \rightarrow \mathbf{k}} = W_{\mathbf{k} \rightarrow \mathbf{k}'}. \quad (1.2.12)$$

Using the Eq. (1.2.12), the scattering term Eq. (1.2.10) for the case of electron-impurity interaction becomes

$$\begin{aligned} \left(\frac{\partial f_{\mathbf{k}}}{\partial t} \right)_{\text{coll}} &= \sum_{\mathbf{k}'} W_{\mathbf{k} \rightarrow \mathbf{k}'} (f_{\mathbf{k}'}(1 - f_{\mathbf{k}}) - f_{\mathbf{k}}(1 - f_{\mathbf{k}'})) \\ &= \sum_{\mathbf{k}'} W_{\mathbf{k} \rightarrow \mathbf{k}'} (f_{\mathbf{k}'} - f_{\mathbf{k}}). \end{aligned} \quad (1.2.13)$$

Similarly, for the scattering of electrons due to the phonons, $W_{\mathbf{k} \rightarrow \mathbf{k}'}$ is written as [3,27]

$$W_{\mathbf{k} \rightarrow \mathbf{k}'} = 2\pi |\langle I | H_{\text{ep}} | F \rangle|^2 \delta(\epsilon_{\mathbf{k}} - \epsilon_{\mathbf{k}'} \pm \omega_{\mathbf{q}}) (n_{\mathbf{q}} + \eta). \quad (1.2.14)$$

Here H_{ep} is the electron-phonon interaction Hamiltonian, I and F corresponds to the initial and final state of the electron respectively, $\omega_{\mathbf{q}}$ is the phonon frequency, \pm sign within the delta function correspond to the absorption ($\eta = 0$) and emission ($\eta = 1$) of phonon respectively, and $n_{\mathbf{q}}$ is the Boson distribution function which is represented as

$$n_{\mathbf{q}} = \frac{1}{e^{\beta\omega_{\mathbf{q}}} - 1}. \quad (1.2.15)$$

Here β is the inverse of the temperature i.e. $\beta = \frac{1}{T}$.

In this case, $W_{\mathbf{k} \rightarrow \mathbf{k}'}$ and $W_{\mathbf{k}' \rightarrow \mathbf{k}}$ relate to each other as [27]

$$W_{\mathbf{k}' \rightarrow \mathbf{k}} = \frac{f_{\mathbf{k}}^0}{f_{\mathbf{k}'}^0} W_{\mathbf{k} \rightarrow \mathbf{k}'}, \quad (1.2.16)$$

where $f_{\mathbf{k}}^0$ is the equilibrium distribution function which is defined as

$$f_{\mathbf{k}}^0 = \frac{1}{e^{\beta(\epsilon_{\mathbf{k}} - \mu)} + 1}. \quad (1.2.17)$$

Here μ is the chemical potential or the reference level to measure the energy of an electron and this distribution function is independent of \mathbf{r} because of the homogeneity assumption.

Using the Eq. (1.2.16) into (1.2.10), we have

$$\left(\frac{\partial f_{\mathbf{k}}}{\partial t} \right)_{\text{coll}} = \sum_{\mathbf{k}'} W_{\mathbf{k} \rightarrow \mathbf{k}'} \left(f_{\mathbf{k}'} \frac{f_{\mathbf{k}}^0}{f_{\mathbf{k}'}^0} - f_{\mathbf{k}} \right). \quad (1.2.18)$$

Substituting Eq. (1.2.13) and (1.2.18) for electron-impurity and electron-phonon interaction respectively in the general form of Boltzmann transport equation (1.2.9), the transport equation becomes an integro-differential equation and hence is complicated to solve to determine the non equilibrium distribution function $f_{\mathbf{k}}(\mathbf{r}, t)$. Therefore, one has to consider an assumption(s) to solve it.

Linearized BTE

Assume that the steady state distribution function does not depart far from the equilibrium i.e.

$$g_{\mathbf{k}} = f_{\mathbf{k}} - f_{\mathbf{k}}^0; \quad g_{\mathbf{k}} \ll f_{\mathbf{k}}^0. \quad (1.2.19)$$

Here $f_{\mathbf{k}}^0$ is the local equilibrium distribution function. A local equilibrium means that the state is described by the slowly varying time and space dependent temperature and chemical potential i.e. $T(\mathbf{r}, t)$ and $\mu(\mathbf{r}, t)$ respectively. It is defined as

$$f_{\mathbf{k}}^0(\mathbf{r}, t) = \left\{ \exp \left(\frac{\epsilon_{\mathbf{k}} - \mu(\mathbf{r}, t)}{T(\mathbf{r}, t)} \right) + 1 \right\}^{-1}. \quad (1.2.20)$$

Substituting Eq. (1.2.19) in (1.2.9) and assuming the constant chemical potential, we have

$$-\mathbf{v}_{\mathbf{k}} \cdot \frac{\partial f_{\mathbf{k}}^0}{\partial T} \nabla T - e\mathbf{E} \cdot \frac{\partial f_{\mathbf{k}}^0}{\partial \mathbf{k}} = - \left(\frac{\partial f_{\mathbf{k}}}{\partial t} \right)_{\text{coll}} + \mathbf{v}_{\mathbf{k}} \cdot \frac{\partial g_{\mathbf{k}}}{\partial \mathbf{r}} + e\mathbf{E} \cdot \frac{\partial g_{\mathbf{k}}}{\partial \mathbf{k}}. \quad (1.2.21)$$

On further simplifications, we get

$$-\mathbf{v}_{\mathbf{k}} \cdot \left(\frac{-(\epsilon_{\mathbf{k}} - \mu)}{T} \nabla T + e\mathbf{E} \right) \frac{\partial f_{\mathbf{k}}^0}{\partial \epsilon_{\mathbf{k}}} = - \left(\frac{\partial f_{\mathbf{k}}}{\partial t} \right)_{\text{coll}} + \mathbf{v}_{\mathbf{k}} \cdot \frac{\partial g_{\mathbf{k}}}{\partial \mathbf{r}}. \quad (1.2.22)$$

This is the linearized form of the Boltzmann transport equation. Here we drop the term of the order of E^2 and higher, since the external fields are assumed to be slowly varying in space.

Furthermore, for the scattering term, the phenomenological assumption is made

$$- \left(\frac{\partial f_{\mathbf{k}}}{\partial t} \right)_{\text{coll}} \simeq \frac{f_{\mathbf{k}} - f_{\mathbf{k}}^0}{\tau_{\mathbf{k}}}. \quad (1.2.23)$$

Here $\tau_{\mathbf{k}}$ is the relaxation time i.e. the time with which the non equilibrium distribution function relax towards local equilibrium state via scattering processes. Also, the former depends only on the mean k value. This assumption Eq. (1.2.23) is known as the

Relaxation Time Approximation (RTA). The essence of this approximation implies that taking into account the fact of local equilibrium the collisions do not change the form of the distribution function. Under this assumption, the linearized BTE Eq. (1.2.22) can be written as

$$-\mathbf{v}_{\mathbf{k}} \cdot \left(\frac{-(\epsilon_{\mathbf{k}} - \mu)}{T} \nabla T + e\mathbf{E} \right) \frac{\partial f_{\mathbf{k}}^0}{\partial \epsilon_{\mathbf{k}}} = \frac{g_{\mathbf{k}}}{\tau_{\mathbf{k}}} + \mathbf{v}_{\mathbf{k}} \cdot \frac{\partial g_{\mathbf{k}}}{\partial \mathbf{r}}. \quad (1.2.24)$$

If the distribution function and the temperature do not depend on the position, then Eq. (1.2.24) becomes

$$-\mathbf{v}_{\mathbf{k}} \cdot e\mathbf{E} \frac{\partial f_{\mathbf{k}}^0}{\partial \epsilon_{\mathbf{k}}} = \frac{g_{\mathbf{k}}}{\tau_{\mathbf{k}}}. \quad (1.2.25)$$

Hence from Eq. (1.2.19) we have

$$f_{\mathbf{k}} = f_{\mathbf{k}}^0 + e\tau_{\mathbf{k}} \mathbf{v}_{\mathbf{k}} \cdot \mathbf{E} \frac{\partial f_{\mathbf{k}}^0}{\partial \epsilon_{\mathbf{k}}}. \quad (1.2.26)$$

This is the required distribution function which includes the effect of scatterings via the relaxation time $\tau_{\mathbf{k}}$. Using it, the transport properties such as electrical conductivity, thermal conductivity and thermoelectric coefficient, etc. can be computed as discussed in the next subsection.

Transport properties

To find the electrical conductivity, let us first define the electrical current density as [28]

$$\mathbf{J} = \frac{2e}{(2\pi)^3} \int \mathbf{v}_{\mathbf{k}} f_{\mathbf{k}} d\mathbf{k}. \quad (1.2.27)$$

In the above equation, the equilibrium part of the distribution function i.e. $f_{\mathbf{k}}^0$ does not contribute to current density. Thus only second term of Eq. (1.2.26) contributes to the current density which on substituting into (1.2.27) gives

$$\mathbf{J} = \frac{e^2}{4\pi^3} \int \tau_{\mathbf{k}} \mathbf{v}_{\mathbf{k}} (\mathbf{v}_{\mathbf{k}} \cdot \mathbf{E}) \left(\frac{\partial f_{\mathbf{k}}^0}{\partial \epsilon_{\mathbf{k}}} \right) d\mathbf{k}. \quad (1.2.28)$$

On comparing the Eq. (1.2.28) with Ohm's law $\mathbf{J} = \sigma \mathbf{E}$, assuming that the field is applied in x-direction and the system has cubic symmetry (which gives $v_x^2 = \frac{v^2}{3}$), the electrical conductivity can be written as

$$\sigma = \frac{e^2}{12\pi^3} \int \tau_{\mathbf{k}} v_{\mathbf{k}}^2 \left(\frac{\partial f_{\mathbf{k}}^0}{\partial \epsilon_{\mathbf{k}}} \right) d\mathbf{k}. \quad (1.2.29)$$

Similarly, the thermal conductivity and the thermoelectric coefficient can be expressed as

$$\sigma S = \frac{e}{12\pi^3 T} \int \tau_{\mathbf{k}} v_{\mathbf{k}}^2 (\epsilon_{\mathbf{k}} - \mu) \left(\frac{\partial f_{\mathbf{k}}^0}{\partial \epsilon_{\mathbf{k}}} \right) d\mathbf{k}, \quad (1.2.30)$$

$$\kappa = \frac{1}{12\pi^3 T} \int \tau_{\mathbf{k}} v_{\mathbf{k}}^2 (\epsilon_{\mathbf{k}} - \mu)^2 \left(\frac{\partial f_{\mathbf{k}}^0}{\partial \epsilon_{\mathbf{k}}} \right) d\mathbf{k}. \quad (1.2.31)$$

Here S and κ represents the Seebeck coefficient and the thermal conductivity respectively [3, 24]. The Seebeck coefficient is the measure of an electric field generated by the thermal gradient and the thermal conductivity measures the amount of heat flow per unit time through a unit area in the presence of thermal gradient.

Now, we consider the case of a simple metal where electrons follow quadratic energy dispersion (i.e. $\epsilon_{\mathbf{k}} = \frac{k^2}{2m}$). In this case, it is found that the temperature dependent transport coefficients (using Eqns. (1.2.29) to (1.2.31)) show different temperature power law behavior for different interactions such as electron-impurity and the electron-phonon interactions. In the case of electron-impurity interactions, the electrical conductivity $\sigma(T)$, the thermal conductivity $\kappa(T)$ and the Seebeck coefficient $S(T)$ show temperature independent behavior. While for the electron-phonon interaction case, in the high temperature regime i.e. when $T \gg \Theta_D$, $\sigma(T) \sim T^{-1}$, $\kappa(T) \sim T^0$ and $S(T) \sim T$, where Θ_D is the maximum temperature cutoff for phonons i.e the Debye temperature. These predictions are verified in several works with experiments findings and thus are agree with them [3, 14, 29–34]. In the low temperature ($T \ll \Theta_D$), $\sigma(T) \sim T^{-5}$, $\kappa(T) \sim T^{-2}$ and $S(T)$ gives kink in its structure due to the presence of the phonon drag [3].

At the end, we conclude that the BTE can be solved under the relaxation time approximation to calculate electrical conductivity, thermal conductivity and Seebeck coefficient to explain their temperature dependent behavior. The general solutions of the BTE are complicated and generally discussed numerically. To get general analytical expressions, one must resort to an alternative approach. One such approach which goes beyond RTA is called the memory function approach. Within this approach one can also discuss the finite frequency cases. This approach is analogous to the Kubo's linear response approach. Before to present the memory function approach, let us first briefly discuss the Kubo approach in the next section.

1.3 Kubo approach

Earlier in Drude and Bloch-Boltzmann approaches, the transport properties have been discussed based on the classical and semi-classical treatment of the motion of interacting carriers respectively. Here, we discuss the quantum mechanical treatment to the theory of electron transport which is known as Kubo's theory of linear response. In this approach, a system is considered in equilibrium state and the small external perturbation is applied to the system. In response to it, the expectation values of observables change from their equilibrium values and can be obtained within this approach to linear order in the strength of perturbation. In the following, we sketch the derivation of the general form of Kubo's formula as well as in particular for the case of electrical conduction.

Let us consider a system which is described by the total Hamiltonian $H = H_0 + H'$, where H_0 is the time independent unperturbed part and H' is the time dependent perturbed part of the Hamiltonian. Here H' is defined as $H' = -F(t)B$, where B is an operator to which the external field couples and $F(t)$ is the strength of the perturbation (like an electric field). We assume that the perturbation is switched on in the past $t = -\infty$. At that time, the expectation value of operator A is represented as $\langle A \rangle = \text{tr}(\rho_0 A)$, where ρ_0 is the equilibrium density matrix. Due to the small applied perturbation, the density matrix changes and it is represented as $\rho(t) = \delta\rho(t) + \rho_0$. Then the equation of motion for $\rho(t)$ is

$$\frac{\partial \rho(t)}{\partial t} = \frac{1}{i\hbar} [H, \rho(t)]. \quad (1.3.1)$$

On substituting the value of $\rho(t)$, keeping the terms in linear order in $F(t)$ and using $\delta\rho(-\infty) = 0$, it becomes

$$\frac{\partial \delta\rho(t)}{\partial t} = -\frac{1}{i\hbar} [H', \rho_0].$$

Now using interaction representation (where $A(t) = e^{-iH_0 t} A e^{-iH_0 t}$), the above equation gives the formal solution as

$$\delta\rho(t) = -\frac{1}{i\hbar} \int_{-\infty}^t dt' [H'(t'), \rho_0]. \quad (1.3.2)$$

Further using the identity

$$[C(t'), \rho_0] = \int_0^\beta d\lambda \rho_0 e^{\lambda H_0} [H_0, C(t')] e^{-\lambda H_0} = -i\hbar \int_0^\beta d\lambda \dot{C}(t' - i\hbar\lambda), \quad (1.3.3)$$

Eq. (1.3.2) can be written as

$$\delta\rho(t) = \int_{-\infty}^t dt' \rho_0 \int_0^\beta d\lambda \dot{H}'(t' - i\hbar\lambda). \quad (1.3.4)$$

Using the above equation, the change in the expectation value of an operator A i.e. $\delta\langle A(t) \rangle$ becomes

$$\begin{aligned} \delta\langle A(t) \rangle &= \int_{-\infty}^t dt' F(t') \int_0^\beta d\lambda \text{tr}(\rho_0 \dot{B}(t' - i\hbar\lambda) A(t)) \\ &= \int_{-\infty}^{\infty} dt' \chi_{AB}(t - t') F(t'). \end{aligned} \quad (1.3.5)$$

Here $\chi_{AB}(t - t')$, the response function is defined as

$$\chi_{AB}(t - t') = \int_0^\beta d\lambda \langle \dot{B}(t' - i\hbar\lambda) A(t) \rangle \Theta(t - t'). \quad (1.3.6)$$

This is known as the Kubo formula in linear response theory. Now we will apply this approach to the case of electrical conduction. We assume that the time dependent and spatially independent electric field is applied to the system in ν direction. This gives the perturbing Hamiltonian as $H' = -e\mathbf{r}E_\nu(t)$. Also, the current density is defined as $J_\mu(t) = -ne\mathbf{v}_\mu(t)$. In this case, the general quantities are defined as $A(t) = J(t)$, $B = r$ and $F(t) = e^{i\omega t}E$. Using these, the electrical conductivity is expressed as

$$\sigma_{\mu\nu}(\omega) = \int_0^\infty dt e^{i\omega t} \int_0^\beta d\lambda \langle J_\nu(-i\hbar\lambda) J_\mu(t) \rangle. \quad (1.3.7)$$

In classical limit $\hbar \rightarrow 0$, it becomes

$$\sigma_{\mu\nu}(\omega) = \beta \int_0^\infty dt e^{i\omega t} \langle J_\nu(0) J_\mu(t) \rangle. \quad (1.3.8)$$

This is known as the Kubo formula for the electrical conductivity. Similarly, this formula can be derived for other transport properties. The limits of applicability of the Kubo approach are as follows:

1. It is based on the linear response theory which is valid at the low magnitude of the perturbing field.

2. This approach is applicable to a system if the latter maintains the local equilibrium.
3. It cannot be applied to calculate the correlation functions in the nonequilibrium state.

Now, we will present the memory function approach in the next section which we use to compute the transport properties in this thesis.

1.4 Memory Function approach

The memory function technique was developed by Zwanzig and Mori [6–8, 11]. It is introduced to describe the non-equilibrium behavior of the system via the time evolution of the correlation functions. It is formulated in several renditions. Among all these, the projection operator formalism, originally developed by Zwanzig, is the most illuminating as it uses many body projection operators to capture the relevant information of many body systems [12, 13]. Latter, it was generalized by Mori to cast the Laplace transform of the auto correlation function into the continued fraction representation [9]. This technique is also very appealing, because it relates the transport coefficients to the interaction energy and deals with the dynamical study of the physical variables [35–37]. The memory function approach enables one to separate the time scales i.e. slow and fast. Here the slow variables means the variables that have long time memory functions i.e. which decays slowly with time and the fast variables are those which have short time memory functions i.e. which decay quickly. More clearly, this can be explained with a following example.

Suppose that a particle is moving through a fluid and its motion is opposed by fluid particles as depicted in Fig. 1.1. The microscopic origin of the phenomena is surely the Coulomb interactions between all the atoms and electrons of the total system. However, if the moving particle is macroscopically large and we focus on its center-of-mass motion, we can reduce the complexity of the problem drastically without compromising with the basic physics. If the center-of-mass velocity of macroscopic particle is small compared to the velocity of the fluid particles, we can separate or project out the center-of-mass coordinates from the rest of the degrees of freedom of the total system.

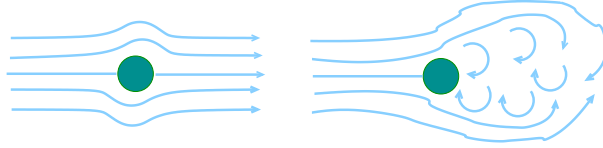


Figure 1.1: In the left panel when the external particle of macroscopic size moves slowly, we see viscous drag with a streamline flow. In this case the time scales corresponding to the macroparticle and the fluid particles are nicely separable. In the right panel, due to the faster motion of a particle within fluid, a turbulence sets in and in such situation, separation of scales are not possible.

In such a situation, we can write its effective equation of motion where the effects of the molecular drag on its motion is incorporated through a drag force. This leads to a very simple and well known equation of motion of the dragged particle which is of the form [38],

$$\ddot{\mathbf{R}} - \gamma \dot{\mathbf{R}} + \mathbf{F} = 0. \quad (1.4.1)$$

Here \mathbf{R} is the position vector of the center-of-mass of the macroscopic particle of unit mass, $\dot{\mathbf{R}}$ and $\ddot{\mathbf{R}}$ represent its time derivative or the velocity and the acceleration respectively and \mathbf{F} is the external force. This is indeed a major simplification of a very complex system. The parameter γ is termed as friction coefficient, viscous coefficient, etc. depending on the contexts. It describes dissipation or the flow of energy and or momentum from the coherent to the incoherent degrees of freedom in a system. It can also be space and time dependent. However when the velocity of the particle becomes large, as seen in the right panel of the Fig. 1.1, turbulence sets in and the idea of separation of scales is no longer obvious. Separation of scales as used in studying the case of a slowly moving particle in a fluid, can be used in quantum systems also. Many such examples can be found in the literature. Since we look at the system within our desired or approximate time scale and length scale, we effectively observe the dissipation of the momentum or energy of the particle as a result of the interaction with other fast variables. The same scenario also may be emerged in other interacting systems to calculate the generalized dissipative constant or the scattering rates. Moreover, in short, the goal of this formalism (the Mori-Zwanzig formalism) is the systematic eval-

uations of the time dependent correlation functions in classical or quantum many body systems [12, 13].

1.4.1 Projectors and Memory functions

In this subsection, we will give the idea to use the projectors or projection operators [12, 13] and describe the mathematical setup to calculate the expressions of the memory functions.

Let us start with a many body system having macroscopically large number of degrees of freedom and examine its macroscopic properties. In classical case, such a system is described by position and momentum variables of the constituent particles. This set of position-momentum variables is called phase space. In quantum cases, these variables are replaced by a set of linearly independent operators. These physical operators have well defined inner product and thus forms a Hilbert space [23]. This is depicted pictorially in the big dark blue circle in Fig. 1.2.

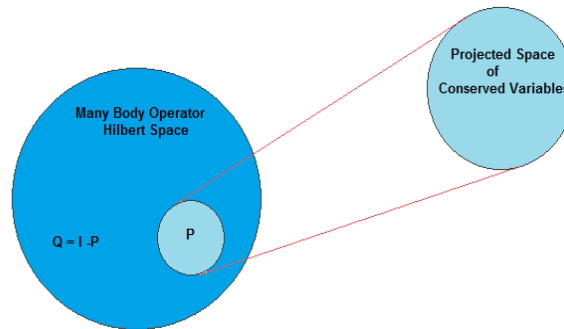


Figure 1.2: A schematic representation of the idea of projection in the memory function formalism. Here the full big circle is the total many body operator Hilbert Space. The Projection of full many body states defined by a few operators residing in the region P is represented by light blue circle. Rests are defined by $I - Q$.

Now studying the low energy consequences of such a large number of variables or operators and their interactions is extremely complicated, if not impossible as mentioned before. To do this job, we need methods which captures the correct low energy

physics. Here the Memory function formalism drastically simplifies the above picture. Basic principle of the memory function formalism is as follows. Suppose we are interested in studying the center-of-mass motion of a system of N number of particles. Then we separate or project out the center-of-mass variable from the others. Here the center-of-mass variable is a macroscopic variable and is defined as a linear combination of the microscopic variables. Now in memory function formalism, it is shown that the effects of the rest of the microscopic variables on the dynamics of the macroscopic variable can be estimated systematically and is cast in a so called *Memory function* [39–52]. The above discussion is applicable to the quantum systems also, except that the classical variables will be replaced by operators. Since we discuss this formalism in a context of the electronic systems, we invoke quantum mechanics from the very beginning and work with operator language henceforth.

Consider an operator A corresponds to some physical observable and obeys the Hamiltonian dynamics. To determine its dynamics, we define an operator \mathcal{L} in the Liouville space i.e. the linear vector space whose elements are represented by linear operators in Hilbert space [36]. These operators are known as superoperators and the operator \mathcal{L} is named as Liouville operator. Its action on an another given operator A produces a new operator or maps its action into its commutator with the Hamiltonian H .

$$\mathcal{L}A = [H, A] = -i\frac{dA}{dt}. \quad (1.4.2)$$

Here $[\dots, \dots]$ is the commutator between two operators. It is to be noted that there is no restriction on the Hamiltonian. It can be non-Hermitian as well, a case of non-equilibrium situation [53]. From Eq. (1.4.2), we see that an operator evolves with time as,

$$A(t) = e^{i\mathcal{L}t}A(0). \quad (1.4.3)$$

To understand the dynamic property of observable in a many body system, the time evolutions of related operators are needed to quantify the correlation between its various components. If such operators are represented as A_i , then their correlation function

matrix $\mathcal{R}(t)$ in terms of its matrix elements is defined as

$$\begin{aligned} R_{ij}(t) &= \langle A_i(t) | A_j(0) \rangle \\ &= \langle A_i(0) e^{-i\mathcal{L}t} | A_j(0) \rangle. \end{aligned} \quad (1.4.4)$$

Here the angular bracket $\langle \dots \rangle$ represents the canonical ensemble average. Now, performing the Laplace transform of Eq. (1.4.4), we obtain

$$\begin{aligned} R_{ij}(z) &= i \int_0^\infty dt e^{izt} R_{ij}(t) \\ &= \left\langle A_i \left| \frac{1}{z - \mathcal{L}} \right| A_j \right\rangle, \quad z = \omega + i\zeta. \end{aligned} \quad (1.4.5)$$

Here z refers the complex frequency and $\zeta \rightarrow 0^+$ is a small positive number. Again, evaluation of $R_{ij}(z)$ is a many body problem with all its associated complications as discussed previously. Further to evaluate the correlation function, we introduce a projection operator P which projects onto the subspace of operators A_i and is defined as [12, 13]

$$\begin{aligned} P &= \sum_{ij} \frac{|A_i\rangle\langle A_j|}{\langle A_i | A_j \rangle} \\ &= \mathbb{I} - Q. \end{aligned} \quad (1.4.6)$$

Here P separates A , the operator corresponding to the observed macroscopic quantity, from the rest of the microscopic degrees of freedom and the role of the Q is just the opposite. A generic projection operator should have the following properties.

$$P^2 = P, \quad PQ = QP = 0, \text{ etc..} \quad (1.4.7)$$

Again considering the correlation function in terms of matrix elements Eq. (1.4.6) and replacing the operator \mathcal{L} by $\mathcal{L}(P + Q)$ in Eq. (1.4.5), we have

$$R_{ij}(z) = \left\langle A_i \left| \frac{1}{z - \mathcal{L}P - \mathcal{L}Q} \right| A_j \right\rangle. \quad (1.4.8)$$

Using the operator identity [12, 13]

$$\frac{1}{X + Y} = \frac{1}{X} - \frac{1}{X} Y \frac{1}{X + Y}, \quad (1.4.9)$$

we can write $R_{ij}(z)$ in the following form

$$R_{ij}(z) = \left\langle A_i \left| \left(\frac{1}{z - \mathcal{L}Q} + \frac{1}{z - \mathcal{L}Q} \mathcal{L}P \frac{1}{z - \mathcal{L}} \right) \right| A_j \right\rangle. \quad (1.4.10)$$

Since $Q|A_j\rangle = 0$, the first term in the right hand side of the above expression simplifies as

$$\begin{aligned} \left\langle A_i \left| \frac{1}{z - \mathcal{L}Q} \right| A_j \right\rangle &= \frac{1}{z} \langle A_i | A_j \rangle \\ &= \frac{1}{z} \chi_{ij}. \end{aligned} \quad (1.4.11)$$

Therefore the expression for $R_{ij}(z)$ can be re-written as

$$R_{ij}(z) = \frac{1}{z} \chi_{ij} + \sum_{lm} \left\langle A_i \left| \frac{1}{z - \mathcal{L}Q} \mathcal{L} \right| A_l \right\rangle \chi_{lm}^{-1} R_{mj}. \quad (1.4.12)$$

In matrix notation, this can be cast in the following form

$$z\mathbb{I} - \mathcal{C}\chi^{-1}\mathcal{R} = \chi. \quad (1.4.13)$$

Here the matrix elements of \mathcal{C} are expressed as

$$C_{il} = \left\langle A_i \left| \frac{z}{z - \mathcal{L}Q} \mathcal{L} \right| A_l \right\rangle. \quad (1.4.14)$$

Further this can be decomposed into two parts by writing the numerator as $z + \mathcal{L}Q - \mathcal{L}Q$ as

$$C_{il} = \langle A_i | \mathcal{L} | A_l \rangle + \left\langle A_i \left| \mathcal{L}Q \frac{1}{z - \mathcal{L}Q} \mathcal{L} \right| A_l \right\rangle. \quad (1.4.15)$$

The first term of the right hand side of the above expression is called the frequency matrix and is defined as

$$L_{il} = \langle A_i | \mathcal{L} | A_l \rangle. \quad (1.4.16)$$

The remaining part of Eq. (1.4.15) contains the effects of the faster degrees of freedom residing in the un-projected part of the Hilbert space and is termed as the memory matrix. It is defined as,

$$\begin{aligned} M_{il}(z) &= \left\langle A_i \left| \mathcal{L}Q \frac{1}{z - Q\mathcal{L}Q} Q\mathcal{L} \right| A_l \right\rangle \\ &= \left\langle \dot{A}_i \left| Q \frac{1}{z - Q\mathcal{L}Q} Q \right| \dot{A}_l \right\rangle. \end{aligned} \quad (1.4.17)$$

Here we use the relation $Q^2 = Q$ to write $M_{il}(z)$ in a symmetric form. This form is very instructive as it defines the memory function in terms of the un-projected part

of the $|\dot{A}\rangle = \mathcal{L}|A\rangle$ and the un-projected part of the Liouville operator \mathcal{L} , i.e. $Q\mathcal{L}Q$. Since the memory function consists of the unprojected degrees of freedom only, it describes the effects of fast modes on the slow modes in a system and accounts for the dissipation in the slow degrees of freedom. Using the above expressions, the correlation function Eq. (1.4.4) between different components of A can be written in a compact notation as,

$$\mathcal{R}(z) = \frac{1}{z\mathbb{I} - [\mathfrak{L} + \mathcal{M}(z)]\chi^{-1}}\chi. \quad (1.4.18)$$

In terms of the matrix elements, it takes the form,

$$\sum_l \left(z\delta_{il} - \sum_s [L_{is} + M_{is}]\chi_{sl}^{-1} \right) R_{ij}(z) = \chi_{ij}. \quad (1.4.19)$$

This completes the general description of the memory function formalism. In the next section, we provide the motivation to apply the above technique to electronic transport.

1.4.2 Application to electronic transport

The usefulness of the memory function formalism to find the correlation function becomes significant when infinite dimensional matrix M has finite number of eigen values [37, 54, 55]. It allows us to treat this formalism for the finite dimensional system to study the dynamical transport properties of the electronic systems. Here our focus is on the time evolution of the current operator and the correlation of its various components in a generic many body system. In our discussions on electronic systems we assume that momentum is the only almost conserved quantity here and thus there is only one slow mode associated with this conservation law. We study the momentum relaxation of a charged particle under external perturbation. Thus the projector operator is defined only in terms of the current operator. This assumption holds if there is no other slow modes associated with any other conservation law or broken symmetry that couples to the charge degrees of freedom. However for simplicity we stick to this picture for the time being.

Now we can start with the expression for memory function as defined in Eq. (1.4.17). In certain situations, we can evaluate the expression in the spirit of perturbation theory. Memory function can be viewed as the self energy of the current-current correlation

function [12]. It has an added advantage that such self energy calculation does not require vertex correction [56]. The latter is extremely important and problematic when it is expressed through the interaction renormalized single particle propagators [24]. Now, for the case of current-current correlation, the general operators are replaced by the current operators J and the memory function Eq. (1.4.17) can be rewritten as [57]

$$M(z) = \left\langle \dot{J} \left| Q \frac{1}{z - Q\mathcal{L}Q} Q \right| \dot{J} \right\rangle. \quad (1.4.20)$$

Here $\dot{J} = [J, H]$, where H is the total Hamiltonian of the system under consideration.

With this, we can conclude that knowing the form of total Hamiltonian (including the perturbation part) and current of a specific system, one can calculate the memory function in a systematic way, hence the transport properties which is the main aim of our thesis. A procedure to calculate the memory function, due to Götze-Wölfle is presented in the next chapter. Further, the limits of the applicability of the memory function approach are as follows:

1. In this approach, the existence of quasiparticle is not essential. Thus, it is applicable to certain strongly correlated systems. There is no restriction on the dimension of the system. In this thesis, I have used the quasiparticle picture to study the transport properties.
2. Within the Götze-Wölfle memory function approach, one can calculate the transport properties perturbatively by considering current as a nearly conserved quantity. If the system has other nearly conserved quantities like total momentum, heat diffusion, etc. as in the case of strongly interacting non-Fermi liquids, one has to use the memory matrix formulation rather than GW approach to include the other slow modes that couples to the electric (thermal in case of thermal conductivity) current.
3. It is valid only if the system is in the local equilibrium.

1.5 Objectives of the present study

To study the effect of perturbative interactions on the transport coefficients, we use the memory function approach and calculate them at zero and finite frequency regimes.

The main objectives of our study are as follows:

1. Studying the generalized Drude scattering rate based on the Götze-Wölfle (GW) approach takes into account the effect of gapped electronic density of states.
2. Exploring the frequency and temperature evolution of the thermal conductivity of metal for the case of the electron-impurity and the electron-phonon interactions. Motivated by recent experimental advancements, we report the results in the finite frequency regimes.
3. Materials with the large figure of merit are required for the operation of nano thermoelectric devices. Motivated by that we study the dynamical thermoelectric coefficient in a metal for the case of electron-impurity and electron-phonon interactions.
4. Exploring the role of various acoustic phonon modes such as longitudinal, transverse and flexural modes considering the electron-phonon interactions in the dynamical thermal conductivity of graphene.
5. Extension of the GW memory function approach taking the high frequency expansion of the memory function for the case of the electron-impurity interaction. We calculate the memory function upto the second moment and show its large contributions in the case of larger interaction strength.

1.6 Overview of chapters

In the next chapter, Chapter 2, we begin with discussion of the Götze-Wölfle (GW) memory function approach. We then present the results of scattering rate predicted by GW to address the effect of electron-phonon interaction in a metal by taking constant electron density of states. We then go beyond this assumption and introduce the gapped density of states and calculate the imaginary part of the memory function or known as generalized Drude scattering rate. Here we discuss the dc (zero frequency limit) and ac imaginary part of the memory function in different temperature and frequency regimes. Then we compare our findings with the phenomenological approach given by Sharapov and Carbotte and discuss our results.

In Chapter 3, we calculate the dynamical thermal conductivity in the case of a metal using the memory function approach. Here for the first time we introduce the thermal memory functions and calculate them to study the effects of electron-impurity and electron-phonon interactions. Then we discuss its asymptotic behavior in different frequency and temperature regimes. Further we compare the results for the zero frequency case with the results obtained by the Boltzmann approach and find good agreement. In addition to this, we make several predictions in the frequency dependent cases for ac thermal conductivity.

In Chapter 4, with the same spirit of the previous chapter, we calculate the frequency dependent thermoelectric transport i.e. the Seebeck coefficient of a metal. First, we discuss the basic relations of the thermoelectric coefficients and then calculate them in various frequency and temperature regimes. Also, we discuss that how the Seebeck coefficient can improve the figure of merit of any material to increase the efficiency of thermoelectric devices.

In Chapter 5, we study the two dimensional system i.e. graphene which is different from the normal three dimensional system. We present the role of various acoustic phonons to the electronic thermal conductivity of graphene. Furthermore, we also discuss the contribution of these phonons to the finite frequency cases.

In Chapter 6, we extend the GW memory function approach to the higher order contribution to the Drude scattering rate. We propose a systematic expansion of the memory function involving its various moments. Then, we calculate the scattering rate upto second moment in the memory function expansion for the case of the electron-impurity interactions. We discuss the contributions from higher moments in the case of larger interaction strength. Finally, in Chapter 7 we present the summary of the dynamical transport coefficients and outlook for the future studies.

Chapter 2

Generalized Drude Scattering Rate: Memory Function approach

Electrical conductivity is one of the important transport property and its study can help us in attaining a better understanding of the electronic interactions in many body systems. These interactions comprise of electron-impurity, electron-phonon, electron-electron interactions which play important role in the frequency dependent generalized scattering rate. Their signatures can be easily grasped by using the experimental data on reflectance to extract $\sigma(\omega, T)$ which can be written in a general way by the memory function expression or the generalized Drude scattering form [12, 56]:

$$\sigma(\omega, T) = \frac{\omega_p^2}{4\pi} \frac{1}{1/\tau(\omega, T) + i\omega(1 + \lambda(\omega, T))}. \quad (2.0.1)$$

Here $1/\tau(\omega, T)$ is the frequency and temperature dependent scattering rate, $\lambda(\omega, T)$ is the frequency and temperature dependent mass enhancement factor and ω_p is the plasma frequency.

On theory side, the derivation of the analytical formulae for these quantities (like $1/\tau(\omega, T)$ and $\lambda(\omega, T)$) is quite complicated and has yet not been calculated by the Bloch-Boltzmann approach as discussed in previous chapter. Owing to the analytical tractability, the memory function formalism was first used in a systematic way to calculate electrical conductivity for the case of a simple metal with various interactions by Götze-Wölfle [56]. Within this approach, they calculated the frequency dependent conductivity with various interactions such as electron-phonon, electron-impurity, electron-magnetic impurity, scattering with localized modes etc. For electron-impurity

interactions they showed that the results are identical to the single particle calculations by using the Bloch-Boltzmann equation with vertex corrections [56]. This is indeed a benchmark and major success of this formalism.

In this chapter, we discuss the case of electron-phonon interaction in the dynamical or frequency dependent electrical conductivity. In Sec. 2.1, we describe the model Hamiltonian of the system. In Sec. 2.2, we first calculate the electrical memory function as done by Götze-Wölfle to provide the background and then we go beyond the assumption of constant electronic density of states. Here we introduce the gapped electronic density of states and calculate the electrical memory function. In Sec. 2.3, we review the approach introduced by Sharapov and Carbotte. Later in Sec. 2.4, we compare our results with the Sharapov-Carbotte results. Finally, we discuss our findings in Sec. 2.5.

2.1 Model Hamiltonian

We consider a system in which conduction electrons interact with phonons. In such system, the total Hamiltonian is given by [56]

$$H = H_0 + H_{\text{ep}} + H_{\text{ph}}, \quad (2.1.1)$$

where H_0 is the Hamiltonian for non-interacting electrons or free band Hamiltonian and is represented as

$$H_0 = \sum_{\mathbf{k}, \sigma} \epsilon_{\mathbf{k}} c_{\mathbf{k}, \sigma}^\dagger c_{\mathbf{k}, \sigma}, \quad (2.1.2)$$

where $\epsilon_{\mathbf{k}}$ is the electron energy dispersion and $c_{\mathbf{k}, \sigma}^\dagger$ ($c_{\mathbf{k}, \sigma}$) is creation (annihilation) operator having wave vector \mathbf{k} and spin σ . The Hamiltonian H_{ep} represents the electron-phonon interaction or known as the perturbing Hamiltonian due to interaction of electrons with phonons and is given by

$$H_{\text{ep}} = \sum_{\mathbf{k}, \mathbf{k}', \sigma} \left[D(\mathbf{k} - \mathbf{k}') c_{\mathbf{k}', \sigma}^\dagger c_{\mathbf{k}, \sigma} b_{\mathbf{k} - \mathbf{k}'} + \text{h.c.} \right]. \quad (2.1.3)$$

Here $b_{\mathbf{k} - \mathbf{k}'}$ ($b_{\mathbf{k} - \mathbf{k}'}^\dagger$) is the annihilation (creation) operator for phonon having momentum $\mathbf{q} = \mathbf{k} - \mathbf{k}'$ and $D(\mathbf{k} - \mathbf{k}')$ is the electron-phonon matrix element. The symbol h.c.

corresponds to the Hermitian conjugate of the first term. Here for simplicity or to understand the low energy dynamics of a metal, we consider only the acoustic phonons. In this case, the electron-phonon matrix element can be specified as [3]

$$D(\mathbf{q}) = \left(\frac{1}{2m_i N \omega_q} \right)^{-1/2} q C(q); \quad \omega_q = c_s q, \quad (2.1.4)$$

where $C(q)$ is the slowly varying function of q , m_i is the ion mass, N is the total number of unit cells, c_s is the sound velocity and ω_q is the phonon frequency.

The third part of Eq. (2.1.1) represents the free phonon Hamiltonian and is described as

$$H_{\text{ph}} = \sum_q \omega_q \left(b_q^\dagger b_q + \frac{1}{2} \right). \quad (2.1.5)$$

With this description of the Hamiltonian, we will proceed for the calculation of the electrical memory functions in the next section.

2.2 Electrical memory functions

According to the Götze-Wölfle approach, the electrical memory function is defined as [56]

$$M(z, T) = z \frac{\chi(z, T)}{\chi_0 - \chi(z, T)} \quad \text{or} \quad \chi(z, T) = \chi_0 \frac{M(z, T)}{z + M(z, T)}, \quad (2.2.1)$$

where $\chi(z, T)$ is the current-current correlation function, χ_0 corresponds to the static limit of the correlation function ($= N_e/m$, N_e is the electron density) and z is the complex frequency ($z = \omega + i\zeta$, $\zeta \rightarrow 0^+$). As discussed in the first chapter, the memory function includes the effect of fast degrees-of-freedom like electron-phonon interactions, etc. on slow degrees-of-freedom which in the present case is the electrical current density. If there are no interactions then current density is a conserved quantity. The decay of a spontaneously generated current fluctuation in a realistic system is due to the electron-phonon or electron-impurity interactions. In metals*, there is clear scale separation in that the time scale over which current density decays is much larger

*In strange metals, transport is controlled by the collective diffusion of energy and charge rather than by quasiparticle or momentum relaxation [58].

than the time scale of the fast degrees-of-freedom electron-phonon or electron-impurity interactions.

The effect of these fast degrees-of-freedom on the slow degrees-of-freedom can be calculated by using the memory function formalism which is an alternative formulation of the linear response theory. In this theory, the linear response of an operator due to perturbation (electron-phonon, electron-impurity) coupled to an another operator is expressed in terms of the correlation function as [59, 60]

$$\chi(z, T) = \langle\langle J; J \rangle\rangle_z = -i \int_0^\infty dt e^{izt} \langle [J(t), J] \rangle. \quad (2.2.2)$$

Here the electrical current J is defined as

$$J = \frac{1}{m} \sum_{\mathbf{k}} e\mathbf{k} \cdot \hat{n} c_{\mathbf{k},\sigma}^\dagger c_{\mathbf{k},\sigma}, \quad (2.2.3)$$

where \hat{n} is the unit vector parallel to the direction of current. In Eq.(2.2.2), $[\dots, \dots]$ denotes the commutator, the inner angular bracket of $\langle\langle \dots \rangle\rangle_z$ represents the ensemble average at temperature T and the outer one represents the Laplace transform of the ensemble average. Thus electrical current density J defined in the above equation is our slow mode as discussed earlier.

In this chapter, we want to discuss the dynamical transport i.e. the dynamical electrical conductivity $\sigma(z, T)$ which is related to the current-current correlation function as follows [24, 59–61]

$$\sigma(z, T) = -i \frac{1}{z} \chi(z, T) + i \frac{\omega_p^2}{4\pi z}. \quad (2.2.4)$$

In the above expression, $\omega_p^2 = 4\pi N_e e^2 / m$ is the square of plasma frequency. Now substituting Eq. (2.2.1) in (2.2.4), the electrical conductivity becomes [27, 56]

$$\sigma(z, T) = \frac{i}{4\pi z + M(z, T)} \omega_p^2. \quad (2.2.5)$$

To calculate $\sigma(z, T)$, we need to calculate the electrical memory function which further relies on the correlation function. This correlation function can be obtained by using the equation of motion [56] i.e. first multiplying $\chi(z, T)$, defined in Eq. (2.2.2) by z and then performing the integration on the right hand side of the equation by parts[†]

[†] $z \langle\langle J; J \rangle\rangle_z = -i \int_0^\infty dt \frac{1}{i} \frac{d(e^{izt})}{dt} \langle [J(t), J] \rangle = \langle [J, J] \rangle - i \int_0^\infty dt e^{izt} \langle [[J, H], J] \rangle$

which express $z\langle\langle J; J \rangle\rangle_z$ as

$$z\langle\langle J; J \rangle\rangle_z = \langle[J, J]\rangle + \langle\langle[J, H]; J\rangle\rangle_z. \quad (2.2.6)$$

Here the first term in the right hand side contains equal time commutator $[J, J]$ which identically vanishes. Thus, $z\langle\langle J; J \rangle\rangle_z = \langle\langle[J, H]; J\rangle\rangle_z$. Again using the equation of motion on $\langle\langle[J, H]; J\rangle\rangle_z$ as done earlier, one obtains

$$z\langle\langle[J, H]; J\rangle\rangle_z = \langle[[J, H], J]\rangle - \langle\langle[J, H]; [J, H]\rangle\rangle_z. \quad (2.2.7)$$

In this equation, the difference is the negative sign in front of the second term of the right hand side which can be proved by the cyclic property of trace operation[‡]. Further for $z = 0$, $\langle[[J, H], J]\rangle = \langle\langle[J, H]; [J, H]\rangle\rangle_{z=0}$. Thus, substituting these back in Eq. (2.2.6) we get

$$z\langle\langle J; J \rangle\rangle_z = \frac{\langle\langle[J, H]; [J, H]\rangle\rangle_{z=0} - \langle\langle[J, H]; [J, H]\rangle\rangle_z}{z}. \quad (2.2.8)$$

Finally, the correlation function can be expressed as

$$\chi(z, T) = \frac{\langle\langle[J, H]; [J, H]\rangle\rangle_{z=0} - \langle\langle[J, H]; [J, H]\rangle\rangle_z}{z^2}. \quad (2.2.9)$$

In Ref. [56], an expansion for $M(z, T) = z\chi(z, T)/\chi_0 (1 + \chi(z, T)/\chi_0 - \dots)$ is used. Basis of this assumption is the smallness of interaction energy as compared to the kinetic energy of free electrons [56]. Using this expansion and on keeping leading order term, the electrical memory function $M(z, T)$ can be written as

$$M(z, T) = z \frac{\chi(z, T)}{\chi_0} = z \frac{\langle\langle J; J \rangle\rangle_z}{\chi_0}. \quad (2.2.10)$$

Substituting Eq. (2.2.8) in the above equation, the electrical memory function becomes

$$M(z, T) = \frac{\langle\langle[J, H]; [J, H]\rangle\rangle_{z=0} - \langle\langle[J, H]; [J, H]\rangle\rangle_z}{z\chi_0}. \quad (2.2.11)$$

Further for this evaluation, we first calculate the commutator of the current and the total Hamiltonian. Since, the electrical current commutes with the free parts of Hamiltonian i.e. H_0 and H_{ph} . Thus $[J, H] = [J, H_{ep}]$ which using Eqs. (2.1.1) and (2.2.2) becomes

$$[J, H] = \frac{1}{m} \sum_{\mathbf{k}\mathbf{k}'\sigma} (\mathbf{k} - \mathbf{k}') \cdot \hat{n} \left(D(\mathbf{k} - \mathbf{k}') c_{\mathbf{k},\sigma}^\dagger c_{\mathbf{k}',\sigma} b_{\mathbf{k}-\mathbf{k}'} - \text{h.c.} \right). \quad (2.2.12)$$

[‡] $\langle\langle[A, H], B\rangle\rangle = \text{Tr}[A, H]B - \text{Tr}B[A, H] = -\text{Tr}A[B, H] + \text{Tr}[B, H]A = -\langle[A, [B, H]]\rangle$

Using the above equation, the correlation function for the case of electron-phonon interaction $\langle\langle [J, H]; [J, H] \rangle\rangle_z$ becomes

$$\begin{aligned} \langle\langle [J, H]; [J, H] \rangle\rangle_z &= \frac{1}{m^2} \sum_{\mathbf{k}\mathbf{k}'\sigma} \sum_{\mathbf{p}\mathbf{p}'\tau} (\mathbf{k} - \mathbf{k}') \cdot \hat{n}(\mathbf{p} - \mathbf{p}') \cdot \hat{n} \\ &\times \left(D(\mathbf{k} - \mathbf{k}') D^*(\mathbf{p} - \mathbf{p}') \langle\langle c_{\mathbf{k}\sigma}^\dagger c_{\mathbf{k}'\sigma} b_{\mathbf{k}-\mathbf{k}'}; c_{\mathbf{p}'\tau}^\dagger c_{\mathbf{p}\tau} b_{\mathbf{p}-\mathbf{p}'}^\dagger \rangle\rangle_z \right. \\ &\left. - D^*(\mathbf{k} - \mathbf{k}') D(\mathbf{p} - \mathbf{p}') \langle\langle c_{\mathbf{k}'\sigma}^\dagger c_{\mathbf{k}\sigma} b_{\mathbf{k}-\mathbf{k}'}^\dagger; c_{\mathbf{p}\tau}^\dagger c_{\mathbf{p}'\tau} b_{\mathbf{p}-\mathbf{p}'} \rangle\rangle_z \right). \end{aligned} \quad (2.2.13)$$

To simplify the above expression, we need to calculate $\langle\langle c_{\mathbf{k},\sigma}^\dagger c_{\mathbf{k}',\sigma} b_{\mathbf{k}-\mathbf{k}'}; b_{\mathbf{p}-\mathbf{p}'}^\dagger c_{\mathbf{p}',\sigma'}^\dagger c_{\mathbf{p},\sigma'} \rangle\rangle_z$ which can be calculated as (using definition Eq. (2.2.2))

$$\begin{aligned} \langle\langle c_{\mathbf{k},\sigma}^\dagger c_{\mathbf{k}',\sigma} b_{\mathbf{k}-\mathbf{k}'}; b_{\mathbf{p}-\mathbf{p}'}^\dagger c_{\mathbf{p}',\sigma'}^\dagger c_{\mathbf{p},\sigma'} \rangle\rangle_z &= \\ -i \int_0^\infty dt e^{izt} \langle [c_{\mathbf{k},\sigma}^\dagger(t) c_{\mathbf{k}',\sigma}(t) b_{\mathbf{k}-\mathbf{k}'}(t); b_{\mathbf{p}-\mathbf{p}'}^\dagger c_{\mathbf{p}',\sigma'}^\dagger c_{\mathbf{p},\sigma'}] \rangle. \end{aligned} \quad (2.2.14)$$

Using $c_{\mathbf{k},\sigma}(t) = c_{\mathbf{k},\sigma} e^{-i\epsilon_{\mathbf{k}} t}$ and performing the integration over time, we have

$$\langle\langle c_{\mathbf{k},\sigma}^\dagger c_{\mathbf{k}',\sigma} b_{\mathbf{k}-\mathbf{k}'}; b_{\mathbf{p}-\mathbf{p}'}^\dagger c_{\mathbf{p}',\sigma'}^\dagger c_{\mathbf{p},\sigma'} \rangle\rangle_z = - \frac{\langle [c_{\mathbf{k},\sigma}^\dagger c_{\mathbf{k}',\sigma} b_{\mathbf{k}-\mathbf{k}'}; b_{\mathbf{p}-\mathbf{p}'}^\dagger c_{\mathbf{p}',\sigma'}^\dagger c_{\mathbf{p},\sigma'}] \rangle}{z - \epsilon_{\mathbf{k}'} + \epsilon_{\mathbf{k}} - \omega_{\mathbf{k}-\mathbf{k}'}}. \quad (2.2.15)$$

Further solving the commutator and ensemble average, the above equation reduces to

$$\langle\langle c_{\mathbf{k},\sigma}^\dagger c_{\mathbf{k}',\sigma} b_{\mathbf{k}-\mathbf{k}'}; b_{\mathbf{p}-\mathbf{p}'}^\dagger c_{\mathbf{p}',\sigma'}^\dagger c_{\mathbf{p},\sigma'} \rangle\rangle_z = - \frac{[f(1-f')(1+n) - f'(1-f)n] \delta_{\mathbf{k},\mathbf{p}} \delta_{\mathbf{k}',\mathbf{p}'} \delta_{\sigma,\sigma'}}{z - \epsilon_{\mathbf{k}'} + \epsilon_{\mathbf{k}} - \omega_{\mathbf{k}-\mathbf{k}'}}. \quad (2.2.16)$$

Here f and n are Fermi and Boson distribution functions as defined in Eqs. (1.2.15) and (1.2.17) in Chapter 1.

Inserting Eq. (2.2.16) into (2.2.14) and hence in Eq. (2.2.11) and then performing the analytic continuation $z \rightarrow \omega + i\zeta$, $\zeta \rightarrow 0^+$, the imaginary part of the electrical memory function[§] can be expressed as

$$\begin{aligned} M''(\omega, T) &= \frac{2\pi}{3} \frac{1}{mN_e} \sum_{\mathbf{k},\mathbf{k}'} |D(\mathbf{k} - \mathbf{k}')|^2 (\mathbf{k} - \mathbf{k}')^2 f_{\mathbf{k}'} (1 - f_{\mathbf{k}}) n_{\mathbf{k}-\mathbf{k}'} \\ &\left[\frac{e^{\beta\omega} - 1}{\omega} \delta(\epsilon_{\mathbf{k}} - \epsilon_{\mathbf{k}'} - \omega_{\mathbf{k}-\mathbf{k}'} + \omega) + (\text{terms with } \omega \rightarrow -\omega) \right]. \end{aligned} \quad (2.2.17)$$

For simplification in the above expression, we use the law of conservation of momentum $\mathbf{q} = \mathbf{k} - \mathbf{k}'$ and assume that the system has cubic symmetry for which

[§] $\lim_{\zeta \rightarrow 0} \frac{1}{a + i\zeta} = P\left(\frac{1}{a}\right) - i\pi\delta(a)$

$((\mathbf{k} - \mathbf{k}') \cdot \hat{n})^2 = \frac{1}{3}|\mathbf{k} - \mathbf{k}'|^2$. Convert the summations over \mathbf{k} and \mathbf{k}' into integrations using $\epsilon_{\mathbf{k}} = \frac{k^2}{2m}$ and $\epsilon_{\mathbf{k}'} = \frac{k'^2}{2m}$ and assuming that \mathbf{k} is pointing along the z-direction and \mathbf{k}' subtends an angle θ with it (at the end, \mathbf{k} integration over all directions and magnitudes is to be performed). Insert an integral $\int dq \delta(q - |\mathbf{k} - \mathbf{k}'|)$ over q to simplify the calculation as given below. Thus the Eq. (2.2.17) becomes

$$M''(\omega, T) = \frac{2}{3} \frac{N^2}{(2\pi)^3 m N_e} \int_0^\infty dq q^2 |D(q)|^2 \int \frac{d\epsilon_{\mathbf{k}}}{v_{\mathbf{k}}} k^2 \int \frac{d\epsilon_{\mathbf{k}'}}{v_{\mathbf{k}'}} k'^2 \int_0^\pi d\theta \sin \theta \delta(q - |\mathbf{k} - \mathbf{k}'|) f_{\mathbf{k}'} (1 - f_{\mathbf{k}}) n_q \left[\frac{e^{\beta\omega} - 1}{\omega} \delta(\epsilon_{\mathbf{k}} - \epsilon_{\mathbf{k}'} - \omega_{\mathbf{k}-\mathbf{k}'} + \omega) + (\text{terms with } \omega \rightarrow -\omega) \right]. \quad (2.2.18)$$

In a typical metal, the Fermi energy is very large (is of the order of 10^4K). On the other hand the experiments are usually performed at temperature of the order of 10^2K . Thus, electrons from a small region of width $k_B T$ (in the present case $k_B = 1$) around the Fermi surface participate in the scattering events. Hence, we assume that the magnitudes of \mathbf{k} and \mathbf{k}' are equal to k_F , the Fermi wave vector. With this, the θ integral can be simplified as:

$$\int_0^\pi d\theta \sin \theta \delta(q - \sqrt{2} k_F \sqrt{1 - \cos \theta}) = \frac{q}{k_F^2}. \quad (2.2.19)$$

Using this and simplifying the above equation, we obtain

$$M''(\omega, T) = \frac{4}{3} \frac{N^2 m^2 \epsilon_F}{(2\pi)^3 N_e k_F^2} \int_0^{q_D} dq q^3 |D(q)|^2 \int_{-\infty}^\infty d\epsilon \frac{n_q}{e^{-\beta(\epsilon - \epsilon_F)} + 1} \times \left[\frac{1}{e^{\beta(\epsilon - \epsilon_F + \omega - \omega_q)} + 1} \frac{e^{\beta\omega} - 1}{\omega} + (\text{terms with } \omega \rightarrow -\omega) \right]. \quad (2.2.20)$$

This is an expression for the imaginary part of the electrical memory function by considering the constant electronic density of states (EDOS) as deduced by Götze-Wölfle [56].

2.2.1 For gapped density of states

In the optical study of strongly correlated systems, the generalized Drude scattering rate is obtained experimentally using the reflectance data. To address these exper-

imental findings, Sharapov and Carbotte have proposed a theoretical approach. This approach is based on several assumptions which have shortcomings as discussed in latter section (Sec. 2.3). Here we have proposed [62] an alternative approach to address the optical measurements which is based on the memory function formalism.

In this section, we extend the GW approach which is based on constant EDOS. To go beyond the latter assumption, we consider a system with a gap around the Fermi surface and introduce the phonon DOS into the GW formalism which generalizes it in a substantial way as explained below. In this case, the electronic density of states is zero in energy region $(-\Delta, \Delta)$. Thus the energy integration in Eq. (2.2.20) has to be modified

$$I = \int_{-\infty}^{\epsilon_F - \Delta} d\epsilon \frac{e^{\beta(\epsilon - \epsilon_F)}}{e^{\beta(\epsilon - \epsilon_F)} + 1} \frac{1}{e^{\beta(\epsilon - \epsilon_F + \omega - \omega_q)} + 1} + \int_{\epsilon_F + \Delta}^{\infty} d\epsilon \frac{e^{\beta(\epsilon - \epsilon_F)}}{e^{\beta(\epsilon - \epsilon_F)} + 1} \frac{1}{e^{\beta(\epsilon - \epsilon_F + \omega - \omega_q)} + 1}. \quad (2.2.21)$$

After simplification we have

$$I = \frac{1}{\beta} \frac{1}{e^{\beta(\omega - \omega_q)} - 1} \log \left\{ \frac{(1 + e^{\beta(-\Delta + \omega - \omega_q)})(1 + e^{\beta\Delta})e^{\beta(\omega - \omega_q)}}{(1 + e^{\beta(\Delta + \omega - \omega_q)})(1 + e^{-\beta\Delta})} \right\}. \quad (2.2.22)$$

Using the simplified version of the energy integral, the imaginary part of electrical memory function can be written as

$$M''(\omega, T) = \frac{\pi^3 N^2 \rho_F^2}{4m k_F^5} \int_0^{q_D} dq q^3 |D(q)|^2 \frac{1}{\beta} n_q \left[\frac{e^{\beta\omega} - 1}{\omega} \frac{1}{e^{\beta(\omega - \omega_q)} - 1} \log \left\{ \left(\frac{1 + e^{\beta\Delta}}{1 + e^{-\beta\Delta}} \right) \left(\frac{1 + e^{-\beta(\Delta - \omega + \omega_q)}}{e^{\beta\Delta} + e^{\beta(\omega_q - \omega)}} \right) \right\} + (\text{terms with } \omega \rightarrow -\omega) \right]. \quad (2.2.23)$$

This is the desired expression for the frequency and temperature dependent imaginary part of electrical memory function. For $\Delta = 0$ and using phonon matrix element Eq. (2.1.4), this expression reduces to the expression calculated by GW in their work [56], as it should. In actual practise (i.e. for an arbitrary form of gap around the Fermi surface), the general expression of the imaginary part of electrical memory function is complicated and difficult to proceed analytically. A general formulae is given in Appendix A. Thus for the simplicity of calculation, here we have discussed it for a hypothetical system. Further to write $M''(\omega, T)$ in the general form, change the

variable ω_q to Ω in above equation which can be rewritten as

$$M''(\omega, T) = \frac{2\pi}{\omega} \int_0^{\omega_D} d\Omega \alpha^2 F(\Omega) \frac{1}{\beta} \left[\frac{e^{\beta\omega} - 1}{e^{\beta(\omega-\Omega)} - 1} \times \frac{1}{e^{\beta\Omega} - 1} \log \left\{ \frac{1 + e^{-\beta(\Delta-\omega+\Omega)}}{1 + e^{-\beta(\Delta+\omega-\Omega)}} \right\} - (\text{terms with } \omega \rightarrow -\omega) \right], \quad (2.2.24)$$

where $\alpha^2 F(\Omega)$ is defined as

$$\alpha^2 F(\Omega) = \frac{\pi^2 N^2 \rho_F^2}{8m k_F^5 c_s^4} \Omega^3 |D(\Omega)|^2. \quad (2.2.25)$$

This is known as phonon spectral function whose form is same as given by Allen [63] $\left(\alpha^2 F(\Omega) = \frac{N(0)}{4v_F^2} \langle\langle |M_{\mathbf{k}\mathbf{k}'}|^2 (v(\mathbf{k}) - v(\mathbf{k}'))^2 \delta(\hbar\Omega_{\mathbf{Q}} - \hbar\Omega) \rangle\rangle \right)$.

Equation (2.2.23) is our main result. To discuss it in various temperature and frequency regimes, we use the electron-phonon matrix element Eq. (2.1.4) and calculate $M''(\omega, T)$ in next subsections.

DC memory function

In the zero frequency limit and assuming $C(q)$ as a constant i.e. $C(q) = 1/\rho_F$ [3], the imaginary part of the electrical memory function Eq. (2.2.23) becomes

$$M''(T) = \frac{1}{8} \pi^3 \frac{N}{m m_i k_F^5} \int_0^{q_D} dq q^5 \frac{1}{(e^{\beta\omega_q} - 1)(e^{-\beta\omega_q} - 1)} \frac{1}{\omega_q} \times \log \left\{ \frac{1 + e^{\beta\Delta}}{1 + e^{-\beta\Delta}} \frac{1 + e^{-\beta(\Delta+\omega_q)}}{e^{\beta\Delta} + e^{\beta\omega_q}} \right\}. \quad (2.2.26)$$

Now consider the case of $T \gg \omega_D, \Delta$, the above equation reduces to

$$M''(T) = \frac{1}{8} \pi^3 \frac{N}{m m_i k_F^5} \int_0^{q_D} dq q^5 \frac{1}{\omega_q} \frac{-1 + \beta\omega_q}{(\beta\omega_q)^2} \log \left\{ \frac{2 - \beta\Delta - \beta\omega_q}{2 - \beta\Delta + \beta\omega_q} \right\}. \quad (2.2.27)$$

On substituting $x = \frac{q\Theta_D}{q_D T}$ (i.e. $\beta\omega_q = x$) where Θ_D is the Debye temperature, the dc electrical memory function reduces to

$$M''(T) = \frac{1}{8} \pi^3 \frac{N q_D^6}{m m_i k_F^5 \Theta_D} \left(\frac{T}{\Theta_D} \right)^5 \int_0^{\beta\Theta_D} dx x^2 (x - 1) \log \left\{ \frac{2 - \beta\Delta - x}{2 - \beta\Delta + x} \right\}. \quad (2.2.28)$$

This expression under case $T \gg \omega_D, \Delta$ is equivalent to

$$M''(T) \approx A \left\{ \frac{T}{\Theta_D} + \frac{\Delta}{\Theta_D} + \frac{1}{T} \left(\frac{\Delta^2}{8\Theta_D} + \frac{8\Delta}{5} - \frac{\Theta_D}{6} \right) \dots \right\}. \quad (2.2.29)$$

where A refers for constant numerical factor.

Similarly for $T \ll \omega_D, \Delta$, the Eq. (2.2.26) becomes

$$M''(T) = -\frac{1}{8}\pi^3 \frac{Nq_D^6}{mm_i k_F^5 \Theta_D} \left(\frac{T}{\Theta_D}\right)^5 \int_0^{\beta\Theta_D} dx x^4 e^{-x} \log \left\{ \frac{e^{\beta\Delta} + e^{-x}}{e^{\beta\Delta} + e^x} \right\}. \quad (2.2.30)$$

The above expression can also be simplified as

$$M''(T) \approx A e^{-\beta\Delta} \left\{ \frac{1}{5} - \frac{3}{4} \left(\frac{T}{\Theta_D}\right)^5 \dots \right\}. \quad (2.2.31)$$

Substituting the Eq. (2.2.30) into (2.2.5), it leads to the expression of dc conductivity for the electron-phonon interaction. Here if we insert gap $\Delta = 0$ in the Eq. (2.2.26), we obtain the results as given in Ref [56].

AC memory function

We proceed again with Eq. (2.2.23) to study frequency dependent behaviour of electrical memory function in different regimes. In the high frequency regime i.e. for $\omega \gg \omega_D$ and using same approximation ($C(q) = 1/\rho_F$) as considered for the dc case, the imaginary part of electrical memory function becomes

$$M''(\omega, T) = \frac{1}{8}\pi^3 \frac{N}{mm_i k_F^5} \int_0^{q_D} dq q^5 \frac{1}{\beta\omega_q} \frac{n}{\omega} \times \left[\log \left(\frac{1 + e^{-\beta(\Delta-\omega)}}{1 + e^{-\beta(\Delta+\omega)}} \right) - e^{\beta\omega_q} \log \left(\frac{1 + e^{-\beta(\Delta+\omega)}}{1 + e^{-\beta(\Delta-\omega)}} \right) \right] \quad (2.2.32)$$

When the gap is smaller than the $|\omega - \omega_D|$ i.e. $\Delta < |\omega - \omega_D|$, the above equation reduces to[¶]

$$M''(\omega, T) = \frac{1}{8}\pi^3 \frac{N}{mm_i k_F^5 \Theta_D} q_D^6 \left(\frac{T}{\Theta_D}\right)^5 \int_0^{\beta\Theta_D} dx x^4 \coth \left(\frac{x}{2}\right). \quad (2.2.33)$$

From this we identify that at high temperature, the imaginary part of electrical memory function becomes temperature and frequency independent. This means the saturation behavior of $M''(\omega, T)$ for $\omega \gg \omega_D$. The reason is that under this condition, the integral approaches to $(\Theta_D/T)^5$ and it cancels with prefactor $(T/\Theta_D)^5$ in Eq. (2.2.24). At low temperature, it varies linearly with temperature as the integral approaches to $(\Theta_D/T)^4$.

[¶]In the opposite case $|\omega - \omega_D| < \Delta$, Eq. (2.2.23) leads to vanishing scattering rate.

In the later section we compare our findings Eq. (2.2.24) with that by the Sharapov-Carbotte approach. Before we compare our results, let us first discuss briefly the approach proposed by Sharapov and Carbotte [64] to study the transport in the next section.

2.3 Sharapov-Carbotte approach

In this approach, Sharapov and Carbotte deduce a relationship between the scattering rate $1/\tau(\omega, T)$ [64], which in our context is termed as memory function, and the electron-phonon spectral function for a system in which electronic density of states cannot be considered as a constant. The motivation behind this approach was to study the frequency and temperature dependencies of the optical conductivity $\sigma(\omega, T)$ data through the Generalized Drude Scattering rate (GDS) $1/\tau(\omega, T)$.

A simple expression for the scattering rate in terms of the electron-phonon spectral function at zero temperature was first derived by Allen [63] to study the effects of electron-phonon interaction in electrical conductivity of metals. Then for the finite temperature, it was extended by Shulga, Dolgov and Maksimov [65]. But in both the formalisms, the Electronic Density Of States (EDOS) at the Fermi energy is considered as a constant. To go beyond this idea, Mitrović and Fiorucci [66] gave a relation for non-constant EDOS, but their result is at zero temperature. Sharapov and Carbotte [64] generalize their result for finite temperatures. In deriving the formula, they begin with the Kubo formula for electrical conductivity

$$\sigma(\omega) = \frac{i}{\omega + i0} \left[\Pi(\omega + i0) + \frac{ne^2}{m} \right]. \quad (2.3.1)$$

Here $\Pi(\omega)$ is the current-current correlation function which can be obtained from imaginary time expression [24]

$$\Pi(i\Omega_m) = \int_0^\beta d\tau e^{i\Omega_m\tau} \langle j(\tau)j(0) \rangle, \quad (2.3.2)$$

where $i\Omega_m = \omega + i0$ and τ is the imaginary time. Further using the definition of electrical current, this expression has been expressed in terms of Green's function and calculated using Matsubara technique [24]. Substituting the resulting expression for

correlation function in Eq. (2.3.1) and comparing that with the expression for the generalized Drude formula Eq. (2.0.1), they derived the frequency and temperature dependent scattering rate. In this derivation, they made several assumptions including the important one on self energy, $|\Sigma(\epsilon + \omega) - \Sigma^*(\epsilon)| \ll \omega$ where $\Sigma(\epsilon)$ is the electronic self energy and * corresponds to the complex conjugate [64]. Based on these, Sharapov and Carbotte gave the following expression for GDS

$$\frac{1}{\tau(\omega, T)} = \frac{\pi}{\omega} \int_0^\infty d\Omega \alpha^2 F(\Omega) \int_{-\infty}^\infty d\omega' \left[\frac{N(\omega' - \Omega)}{N(0)} + \frac{N(-\omega' + \Omega)}{N(0)} \right] [n(\Omega) + f(\Omega - \omega')] [f(\omega' - \omega) - f(\omega' + \omega)], \quad (2.3.3)$$

where $\alpha^2 F(\omega)$ is the phonon spectral function, $N(\omega)$ is the electronic density of states and $N(0)$ is the normalization factor. Thus we conclude that by knowing the form of the phonon spectral function and the electronic density of states of a specific system, one can obtain the behavior of the generalized Drude scattering rate.

2.4 Comparison of GW and SC approach

To compare our approach Eq. (2.2.24) with SC approach Eq. (2.3.3), we have done calculations using models for electronic density of states and the phonon spectral function. First in SC approach, for the electronic density of states, we use a square well type model with center at Fermi energy and considered a gap of 2Δ around it. This model is considered for the simplicity of the analytical treatment of our calculation and it is similar to the density of states of the quantum well. However, the consideration of the gapped density of states is important to understand the behavior of various system such as conventional and unconventional superconductors. Same gap is taken in our approach Eq. (2.2.24) for comparison. Second, for the phonon spectral function, $\alpha^2 F(\Omega)$, we modelled it as Lorentzian of the type $\frac{\Gamma \Omega}{(\Omega - \Omega_E)^2 + (\Gamma)^2}$ where Ω_E represent the phonon peak frequency and Γ is the width of the Lorentzian [67–69]. Thus for comparison, we use the same form of $\alpha^2 F(\Omega)$ in SC approach and our approach. In the whole analysis, we have fixed the value of Ω_E and Γ as 0.02eV and 0.04eV respectively in both approaches. The value of Debye frequency (the upper limit of phonon frequency integration Eq. (2.2.24)) is very much high as compared to the Lorentzian width, hence ω_D does not give any effect in whole calculation. To compare the results

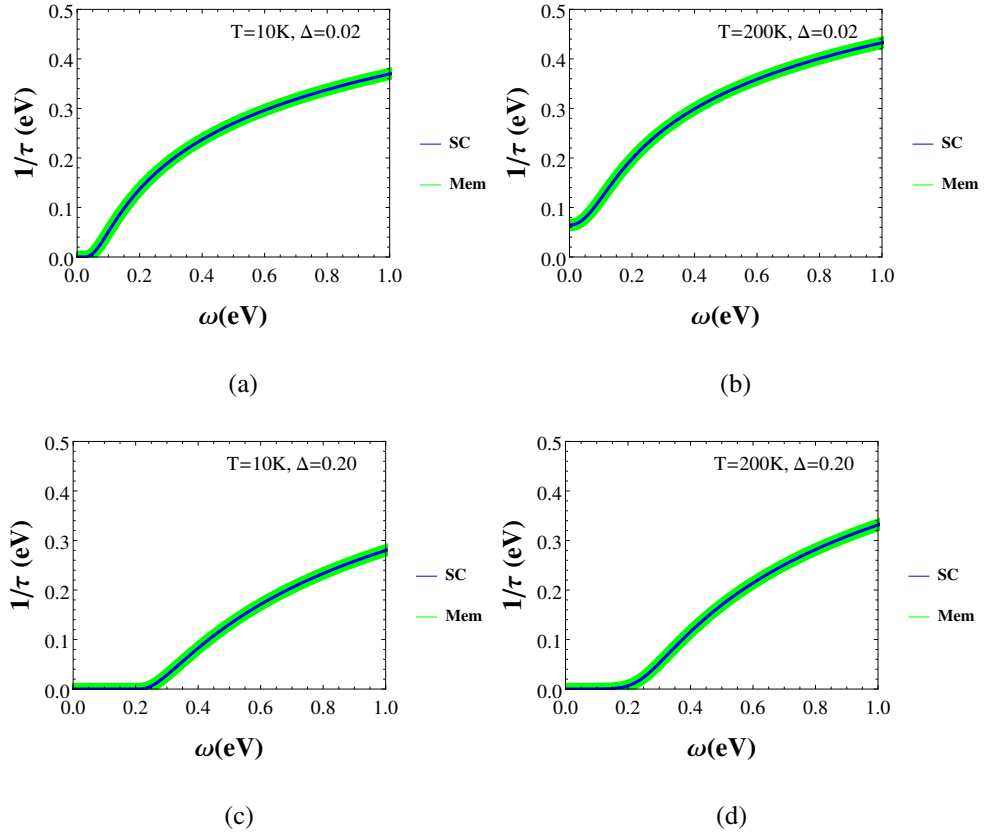


Figure 2.1: Comparison plot of scattering rate $1/\tau(\omega, T)(=M''(\omega, T))$ calculated using Memory function approach (Mem, solid, green) and Sharapov-Carbotte approach (SC, solid, blue) at temperature $T= 10\text{K}$ and 200K and at gap $\Delta = 0.02\text{eV}$ and 0.20eV . The agreement is excellent.

from both the approaches, the frequency dependent scattering rate has been plotted at different temperatures. In Fig. 2.1, we can observe an excellent agreement between both the approaches. As the gap magnitude is increased, the scattering rate shows suppression upto the frequency $\omega \sim \Delta$ as expected (compare Figs. 2.1(a) and 2.1(c)). These results are qualitatively in agreement with the experimental results [70, 71].

In Fig. 2.2, we plot $1/\tau(\omega \rightarrow 0, T)$ as a function of temperature T . Here we can observe that the scattering rate using memory function approach gives more magnitude over the SC approach. In Fig. 2.2(a) i.e. in zero frequency limit, the ratio $\left| \frac{1/\tau_{MF} - 1/\tau_{SC}}{1/\tau_{MF}} \right|_{100K}$, where $1/\tau_{MF}$ and $1/\tau_{SC}$ represents the scattering rate by memory function technique and SC technique respectively, is 0.7 which becomes 0.4 at $\omega = 0.05\text{eV}$ (as shown in Fig. 2.2(b)) and at $\omega = 0.5\text{eV}$ it further reduce to 0.031 (as

shown in Fig. 2.2(c). This shows that the ratio for scattering rates using memory function approach and SC approach reduces as we go from dc limit to finite frequency limit.

Thus we notice that there are discrepancies between the two approaches in the low

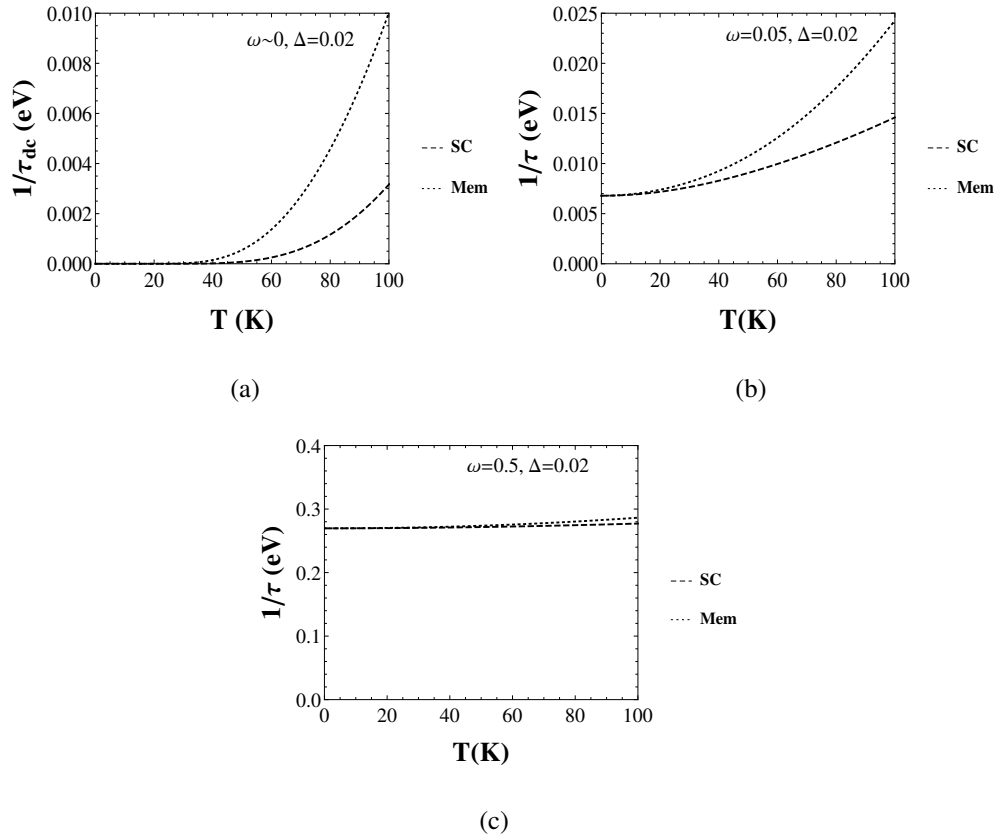


Figure 2.2: Temperature variation of scattering rate with two different approaches namely memory function (Mem, dotted) and Sharapov-Carbotte (SC, dashed) at gap 0.02eV. (a) dc case (b) at $\omega = 0.05$ eV (c) at $\omega = 0.5$ eV.

frequency ($\omega \rightarrow 0$) limit. But both approaches explain the Holstein's mechanism at $T = 0$ K [72,73] (as shown in Figs. 2.2(b), 2.2(c)). This means that at finite frequency and at zero temperature (where thermally excited phonons are not present), there is a finite scattering rate. This attributes due to the generation of phonons along with the electron-hole excitations with the absorption of photon quanta. This mechanism is known as Holstein mechanism [72,73].

Next, we have plotted $1/\tau_{dc}$ at different temperatures as a function of Δ and compare the both approaches (Fig. 2.3). Here we observe that $1/\tau_{dc}$ decreases with the increase of gap energy Δ . Also, we find that the difference between the magnitudes

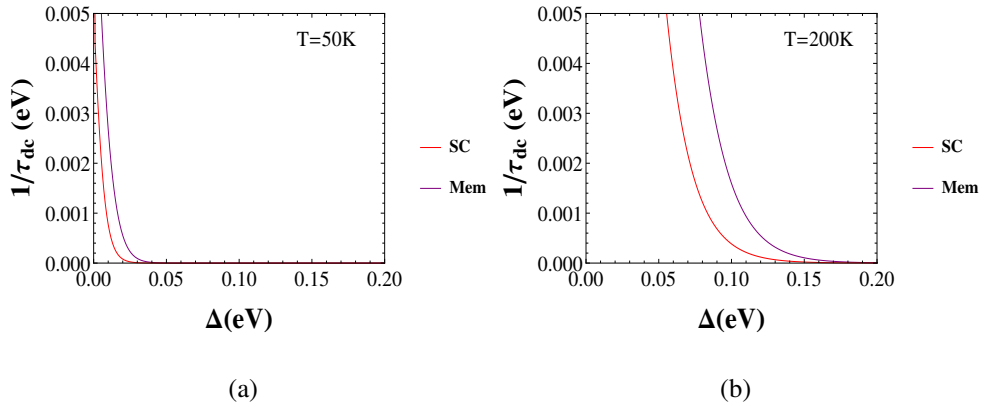


Figure 2.3: Comparison of dc scattering rate ($1/\tau_{dc}$) as a function of Δ using Memory function approach (Mem, Purple) and Sharapov-Carbotte approach (SC, Red) at various temperatures 50K and 200K.

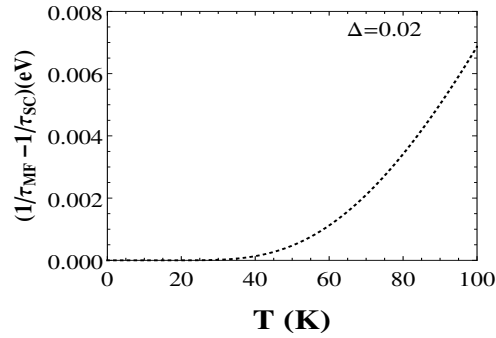


Figure 2.4: Variation of difference $= (1/\tau_{MF} - 1/\tau_{SC})$ of dc scattering rate with temperature calculated by two different approaches MF and SC at $\Delta = 0.02\text{eV}$.

of $1/\tau_{SC}$ and $1/\tau_{MF}$ is not much dependent on Δ , but it does increase with increasing temperature. These discrepancies observed in the dc limit are discussed below.

To illustrate these discrepancies, we have plotted the difference in the magnitudes of scattering rates calculated by both approaches. The difference $(1/\tau_{MF} - 1/\tau_{SC})$ at $\Delta = 0.02\text{eV}$ is plotted in Fig. 2.4. Here we find that this difference increases with the rise of temperature. The reason behind this difference in the low frequency case is the assumption made by SC i.e. $\omega \gg |\Sigma(\epsilon + \omega) - \Sigma^*(\epsilon)|$ which becomes more severe in high temperature regime. To clarify this fact, we plot the quantity $|\Sigma(\epsilon + \omega) - \Sigma^*(\epsilon)|$ as a function of temperature in Fig. 2.5 (where the expression used for $\Sigma(\omega)$ has been given in Ref. [64]). It shows that the magnitude of the difference of self energy increases with the temperature. This shows the stronger violation of

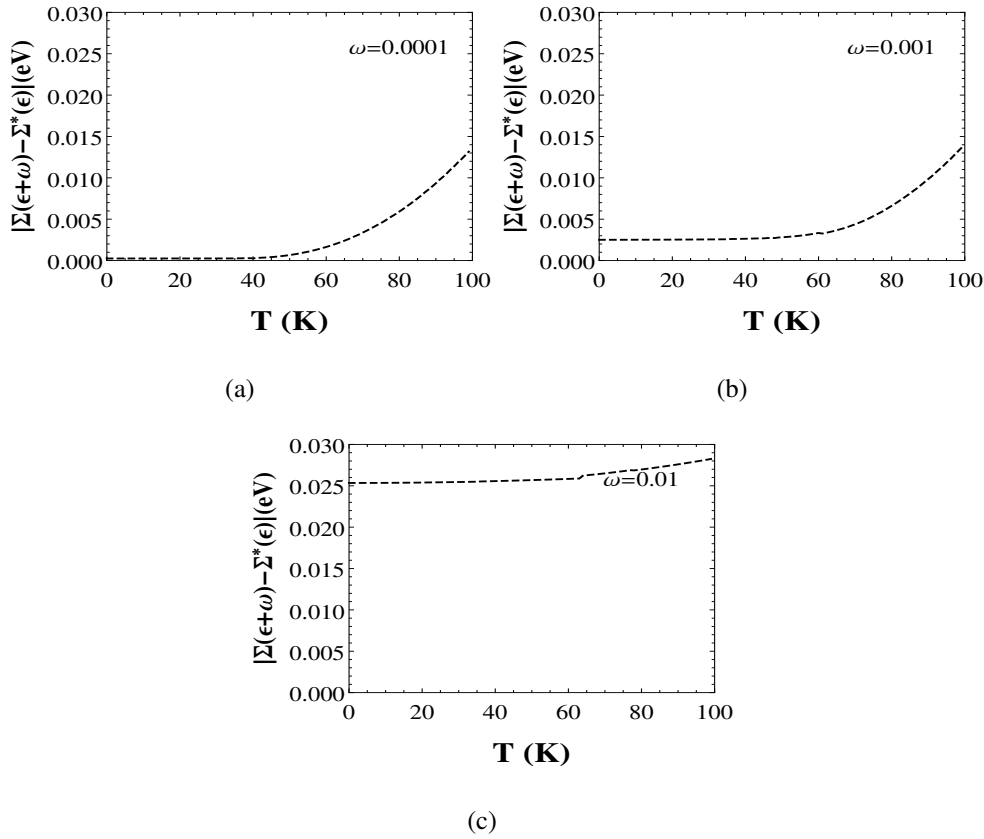


Figure 2.5: Plot of $|\Sigma(\epsilon + \omega) - \Sigma^*(\epsilon)|$ with temperature at different frequencies such as (a) $\omega = 0.0001\text{eV}$, (b) $\omega = 0.001\text{eV}$ and (c) $\omega = 0.01\text{eV}$. Here $\Sigma(\omega)$ represents the self energy and * corresponds to the conjugate.

the condition $\omega \gg |\Sigma(\epsilon + \omega) - \Sigma^*(\epsilon)|$ in high temperature limit. It implies that SC formalism is not appropriate to study the dc behavior and the disagreement is severe at high temperature, but it is quite reasonable for the finite frequency case.

2.5 Conclusion

In this chapter, we look at the case of the electrical conductivity of a metal discussed by Götze-Wölfle and extend their approach by considering the non constant electronic density of states. Here we have considered a phenomenological gap around the Fermi surface and analyzed its impact on the scattering rate. The calculations of the scattering rate have been done by two different approaches namely (1) memory function (MF) and (2) Sharapov-Carbotte (SC).

In a nutshell, the concluding remarks of this chapter are as follows:

- 1 The finite frequency scattering rate using memory function formula is in excellent agreement with the same obtained from SC formula as shown in Fig. 2.1.
- 2 Assumptions made in these two different approaches are consistent at finite frequencies.
- 3 In the case of low frequency, significant discrepancy for the scattering rate between the two approaches (Figs. 2.2(a) and 2.3) has been observed.
- 4 There is also decrease in the dc scattering rate with the increase in gap and the difference between the magnitudes of the scattering rate by two approaches does not depend much on gap.
- 5 This discrepancy is due to the assumption $\omega \gg |\Sigma(\epsilon + \omega) - \Sigma^*(\epsilon)|$ made in the SC approach which becomes severe in high temperature regime.
- 6 No such assumption has been obtained in MF formalism.
- 7 Thus, the MF formalism is better choice to calculate frequency and temperature dependent scattering rate.

Chapter 3

Dynamical Thermal Conductivity of metals

In this chapter, we apply generalized version of the Götze-Wölfle memory function formalism to a very interesting problem of dynamical thermal conductivity of metals. Before to start this problem, we first give the brief introduction about the concept of thermal conductivity.

The knowledge of the properties of the metals are very important for industrial development [69,74–77]. These properties include appearance, malleability and ductility, ability to conduct heat, etc. Among them, the most important criteria is how the metal conducts heat. To answer this question, there is one transport property known as thermal conductivity that quantifies the ability of the material to conduct heat. Understanding this heat conduction process is an interesting issue of the scientific research. In this direction, several methods based on the Kubo formalism and the Bloch-Boltzmann method have been applied to calculate thermal conductivity of metals [3]. These are discussed in the zero frequency limit and are well verified. However, the notion of the frequency dependent thermal conductivity was not previously known and hence was not addressed in theoretical discussions.

Recently, the notion of the dynamical thermal conductivity is introduced by Volz et al. [78]. With this idea, the recent experiments access frequency in which dependence of the thermal conductivity on frequency cannot be ignored. There it is introduced in the context of its usefulness for the thermal design of microsystems and nanosystems

which operates at several GHz clock frequency. Cooling of the Joule heating in such systems is an important issue [78] and it requires detailed understanding of the frequency dependence of the thermal conductivity. In reference [78], the dynamical thermal conductivity is introduced in the context of phonon mediated thermal transport in Si crystals. However, in the case of metals, and particularly at certain oscillating frequency, the electronic contributions to the thermal conductivity under local thermal equilibrium condition may predominate. We consider this scenario and present in the chapter a careful theoretical analysis of the frequency dependent electronic thermal conductivity of metals in various regimes of interest [79]. In a recent computer simulation using molecular dynamics technique, it is found that the phononic thermal conductivity reduces in magnitude at high frequencies [78]. Experimentally, it is also studied in the context of semiconductor alloys and it is found that the magnitude of the phononic thermal conductivity reduces as the frequency increases [80].

Theoretically, the electronic and the phononic dynamical thermal conductivity is discussed recently by Shastry [81] and others [82–85] in different contexts such as in open systems, strongly correlated systems, semiconductor crystals, etc. In the present chapter, we explicitly derive the various expressions for the electronic thermal conductivity in case of a metal using the memory function formalism. First, in Sec. 3.1, we give the basic definition of the thermal conductivity and then give its relation to the memory function. In Sec. 3.2, we calculate the thermal memory functions for the case of the electron-impurity and electron-phonon interactions in a metal. Then, we present our results in Sec. 3.3 and give the conclusion of our results in Sec. 3.4.

3.1 Thermal Conductivity

According to the Kinetic theory, the thermal conductivity is defined as the rate of flow of heat across a unit area of cross section in a unit temperature gradient [14, 24] i.e.

$$J_Q = -\kappa \nabla T. \quad (3.1.1)$$

Here ∇T is the temperature gradient, κ is the thermal conductivity, and J_Q is the thermal current density and is defined as [24],

$$J_Q = \frac{1}{m} \sum_{\mathbf{k}} \mathbf{k} \cdot \hat{n}(\epsilon_{\mathbf{k}} - \mu) c_{\mathbf{k}}^\dagger c_{\mathbf{k}}. \quad (3.1.2)$$

In Eq.(3.1.1) κ , the thermal conductivity, describes the response due to the change in the temperature gradient and is generally analyzed by various approaches where the gradient of the temperature is considered as static. In the present work, we assume that ∇T is not static and oscillates with the frequency ω . This oscillation leads to the dynamical variation of the thermal conductivity. Here it is to be noted that while oscillating the temperature at one of the end of the bath, the local thermal equilibrium must be maintained. This impose the condition that the oscillating frequency should be greater than the scattering rate. Under this condition, we can define the thermal current density by Fourier law and calculate the thermal conductivity by using memory function formula.

To calculate it, we employ the memory function approach. In this approach, the dynamical thermal conductivity at a complex frequency z and temperature T is defined as [79]

$$\kappa(z, T) = \frac{i}{T} \frac{\chi_{QQ}^0(T)}{z + M_{QQ}(z, T)}, \quad (3.1.3)$$

where $\chi_{QQ}^0(T)$ is the static thermal current thermal current correlation function and $M_{QQ}(z, T)$ is the thermal memory function.

It is known that, within the perturbation theory, the thermal memory function can be expressed to leading order in the interaction strength as (derivation of this equation is given in Appendix C)

$$M_{QQ}(z, T) = \frac{\langle\langle [J_Q, H]; [J_Q, H] \rangle\rangle_{z=0} - \langle\langle [J_Q, H]; [J_Q, H] \rangle\rangle_z}{z \chi_{QQ}^0(T)}. \quad (3.1.4)$$

This is the complex memory function in which the imaginary part of the memory function describes the thermal scattering rate due to the presence of different interactions such as electron-impurity and electron-phonon interactions and its real part describes the mass enhancement factor. In the present work, we focus on the thermal scattering rate which leads to the real part of the thermal conductivity. Here for simplicity, we have ignored the mass enhancement contribution to the thermal conductivity as the thermal conductivity is mainly controlled by the thermal scattering rate [56].

3.2 Thermal Memory functions

Using the definitions of the thermal current and the Hamiltonian, let us focus on the calculation of the thermal memory function and hence the thermal conductivity.

3.2.1 Electron-Impurity Interaction

Consider a system in which electrons interact only with impurities, the total Hamiltonian in this case is given in the form $H = H_0 + H_{\text{imp}}$, where the form of unperturbed Hamiltonian H_0 is given in Eq. (2.1.2) and the perturbing part H_{imp} is defined as

$$H_{\text{imp}} = N^{-1} \sum_i \sum_{\mathbf{k}\mathbf{k}'\sigma} \langle \mathbf{k} | U^i | \mathbf{k}' \rangle c_{\mathbf{k}\sigma}^\dagger c_{\mathbf{k}'\sigma}, \quad (3.2.1)$$

where U^i refers to the impurity interaction strength, sum over i index refers to the number of impurity sites and N represents the number of lattice cells.

Using the form of Hamiltonians Eqs. (2.1.2) and (3.2.1) and the expression of thermal current Eq. (3.1.2), the thermal memory function can be calculated from Eq. (3.1.4) for the case of the electron-impurity interaction. In this direction, we first calculate the commutator between J_Q and H . Due to the fact that J_Q and H_0 commutes with each other, we left with $[J_Q, H_{\text{imp}}]$. Thus $[J_Q, H] = [J_Q, H_{\text{imp}}]$ which is given as

$$[J_Q, H] = \frac{1}{mN} \sum_i \sum_{\mathbf{k}\mathbf{k}'\sigma} \langle \mathbf{k} | U^i | \mathbf{k}' \rangle \{ \mathbf{k}(\epsilon_{\mathbf{k}} - \mu) - \mathbf{k}'(\epsilon_{\mathbf{k}'} - \mu) \} \cdot \hat{n} c_{\mathbf{k}\sigma}^\dagger c_{\mathbf{k}'\sigma}. \quad (3.2.2)$$

Using the above commutation relation, the Laplace transform and the thermal average of the inner product $\langle \langle [J_Q, H]; [J_Q, H] \rangle \rangle_z$ becomes

$$= \frac{1}{m^2 N^2} \sum_{ij} \sum_{\mathbf{k}\mathbf{k}'\sigma} \sum_{\mathbf{p}\mathbf{p}'\tau} \langle \mathbf{k} | U^i | \mathbf{k}' \rangle \langle \mathbf{p} | U^j | \mathbf{p}' \rangle \{ \mathbf{k}(\epsilon_{\mathbf{k}} - \mu) - \mathbf{k}'(\epsilon_{\mathbf{k}'} - \mu) \} \cdot \hat{n} \{ \mathbf{p}(\epsilon_{\mathbf{p}} - \mu) - \mathbf{p}'(\epsilon_{\mathbf{p}'} - \mu) \} \cdot \hat{n} \langle \langle c_{\mathbf{k}\sigma}^\dagger c_{\mathbf{k}'\sigma}; c_{\mathbf{p}\tau}^\dagger c_{\mathbf{p}'\tau} \rangle \rangle_z. \quad (3.2.3)$$

Now we consider the case of dilute impurity i.e. $i = j$ which means that we have neglected the interference terms i.e. terms that corresponds to $i \neq j$ and perform the ensemble average followed by integration over time using the definition for correlation

function Eq. (2.2.2) . This yield Eq. (3.2.3) in the following form

$$= \frac{2N_{\text{imp}}}{m^2 N^2} \sum_{\mathbf{k}\mathbf{k}'} |\langle \mathbf{k} | U | \mathbf{k}' \rangle|^2 [\{ \mathbf{k}(\epsilon_{\mathbf{k}} - \mu) - \mathbf{k}'(\epsilon_{\mathbf{k}'} - \mu) \} \cdot \hat{n}]^2 \frac{f_{\mathbf{k}} - f_{\mathbf{k}'}}{z + \epsilon_{\mathbf{k}} - \epsilon_{\mathbf{k}'}}. \quad (3.2.4)$$

Here N_{imp} represents the impurity concentration, the factor 2 is due to the electronic spin degeneracy and $f_{\mathbf{k}} = \frac{1}{e^{\beta(\epsilon_{\mathbf{k}} - \mu)} + 1}$ is the Fermi distribution function and β is the inverse of the temperature.

Using the above Eq. (3.2.4) in (3.1.4) and then performing the analytic continuation $z \rightarrow \omega + i\zeta$, $\zeta \rightarrow 0^+$, the imaginary part of the thermal memory function can be written as

$$M''_{QQ}(\omega, T) = \frac{2\pi}{N^2} \frac{N_{\text{imp}}}{\chi_{QQ}^0(T) m^2} \sum_{\mathbf{k}\mathbf{k}'} |\langle \mathbf{k} | U | \mathbf{k}' \rangle|^2 [\{ \mathbf{k}(\epsilon_{\mathbf{k}} - \mu) - \mathbf{k}'(\epsilon_{\mathbf{k}'} - \mu) \} \cdot \hat{n}]^2 \times \frac{f_{\mathbf{k}} - f_{\mathbf{k}'}}{\omega} \delta(\omega + \epsilon_{\mathbf{k}} - \epsilon_{\mathbf{k}'}). \quad (3.2.5)$$

Further to reduce the Eq. (3.2.5), we assume that the system has cubic symmetry. Then on averaging over all directions, we obtain

$$[\{ \mathbf{k}(\epsilon_{\mathbf{k}} - \mu) - \mathbf{k}'(\epsilon_{\mathbf{k}'} - \mu) \} \cdot \hat{n}]^2 = \frac{1}{3} |\mathbf{k}(\epsilon_{\mathbf{k}} - \mu) - \mathbf{k}'(\epsilon_{\mathbf{k}'} - \mu)|^2. \quad (3.2.6)$$

Using the above Eq. (3.2.6) along with the assumption of point like impurities (i.e. momentum independent character of U), the Eq. (3.2.5) can be written in the integral form

$$M''_{QQ}(\omega, T) = \frac{U^2 N_{\text{imp}}}{3(2\pi)^5 m^2 \chi_{QQ}^0(T)} \int \frac{d\epsilon_{\mathbf{k}}}{v_{\mathbf{k}}} k^2 \sin \theta d\theta d\phi \int \frac{d\epsilon_{\mathbf{k}'}}{v_{\mathbf{k}'}} k'^2 \sin \theta' d\theta' d\phi' |\mathbf{k}(\epsilon_{\mathbf{k}} - \mu) - \mathbf{k}'(\epsilon_{\mathbf{k}'} - \mu)|^2 \frac{f_{\mathbf{k}} - f_{\mathbf{k}'}}{\omega} \delta(\omega + \epsilon_{\mathbf{k}} - \epsilon_{\mathbf{k}'}). \quad (3.2.7)$$

Following the assumptions used in Chapter 2 (for details refer page 27) to simplify the expression of the memory function, the magnitudes of \mathbf{k} and \mathbf{k}' can be considered equal to k_F . Thus, the imaginary part of the thermal memory function takes the form

$$M''_{QQ}(\omega, T) = \frac{N_{\text{imp}} U^2 k_F^4}{6\pi^3 \chi_{QQ}^0(T)} \int d\epsilon [(\epsilon_{\mathbf{k}} - \mu)^2 + (\epsilon_{\mathbf{k}} - \mu + \omega)^2] \times \frac{f(\epsilon_{\mathbf{k}} - \mu) - f(\epsilon_{\mathbf{k}} - \mu + \omega)}{\omega}. \quad (3.2.8)$$

Substituting $\frac{\epsilon_{\mathbf{k}} - \mu}{T} = \eta$ and $\frac{\omega}{T} = x$, the above expression can be written in simpler form as

$$M''_{QQ}(\omega, T) = \frac{N_{\text{imp}} U^2 k_F^4 T^2}{6\pi^3 \chi_{QQ}^0(T)} \int_0^\infty d\eta \frac{\eta^2 + (\eta + x)^2}{x} \left[\frac{1}{e^\eta + 1} - \frac{1}{e^{\eta+x} + 1} \right]. \quad (3.2.9)$$

$$M''_{QQ}(\omega, T) = \frac{N_{\text{imp}} U^2 k_F^4 T^2}{6\pi^3 \chi_{QQ}^0(T)} \left\{ \frac{\pi^2}{6} + x \log \left(\frac{2e^x}{1 + e^x} \right) + 2Li_2(-e^{-x}) + \frac{4}{x} Li_3(-e^{-x}) + 3\zeta(3) \right\}.$$

This is the final expression for the imaginary part of the thermal memory function due to the electron-impurity interaction and is our main result. Further in various frequency and temperature limits, its behavior can be discussed as follows:

Case-I: In the dc limit i.e. $\omega \rightarrow 0$

In this limit, the Eq. (3.2.9) reduces to

$$M''_{QQ}(T) = \frac{N_{\text{imp}} U^2 k_F^4 T^2}{3\pi^3 \chi_{QQ}^0(T)} \int_0^\infty d\eta \frac{\eta^2 e^\eta}{(e^\eta + 1)^2} \quad (3.2.10)$$

$$= \frac{N_{\text{imp}} U^2 k_F^4 T^2}{18\pi \chi_{QQ}^0(T)} \quad (3.2.11)$$

This concludes that the temperature dependent imaginary part of the thermal memory function, also known as thermal scattering rate, $1/\tau_{th}$, varies with temperature as $T^2/\chi_{QQ}^0(T)$. Since the static correlation function $\chi_{QQ}^0(T)$ is directly proportional to the square of temperature (proof is given in Appendix B.1). Thus, $1/\tau_{th}$ in the zero frequency limit is expressed as

$$M''_{QQ}(T) \propto T^0 \quad \text{or} \quad \text{constant}. \quad (3.2.12)$$

This yields that the thermal scattering rate does not show temperature dependent behavior in the case of electron-impurity interaction. On the other hand, due to the symmetry relations of the thermal memory function, its real part becomes identically zero in the dc limit [56]. On substituting this in the expression for the thermal conductivity Eq. (3.1.3), we find that the real part of the thermal conductivity depends on the temperature as

$$\text{Re}[\kappa(T)] = \frac{1}{T} \frac{\chi_{QQ}^0(T)}{M''_{QQ}(T)}. \quad (3.2.13)$$

Using Eqs. (3.2.11) and (B.1.2) (as mentioned in the Appendix B.1), the above equation for the thermal conductivity reduces to

$$\begin{aligned} \text{Re}[\kappa(T)] &= \frac{1}{72} \frac{\pi k_F^2}{N_{\text{imp}} U^2 m^2} T \\ \text{i.e., } \text{Re}[\kappa(T)] &\propto T. \end{aligned} \quad (3.2.14)$$

This result is in accord with the result predicted earlier using Bloch-Boltzmann's equation approach Eq. (D.1.10) in Appendix D.1.

Case-II: In the finite frequency limit

In the high frequency limit i.e. $\omega \gg T$, the imaginary part of the thermal memory function Eq. (3.2.9) approximately becomes

$$\begin{aligned} M''_{QQ}(\omega, T) &\approx \frac{N_{\text{imp}} U^2 k_F^4 T^2}{6\pi^3 \chi_{QQ}^0(T)} \int_0^\infty d\eta x \left[\frac{1}{e^\eta + 1} - \frac{1}{e^{\eta+x} + 1} \right]. \\ &\approx \frac{N_{\text{imp}} U^2 k_F^4 T^2 \log 2 \omega}{6\pi^3 \chi_{QQ}^0(T) T}. \end{aligned} \quad (3.2.15)$$

This yields that the thermal memory function or the thermal scattering rate approximately varies linearly with the frequency and inversely with the temperature (as $\chi_{QQ}^0(T) \sim T^2$). While in the opposite case $\omega \ll T$, the leading order term in the Eq. (3.2.9) becomes

$$\begin{aligned} M''_{QQ}(\omega, T) &\approx \frac{N_{\text{imp}} U^2 k_F^4 T^2}{6\pi^3 \chi_{QQ}^0(T)} \int_0^\infty d\eta \frac{\eta^2}{e^\eta + 1} \left(2 - \frac{\omega}{T} \right) \\ &\approx \frac{N_{\text{imp}} U^2 k_F^4 T^2 \zeta(3)}{4\pi^3 \chi_{QQ}^0(T)} \left(2 - \frac{\omega}{T} \right) \\ &\approx A + B \frac{\omega}{T}, \end{aligned} \quad (3.2.16)$$

where A and B are constants.

These results are summarized in the Table 3.1.

3.2.2 Electron-Phonon Interaction

Now we consider that the system has only electron-phonon interactions as considered for the calculation of electrical memory function in Chapter 2. Then, the thermal memory function can be calculated in a similar fashion as is done in the case of impurity interactions in the previous section. Here the total Hamiltonian is considered as $H = H_0 + H_{\text{ep}} + H_{\text{ph}}$ (the parts of Hamiltonian are defined in Eq. (2.1.2), (2.1.3)

Table 3.1: The results of thermal memory function and the real part of the thermal conductivity due to the electron-impurity interaction in different frequency and temperature domains.

Regimes	Thermal memory function $1/\tau_{\text{th}}$ or M''_{QQ}	Thermal conductivity, κ
$\omega = 0$	T^0	T
$\omega \gg T$	$T^{-1}\omega$	ω^{-1}
$\omega \ll T$	T^0	T

and (2.1.5)). The thermal current commutes with the free electron and the free phonon parts of the Hamiltonian. Thus, we are left with the commutator of the thermal current J_Q and the interaction term H_{ep} which is expressed as

$$[J_Q, H_{\text{ep}}] = \frac{1}{m} \sum_{\mathbf{k}\mathbf{k}'\sigma} \{ \mathbf{k}(\epsilon_{\mathbf{k}} - \mu) - \mathbf{k}'(\epsilon_{\mathbf{k}'} - \mu) \} \cdot \hat{n} \left(D(\mathbf{k} - \mathbf{k}') c_{\mathbf{k}\sigma}^\dagger c_{\mathbf{k}'\sigma} b_{\mathbf{k}-\mathbf{k}'} - \text{h.c.} \right). \quad (3.2.17)$$

This commutation relations yield the Laplace transform and ensemble average of the inner product, $\langle\langle [J_Q, H_{\text{ep}}]; [J_Q, H_{\text{ep}}] \rangle\rangle_z$ in the following form

$$\begin{aligned} &= \frac{1}{m^2} \sum_{\mathbf{k}\mathbf{k}'\sigma} \sum_{\mathbf{p}\mathbf{p}'\tau} \{ \mathbf{k}(\epsilon_{\mathbf{k}} - \mu) - \mathbf{k}'(\epsilon_{\mathbf{k}'} - \mu) \} \cdot \hat{n} \{ \mathbf{p}(\epsilon_{\mathbf{p}} - \mu) - \mathbf{p}'(\epsilon_{\mathbf{p}'} - \mu) \} \cdot \hat{n} \\ &\quad \left(D(\mathbf{k} - \mathbf{k}') D^*(\mathbf{p} - \mathbf{p}') \langle\langle c_{\mathbf{k}\sigma}^\dagger c_{\mathbf{k}'\sigma} b_{\mathbf{k}-\mathbf{k}'}; c_{\mathbf{p}'\tau}^\dagger c_{\mathbf{p}\tau} b_{\mathbf{p}-\mathbf{p}'}^\dagger \rangle\rangle_z \right. \\ &\quad \left. - D^*(\mathbf{k} - \mathbf{k}') D(\mathbf{p} - \mathbf{p}') \langle\langle c_{\mathbf{k}'\sigma}^\dagger c_{\mathbf{k}\sigma} b_{\mathbf{k}-\mathbf{k}'}^\dagger; c_{\mathbf{p}\tau}^\dagger c_{\mathbf{p}'\tau} b_{\mathbf{p}-\mathbf{p}'} \rangle\rangle_z \right). \end{aligned} \quad (3.2.18)$$

On further simplifications, the above expression reduces to

$$\begin{aligned} \langle\langle [J_Q, H_{\text{ep}}]; [J_Q, H_{\text{ep}}] \rangle\rangle_z &= \frac{2}{m^2} \sum_{\mathbf{k}\mathbf{k}'} \left[\{ \mathbf{k}(\epsilon_{\mathbf{k}} - \mu) - \mathbf{k}'(\epsilon_{\mathbf{k}'} - \mu) \} \cdot \hat{n} \right]^2 |D(\mathbf{k} - \mathbf{k}')|^2 \\ &\quad \times \left\{ f_{\mathbf{k}}(1 - f_{\mathbf{k}'}) (1 + n_{\mathbf{k}-\mathbf{k}'} - (1 - f_{\mathbf{k}}) f_{\mathbf{k}'} n_{\mathbf{k}-\mathbf{k}'}) \right\} \\ &\quad \times \left\{ \frac{1}{z + \epsilon_{\mathbf{k}} - \epsilon_{\mathbf{k}'} - \omega_{\mathbf{k}-\mathbf{k}'}} - \frac{1}{z + \epsilon_{\mathbf{k}'} - \epsilon_{\mathbf{k}} + \omega_{\mathbf{k}-\mathbf{k}'}} \right\}, \end{aligned} \quad (3.2.19)$$

where n is the Boson distribution function (see Eq. (1.2.16)).

Substituting the above Eq. (3.2.19) in the thermal memory function Eq. (3.1.4) and then performing the analytic continuation $z \rightarrow \omega + i\zeta$, $\zeta \rightarrow 0^+$, the imaginary part of the thermal memory function can be written as

$$M''_{QQ}(\omega, T) = \frac{2\pi}{\chi_{QQ}^0(T)m^2} \sum_{\mathbf{k}\mathbf{k}'} [\{\mathbf{k}(\epsilon_{\mathbf{k}} - \mu) - \mathbf{k}'(\epsilon_{\mathbf{k}'} - \mu)\} \cdot \hat{n}]^2 |D(\mathbf{k} - \mathbf{k}')|^2 (1 - f_{\mathbf{k}}) \\ \times f_{\mathbf{k}'} n_{\mathbf{k}-\mathbf{k}'} \left\{ \frac{e^{\omega/T} - 1}{\omega} \delta(\epsilon_{\mathbf{k}} - \epsilon_{\mathbf{k}'} - \omega_{\mathbf{k}-\mathbf{k}'} + \omega) + (\text{terms with } \omega \rightarrow -\omega) \right\}. \quad (3.2.20)$$

To evaluate the above equation, we use the law of conservation of energy $\epsilon_{\mathbf{k}} = \epsilon_{\mathbf{k}'} - \omega_q$ and the law of conservation of momentum $\mathbf{q} = \mathbf{k}' - \mathbf{k}$ which simplify a factor appearing in the Eq. (3.2.20) as follows

$$[\{\mathbf{k}(\epsilon_{\mathbf{k}} - \mu) - \mathbf{k}'(\epsilon_{\mathbf{k}'} - \mu)\} \cdot \hat{n}]^2 = [\{\omega_q \mathbf{k}' + (\epsilon_{\mathbf{k}} - \mu) \mathbf{q}\} \cdot \hat{n}]^2. \quad (3.2.21)$$

For simplicity, we consider that the system has cubic symmetry as considered in the impurity case. Then on averaging over all directions, we obtain

$$[\{\omega_q \mathbf{k}' + (\epsilon_{\mathbf{k}} - \mu) \mathbf{q}\} \cdot \hat{n}]^2 = \frac{1}{3} \{ \omega_q^2 k'^2 + q^2 (\epsilon_{\mathbf{k}} - \mu)^2 + \omega_q (\epsilon_{\mathbf{k}} - \mu) q^2 \}. \quad (3.2.22)$$

Substituting the Eq. (3.2.22) in (3.2.20) and converting the summations into integrals, we get

$$M''_{QQ}(\omega, T) = \frac{N^2}{3\chi_{QQ}^0(T)m^2(2\pi)^5} \int \frac{d\epsilon_{\mathbf{k}}}{v_{\mathbf{k}}} k^2 \sin \theta d\theta d\phi \int \frac{d\epsilon_{\mathbf{k}'}}{v_{\mathbf{k}'}} k'^2 \sin \theta' d\theta' d\phi' \int dq \\ \times |D(q)|^2 \delta(q - |\mathbf{k} - \mathbf{k}'|) (1 - f_{\mathbf{k}}) f_{\mathbf{k}'} n_{\mathbf{k}-\mathbf{k}'} \\ \times \{ \omega_q^2 k'^2 + q^2 (\epsilon_{\mathbf{k}} - \mu)^2 + \omega_q (\epsilon_{\mathbf{k}} - \mu) q^2 \} \\ \times \left\{ \frac{e^{\omega/T} - 1}{\omega} \delta(\epsilon_{\mathbf{k}} - \epsilon_{\mathbf{k}'} - \omega_{\mathbf{k}-\mathbf{k}'} + \omega) + (\text{terms with } \omega \rightarrow -\omega) \right\}. \quad (3.2.23)$$

Following the argument as quoted in the Chapter 2 (refer page 31), for low energy scattering, we consider the magnitudes of \mathbf{k} and \mathbf{k}' of the order of \mathbf{k}_F . With these facts and solving one of the energy integrals, the above Eq. (3.2.23) reduces to

$$M''_{QQ}(\omega, T) = \frac{N^2}{12\pi^3} \frac{1}{\chi_{QQ}^0(T)} \int_0^\infty d\eta \int_0^{q_D} dq q |D(q)|^2 \{ \omega_q^2 k_F^2 + q^2 \eta^2 T^2 + \omega_q \eta T q^2 \} \\ \times \frac{1}{e^y - 1} \frac{1}{e^{-\eta} + 1} \left[\frac{1}{e^{\eta-y-x} + 1} \frac{e^x - 1}{x} + (\text{terms with } \omega \rightarrow -\omega) \right]. \quad (3.2.24)$$

Here we introduce new dimensionless variables $\frac{\epsilon_{\mathbf{k}} - \mu}{T} = \eta$, $\frac{\omega_q}{T} = y$ and $\frac{\omega}{T} = x$. Now integrating over η , we obtain

$$M''_{QQ}(\omega, T) = \frac{N^2 T^6}{12\pi \chi_{QQ}^0(T)} \left(\frac{q_D}{\Theta_D}\right)^4 \int_0^{\Theta_D/T} dy y^3 |D(y)|^2 \left[\frac{(x-y)}{e^{x-y}-1} \frac{e^x-1}{x(e^y-1)} \left\{ \frac{k_F^2}{\pi^2} \left(\frac{\Theta_D}{q_D T}\right)^2 + \frac{1}{3} + \frac{(x-y)^2}{\pi^2} + \frac{1}{2\pi^2} y(x-y) \right\} + (\text{terms with } \omega \rightarrow -\omega) \right]. \quad (3.2.25)$$

Substituting the phonon matrix element using the Eq. (2.1.4), the thermal memory function is simplified to

$$M''_{QQ}(\omega, T) = \frac{N}{24\pi m_i \rho_F^2} \frac{T^7}{\chi_{QQ}^0(T)} \left(\frac{q_D}{\Theta_D}\right)^6 \int_0^{\Theta_D/T} dy y^4 \left[\frac{(x-y)}{e^{x-y}-1} \frac{e^x-1}{x(e^y-1)} \left\{ \frac{k_F^2}{\pi^2} \left(\frac{\Theta_D}{q_D T}\right)^2 + \frac{1}{3} + \frac{(x-y)^2}{3\pi^2} + \frac{1}{2\pi^2} y(x-y) \right\} + (\text{terms with } \omega \rightarrow -\omega) \right]. \quad (3.2.26)$$

This is the frequency and the temperature dependent thermal memory function for the case of electron-phonon interaction. It can be further simplified by using the integral which we have shown in Eq. (G.0.4) in Appendix G. Here we discuss it in certain regimes of temperature and frequency as follows:

Case-I: In the dc limit i.e. $\omega \rightarrow 0$

In this limit, the Eq. (3.2.26) reduces to

$$M''_{QQ}(T) = \frac{N}{12\pi m_i \rho_F^2} \frac{T^7}{\chi_{QQ}^0(T)} \left(\frac{q_D}{\Theta_D}\right)^6 \int_0^{\Theta_D/T} dy \frac{y^5 e^y}{(e^y-1)^2} \times \left\{ \frac{k_F^2}{\pi^2 T^2} \left(\frac{\Theta_D}{q_D}\right)^2 + \frac{1}{3} - \frac{1}{6\pi^2} y^2 \right\}. \quad (3.2.27)$$

The closed form of the above expression can be obtained by solving the integral which gives the result in the form of PolyLogs (as shown in Eq. (G.0.5)) and then simplifying by substitution of the upper and lower limits of integration. Here we discuss the above equation in high and low temperature limit. In the high temperature limit i.e. when the temperature is much greater than the Debye temperature ($T \gg \Theta_D$), the second term within the curly brackets contributes more as compared to the other terms. Because the other terms varies inversely as square of the temperature, they contribute less than

the second term (i.e. $1/3$). Hence, the thermal memory function $M''_{QQ}(T)$ with leading term can be approximated as

$$M''_{QQ}(T) \approx \frac{N}{36\pi m_i \rho_F^2} \frac{T^7}{\chi_{QQ}^0(T)} \left(\frac{q_D}{\Theta_D}\right)^6 \int_0^{\Theta_D/T} dy \frac{y^5 e^y}{(e^y - 1)^2}.$$

$$M''_{QQ}(T) = \frac{N\Theta_D^4}{144\pi m_i \rho_F^2} \left(\frac{q_D}{\Theta_D}\right)^6 \frac{T^3}{\chi_{QQ}^0(T)}. \quad (3.2.28)$$

Thus on considering the temperature variation of the static thermal correlation function (Eq. B.1.2 in Appendix B.1), we find that the imaginary part of the dc thermal memory function varies linearly with the temperature in the high temperature regime. On substituting this in Eq. (3.1.3), we find that the real part of the thermal conductivity varies as

$$\text{Re}[\kappa(T)] = \text{constant}. \quad (3.2.29)$$

In the low temperature limit i.e. when the temperature is much less than the Debye temperature ($T \ll \Theta_D$), the first term and the third term in the Eq. (3.2.27) contributes more to the thermal memory function as compared to the second term. We know that q_D is generally much smaller than the k_F , then the first term dominates over third term. Thus using this fact $M''_{QQ}(T)$ becomes

$$M''_{QQ}(T) \approx \frac{Nk_F^2}{12\pi^3 m_i \rho_F^2} \left(\frac{q_D}{\Theta_D}\right)^6 \frac{T^5}{\chi_{QQ}^0(T)} \int_0^\infty dy y^5 \frac{e^y}{(e^y - 1)^2}$$

$$\approx \frac{10Nk_F^2 \zeta(5)}{\pi^3 m_i \rho_F^2} \left(\frac{q_D}{\Theta_D}\right)^6 \frac{T^5}{\chi_{QQ}^0(T)} \quad (3.2.30)$$

The above equation tells that the imaginary part of the thermal memory function or the thermal scattering rate varies as T^3 ($1/\tau_{\text{th}} \propto T^3$ as $\chi_{QQ}^0(T) \sim T^2$). Thus, we find that the real part of the thermal conductivity Eq. (3.1.3) which varies inversely as square of the temperature i.e.

$$\text{Re}[\kappa(T)] \propto T^{-2}. \quad (3.2.31)$$

These results in different temperature regimes are in accord with the results obtained from the Bloch-Boltzmann equation approach (details are given in Appendix D.2) and with the experimental results [29, 31, 86].

Case-II: In the finite frequency case

In the high frequency limit i.e. when frequency is much higher than the Debye frequency ($\omega \gg \omega_D$), the thermal memory function Eq. (3.2.26) becomes

$$M''_{QQ}(\omega, T) \approx \frac{N}{12\pi m_i \rho_F^2} \frac{T^7}{\chi_{QQ}^0(T)} \left(\frac{q_D}{\Theta_D} \right)^6 \int_0^{\Theta_D/T} dy \frac{y^4}{e^y - 1} \times \left\{ \frac{k_F^2}{\pi^2} \left(\frac{\Theta_D}{q_D T} \right)^2 + \frac{1}{3} + \frac{1}{3\pi^2} \frac{\omega^2}{T^2} \right\}. \quad (3.2.32)$$

In the low temperature limit i.e. $\omega \gg \Theta_D \gg T$, the first term and the third term are the leading order terms in the thermal memory function. Further, in the limit $\omega \gg T$,

$$M''_{QQ}(\omega, T) \approx \frac{2N\zeta(5)}{\pi m_i \rho_F^2} \frac{T^7}{\chi_{QQ}^0(T)} \left(\frac{q_D}{\Theta_D} \right)^6 \left\{ \frac{k_F^2}{\pi^2} \left(\frac{\Theta_D}{q_D T} \right)^2 + \frac{1}{3\pi^2} \frac{\omega^2}{T^2} \right\}. \quad (3.2.33)$$

In the high temperature limit i.e. $T \gg \omega \gg \Theta_D$, the second term of Eq. (3.2.32) contributes more over the other terms. Thus, the imaginary part of the thermal memory function in this regime becomes

$$M''_{QQ}(\omega, T) \approx \frac{N}{36\pi m_i \rho_F^2} \left(\frac{q_D}{\Theta_D} \right)^6 \frac{T^7}{\chi_{QQ}^0(T)} \int_0^{\Theta_D/T} dy \frac{y^4}{e^y - 1}. \quad (3.2.34)$$

On solving the integral in the above limits, we obtain the integral as $(\Theta_D/T)^4$. Thus,

$$M''_{QQ}(\omega, T) \propto T. \quad (3.2.35)$$

In the case, when $\omega \gg T \gg \Theta_D$, the third term of Eq. (3.2.32) contributes to the thermal memory function as

$$M''_{QQ}(\omega, T) \approx \frac{N}{36\pi^3 m_i \rho_F^2} \frac{T^7}{\chi_{QQ}^0(T)} \left(\frac{q_D}{\Theta_D} \right)^6 \frac{\omega^2}{T^2} \int_0^{\Theta_D/T} dy \frac{y^4}{e^y - 1}. \quad (3.2.36)$$

In the above mentioned frequency and temperature regime, the integral gives $(\Theta_D/T)^4$. Thus the thermal memory function varies as ω^2/T . All these limiting cases are collected in Table 3.2

Similarly in the low frequency limit i.e. when the frequency is much smaller than the Debye frequency ($\omega \ll \omega_D$), the Eq. (3.2.26) is written as

$$M''_{QQ}(\omega, T) \approx \frac{N}{24\pi m_i \rho_F^2} \frac{T^7}{\chi_{QQ}^0(T)} \left(\frac{q_D}{\Theta_D} \right)^6 \frac{e^{\omega/T}}{\omega/T} \times \int_0^{\Theta_D/T} dy \frac{y^5 e^y}{(e^y - 1)^2} \left\{ \frac{k_F^2}{\pi^2} \left(\frac{\Theta_D}{q_D T} \right)^2 + \frac{1}{3} - \frac{y^2}{6\pi^2} \right\} \quad (3.2.37)$$

The closed form of the above equation can be obtained similar to Eq. (3.2.27).

In the limit $\Theta_D \gg \omega \gg T$,

$$\begin{aligned} M''_{QQ}(\omega, T) &\approx \frac{Nk_F^2}{24\pi^3 m_i \rho_F^2} \frac{T^5}{\chi_{QQ}^0(T)} \left(\frac{q_D}{\Theta_D}\right)^4 \frac{e^{\omega/T}}{\omega/T} \int_0^\infty dy \frac{y^5 e^y}{(e^y - 1)^2}. \\ &\approx \frac{5Nk_F^2 \zeta(5)}{\pi^3 m_i \rho_F^2} \frac{T^5}{\chi_{QQ}^0(T)} \left(\frac{q_D}{\Theta_D}\right)^4 \frac{e^{\omega/T}}{\omega/T} \end{aligned} \quad (3.2.38)$$

And in the limit $T \gg \Theta_D \gg \omega$,

$$M''_{QQ}(\omega, T) \approx \frac{N}{36\pi m_i \rho_F^2} \frac{T^7}{\chi_{QQ}^0(T)} \left(\frac{q_D}{\Theta_D}\right)^6 \int_0^{\Theta_D/T} dy \frac{y^5 e^y}{(e^y - 1)^2}. \quad (3.2.39)$$

Under this limit, the integral over y yields $(\Theta_D/T)^4$. Hence the thermal memory function becomes

$$M''_{QQ}(\omega, T) \propto T. \quad (3.2.40)$$

This shows the linear temperature variation and frequency independent character of the thermal scattering rate in the regime $T \gg \Theta_D \gg \omega$.

In the case when $\Theta_D \gg T \gg \omega$, the Eq. (3.2.37) becomes

$$\begin{aligned} M''_{QQ}(\omega, T) &\approx \frac{Nk_F^2}{12\pi^3 m_i \rho_F^2} \frac{T^5}{\chi_{QQ}^0(T)} \left(\frac{q_D}{\Theta_D}\right)^4 \int_0^\infty dy \frac{y^5 e^y}{(e^y - 1)^2}. \\ &\approx \frac{10Nk_F^2 \zeta(5)}{12\pi^3 m_i \rho_F^2} \frac{T^5}{\chi_{QQ}^0(T)} \left(\frac{q_D}{\Theta_D}\right)^4 \end{aligned} \quad (3.2.41)$$

From the above equation, we find that $M''_{QQ}(\omega, T)$ varies as T^3 and it shows frequency independent behavior.

We summarize the above results in the Table 3.2. These analytical predictions of the dynamical behavior of the thermal memory functions in different temperature and frequency domains are supplemented by numerical calculation in the next section.

3.3 Results and Discussion

In this section, we have plotted and discussed the imaginary part of the dynamical thermal memory functions $M''_{QQ}(\omega, T)$ for the case of the electron-impurity and electron-phonon interactions (i.e. Eqs. (3.2.9) and (3.2.26)). To extract the characteristic frequency dependent and temperature dependent behavior of $M''_{QQ}(\omega, T)$, we suitably normalize it in various cases.

Table 3.2: The results of thermal memory function and the real part of the thermal conductivity due to the electron-phonon interaction in different frequency and temperature domains.

Regimes	Thermal memory function $1/\tau_{\text{th}}$ or M''_{QQ}	Thermal conductivity, κ
$\omega = 0, T \gg \Theta_D$	T^1	T^0
$\omega = 0, T \ll \Theta_D$	T^3	T^{-2}
$\omega \ll T \ll \Theta_D$	T^3	$T^4\omega^{-2}$
$\omega \ll \Theta_D \ll T$	T^1	$T^2\omega^{-2}$
$T \ll \omega \ll \Theta_D$	$T^4\omega^{-1}e^{\omega/T}$	$T^5\omega^{-3}e^{\omega/T}$
$\Theta_D \ll \omega \ll T$	T^1	$T^2\omega^{-2}$
$\Theta_D \ll T \ll \omega$	$T^{-1}\omega^2$	$T^0\omega^0$
$T \ll \Theta_D \ll \omega$	$T^3(a + b\omega^2)$	$T^4(A\omega^{-2} + B)$

First for the impurity interaction, we plot $M''_{QQ}(\omega, T)/M''_0$ where M''_0 is frequency and temperature independent constant ($= 2k_F^4 m/\pi^5 N_e$), as a function of frequency at a fixed temperature using the Eq. (3.2.9) in Fig. 3.1. Here we consider impurity concentration $N_{\text{imp}} = 0.001$ and interaction strength $U = 0.1\text{eV}$. It is found that the normalized thermal scattering rate increases linearly with the frequency in the range where the frequency is very high as compared to the temperature (as shown in Fig. 3.1(a)). This linear feature becomes more prominent as the temperature is lowered. For example in Fig. 3.1(b), the purple curve drawn at $T = 200\text{K}$ start showing a linear behavior above a frequency lower than that of the other two curves drawn at higher temperatures such as 300K and 400K. The low frequency regime $\omega \ll T$ of the plot is more elaborated in Fig. 3.1(b) which shows deviations from linearity. Also in both the regimes, the thermal scattering rate due to the impurity interaction decreases with the rise in temperature. These features are in accord with our asymptotic analytical predictions (Table 3.1).

In the zero frequency limit, the thermal scattering rate Eq. (3.2.11) becomes tem-

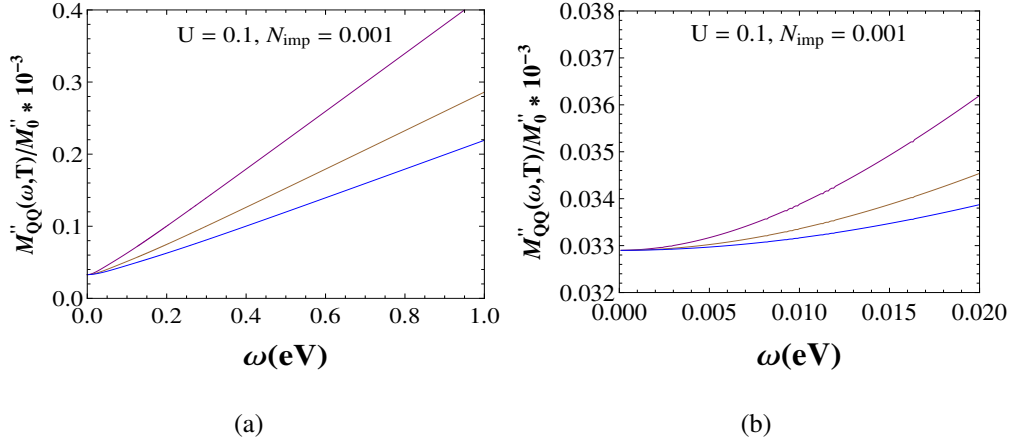


Figure 3.1: (a): The imaginary part of the thermal memory function for the case of electron-impurity interaction is plotted with frequency at different temperatures such as 200 (purple), 300 (brown) and 400K (blue) at fixed interaction strength U and impurity concentration N_{imp} . (b): The low frequency regime of Fig. 3.1(a) is elaborated.

perature independent. The same result can be obtained using Boltzmann approach as mentioned in Appendix D.1. This feature is also in accord with the experimental findings [3, 5].

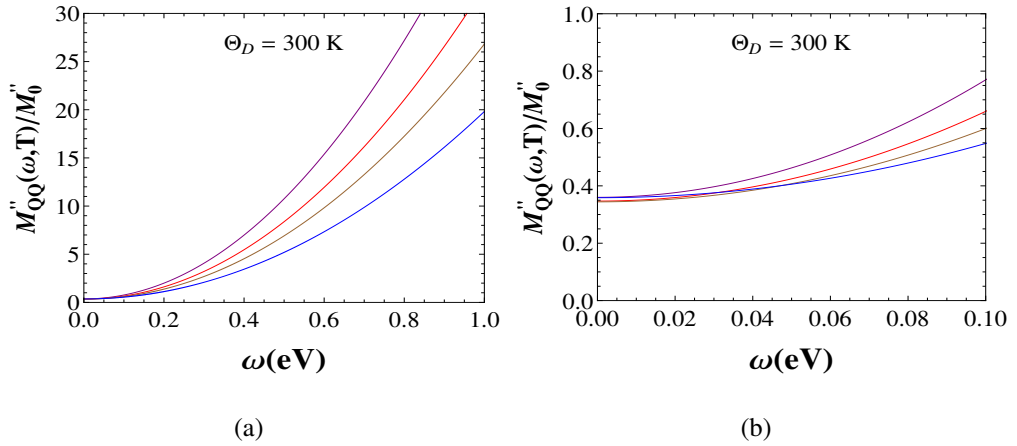


Figure 3.2: (a): The imaginary part of the thermal memory function for electron-phonon interaction is plotted with frequency at different temperatures such as 200 (purple), 250 (red), 300 (brown) and 400K (blue) at fixed Debye temperature $\Theta_D = 300\text{K}$. (b): The low frequency regime of Fig. 3.2(a) is elaborated.

For the electron-phonon interaction, the frequency dependent behavior of the normalized thermal scattering rate Eq. (3.2.26) is shown in Fig. 3.2 at different temper-

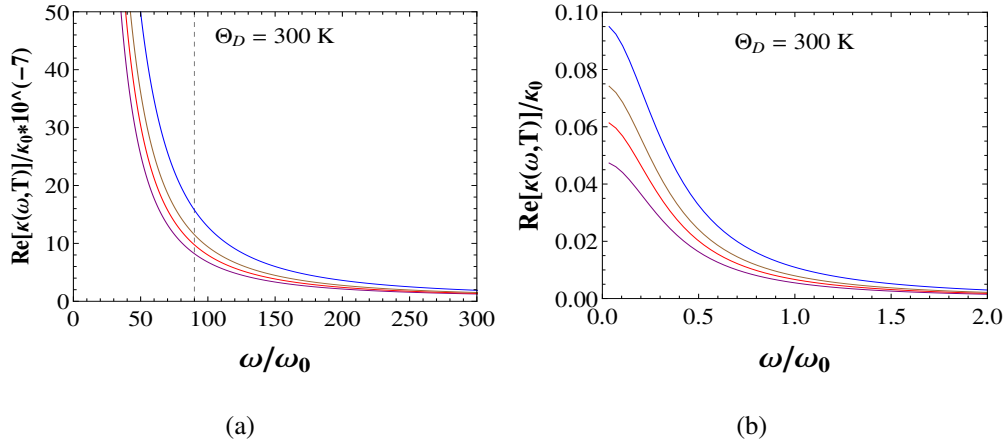


Figure 3.3: (a). The normalized frequency dependent thermal conductivity is plotted with the ratio ω/ω_0 for electron-phonon interaction at different temperatures such as 200 (purple), 250 (red), 300 (brown) and 400K (blue) and at Debye temperature $\Theta_D = 300$ K. Here the dashed line corresponds to the scale for Debye frequency cutoff i.e. ω_D/ω_0 . (b). The low frequency regime of Fig. 3.3(a) is elaborated.

atures. Here the Debye temperature Θ_D is kept fixed at 300K. In Fig. 3.2(a), we observe that in the high frequency regime ($\omega \gg \Theta_D$), the scaled thermal memory function M''_{QQ}/M''_0 ($M''_0 = Nm q_D^6/6\pi^3 m_i \rho_F^2 N_e \Theta_D$) increases as the frequency increases. While in the low frequency regime ($\omega \ll \omega_D$), it becomes constant. To see the zoomed low frequency behavior, we replot the same curves within a small frequency regime (as shown in Fig. 3.2(b)). We also observe that the magnitude of the thermal memory function reduces with the increase in temperature. However, the exact temperature dependence in the low frequency regime depends on whether the temperature is greater or lower than the Debye temperature. The detail asymptotic behaviors are obtained analytically in previous section (3.2) and given in Table 3.2.

In Fig. 3.3, the real part of the thermal conductivity in case of electron-phonon interaction using Eq. (3.1.3) is plotted as a function of frequency at a fixed Debye temperature Θ_D and at different temperatures. Here we have scaled the frequency with parameter ω_0 ($= Nm q_D^6/6\pi^3 m_i \rho_F^2 N_e \Theta_D$), which has the dimension of energy and scaled the real part of the thermal conductivity $\text{Re}[\kappa(\omega, T)]$ with κ_0 ($= \pi^2 N_e/4m\omega_0$). It is observed that the thermal conductivity decays with the increase in frequency (as shown in Fig. 3.3). Also, with the increase of temperature, the thermal conductivity increases.

This detailed behavior can be understood as follows. Our calculation is limited to a perturbative regime i.e. $M''_{QQ}(\omega, T) \ll \omega$, thus $\text{Re}[\kappa(\omega, T)] \sim \chi_{QQ}^0/T \times M''_{QQ}(\omega, T)/\omega^2$. As the static thermal current thermal current correlation function, $\chi_{QQ}^0(T) \sim T^2$, the real part of the thermal conductivity becomes $\text{Re}[\kappa(\omega, T)] \sim TM''_{QQ}(\omega, T)/\omega^2$. Under this condition, the increase in the thermal conductivity due to the increase in temperature is governed by the factor $TM''_{QQ}(\omega, T)$ which is an increasing function of temperature. Using this relation and Table 3.2, various regimes of Fig. 3.3 can be understood. For example, in the regimes

1. $T \ll \omega \ll \omega_D$, $\text{Re}[\kappa(\omega, T)] \sim T^5 \frac{e^{\omega/T}}{\omega^3}$,
2. $T \gg \omega \gg \omega_D$, $\text{Re}[\kappa(\omega, T)] \sim \frac{T^2}{\omega^2}$,
3. $\omega \gg \omega_D \gg T$, $\text{Re}[\kappa(\omega, T)] \sim T^4 \left(\frac{a}{\omega^2} + b \right)$,

where $a(= 2N\zeta(5)q_D^4/\pi^3 m_i \rho_F^2 \Theta_D^4)$ and $b(= 2N\zeta(5)q_D^6/3\pi^3 m_i \rho_F^2 \Theta_D^6)$ are constants. The detailed asymptotic results of the thermal conductivity due to the electron-phonon and the electron-impurity interactions are given in Table 3.2 and 3.1. *These signatures are new predictions from our formalism and can be verified in future experiments.*

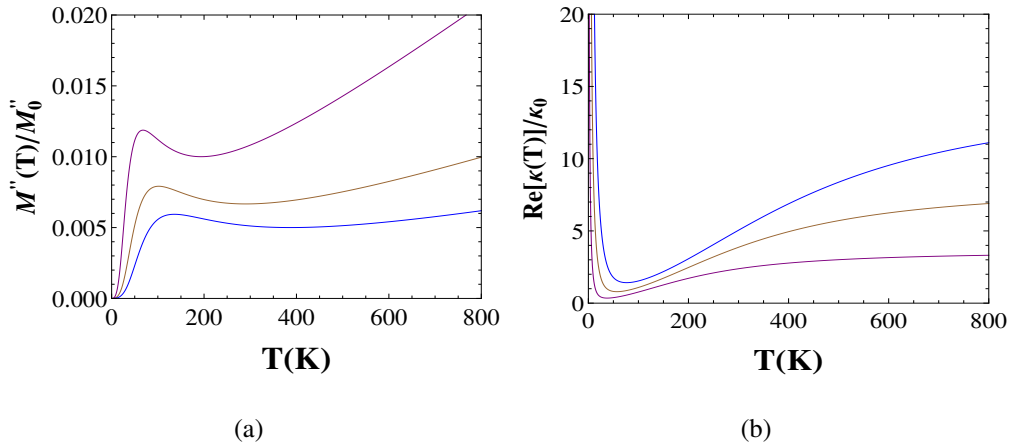


Figure 3.4: (a): Plot of temperature dependent normalized dc imaginary part of the thermal memory function for electron-phonon interaction at different Debye temperatures such as 200 (purple), 300 (brown) and 400K (blue). (b): The variation of the normalized thermal conductivity with T at same Debye temperatures.

Now in the dc limit, we plot $M''_{QQ}(T)/M_0''$ as a function of temperature T at different Debye's temperatures in Fig. 3.4(a). Here we find three important features. One

is the increase of the thermal scattering rate with temperature in the low temperature regime ($\sim T^3$, refer Table 3.2). Second, it increases linearly with the temperature at high temperature regime. Third, in the intermediate regime around the Debye temperature, there is a minima in the thermal scattering rate. These features (at high and low temperatures namely T^3 at $T \ll \Theta_D$ and T at $T \gg \Theta_D$) are in agreement with experiments [29, 31, 86]. In Fig. 3.4(b), using Eq. (3.1.3), the normalized thermal conductivity has been plotted with temperature T . This shows that it decreases as T^{-2} in the low temperature regime and becomes constant in the high temperature regime. These results are consistent with the results derived using Boltzmann approach in Appendix D.2. In the intermediate temperature regime, it passes through a minimum. This minimum in the thermal conductivity plot is an artifact of neglecting contributions from the Umklapp process in the memory function. Such minima occurs near the Debye temperature where Umklapp process becomes important. The same peculiarity is also found in Bloch-Boltzmann theory when Umklapp processes are neglected [3, 87].

3.4 Conclusion

In this chapter, we present analytical calculation of the dynamical thermal conductivity of metal for electron-impurity and electron-phonon interactions. We discuss the results in different frequency and temperature domains. Since in the zero frequency limit (dc limit) behavior of the thermal conductivity of metals is well known, we consider the dc results from the Bloch-Boltzmann approach and the experimental findings as a benchmark and compare our results with them.

According to the memory function formalism, the total thermal memory function is the thermal-current thermal-current correlation function which captures the role of the impurity and the electron-phonon interactions. This leads to the thermal memory function as the sum of the memory functions due to the electron-impurity interactions and the electron-phonon interactions which further result in the total thermal conductivity.

In a nutshell, the concluding remarks of this chapter are as follows:

1. The thermal memory function due to the impurity interaction shows the temperature independent behavior Eq. (3.2.12). Thus the thermal conductivity $\kappa(T)$ shows linear temperature behavior Eq. (3.2.14).
2. Due to the electron-phonon interactions, the thermal memory function and the thermal conductivity in the dc limit show:

$$\text{a. } M''_{QQ}(T) \sim T^3; \kappa(T) \sim T^{-2}, \quad T \ll \Theta_D,$$

$$\text{b. } M''_{QQ}(T) \sim T; \kappa(T) \sim T^0, \quad T \gg \Theta_D.$$

3. If we consider the impurity and phonon contributions together, we see that the total thermal conductivity can be expressed in an empirical form as,

$$\begin{aligned} \frac{1}{\kappa_{\text{total}}(T)} &= \frac{1}{\kappa_{\text{imp}}(T)} + \frac{1}{\kappa_{\text{ep}}(T)}. \\ &\sim \begin{cases} \frac{A}{T} + BT^2, & T \ll \Theta_D \\ \frac{A}{T} + C, & T \gg \Theta_D. \end{cases} \end{aligned} \quad (3.4.1)$$

Here, the first term and the second term are due to the electron-impurity and the electron-phonon interactions respectively and A , B and C are material dependent constants.

4. The results in the zero frequency limit (dc limit) are in accord with the results calculated using Bloch-Boltzmann approach [3, 5] and also with the experimental findings [3, 29, 86].
5. In the finite frequency cases we have several new predictions depending on the relative values of the frequency ω , temperature T and the Debye frequency ω_D (as refer in Table 3.1 and 3.2). This is the main contribution of this chapter.
6. Moreover, the present approach can also be used to study other transport properties such as thermo-electric coefficients etc.

Chapter 4

Dynamical Thermoelectric Coefficient of metals

For the future technological advancements, the theoretical and the practical understanding of the thermoelectric devices are of fundamental important [88–90]. These are the devices which possess the ability to convert the thermal energy into electrical energy and hence recognized for the energy conversion processes [91–93]. In this quest, the knowledge of the efficiency of these devices is essential which is characterized by the figure of merit, $ZT = S^2\sigma T/\kappa$ where S is the Seebeck coefficient, σ is the electrical conductivity, κ is the thermal conductivity and T is the temperature [14]. This ensures that larger the value of ZT , higher is the efficiency of the thermoelectric device. Enormous efforts have been made in order to increase the figure of merit. In the steady state, it can be increased by increasing the product of the electrical conductivity and square of the Seebeck coefficient i.e. σS^2 or by decreasing the thermal conductivity κ . But in this pathway, there is a well known relation between the thermal conductivity and the electrical conductivity, known as Wiedemann-Franz law [17]. The latter makes it difficult to decrease κ without the decrease of σ . Thus, an alternative approach known as dynamical approach is required to make this pathway easier [94]. This approach is beyond the above mentioned restriction and includes the frequency dependent behavior of the transport coefficients. The details of this approach is discussed in Chapter 1. Here we find that the Seebeck coefficient is higher at higher external driving frequencies, thus it leads to a greater figure of merit as the

Wiedemann-Franz law is no more valid in the finite frequency case:

$$\frac{\kappa(\omega, T)}{T\sigma(\omega, T)} = \frac{TM''_{QQ}(\omega, T)}{M''(\omega, T)} \left(\frac{\omega^2 + (M'''(\omega, T))^2}{\omega^2 + (M''_{QQ}(\omega, T))^2} \right), \quad (4.0.1)$$

where $M''_{QQ}(\omega, T)$ and $M''(\omega, T)$ are thermal and electrical memory functions or known as scattering rates respectively. The right hand side of the above equation is not a constant. Thus Wiedemann-Franz restriction is not applicable.

Another importance of this study is due to the recent demand of the microelectronic and optoelectronic devices, working at several Giga Hertz frequencies i.e. *GHz* clock frequencies [78, 80]. The basic working principle of these devices involves various frequency dependent thermal transport coefficients. Thus the quest of making the thermoelectric devices more efficient requires the understanding of the frequency and the temperature dependences of various transport quantities. So far, the dynamical nature of the electrical conductivity and the thermal conductivity have been studied in recent years [56, 62, 79, 95, 96]. The study of the Seebeck coefficient is an important parameter to determine the figure of merit and was not studied previously in detail especially in the dynamical regime.

In the present chapter, we first define the thermoelectric coefficients in Sec. 4.1. Then in Sec. 4.2, we introduce the thermoelectric memory functions and calculate them and the Seebeck coefficient for the case of electron-impurity and electron-phonon interactions in a metal. In Sec. 4.3, we present our results with discussion and latter we give conclusion in Sec. 4.4.

4.1 Thermoelectric Coefficients

In the linear response theory, the electric field and the temperature gradient are related to the electric current and the thermal current as follows [14, 24].

$$\mathbf{J} = \sigma\mathbf{E} - \alpha\nabla T. \quad (4.1.1)$$

$$\mathbf{J}_Q = \tilde{\alpha}\mathbf{E} - \kappa\nabla T. \quad (4.1.2)$$

These equations tell that the generation of charge current and the flow of heat can be a consequence of either electric field or temperature gradient or both. Here κ is the ther-

mal conductivity, σ is the electrical conductivity, α is the thermoelectric conductivity, and $\tilde{\alpha}$ is the electrothermal conductivity.

Consider that the system is electrically insulated. Thus, there is no electric current flow in the system i.e. $J = 0$. Then, Eq. (4.1.1) can be written as

$$\frac{E}{\nabla T} = \frac{\alpha}{\sigma}. \quad (4.1.3)$$

The Seebeck coefficient S is defined as the electric field generated by a thermal gradient in the absence of electric current [14]

$$S = -\frac{E}{\nabla T} = -\frac{\alpha}{\sigma}. \quad (4.1.4)$$

Here the sign indicates the sign of the charge carriers.

The Peltier coefficient is defined as the flow of heat due to the electric current. According to the Kelvin relation, it can be expressed as [22]

$$\Pi = ST. \quad (4.1.5)$$

Similarly, the Thomson coefficient which is related to the phenomenon of reversible heating or cooling in a current carrying material is defined as [22]

$$\mu_T = T \frac{dS}{dT} \quad (4.1.6)$$

We see that all these coefficients are related Eqs. (4.1.4) - (4.1.6) and the calculation of the Seebeck coefficient is sufficient to understand the others. The former is the ratio of the thermoelectric conductivity and the electrical conductivity which are calculated in the later sections.

4.2 Thermoelectric Memory Functions

Following the same idea of the previous chapters, the thermoelectric conductivity can be calculated via the thermal-current electric-current correlation function which relates the former via the corresponding memory function as

$$\alpha(z, T) = \frac{i}{T} \frac{\chi_Q^0(T)}{z + M_Q(z, T)}. \quad (4.2.1)$$

Here $\chi_Q^0(T)$ is the static thermal-current electric-current correlation function and $M_Q(z, T)$ is the thermoelectric memory function. Further, the latter is related to the correlation function as

$$M_Q(z, T) = z \frac{\chi_Q(z, T)}{\chi_Q^0(T) - \chi_Q(z, T)}, \quad (4.2.2)$$

where $\chi_Q(z, T)$ according to the linear response theory is defined as [59, 60, 97]

$$\chi_Q(z, T) = \langle\langle J_Q; J \rangle\rangle_z = -i \int_0^\infty dt e^{izt} \langle [J_Q(t), J] \rangle. \quad (4.2.3)$$

Further, this correlation function using equation of motion can be expressed in a similar fashion as the electric-current electric-current correlation function in Chapter 2. To deal with thermal-current electric-current correlation function, here we replace the electric currents J by J_Q and J . Thus, $\chi_Q(z, T)$ can be written as

$$\chi_Q(z, T) = \frac{\langle\langle [J_Q, H]; [J, H] \rangle\rangle_{z=0} - \langle\langle [J_Q, H]; [J, H] \rangle\rangle_z}{z^2}. \quad (4.2.4)$$

Substituting this correlation function in Eq. (4.2.2), then expanding the memory function expression as $M_Q(z, T) = \chi_Q(z, T)/\chi_Q^0 (1 + \chi_Q(z, T)/\chi_Q^0 - \dots)$ and keeping the leading order term [62, 79], the thermoelectric memory function $M_Q(z, T)$ can be expressed as

$$M_Q(z, T) = \frac{\langle\langle [J_Q, H]; [J, H] \rangle\rangle_{z=0} - \langle\langle [J_Q, H]; [J, H] \rangle\rangle_z}{z\chi_Q^0(T)}. \quad (4.2.5)$$

Knowing the commutation relations between the currents and Hamiltonian, it can be calculated for different type of interactions such as electron-impurity and electron-phonon.

4.2.1 Electron-Impurity Interaction

We want to calculate $M_Q(z, T)$ for a system in which the total Hamiltonian is defined by $H = H_0 + H_{\text{imp}}$ due to the presence of electron-impurity interaction. First, we calculate the Laplace transform and thermal average of the inner product $\langle\langle [J_Q, H]; [J, H] \rangle\rangle_z$ which requires the commutation relations between the currents and the Hamiltonian. The commutator between the electric current and the Hamiltonian is given by $[J, H] =$

$[J, H_0] + [J, H_{\text{imp}}]$. As the electric current and the unperturbed Hamiltonian commutes with each other, we have

$$[J, H] = \frac{1}{mN} \sum_i \sum_{\mathbf{k}\mathbf{k}'\sigma} \langle \mathbf{k} | U^i | \mathbf{k}' \rangle \{ \mathbf{k} - \mathbf{k}' \} \cdot \hat{n} c_{\mathbf{k}\sigma}^\dagger c_{\mathbf{k}'\sigma}. \quad (4.2.6)$$

Similarly, the commutator of thermal current and Hamiltonian is given by

$$[J_Q, H] = \frac{1}{mN} \sum_i \sum_{\mathbf{k}\mathbf{k}'\sigma} \langle \mathbf{k} | U^i | \mathbf{k}' \rangle \{ \mathbf{k}(\epsilon_{\mathbf{k}} - \mu) - \mathbf{k}'(\epsilon_{\mathbf{k}'} - \mu) \} \cdot \hat{n} c_{\mathbf{k}\sigma}^\dagger c_{\mathbf{k}'\sigma}. \quad (4.2.7)$$

Using the above relations, the correlation function $\langle\langle [J_Q, H]; [J, H] \rangle\rangle_z$ becomes

$$\begin{aligned} &= \frac{1}{m^2 N^2} \sum_{ij} \sum_{\mathbf{k}\mathbf{k}'\sigma} \sum_{\mathbf{p}\mathbf{p}'\tau} \langle \mathbf{k} | U^i | \mathbf{k}' \rangle \langle \mathbf{p} | U^j | \mathbf{p}' \rangle \\ &\quad \times \{ \mathbf{k} - \mathbf{k}' \} \cdot \hat{n} \{ \mathbf{p}(\epsilon_{\mathbf{p}} - \mu) - \mathbf{p}'(\epsilon_{\mathbf{p}'} - \mu) \} \cdot \hat{n} \langle\langle c_{\mathbf{k}\sigma}^\dagger c_{\mathbf{k}'\sigma}; c_{\mathbf{p}\tau}^\dagger c_{\mathbf{p}'\tau} \rangle\rangle_z. \end{aligned} \quad (4.2.8)$$

By considering the case of dilute impurity (i.e. $i = j$ case and neglect the terms $i \neq j$), performing ensemble average, and integrating over time, Eq. (4.2.8) reduces to

$$\begin{aligned} \langle\langle [J_Q, H]; [J, H] \rangle\rangle_z &= \frac{2N_{\text{imp}}}{m^2 N^2} \sum_{\mathbf{k}\mathbf{k}'} |\langle \mathbf{k} | U | \mathbf{k}' \rangle|^2 \{ \mathbf{k} - \mathbf{k}' \} \cdot \hat{n} \\ &\quad \times \{ \mathbf{k}(\epsilon_{\mathbf{k}} - \mu) - \mathbf{k}'(\epsilon_{\mathbf{k}'} - \mu) \} \cdot \hat{n} \times \frac{f_{\mathbf{k}} - f_{\mathbf{k}'}}{z + \epsilon_{\mathbf{k}} - \epsilon_{\mathbf{k}'}} \end{aligned} \quad (4.2.9)$$

Here $f_{\mathbf{k}}$ is the Fermi distribution function. Substituting Eq. (4.2.9) in the thermoelectric memory function Eq. (4.2.5) and performing the analytic continuation using $z \rightarrow \omega + i\zeta$, $\zeta \rightarrow 0^+$, the imaginary part of the thermoelectric memory function* takes the form

$$\begin{aligned} M_Q''(\omega, T) &= \frac{2\pi N_{\text{imp}}}{\chi_Q^0(T) m^2 N^2} \sum_{\mathbf{k}\mathbf{k}'} |\langle \mathbf{k} | U | \mathbf{k}' \rangle|^2 \left[\{ \mathbf{k} - \mathbf{k}' \} \cdot \hat{n} \right. \\ &\quad \left. \times \{ \mathbf{k}(\epsilon_{\mathbf{k}} - \mu) - \mathbf{k}'(\epsilon_{\mathbf{k}'} - \mu) \} \cdot \hat{n} \right] \frac{f_{\mathbf{k}} - f_{\mathbf{k}'}}{\omega} \delta(\omega + \epsilon_{\mathbf{k}} - \epsilon_{\mathbf{k}'}). \end{aligned} \quad (4.2.10)$$

Further, assuming the cubic symmetry of the system and using the laws of conservation of energy and conservation of momentum, the part within the square brackets of above equation can be written as

$$\{ \mathbf{k} - \mathbf{k}' \} \cdot \hat{n} \{ \mathbf{k}(\epsilon_{\mathbf{k}} - \mu) - \mathbf{k}'(\epsilon_{\mathbf{k}'} - \mu) \} \cdot \hat{n} = \frac{1}{3} [(\epsilon_{\mathbf{k}} - \mu)k^2 + (\epsilon_{\mathbf{k}'} - \mu)k'^2]. \quad (4.2.11)$$

* $\lim_{\zeta \rightarrow 0} \frac{1}{a + i\zeta} = P \left(\frac{1}{a} \right) - i\pi\delta(a)$

Now we assume that the impurity strength U is independent of momentum and consider the fact that due to large Fermi energy, electrons from a small region of width $k_B T$ (here we set $k_B = 1$) around the Fermi surface participate in scattering events. Using these considerations and Eq. (4.2.11), the thermoelectric memory function Eq. (4.2.10) in the integral form reduces to

$$M_Q''(\omega, T) = \frac{N_{\text{imp}} U^2 k_F^4}{6\pi^3 \chi_Q^0(T)} \int_0^\infty d\epsilon \left\{ 2(\epsilon_{\mathbf{k}} - \mu) + \omega \right\} \frac{f(\epsilon_{\mathbf{k}}) - f(\epsilon_{\mathbf{k}} + \omega)}{\omega}. \quad (4.2.12)$$

Defining the new dimensionless variables $\frac{\epsilon_{\mathbf{k}} - \mu}{T} = \eta$ and $\frac{\omega}{T} = x$ and substituting it in Eq. (4.2.12) we have

$$M_Q''(\omega, T) = \frac{N_{\text{imp}} U^2 k_F^4 T}{6\pi^3 \chi_Q^0(T)} \int_0^\infty d\eta \frac{2\eta + x}{x} \left(\frac{1}{e^\eta + 1} - \frac{1}{e^{\eta+x} + 1} \right). \quad (4.2.13)$$

After performing the integration, the above expression reduces to

$$M_Q''(\omega, T) = \frac{N_{\text{imp}} U^2 k_F^4 T}{6\pi^3 \chi_Q^0(T)} \left\{ \frac{\pi^2}{6x} + \log 2 - \log \left(1 + e^{-x} \right) + \frac{2\text{Li}_2(-e^{-x})}{x} \right\}. \quad (4.2.14)$$

This is an expression for the imaginary part of the thermoelectric memory function in the presence of electron-impurity interaction. Its behavior can be discussed in different frequency and temperature regimes as follows.

Case-I The zero frequency limit i.e. $\omega \rightarrow 0$:

In this limit, Eq. (4.2.13) can be written as

$$M_Q''(T) = \frac{N_{\text{imp}} U^2 k_F^4 T}{3\pi^3 \chi_Q^0(T)} \int_0^\infty d\eta \frac{\eta e^\eta}{(e^\eta + 1)^2}. \quad (4.2.15)$$

Substituting the expression of the static thermoelectric correlation function (Eq. (B.2.2) in Appendix B.2), we obtain

$$\begin{aligned} M_Q''(T) &= \frac{N_{\text{imp}} U^2 k_F}{\pi \log 2} \int_0^\infty d\eta \frac{\eta e^\eta}{(e^\eta + 1)^2}. \\ &\approx \frac{N_{\text{imp}}}{\pi} U^2 k_F. \end{aligned} \quad (4.2.16)$$

Thus, in the zero frequency limit, $M_Q''(T)$ behaves independent of the temperature. Using this temperature variation of $M_Q''(T)$, the thermoelectric response function, Eq. (4.2.1) in the zero frequency limit becomes

$$\alpha(T) = \frac{1}{T} \frac{\chi_Q^0(T)}{M_Q''(T)} \quad (4.2.17)$$

Using Eqs. (4.2.16) and (B.2.2) (as mentioned in Appendix B.2), the thermoelectric response function Eq. (4.2.17) approximately becomes

$$\alpha(T) \approx \frac{1}{N_{\text{imp}} U^2 \log 2}. \quad (4.2.18)$$

Thus we conclude that the thermoelectric conductivity shows temperature independent behavior in the case of electron-impurity.

Case-II The finite frequency regime

In the high frequency limit i.e. $\omega \gg T$, the Eq. (4.2.13) reduces to

$$\begin{aligned} M_Q''(\omega, T) &\approx \frac{N_{\text{imp}} U^2 k_F^4 T}{6\pi^3 \chi_Q^0(T)} \left(\frac{1 - 2e^{-\omega/T}}{\omega/T} + e^{-\omega/T} + \log 2 \right). \\ &\approx \frac{N_{\text{imp}} U^2 k_F^4 T}{6\pi^3 \chi_Q^0(T)} \log 2. \\ &= \frac{N_{\text{imp}} U^2 m k_F}{\pi}. \end{aligned} \quad (4.2.19)$$

Here for calculation, we use the Eq. (B.2.2) for the static correlation function $\chi_Q^0(T)$. In the opposite case, when $\omega \ll T$, the imaginary part of the thermoelectric memory function Eq. (4.2.13) with the leading order term becomes

$$\begin{aligned} M_Q''(\omega, T) &\approx \frac{N_{\text{imp}} U^2 k_F^4 T}{18\pi^3 \chi_Q^0(T)} \\ &= \frac{N_{\text{imp}} U^2 m k_F}{3\pi \log 2}. \end{aligned} \quad (4.2.20)$$

These asymptotic results are collected in Table 4.1.

Using these results, the Seebeck coefficient for the case of electron-impurity interaction can be calculated in the following subsection.

Seebeck Coefficient

As discussed earlier that the Seebeck coefficient is the ratio of the thermoelectric and electrical response functions. Thus, to calculate it, we require $\alpha(z, T)$ and $\sigma(z, T)$.

The $\sigma(z, T)$, known as electrical conductivity can be calculated with the following relation which relates the electrical conductivity with the memory function (as discussed in Chapter 2, Eq. (2.2.5)) [27, 56].

$$\sigma(z, T) = i \frac{\chi_0}{z + M(z, T)}, \quad (4.2.21)$$

Table 4.1: The thermoelectric and electrical scattering rates or memory functions due to the electron-impurity interaction in different frequency and temperature domains.

Regimes	Thermoelectric memory function $1/\tau_{te}$ or $M''_Q(\omega, T)$	Electrical memory function $1/\tau_e$ or $M''(\omega, T)$
$\omega = 0$	T^0	T^0
$\omega \gg T$	$\log 2 + T\omega^{-1}$	$T\omega^{-1}$
$\omega \ll T$	T^0	T^0

where χ_0 is the static electric-current electric-current correlation function and $M(z, T)$ is the electrical memory function.

Following the same procedure of the thermoelectric memory function, the imaginary part of the electrical memory function for the case of electron-impurity interaction is written as [56]

$$\begin{aligned}
 M''(\omega, T) &= \frac{N_{\text{imp}}U^2k_F^4}{6\pi^3\chi_0} \int_0^\infty d\eta \frac{1}{x} \left(\frac{1}{e^\eta + 1} - \frac{1}{e^{\eta+x} + 1} \right). \\
 &= \frac{N_{\text{imp}}U^2k_F^4}{6\pi^3\chi_0} \frac{1}{x} \left(1 + \log 2 - \log(1 + e^x) \right). \quad (4.2.22)
 \end{aligned}$$

Here $x = \omega/T$ and $\chi_0 = N_e/m$. The detailed calculation of this expression will be discussed in Sec. 6.2 of Chapter 6.

In the zero frequency limit i.e. $\omega \rightarrow 0$, the above integral equation can be expressed as

$$\begin{aligned}
 M''(T) &= \frac{N_{\text{imp}}U^2k_F^4}{6\pi^3\chi_0} \int_0^\infty d\eta \frac{e^\eta}{(e^\eta + 1)^2}. \\
 &\approx \frac{N_{\text{imp}}U^2k_F^4}{12\pi^3\chi_0}. \quad (4.2.23)
 \end{aligned}$$

This shows the temperature independent behavior of the electrical memory function. Further, on substituting Eq. (4.2.23) in (4.2.21) by taking the zero frequency limit of $\sigma(z, T)$ ($= \chi_0/M''(T)$), we find that the electrical conductivity shows temperature independent behavior in case of the electron-impurity interaction. Using the thermoelectric and electrical memory functions, the Seebeck coefficient is calculated as follows.

In the zero frequency limit, the Seebeck coefficient is

$$\begin{aligned} S(T) &= \frac{\alpha(T)}{\sigma(T)} \\ &= \frac{1}{T} \frac{\chi_Q^0(T)}{\chi_0} \frac{M''(T)}{M_Q''(T)}. \end{aligned} \quad (4.2.24)$$

Using Eqs. (4.2.16), (4.2.23) and (B.2.2), we find that the Seebeck coefficient in the zero frequency limit shows temperature independent behavior for the case of electron-impurity interaction [3].

On the other hand, in the finite frequency case the Seebeck coefficient $S(z, T)$ is written as

$$S(z, T) = \frac{1}{T} \frac{\chi_Q^0(T)}{\chi_0} \frac{z + M(z, T)}{z + M_Q(z, T)}. \quad (4.2.25)$$

Thus, the real part of the Seebeck coefficient becomes

$$\text{Re}[S(\omega, T)] = \frac{1}{T} \frac{\chi_Q^0(T)}{\chi_0} \frac{\omega^2 + M''(\omega, T)M_Q''(\omega, T)}{\omega^2 + (M_Q''(\omega, T))^2}. \quad (4.2.26)$$

Substituting the imaginary part of the electrical and the thermoelectric memory functions, Eqs. (4.2.13) and (4.2.22), we can discuss the frequency variation of the Seebeck coefficient for the case of the electron-impurity interaction. This is done in Sec. 4.3 after discussing the case of electron-phonon interaction.

4.2.2 Electron-Phonon Interaction

In the presence of electron-phonon interaction in a system, the total Hamiltonian is described by $H = H_0 + H_{\text{ep}} + H_{\text{ph}}$. With this Hamiltonian (the details of which are given in Sec. 2.1 of Chapter 2) and using the commutation relations defined in Eq. (2.2.12) and (3.2.17), the inner product $\langle\langle [J_Q, H]; [J, H] \rangle\rangle_z$ can be written as

$$\begin{aligned} &= \frac{2}{m^2} \sum_{\mathbf{k}\mathbf{k}'} \left[\{\mathbf{k} - \mathbf{k}'\} \cdot \hat{n} \{ \mathbf{k}(\epsilon_{\mathbf{k}} - \mu) - \mathbf{k}'(\epsilon_{\mathbf{k}'} - \mu) \} \cdot \hat{n} \right] \\ &\quad \times |D(\mathbf{k} - \mathbf{k}')|^2 f_{\mathbf{k}'}(1 - f_{\mathbf{k}}) n_{\mathbf{k}-\mathbf{k}'} \left(e^{\beta(\epsilon_{\mathbf{k}'} - \epsilon_{\mathbf{k}} + \omega_{\mathbf{k}-\mathbf{k}'})} - 1 \right) \\ &\quad \times \left\{ \frac{1}{z - \epsilon_{\mathbf{k}'} + \epsilon_{\mathbf{k}} - \omega_{\mathbf{k}-\mathbf{k}'}} - \frac{1}{z + \epsilon_{\mathbf{k}'} - \epsilon_{\mathbf{k}} + \omega_{\mathbf{k}-\mathbf{k}'}} \right\}. \end{aligned} \quad (4.2.27)$$

Here $n_{\mathbf{k}-\mathbf{k}'}$ is a Boson distribution function.

Putting Eq. (4.2.27) in the thermoelectric memory function Eq. (4.2.5), the imaginary

part of the thermoelectric memory function after performing analytic continuation $z \rightarrow \omega + i\zeta$, $\zeta \rightarrow 0^+$ can be expressed as

$$M_Q''(\omega, T) = \frac{2\pi}{\chi_Q^0(T)m^2} \sum_{\mathbf{k}\mathbf{k}'} \left[\{\mathbf{k} - \mathbf{k}'\} \cdot \hat{n} \{ \mathbf{k}(\epsilon_{\mathbf{k}} - \mu) - \mathbf{k}'(\epsilon_{\mathbf{k}'} - \mu) \} \cdot \hat{n} \right] |D(\mathbf{k} - \mathbf{k}')|^2 \\ \times (1 - f_{\mathbf{k}}) f_{\mathbf{k}'} n_{\mathbf{k}-\mathbf{k}'} \left\{ \frac{e^{\omega/T} - 1}{\omega} \delta(\epsilon_{\mathbf{k}} - \epsilon_{\mathbf{k}'} - \omega_{\mathbf{k}-\mathbf{k}'} + \omega) \right. \\ \left. + (\text{terms with } \omega \rightarrow -\omega) \right\}. \quad (4.2.28)$$

To simplify the above expression, we use the law of conservation of energy $\epsilon_{\mathbf{k}} = \epsilon_{\mathbf{k}'} - \omega_q$ and the law of conservation of momentum $\mathbf{k}' - \mathbf{k} = \mathbf{q}$. Thus, the factor within the square brackets of above equation becomes

$$\{\mathbf{k} - \mathbf{k}'\} \cdot \hat{n} \{ \mathbf{k}(\epsilon_{\mathbf{k}} - \mu) - \mathbf{k}'(\epsilon_{\mathbf{k}'} - \mu) \} \cdot \hat{n} = \mathbf{q} \cdot \hat{n} \{ \mathbf{q} \cdot \hat{n}(\epsilon_{\mathbf{k}} - \mu) + \mathbf{k}' \cdot \hat{n} \omega_{\mathbf{q}} \}. \quad (4.2.29)$$

For simplifications, we consider that the system has cubic symmetry, thus the averaging over all the directions reduces the above expression as $1/3 (q^2(\epsilon_{\mathbf{k}} - \mu) - k'^2 \omega_{\mathbf{q}})$. Using this relation and converting the summations into integrals along with introducing the new dimensionless variables $\frac{\epsilon_{\mathbf{k}} - \mu}{T} = \eta$, $\frac{\omega}{T} = x$ and $\frac{\omega_q}{T} = y$, the imaginary part of the thermoelectric memory function Eq. (4.2.28) becomes

$$M_Q''(\omega, T) = \frac{N^2 T^3}{12\pi^3 \chi_Q^0(T)} \left(\frac{q_D}{\Theta_D} \right)^2 \int_0^\infty d\eta \int_0^{\Theta_D/T} dy |D(y)|^2 \frac{y}{e^y - 1} \frac{1}{e^{-\eta} + 1} \\ \left\{ \eta \left(\frac{q_D T}{\Theta_D} \right)^2 y^2 - k_F^2 y \right\} \left[\frac{e^x - 1}{x(e^{\eta-y+x} + 1)} + (\text{terms with } \omega \rightarrow -\omega) \right]. \quad (4.2.30)$$

Substituting the phonon matrix element Eq. (2.1.4) and solving the integral over η , we obtain

$$M_Q''(\omega, T) = \frac{NT^4}{48\pi^3 m_i \rho_F^2 \chi_Q^0(T)} \left(\frac{q_D}{\Theta_D} \right)^4 \int_0^{\Theta_D/T} dy \frac{y^2}{e^y - 1} \left\{ \frac{x - y}{e^{x-y} - 1} \frac{e^x - 1}{x} \right. \\ \left. \left((x - y) \left(\frac{q_D T}{\Theta_D} \right)^2 y^2 - 2k_F^2 y \right) + (\text{terms with } \omega \rightarrow -\omega) \right\}. \quad (4.2.31)$$

This is the final expression of the imaginary part of the thermoelectric memory function in the case of the electron-phonon interaction. The analytic closed form of the above

equation can be obtained by solving the integral whose solution is given in Eq. (G.0.6). Here we discuss it in different limits of frequency and temperature as follows.

Case-I The zero frequency limit:

In this limit i.e. $\omega \rightarrow 0$, the magnitude of the imaginary part of the thermoelectric memory function Eq. (4.2.31) reduces as

$$M_Q''(T) = \frac{NT^4}{24\pi^3 m_i \rho_F^2 \chi_Q^0(T)} \left(\frac{q_D}{\Theta_D} \right)^4 \int_0^{\Theta_D/T} dy \frac{y^4 e^y}{(e^y - 1)^2} \left\{ \left(\frac{q_D T}{\Theta_D} \right)^2 y^2 + 2k_F^2 \right\}. \quad (4.2.32)$$

Further, for high and low temperature regimes, this expression can be discussed as follows:

In the high temperature regime i.e. $T \gg \Theta_D$, the first term within a bracket of Eq. (4.2.32), i.e. $(q_D T / \Theta_D)^2 y^2$, gives more contribution to $M_Q''(T)$. Thus, the latter becomes

$$\begin{aligned} M_Q''(T) &\approx \frac{NT^6}{24\pi^3 m_i \rho_F^2 \chi_Q^0(T)} \left(\frac{q_D}{\Theta_D} \right)^6 \int_0^{\Theta_D/T} dy \frac{y^6 e^y}{(e^y - 1)^2}. \\ &\approx \frac{N}{24\pi^3 m_i \rho_F^2} \frac{q_D^6}{\Theta_D} \frac{T}{\chi_Q^0(T)}. \end{aligned} \quad (4.2.33)$$

In the opposite case when $T \ll \Theta_D$, Eq. (4.2.32) becomes

$$M_Q''(T) \approx \frac{2Nk_F^2}{\pi^3 m_i \rho_F^2} \left(\frac{q_D}{\Theta_D} \right)^4 \frac{T^4}{\chi_Q^0(T)}. \quad (4.2.34)$$

Thus, from these above expressions we find that the imaginary part of the thermoelectric memory function in the zero frequency limit is proportional to $T/\chi_Q^0(T)$ in the high and $T^4/\chi_Q^0(T)$ in the low temperature regimes. The static thermoelectric correlation function $\chi_Q^0(T)$ varies linearly with the temperature (as given in Appendix B.2). Thus, $M_Q''(T)$ varies as T^3 in the low temperature regime and becomes constant in the high temperature regime. Substituting this in Eq. (4.2.1), we find that the thermoelectric response function in the zero frequency limit shows temperature dependence as

$$\alpha(T) = \frac{1}{T} \frac{\chi_Q^0(T)}{M_Q''(T)}. \quad (4.2.35)$$

Hence, it varies as T^{-3} in the low temperature regime and becomes temperature independent in the high temperature regime i.e.

$$\alpha(T) \propto \begin{cases} T^{-3}, & T \ll \Theta_D \\ \text{constant}, & T \gg \Theta_D \end{cases} \quad (4.2.36)$$

Case-II The finite frequency regime:

In finite frequency regimes, we study the general expression Eq. (4.2.31) in the two limiting cases and then analyze this expression numerically.

In the high frequency limit i.e. when the frequency is more than the Debye frequency ($\omega \gg \omega_D$), the imaginary part of the thermoelectric memory function Eq. (4.2.31) can be written as

$$\begin{aligned} M_Q''(\omega, T) &\approx \frac{Nk_F^2}{12\pi^3 m_i \rho_F^2} \left(\frac{q_D}{\Theta_D} \right)^4 \frac{T^4}{\chi_Q^0(T)} \int_0^{\Theta_D/T} dy \frac{y^3}{e^y - 1}. \\ &\approx \frac{Nk_F^2}{12\pi^3 m_i \rho_F^2} \left(\frac{q_D}{\Theta_D} \right)^4 \frac{T^4}{\chi_Q^0(T)} \begin{cases} \frac{\pi^4}{15}, & T \ll \Theta_D \\ \frac{1}{3} \left(\frac{\Theta_D}{T} \right)^3, & T \gg \Theta_D. \end{cases} \end{aligned} \quad (4.2.37)$$

On substituting the temperature variation of $\chi_Q^0(T)$ (as shown in Appendix B.2), the thermoelectric memory function shows temperature dependencies as

$$M_Q''(\omega, T) \propto \begin{cases} T^3, & T \ll \Theta_D \\ \text{constant}, & T \gg \Theta_D. \end{cases} \quad (4.2.38)$$

This implies that the imaginary part of the thermoelectric memory function in case of the electron-phonon interaction shows frequency independent and temperature dependent behavior at high frequency regime. It shows T^3 behavior in the low temperature regime and temperature independent behavior in the high temperature regime.

Similarly in the low frequency regime i.e. $\omega \ll \omega_D$, $M_Q''(\omega, T)$ Eq. (4.2.31) in the leading order is given by

$$\begin{aligned} M_Q''(\omega, T) &\approx \frac{N}{24\pi^3 m_i \rho_F^2} \left(\frac{q_D}{\Theta_D} \right)^4 \frac{T^5}{\chi_Q^0(T)} \frac{\sinh(\omega/T)}{\omega} \\ &\quad \times \int_0^{\Theta_D/T} dy \frac{y^4 e^y}{(e^y - 1)^2} \left\{ \left(\frac{q_D T}{\Theta_D} \right)^2 y^2 + 2k_F^2 \right\}. \end{aligned} \quad (4.2.39)$$

Now in the limit $\omega \gg T$,

$$M_Q''(\omega, T) \approx \frac{N\pi k_F^2}{45m_i \rho_F^2} \left(\frac{q_D}{\Theta_D} \right)^4 \frac{e^{\omega/T}}{\omega} \frac{T^5}{\chi_Q^0(T)}. \quad (4.2.40)$$

In the opposite case, i.e. $\omega \ll T$,

$$M_Q''(\omega, T) \approx \frac{N}{24\pi^3 m_i \rho_F^2} \left(\frac{q_D}{\Theta_D} \right)^4 \frac{T^4}{\chi_Q^0(T)} \begin{cases} \frac{8\pi^4}{15} k_F^2, & \text{at } T \ll \Theta_D \\ \frac{1}{5} q_D^2 \left(\frac{\Theta_D}{T} \right)^3, & \text{at } T \gg \Theta_D \end{cases}. \quad (4.2.41)$$

This concludes that the finite frequency imaginary part of the thermoelectric memory function shows frequency dependence of the form $e^{\omega/T}/\omega$ in the regime where the frequency is in between the value of temperature T and Debye temperature Θ_D and becomes frequency independent in the other cases. There is also different temperature dependencies within the different regimes depending on whether the temperature is greater or lesser than the Debye temperature. The details of these asymptotic results are discussed in latter section Sec. 4.3 and are collected in Table 4.2.

Table 4.2: The thermoelectric and electrical scattering rates or memory functions due to the electron-phonon interaction in different frequency and temperature domains.

Regimes	Thermoelectric memory function	Electrical memory function
	$1/\tau_{te}$ or $M_Q''(\omega, T)$	$1/\tau_e$ or $M''(\omega, T)$
$\omega = 0, T \gg \Theta_D$	T^0	T^1
$\omega = 0, T \ll \Theta_D$	T^3	T^5
$\omega \gg T \gg \Theta_D$	T^0	T^1
$\omega \gg \Theta_D \gg T$	T^3	T^5
$T \gg \omega \gg \Theta_D$	T^0	T^1
$T \ll \omega \ll \Theta_D$	$T^4 \omega^{-1} e^{\omega/T}$	$T^6 \omega^{-1} e^{\omega/T}$
$\omega \ll \Theta_D \ll T$	T^3	T^5
$\omega \ll T \ll \Theta_D$	T^0	T^1

Seebeck Coefficient

For the case of electron-phonon interaction, the Seebeck coefficient can be calculated in a similar way as done for the case of electron-impurity interaction.

In this case, the electrical memory function in the finite frequency case and in the zero frequency limit can be written as [27, 56, 62]

$$M''(\omega, T) = \frac{N}{24\pi^3 m_i \rho_F^2} \left(\frac{q_D}{\Theta_D} \right)^6 \frac{T^5}{\chi_0} \int_0^{\Theta_D/T} dy \frac{y^4}{(e^y - 1)} \left\{ \frac{x - y}{e^{x-y} - 1} \frac{e^x - 1}{x} + (\text{terms with } \omega \rightarrow -\omega) \right\}, \quad (4.2.42)$$

and

$$M''(T) = \frac{N}{12\pi^3 m_i \rho_F^2} \left(\frac{q_D}{\Theta_D} \right)^6 \frac{T^5}{\chi_0} \begin{cases} 124.4, & T \ll \Theta_D \\ \frac{1}{4} \left(\frac{\Theta_D}{T} \right)^4, & T \gg \Theta_D, \end{cases} \quad (4.2.43)$$

respectively. The details of this expressions are given in Chapter 2. Substituting this zero frequency electrical memory function Eq. (4.2.43) in Eq. (4.2.21), we find that the electrical conductivity in this limit proportional to

$$\sigma(T) \propto \begin{cases} T^{-5}, & T \ll \Theta_D \\ T^{-1}, & T \gg \Theta_D. \end{cases} \quad (4.2.44)$$

On the other hand, we have also discussed that the thermoelectric conductivity $\alpha(T)$ shows T^{-3} and a temperature independent behavior in the low and the high temperature regimes respectively. Substituting these variations into Eq. (4.1.4), the Seebeck coefficient in the electron-phonon interaction case shows temperature dependence as follows

$$S(T) \propto \begin{cases} T^2, & \text{at } T \ll \Theta_D \\ T, & \text{at } T \gg \Theta_D. \end{cases} \quad (4.2.45)$$

Similarly for the finite frequency case, substituting Eqs. (4.2.31) and (4.2.42) in (4.2.26), the frequency variation of the Seebeck coefficient for the case of the electron-phonon interaction can be analyzed and discussed which is presented in the next section.

4.3 Results and Discussion

In this section, we have presented the results for the imaginary part of the thermoelectric memory function and the corresponding thermoelectric coefficient in different temperature and frequency regimes.

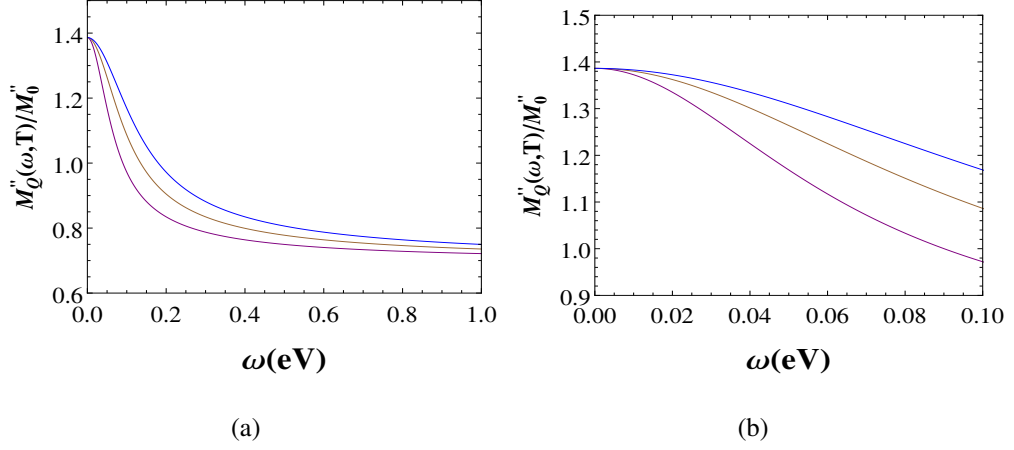


Figure 4.1: (a): Plot of the imaginary part of the thermoelectric memory function for impurity case at different temperatures such as 200K (purple), 300K (brown) and 400K (blue). (b): The low frequency regime of $M_Q''(\omega, T)/M_0''$ of Fig. 4.1(a) is elaborated.

In Fig. 4.1, we plot the imaginary part of the normalized thermoelectric memory function Eq. (4.2.13) $M_Q''(\omega, T)/M_0''$, where $M_0'' = 2k_F^4 m N_{\text{imp}} U^2 / 3\pi^4 N_e$, due to the electron-impurity interaction as a function of ω and at different temperatures. Here we observe that the thermoelectric memory function at low frequency i.e. $\omega \ll T$ shows frequency and temperature independent behavior (as shown in Fig. 4.1(a)). In the intermediate regime, it decays with the increase of the frequency (as shown in Fig. 4.1(b)). Also it increases with the increase of the temperature. Finally, at high frequency i.e. $\omega \gg T$, it saturates to constant value (Fig. 4.1(a)).

In Fig. 4.2, the real part of the normalized Seebeck coefficient $\text{Re}[S(\omega, T)]/S_0$ for the case of electron-impurity interaction is shown as a function of ω/ω_0 , ($\omega_0 = 2k_F^4 m N_{\text{imp}} U^2 / 3\pi^4 N_e$) and at different temperatures. Here, we observe that first it starts to decrease with the rise of the frequency and shows a dip at a certain frequency (as shown in Fig. 4.2(a)). Then, in the high frequency regime, it saturates to the constant value. Also, with the rise of temperature, $\text{Re}[S(\omega, T)]/S_0$ increases in the low frequency regime and becomes independent of the temperature in the high frequency regime. This behavior can be understood from Eq. (4.2.26) as follows:

In the high frequency regime, Eq. (4.2.26) can be written as

$$\begin{aligned} \text{Re}[S(\omega, T)] &\approx \frac{1}{T} \frac{\chi_Q^0(T)}{\chi_0} \\ &\approx \text{constant}. \end{aligned} \quad (4.3.1)$$

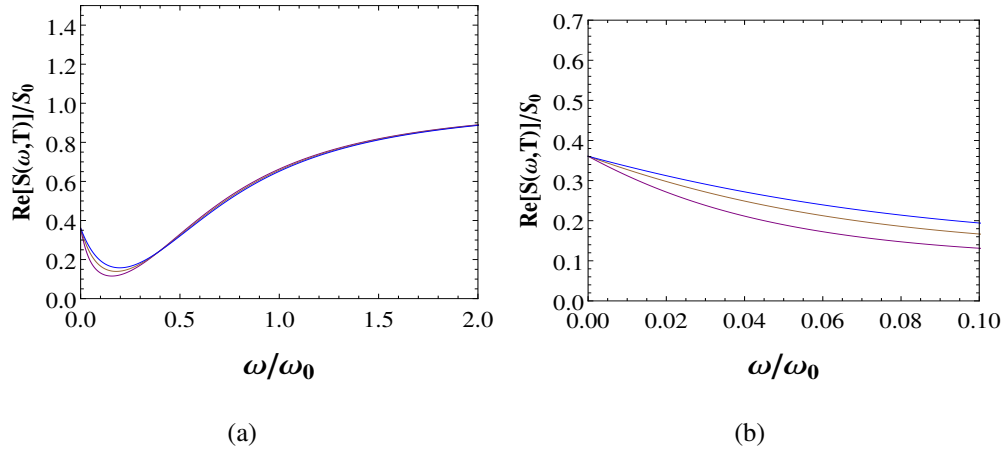


Figure 4.2: (a): Plot of the real part of the normalized Seebeck coefficient for impurity case at different temperatures such as 200K (purple), 300K (brown) and 400K (blue). (b): The low frequency regime of $\text{Re}[S(\omega, T)]/S_0$ of Fig. 4.2(a) is elaborated.

This feature is depicted in Fig. 4.2(a).

Now, in the low frequency regime i.e. $\omega \rightarrow 0$, Eq. (4.2.26) is approximated as

$$\lim_{\omega \rightarrow 0} \text{Re}[S(\omega, T)] \approx \lim_{\omega \rightarrow 0} \frac{1}{T} \frac{\chi_Q^0(T)}{\chi_0} \frac{M''(\omega, T)}{M_Q''(\omega, T)}. \quad (4.3.2)$$

Thus in the zero frequency limit, $\text{Re}[S(\omega, T)]$ shows a constant value as given by above expression.

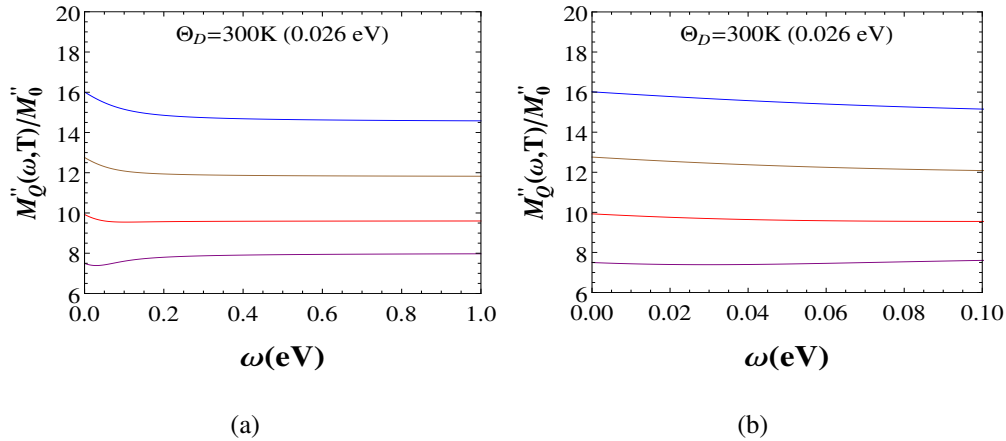


Figure 4.3: (a): Plot of imaginary thermoelectric memory function for phonon case at different temperatures such as 200K (purple), 250K (red), 300K (brown), 350K (blue). (b): The low frequency regime of Fig. 4.3(a).

In Fig. 4.3, we plot the frequency and the temperature dependent normalized imagi-

nary part of the thermoelectric memory function $M_Q''(\omega, T)/M_0''$ for case of the electron-phonon interaction, where $M_0'' = Nm q_D^6 / 6\pi^5 m_i N_e \rho_F^2 \Theta_D$. Here, we keep the Debye temperature Θ_D fixed at 300K i.e. 0.026eV and look at the frequency dependence at different temperatures. We observe that the thermoelectric memory function shows frequency variation below 0.2eV. While in other region $\omega \gg 0.2\text{eV}$, it shows frequency independent behavior (Fig. 4.3(a) and 4.3(b)). Along with the frequency character, we also observe the temperature behavior. In throughout the frequency region, it increases with the increase of the temperature (Fig. 4.3(a) and 4.3(b)).

Now, in Fig. 4.4 we plot the imaginary part of the thermoelectric memory function in the zero frequency limit as a function of temperature. Here, we consider different values of the Debye temperature such as 200, 300 and 400K. It is found that $M_Q''(T)/M_0''$ first increases with the increase of temperature and then saturates to a constant value at a temperature above the Debye temperature.

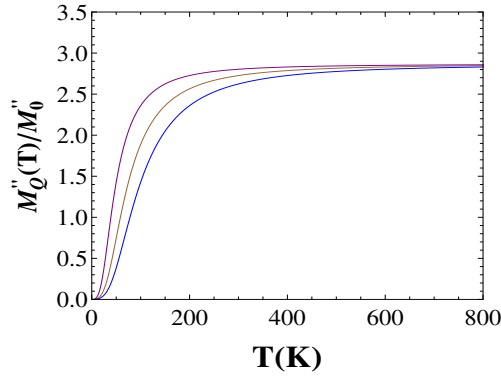


Figure 4.4: Plot of imaginary part of the dc thermoelectric memory function for phonon case at different Debye temperatures such as 200(purple), 300(brown) and 400K(blue).

In Fig. 4.5, we plot the real part of the frequency and temperature dependent normalized Seebeck coefficient $\text{Re}[S(\omega, T)]/S_0$ with ω/ω_0 (using Eq. (4.2.26)) at different temperatures. Here $\omega_0 (= Nm q_D^6 / 6\pi^5 m_i N_e \rho_F^2 \Theta_D)$ in the energy units is a normalizing parameter. We have kept the Debye temperature fixed at 300K. In Fig. 4.5(a), we observe that $\text{Re}[S(\omega, T)]/S_0$ is independent of frequency and temperature in the high frequency regime (i.e. $\omega \gg \omega_D$ as shown in the regime right to the dashed line within the plot). In contrast, there is strong frequency and temperature dependence in the low frequency regime. To elaborate the low frequency regime, we replot the real part of the Seebeck coefficient in Fig. 4.5(b). Here we find that the later increases

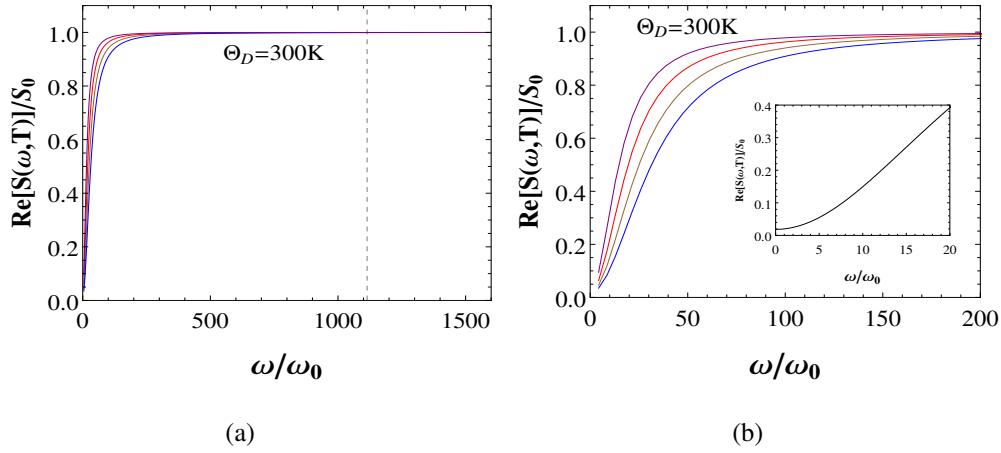


Figure 4.5: (a): Plot of finite frequency real part of the normalized Seebeck coefficient at different temperatures such as 200(purple), 250(red), 300(brown), 350(blue) and 375K(magenta) at fixed Debye temperature 300K. Here the dotted line corresponds to the Debye cutoff i.e. ω_D/ω_0 , where ω_0 is the constant scale parameter having dimensions of energy. (b): The low ω/ω_0 regime of Fig. 4.5(a) is elaborated. Here ω_0 is a normalizing parameter.

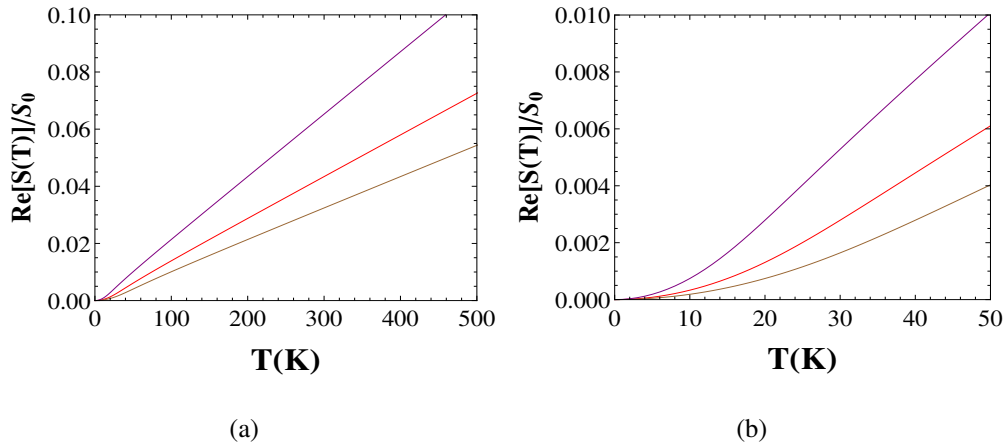


Figure 4.6: (a): Plot of the real part of the normalized Seebeck coefficient in zero frequency limit at different Debye temperatures such as 200 (purple), 300 (red) and 400K (brown). (b): The low temperature regime of $\text{Re}[S(\omega, T)]/S_0$ of Fig. 4.6(a) is elaborated.

with the increase in frequency. While with the rise in temperature, the magnitude of $\text{Re}[S(\omega, T)]/S_0$ reduces. The saturation at high frequencies can be understood from the formula Eq. (4.2.26) as explained above. Also the suppression of the normalized Seebeck coefficient with the increase in temperature can be understood by recognizing the enhanced scattering of quasiparticles at higher temperature. At very low frequency,

we show the same plot at temperature 300K within the inset of Fig. 4.5(b). We can see from the inset that near the zero frequency, $\text{Re}[S(\omega, T)]/S_0$ approaches to the constant value.

For the zero frequency case, $\text{Re}[S(T)]/S_0$ (using Eq. (4.2.26)) is plotted as a function of temperature at different Debye temperatures such as 200, 300 and 400K in Fig. (4.6). It is observed that $\text{Re}[S(T)]/S_0$ increases linearly with the rise of temperature. Also, its linear behavior is more pronounced at the temperature more than the Debye temperature. This linear behavior feature is in accord with the result calculated by Boltzmann approach (Mott formula) and with the experimental findings [3, 14]. However, at very low temperature ($T \ll \Theta_D$), it is quadratic in temperature (refer Eq. (4.2.45)). Experimentally, this regime is dominated by the phonon drag effects and these are not considered in the present formalism [3].

4.4 Conclusion

Making highly efficient thermoelectric devices, one needs materials with large figure of merit ($ZT = S^2\sigma T/\kappa$). As discussed earlier, one possible route to increase ZT is to look beyond the static limit and look for the frequency dependent case. In this connection the understanding of the frequency dependence of the Seebeck coefficient $S(\omega, T)$ is extremely important and is attempted here.

In a nutshell, the concluding remarks of this chapter are as follows:

1. In the case of electron-impurity interactions, the Seebeck coefficient in the zero frequency limit shows temperature independent behavior.
2. In the case of electron-phonon interactions, $S(T)$ shows
 - a Linear temperature dependent behavior in high temperature regime ($T \gg \Theta_D$)
 - b Quadratic temperature dependent behavior in low temperature regime ($T \ll \Theta_D$).

3. In the finite frequency regimes, $S(\omega, T)$ in the case of electron-impurity interactions decays with the increase in frequency in the low frequency regime and then after passing through a minimum, it becomes constant in the high frequency regime.
4. In the case of the electron-phonon interactions, it rises with the frequency in the regime where $\omega \ll \omega_D$ and in the opposite case i.e. $\omega \gg \omega_D$, it saturates.
5. These new predictions insure that the phonon interaction plays an important role in the dynamical behavior of the Seebeck coefficient and hence can help in improving the figure of merit.
6. In addition to these, we have also reported that the thermoelectric memory function in the zero frequency limit for the case of
 - a electron-impurity interaction shows temperature independent behavior.
 - b electron-phonon interaction shows T^3 behavior in the low temperature regime, and temperature independent in the high temperature regime.
7. In the finite frequency case, it shows frequency variation depending on the relative strengths of the temperature T , frequency ω , and Debye frequency ω_D (refer Table 4.1 and 4.2).

Chapter 5

Dynamical Thermal Conductivity of Graphene

In the previous chapters, we have calculated the transport properties of three dimensional metals both in zero frequency and finite frequency regimes using the memory function technique and produced several new results. This chapter deals with an investigation which is performed on a very important two dimensional system, namely Graphene using the techniques developed and applied to three dimensional systems i.e., metals in the previous chapters. Before we proceed for calculation, we first briefly introduce the system i.e., graphene.

Graphene is a two dimensional (2D) material [98,99] and is made of carbon atoms arranged in a honeycomb structure. Being 2D in nature and having linear electron dispersion relation, it creates a lot of attention both in the fundamental and applied research due to its unique electrical, magnetic, thermal, optical and mechanical properties. These properties include anomalous high electrical conductivity, high thermal conductivity, effect of impurities on the electric properties, etc. [100–113] which make the use of this material quite promising for the fabrication or design of the electronic devices. These unique properties are due to its one of the interesting aspect i.e. linear electron energy dispersion which differs from normal metals having quadratic energy dispersion. This energy dispersion of graphene is expressed as

$$E_{\pm} = \pm v_F |\mathbf{k}|. \quad (5.0.1)$$

Here we set $\hbar = 1$ and v_F represents the Fermi velocity. Also the sign \pm corresponds to

the conduction (+) and valence (−) bands. These dispersions lead to form a structure known as Dirac cones and the points, where the Dirac cones of electrons and holes touch each other and give rise to a valley degeneracy $g_v = 2$ [114]. In our calculations, we have simply taken into account this degeneracy factor and do not discuss the intervalley scattering mechanisms in the transport of graphene. Specifically, we present here the thermal conductivity of graphene due to electron-phonon scattering mechanism.

In the literature, it is argued that the thermal conductivity of graphene is high [115, 116] and is mainly contributed by the phonons and the electronic contribution is small [117, 118]. However, electrons and phonons provide different temperature dependence to the electronic and phononic thermal conductivities in low and high temperature limits. In the high temperature limit, due to large number of phonons the electronic thermal conductivity show temperature independent behavior [3, 5, 62] due to the scattering by electron-phonon interactions. On the other hand, the phononic thermal conductivity shows T^{-1} temperature behavior due to the dominating scattering mechanism by phonon-phonon interactions. In the opposite limit i.e. the low temperature limit, the electronic and the phononic thermal conductivities are due to the interactions of electrons and phonons with impurities, boundaries, defects, etc. In the literature, the thermal conductivity of graphene due to phonons has been extensively studied [115–118]. However, the electronic thermal conductivity of graphene is less studied topic [119]. In the present chapter, we describe our study of the electronic thermal conductivity. For the accurate determination of the total thermal conductivity, it is important to have detailed theoretical models for both type of conductivities. In the present context, we use the memory function approach by which both the zero and the finite frequency behavior of the thermal conductivity can be calculated or explained with much ease.

In case of metals, it has been find that in the low temperature regime i.e. $T \ll \Theta_D$ (Θ_D being the Debye temperature) only the acoustic phonons within the phonon sphere of radius k_{ph} with $k_{\text{ph}} \ll k_D$ (where k_D is the radius of Debye sphere) play a role in the electronic thermal conductivity [3, 5, 62]. In these three dimensional systems, it leads to T^{-2} behavior of the electronic thermal conductivity in $T \ll \Theta_D$ regime. In such

systems, the radius of the Fermi sphere is larger than the radius of the Debye sphere i.e. $2k_F \gg k_D$. Thus all phonons can scatter off the electrons. But in the systems where $k_F \ll k_D$ (in graphene and other low density systems), only small number of phonons can scatter off the electrons. These phonons are restricted within the energy range $v_s k_{\text{ph}} \leq 2v_s k_F$. This can be explained by introducing the new temperature scale known as Bloch Grüneisen (BG) temperature which is smaller than the Debye temperature [120]. This scale defines two regimes i.e. low temperature ($T \ll \Theta_{\text{BG}}$) and high temperature ($T \gg \Theta_{\text{BG}}$) regimes for the electron-phonon interaction in graphene. In the low temperature regime ($T \ll \Theta_{\text{BG}}$), the acoustic phonons with linear dispersion relation yield inverse temperature behavior to the electronic thermal conductivity i.e. T^{-1} and then change to the temperature independent behavior in the high temperature regime ($T \gg \Theta_{\text{BG}}$) [119, 121]. However, because of the two dimensional nature of the graphene, there are also other acoustic phonons known as flexural phonons or out of plane phonons which obey quadratic dispersion relation and hence give different power law behavior to the electronic thermal conductivity. Thus the role of the different acoustic phonons is very important to understand the transport or the electronic thermal conductivity of graphene.

In this chapter, we first set the theoretical framework of the problem in Sec. 5.1. Here we discuss the phonon dispersion relations and give the description of the electronic thermal conductivity of graphene for different acoustic phonons. In Sec. 5.2, we present the results in zero and finite frequency regimes. Finally, in Sec. 5.3 we conclude the chapter.

5.1 Theoretical Framework

We consider a two dimensional graphene with only electron-phonon interaction and intraband transitions within this system. The Hamiltonian of such a system is described as $H = H_0 + H_{\text{ep}} + H_{\text{ph}}$. Here the unperturbed parts H_0 and H_{ph} are defined by Eqs. (2.1.2) and (2.1.5) respectively. And the perturbed part of Hamiltonian H_{ep} is defined by the Eq. (2.1.3) as for the case of normal metals. While the difference in the present case comes from the form of the electron-phonon matrix element (which

is specified in Chapter 2 Sec. 2.1 Eq. (2.1.4) for the case of metals). In the case of graphene, the latter is represented as [114,122]

$$D(\mathbf{q}) = \frac{D_0 q}{\sqrt{2\rho_m \omega_q}} \left\{ 1 - \left(\frac{q}{2k_F} \right)^2 \right\}^{1/2}. \quad (5.1.1)$$

Here D_0 is the deformation potential coupling constant, ρ_m is the graphene mass density, k_F is the Fermi wave vector and ω_q is the phonon energy dispersion. Contrary to the case of metal, here the extra q dependence comes from the factor $\left\{ 1 - \left(\frac{q}{2k_F} \right)^2 \right\}^{1/2}$. The consequence of this factor is the suppression of the backscattering in graphene [121, 123]. Further, this is valid for the case of intraband transitions that we have considered in our study.

5.1.1 Phonon Dispersion relations

Before proceeding to calculate the thermal scattering rate and the corresponding thermal conductivity of graphene, for the sake of completeness, we will first discuss the phonon dispersion relations in this subsection.

The thermal transport due to the electron-phonon interaction significantly depends on the characteristics of the phonon which are further determined by the two dimensional structure of the graphene. In graphene, there are two carbon atoms per hexagonal unit cell which gives six phonon branches in the dispersion spectrum. These are three acoustic and three optical branches namely LA(Longitudinal Acoustic), TA(Transverse Acoustic), LO(Longitudinal Optical), TO(Transverse Optical), ZA(Flexural Acoustic) and ZO(Flexural Optical). The TA and TO phonons are due to the transverse vibrations within the graphene plane and LA, LO are due to the longitudinal vibrations within the graphene plane. The other modes such as ZA, ZO are due to the oscillations of phonons in the direction normal to the longitudinal and transverse phononic modes. These phononic modes are also referred to the out of plane modes [124]. Among these, the optical phonons usually have higher energies than the acoustic phonons. And in the present work our main focus is on the low temperature behavior (i.e. below the Debye temperature) of the electronic thermal conductivity. Thus, for the time being we ignore the contribution of optical phonons and consider only acoustic phonons henceforth. The schematic representation of these phonons is shown in Fig. 5.1.

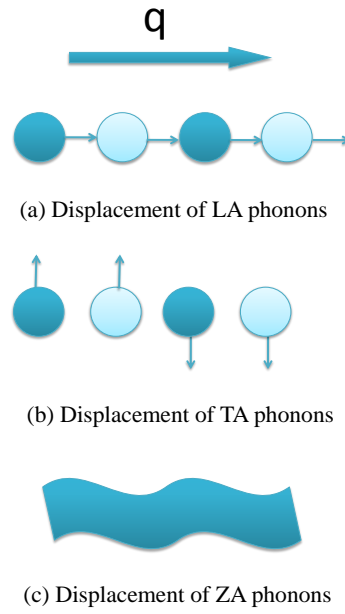


Figure 5.1: Schematic representation of the displacement of acoustic in plane and out of plane phonon modes.

From the phonon dispersion spectra, it has been found that these modes follow different dispersion relations. The LA and TA modes follow the linear dispersion relations [124, 125] i.e.,

$$\begin{aligned}\omega_{\text{LA}} &\approx v_{\text{LA}}q \\ \omega_{\text{TA}} &\approx v_{\text{TA}}q,\end{aligned}\tag{5.1.2}$$

where v_{LA} and v_{TA} are the longitudinal and transverse phonon velocities and $v_{\text{LA}} = 21.3 \times 10^3 \text{ms}^{-1}$, $v_{\text{TA}} = 14.1 \times 10^3 \text{ms}^{-1}$. [125]

The other acoustic phonon ZA approximately follows the quadratic dispersion relation as [124, 126]

$$\omega_{\text{ZA}} \approx \alpha q^2.\tag{5.1.3}$$

Here the parameter $\alpha = \left(\frac{s}{\rho_m}\right)^{1/2}$, where s is the bending stiffness of the graphene, ρ_m is the graphene mass density and $\alpha = 4 \times 10^{-7} \text{m}^2 \text{s}^{-1}$. [127]

5.1.2 Mathematical Calculations

As discussed in Chapter 3, the thermal conductivity Eq. (3.1.3) can be calculated using the memory function formalism by calculating the thermal memory function or thermal scattering rate Eq. (3.1.4). Thus with the definitions of the thermal current Eq. (3.1.2) and the model Hamiltonian (described in Chapter 2 Sec. 2.1), the imaginary part of the thermal memory function can be expressed as*

$$\begin{aligned}
 M''_{QQ}(\omega, T) &= \frac{4\pi}{\chi_{QQ}^0(T)m^2} \sum_{\mathbf{k}\mathbf{k}'} [\{\mathbf{k}(\epsilon_{\mathbf{k}} - \mu) - \mathbf{k}'(\epsilon_{\mathbf{k}'} - \mu)\} \cdot \hat{n}]^2 |D(\mathbf{k} - \mathbf{k}')|^2 \\
 &\quad \times (1 - f_{\mathbf{k}}) f_{\mathbf{k}'} n_{\mathbf{q}-\mathbf{k}'} \left\{ \frac{e^{\omega/T} - 1}{\omega} \delta(\epsilon_{\mathbf{k}} - \epsilon_{\mathbf{k}'} - \omega_{\mathbf{q}-\mathbf{k}'} + \omega) \right. \\
 &\quad \left. + (\text{terms with } \omega \rightarrow -\omega) \right\}. \tag{5.1.4}
 \end{aligned}$$

Here $f_{\mathbf{k}} = \frac{1}{e^{\beta(\epsilon_{\mathbf{k}} - \mu)} + 1}$ and $n_{\mathbf{q}} = \frac{1}{e^{\beta\omega_{\mathbf{q}}} - 1}$ are the Fermi and the Boson distribution functions, β is the inverse of the temperature and factor 4 is for the two spin and two valley degeneracies.

To simplify Eq. (5.1.4), we convert the summations over momentum indices into the two dimensional energy integrals using the linear electron energy dispersion relation $\epsilon_{\mathbf{k}} = v_F k$ and $\epsilon_{\mathbf{k}'} = v_F k'$, where v_F is the Fermi velocity. *This linear dispersion relation distinguishes the characteristics of the graphene from those of the three dimensional normal metals which follows the quadratic dispersion relation.* Further these simplifications along with integrations over the angular parts yield

$$\begin{aligned}
 M''_{QQ}(\omega, T) &= \frac{\epsilon_F^2 D_0^2}{4\pi^2 m^2 \rho_m v_F^4 k_F \chi_{QQ}^0(T)} \int d\epsilon_{\mathbf{k}} \int_0^\lambda dq \frac{q^2}{\omega_q} \sqrt{1 - \left(\frac{q}{2k_F}\right)^2} \\
 &\quad \left\{ \omega_q^2 k_F^2 + (\epsilon_{\mathbf{k}} - \mu)^2 q^2 + \frac{\omega_q(\epsilon_{\mathbf{k}} - \mu)}{2} q^2 \right\} (1 - f(\epsilon_{\mathbf{k}})) n_{\mathbf{q}} \\
 &\quad \left\{ \frac{e^{\omega/T} - 1}{\omega} f(\epsilon_{\mathbf{k}} - \omega_q + \omega) + (\text{terms with } \omega \rightarrow -\omega) \right\}. \tag{5.1.5}
 \end{aligned}$$

Here we use the expression for the electron-phonon matrix element given in Eq. (5.1.1) and the symbol λ corresponds to the upper cut off value of the phonon momentum. Since in normal metals, the Fermi sphere is very large as compared to the Debye

*The details of the calculation of this expression is given in Sec. 3.2.2 Chapter 3.

sphere, the phonons residing in the Debye sphere participate in scattering events and we restrict λ to q_D , q_D being the Debye momentum. While in the case of graphene, this is not the case due to the smaller Fermi surface than the Debye surface. This allows only phonons residing below the Fermi surface to participate in the scattering phenomenon, hence restrict the upper cut off value of q integral to $2k_F$ (the idea of the Bloch-Grüneisen temperature). Further the above equation Eq. (5.1.5) for graphene can be solved for various acoustic phonons as discussed in the following subsections.

Longitudinal/Transverse Acoustic Phonons (LA/TA)

To calculate $M_{QQ}(z, T)$ for the Longitudinal and the Transverse acoustic phonons (having linear dispersion relation), we define few dimensionless quantities such as $\frac{\epsilon_{\mathbf{k}} - \mu}{T} = \eta$, $\frac{\omega_q}{T} = y$ and $\frac{\omega}{T} = x$, where $\omega_q = v_s q$, $v_s \equiv (v_{LA}, v_{TA})$. Using these variables and then performing the integral over variable η , Eq. (5.1.5) becomes

$$M''_{QQ}(\omega, T) = \frac{\epsilon_F^2 D_0^2}{4\pi^2 m^2 \rho_m v_F^4 v_s^5 k_F} \frac{T^6}{\chi_{QQ}^0(T)} \int_0^{\Theta_{BG}/T} dy \frac{y^3}{e^y - 1} \left(1 - \frac{y^2 T^2}{2\Theta_{BG}^2} \right) \times \left\{ \frac{x-y}{e^{x-y} - 1} \frac{e^x - 1}{x} \left(\frac{\Theta_{BG}^2}{4T^2} + \frac{\pi^2}{3} + \frac{(x-y)^2}{3} + \frac{y(x-y)}{4} \right) + (\text{terms with } \omega \rightarrow -\omega) \right\}. \quad (5.1.6)$$

Here Θ_{BG} is the Bloch-Grüneisen temperature and is equal to $2k_F v_s$. The analytic closed form of the integral over y variable is calculated by Mathematica and is given in Eq. (G.0.7). Further, in different frequency and temperature regimes it can be solved analytically and is discussed as follows:

Case-I: The zero frequency limit i.e. $\omega \rightarrow 0$

In this limit in Eq. (5.1.6), $M''_Q(T)$ becomes

$$M''_{QQ}(T) = \frac{\epsilon_F^2 D_0^2}{2\pi^2 m^2 \rho_m A v_F^4 v_s^5 k_F} \frac{T^6}{\chi_{QQ}^0(T)} \int_0^{\Theta_{BG}/T} dy \frac{y^4 e^y}{(e^y - 1)^2} \left(1 - \frac{y^2 T^2}{2\Theta_{BG}^2} \right) \times \left\{ \frac{\Theta_{BG}^2}{4T^2} + \frac{\pi^2}{3} + \frac{y^2}{12} \right\}. \quad (5.1.7)$$

The closed analytic form of this expression is given in Eq. (G.0.8). Here, we find that $M''_{QQ}(T)$ for the case of interaction of the electrons with the longitudinal or transverse phonons leads to different temperature dependence in different regimes. In the high temperature regime ($T \gg \Theta_{BG}$), the term $\pi^2/3$ within the curly brackets of above

equation and in the low temperature regime ($T \ll \Theta_{\text{BG}}$), first and last term contribute more to the thermal memory function. Hence it obtains the temperature behavior as

$$M''_{QQ}(T) \propto \begin{cases} T, & T \gg \Theta_{\text{BG}} \\ T^2, & T \ll \Theta_{\text{BG}}. \end{cases} \quad (5.1.8)$$

Using this, the electronic thermal conductivity can be calculated as follows.

The electronic thermal conductivity Eq. (3.1.3) in the zero frequency limit can be written as [62]

$$\kappa(T) = \frac{1}{T} \frac{\chi_{QQ}^0(T)}{M''_{QQ}(T)} \approx \frac{T}{M''_{QQ}(T)}. \quad (5.1.9)$$

Here we use the temperature variation of the static correlation function $\chi_{QQ}^0(T)$ (as discussed in Appendix B.3). Thus the electronic thermal conductivity depends inversely on the thermal memory function. From Eqs. (5.1.7) and (5.1.9), we find that $\kappa(T)$ for the case of LA and TA phonons varies inversely with the temperature and saturates at the low and the high temperature regimes (as shown in Table 5.1). These are in accord with the results in the literature [119, 121].

Case-II: Finite frequency regimes

In the finite frequency regime, the thermal memory function and the corresponding thermal conductivity can be calculated in different temperature and the frequency regimes depending on the relative strengths of frequency ω , temperature T and Bloch-Grüneisen temperature Θ_{BG} . These limiting cases are calculated as follows.

1. When the frequency, ω is high as compared to T and Θ_{BG} , the thermal memory function for LA/TA phonons, Eq. (5.1.6) reduces as

$$M''_{QQ}(\omega, T) = \frac{\epsilon_F^2 D_0^2}{6\pi^2 m^2 \rho_m v_F^4 v_s^5 k_F} \frac{T^6}{\chi_{QQ}^0(T)} \frac{\omega^2}{T^2} \int_0^{\Theta_{\text{BG}}/T} dy \frac{y^3}{e^y - 1} \left(1 - \frac{y^2 T^2}{2\Theta_{\text{BG}}^2} \right). \quad (5.1.10)$$

Further, the above equation in the closed form is given in Eq. (G.0.9) which in different temperature regimes gives the thermal memory function as

$$M''_{QQ}(\omega, T) \propto \begin{cases} \omega^2 T^{-1}, & \omega \gg T \gg \Theta_{\text{BG}} \\ \omega^2 T^2, & \omega \gg \Theta_{\text{BG}} \gg T. \end{cases} \quad (5.1.11)$$

2. In the opposite case, when ω is smaller than T and Θ_{BG} , Eq. (5.1.6) becomes

$$M''_{QQ}(\omega, T) = \frac{\epsilon_F^2 D_0^2}{2\pi^2 m^2 \rho_m v_F^4 v_s^5 k_F} \frac{T^6}{\chi_{QQ}^0(T)} \int_0^{\Theta_{\text{BG}}/T} dy \frac{y^4 e^y}{(e^y - 1)^2} \left(1 - \frac{y^2 T^2}{2\Theta_{\text{BG}}^2}\right) \times \left(\frac{\Theta_{\text{BG}}^2}{4T^2} + \frac{\pi^2}{3} + \frac{y^2}{12}\right). \quad (5.1.12)$$

The integral in this equation is similar to the integral of Eq. (5.1.7) and is given in Eq. (G.0.8). In limiting cases, it further reduces to

$$M''_{QQ}(\omega, T) \propto \begin{cases} T^2, & \omega \ll T \ll \Theta_{\text{BG}} \\ T, & \omega \ll \Theta_{\text{BG}} \ll T. \end{cases} \quad (5.1.13)$$

3. In the intermediate regimes, the thermal memory function Eq. (5.1.6) shows temperature and frequency dependent behavior as

$$M''_{QQ}(\omega, T) \propto \begin{cases} T^3 \omega^{-1} e^{\omega/T}, & T \ll \omega \ll \Theta_{\text{BG}} \\ T, & \Theta_{\text{BG}} \ll \omega \ll T. \end{cases} \quad (5.1.14)$$

These asymptotic results are shown in Table 5.1.

Now from Eq. (3.1.3), the real part of the electronic thermal conductivity is expressed as

$$\text{Re}[\kappa(\omega, T)] = \frac{\chi_{QQ}^0(T)}{T} \frac{M''_{QQ}(\omega, T)}{\omega^2 + [M''_{QQ}(\omega, T)]^2}, \quad (5.1.15)$$

where $M''_{QQ}(\omega, T)$ for different regimes are given in Table 5.1. In the perturbative regime of small electron-phonon couplings, we assume that the frequency dependent thermal memory function is small. Using this assumption, Eq. (5.1.15) can be written as [62, 95]

$$\text{Re}[\kappa(\omega, T)] \approx \frac{\chi_{QQ}^0(T)}{T} \frac{M''_{QQ}(\omega, T)}{\omega^2} \approx \frac{T M''_{QQ}(\omega, T)}{\omega^2}. \quad (5.1.16)$$

Here we use the temperature variation of the static correlation function (shown in Appendix B.3). Substituting the variation of the temperature and the frequency dependent thermal memory function of graphene, we conclude that the electronic thermal conductivity of graphene at high frequency shows frequency independent behavior. While at the low frequency, it gives large conductivity due to the weakly frequency dependent behavior of the thermal memory function. These behaviors are summarized in Table 5.1 and discussed in Sec. 5.2.

Table 5.1: The results of thermal memory function and the thermal conductivity of graphene for the interaction of electrons with LA/TA and ZA phonons in different frequency and temperature domains.

Regimes	LA/TA phonons		ZA phonons	
	Thermal memory function	Thermal conductivity,	Thermal memory function	Thermal conductivity,
	$1/\tau_{\text{th}}$ or M''_{QQ}	κ	$1/\tau_{\text{th}}$ or M''_{QQ}	κ
$\omega = 0, T \gg \Theta_{\text{BG}}$	T^1	T^0	T^1	T^0
$\omega = 0, T \ll \Theta_{\text{BG}}$	T^2	T^{-1}	$T^{1/2}$	$T^{1/2}$
$\omega \ll T \ll \Theta_{\text{BG}}$	T^2	$T^3\omega^{-2}$	$T^{1/2}$	$T^{3/2}\omega^{-2}$
$\omega \ll \Theta_{\text{BG}} \ll T$	T^1	$T^2\omega^{-2}$	T^1	$T^2\omega^{-2}$
$T \ll \omega \ll \Theta_{\text{BG}}$	$T^3\omega^{-1}e^{\omega/T}$	$T^4\omega^{-3}e^{\omega/T}$	$T^{5/2}\omega^{-1}e^{\omega/T}$	$T^{7/2}\omega^{-3}e^{\omega/T}$
$\Theta_{\text{BG}} \ll \omega \ll T$	T^1	$T^2\omega^{-2}$	T^1	$T^2\omega^{-2}$
$\Theta_{\text{BG}} \ll T \ll \omega$	$T^{-1}\omega^2$	$T^0\omega^0$	$T^{-1}\omega^2$	$T^0\omega^0$
$T \ll \Theta_{\text{BG}} \ll \omega$	$T^2\omega^2$	T^3	$\omega^2T^{-1/2}$	$T^{1/2}$

Flexural Acoustic Phonons (ZA)

Now, in the case of the flexural acoustic phonons having quadratic dispersion [126] i.e. $\omega_q = \alpha q^2$, the thermal memory function can be computed in a similar fashion as done in the case of the LA/TA phonons.

Following the same procedure, the Eq. (5.1.5) for ZA phonons is written as

$$\begin{aligned}
 M''_{QQ}(\omega, T) = & \frac{\epsilon_F^2 D_0^2}{8\pi^2 m^2 \rho_m v_F^4 \alpha^{3/2} k_F} \frac{T^{7/2}}{\chi_{QQ}^0(T)} \int_0^{\Theta_{\text{BG}}/T} dy \frac{y^{1/2}}{e^y - 1} \left(1 - \frac{yT}{8\Theta_{\text{BG}}} \right) \\
 & \times \left\{ \frac{x-y}{e^{x-y} - 1} \frac{e^x - 1}{x} \left(\frac{\Theta_{\text{BG}}}{4T} y + \frac{\pi^2}{3} + \frac{(x-y)^2}{3} + \frac{y(x-y)}{4} \right) \right. \\
 & \left. + (\text{terms with } \omega \rightarrow -\omega) \right\}. \tag{5.1.17}
 \end{aligned}$$

This is analyzed in different frequency and temperature regimes as follows.

Case-I: The zero frequency limit i.e. $\omega \rightarrow 0$

Using this limit in Eq. (5.1.17), we have

$$M''_{QQ}(\omega, T) = \frac{\epsilon_F^2 D_0^2}{4\pi^2 m^2 \rho_m v_F^4 \alpha^{3/2} k_F} \frac{T^{7/2}}{\chi_{QQ}^0(T)} \int_0^{\Theta_{BG}/T} dy \frac{y^{3/2} e^y}{(e^y - 1)^2} \left(1 - \frac{yT}{8\Theta_{BG}}\right) \times \left(\frac{\Theta_{BG}}{4T} y + \frac{\pi^2}{3} + \frac{y^2}{12}\right). \quad (5.1.18)$$

The above equation shows that the *thermal memory function* $M''_{QQ}(T)$ varies as a square root and linearly with temperature at $T \gg \Theta_{BG}$ and $T \ll \Theta_{BG}$ respectively (shown in Table 5.1). Accordingly, the electronic thermal conductivity Eq. (5.1.9) leads to the $T^{1/2}$ power law behavior in the low temperature regime and temperature independent behavior in the high temperature regime.

Case-II: Finite frequency regimes

In this regime, the thermal memory function for the case of flexural phonons in different regimes can be discussed as follows.

1. When ω is higher than T and Θ_{BG} , Eq. (5.1.17) reduces to

$$M''_{QQ}(\omega, T) = \frac{\epsilon_F^2 D_0^2}{12\pi^2 m^2 \rho_m v_F^4 \alpha^{3/2} k_F} \frac{T^{7/2}}{\chi_{QQ}^0(T)} \frac{\omega^2}{T^2} \int_0^{\Theta_{BG}/T} dy \frac{y^{1/2}}{e^y - 1} \left(1 - \frac{yT}{8\Theta_{BG}}\right). \quad (5.1.19)$$

Further at different values of T and Θ_{BG} , the above equation can be expressed as

$$M''_{QQ}(\omega, T) \propto \begin{cases} \omega^2 T^{-1}, & \omega \gg T \gg \Theta_{BG} \\ \omega^2 T^{-1/2}, & \omega \gg \Theta_{BG} \gg T. \end{cases} \quad (5.1.20)$$

2. In the opposite case, when ω is smaller than T and Θ_{BG} , Eq. (5.1.17) becomes

$$M''_{QQ}(\omega, T) = \frac{\epsilon_F^2 D_0^2}{8\pi^2 m^2 \rho_m v_F^4 \alpha^{3/2} k_F} \frac{T^{7/2}}{\chi_{QQ}^0(T)} \int_0^{\Theta_{BG}/T} dy \frac{y^{3/2} e^y}{(e^y - 1)^2} \left(1 - \frac{yT}{8\Theta_{BG}}\right) \times \left(\frac{\Theta_{BG}}{4T} y + \frac{\pi^2}{3} + \frac{y^2}{12}\right). \quad (5.1.21)$$

The above equation further reduces to

$$M''_{QQ}(\omega, T) \propto \begin{cases} T^{1/2}, & \omega \ll T \ll \Theta_{BG} \\ T^1, & \omega \ll \Theta_{BG} \ll T. \end{cases} \quad (5.1.22)$$

3. In the intermediate regime, Eq. (5.1.17) gives

$$M''_{QQ}(\omega, T) \propto \begin{cases} T^{5/2} \omega^{-1} e^{\omega/T}, & T \ll \omega \ll \Theta_{BG} \\ T^1, & \Theta_{BG} \ll \omega \ll T. \end{cases} \quad (5.1.23)$$

Using these results, the thermal conductivity for the case of flexural phonons can be calculated same as for the case of LA/TA phonons and the results are shown in Table 5.1. From this analysis, we observed that the frequency variation for $M''_{QQ}(\omega, T)$ and the corresponding $\kappa(\omega, T)$ is same as the case for the longitudinal or the transverse phonons. But the temperature variations are different. At temperatures higher than the BG temperature, the ZA phonons show identical temperature dependence as the LA/TA phonons do. On the other hand, *at temperature lower than the BG temperature, the temperature dynamics of ZA phonons is different from the LA/TA phonons.*

5.2 Results

5.2.1 Thermal Conductivity in zero frequency limit

In Fig. 5.2, $M''_{QQ}(T)$ Eq. (5.1.7) is plotted as a function of T for LA and TA phonons at different Θ_{BG} which depends on the carrier density n . Here we separately plot

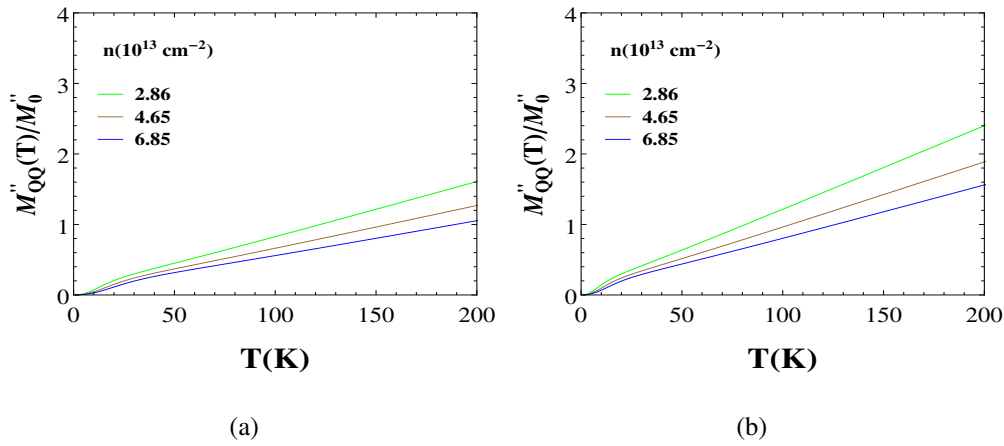


Figure 5.2: The imaginary part of the thermal memory function for the longitudinal and transverse acoustic phonons are plotted with temperature at different $\Theta_{BG} \propto \sqrt{n}$, where n is in the units of 10^{13} cm^{-2} . (a): for the longitudinal acoustic (LA) phonons, $\Theta_{BG} = 57\sqrt{n}\text{K}$ and (b): for the transverse acoustic (TA) phonons, $\Theta_{BG} = 38\sqrt{n}\text{K}$.

it by setting $\Theta_{BG} \approx 57\sqrt{n}$ and $\Theta_{BG} \approx 38\sqrt{n}$ (where n is in the units of 10^{13} cm^{-2}) for the LA and the TA phonons respectively. Also, we have scaled the $M''_{QQ}(T)$ with $M''_0 \left(= \frac{6\epsilon_F^2 D_0^2}{\pi^3 \rho_m v_F^3 v_s^5 k_F} \right)$. It is observed that the thermal memory function increases

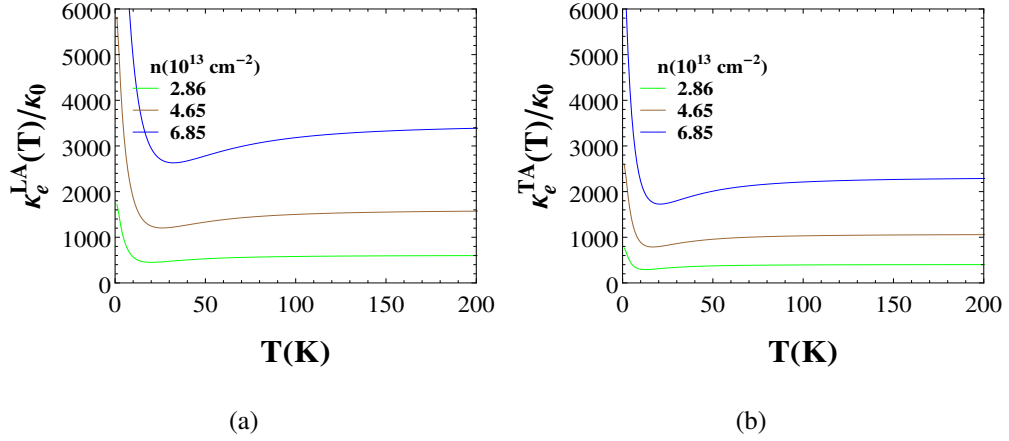


Figure 5.3: The Thermal Conductivity for the (a): longitudinal (LA) and (b): transverse acoustic (TA) phonons are plotted with temperature at different $\Theta_{BG} \propto \sqrt{n}K$, where n is in the units of 10^{13} cm^{-2} .

linearly with increase in the temperature in the high temperature $T \gg \Theta_{BG}$ and non linearly in the low temperature $T \ll \Theta_{BG}$ regimes. Also, it decreases with the increase in the carrier density or Θ_{BG} . This decrease is due to the onset of scattering via large momentum phonons as full backscattering condition i.e. $2k_F = q_c$, where q_c is the critical phonon momentum, leads to larger q_c with large k_F and k_F is the monotonically increasing function of carrier density. Further on comparing the Fig. 5.2(a) and 5.2(b), it is found that the magnitude of the thermal memory function for the TA phonons is more than the LA phonons. This is due to the low phonon velocity of the TA phonons.

The corresponding electronic thermal conductivity for LA and TA phonons is shown in Fig. 5.3. Here for $T \ll \Theta_{BG}$, the thermal conductivity reduces with the increase in T and for $T \gg \Theta_{BG}$, it saturates. These observed features are in accord with the results in the literature [119, 121]. In the intermediate regime i.e. around Θ_{BG} , the small dip is observed which is due to the consideration of the normal process scattering only in the system and we have not taken into account the U-processes (as discussed in Chapter 3, Sec. 3.3).

For the flexural (ZA) phonons, $M''_{QQ}(T)$ Eq. (5.1.18) is shown as a function of temperature in Fig. 5.4. Here we have set $\Theta_{BG} \approx 0.1n$. Such small Θ_{BG} ensures that these phonons play significant role in the low temperature behavior of the thermal conductivity of graphene. Here the value of M''_0 is $3\epsilon_F^2 D_0^2 / \pi^3 \rho_m v_F^3 k_F^4 \alpha^{5/2}$. It is observed that

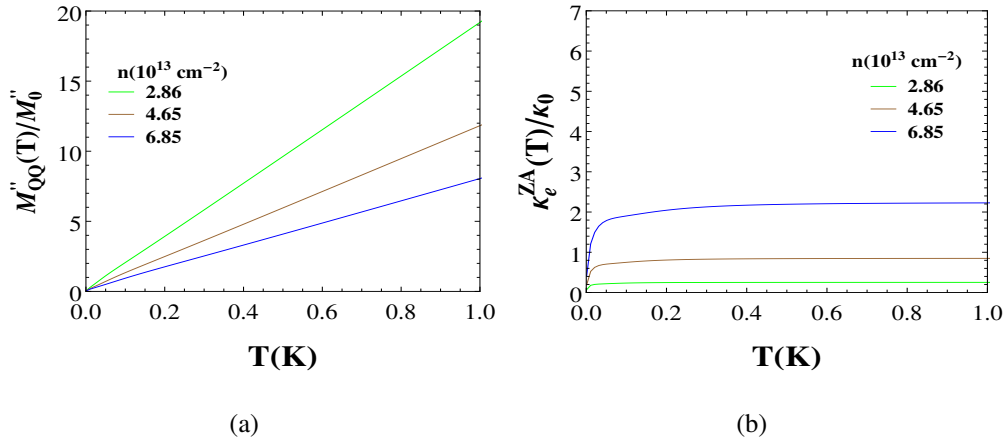


Figure 5.4: (a): The thermal memory function for the flexural acoustic phonons (ZA) is plotted with temperature at different $\Theta_{BG} = 0.1nK$, where n is in the units of 10^{13} cm^{-2} and (b): the corresponding thermal conductivity.

the thermal memory function increases with the increase in the temperature by power law $T^{1/2}$ which further results the increase in the thermal conductivity as $T^{1/2}$ law. But at the high temperature, it increases linearly similar to the case of LA/TA phonons and further it results in the temperature independent thermal conductivity (Fig. 5.4(b)).

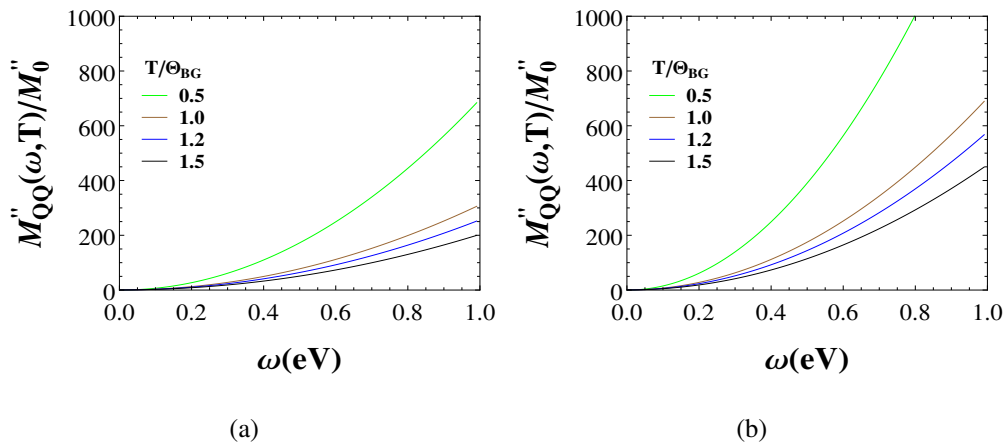


Figure 5.5: The frequency and temperature dependent thermal memory function or the thermal scattering rate for the (a): longitudinal and (b): transverse acoustic phonons are plotted with frequency at different T/Θ_{BG} ratio.

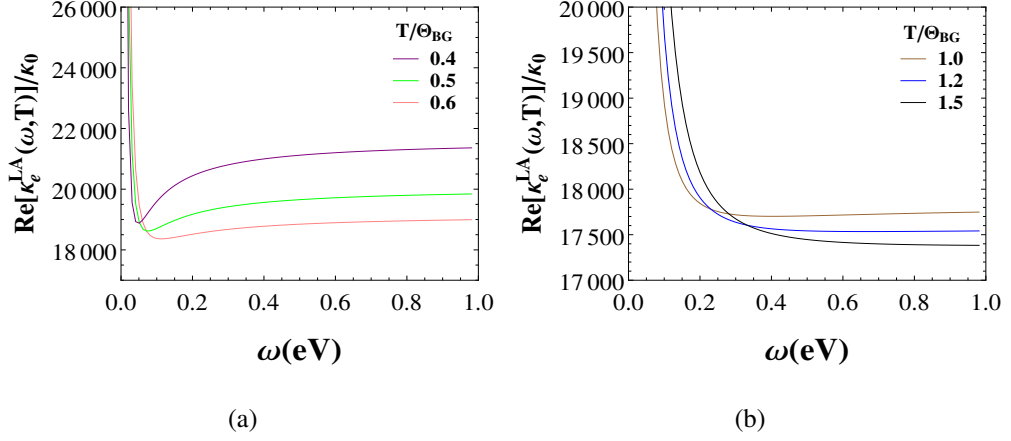


Figure 5.6: The frequency and temperature dependent thermal conductivity for the longitudinal acoustic phonons is plotted with frequency at different T/Θ_{BG} ratio.

5.2.2 Thermal Conductivity in finite frequency regime

In Fig. 5.5 and 5.8(a), we find that in the high frequency regime, the thermal memory function increases with increase in frequency. While in the low frequency regime, it shows saturation behavior. Next, using this variation, we plot the real part of the thermal conductivity Eq. (5.1.15) in Fig. 5.6, 5.7 and 5.8(b). From the frequency behavior of the thermal conductivity, we observe that it shows $1/\omega^2$ behavior in the high frequency regime. This frequency dependent behavior of $\kappa(\omega, T)$ is identical to the

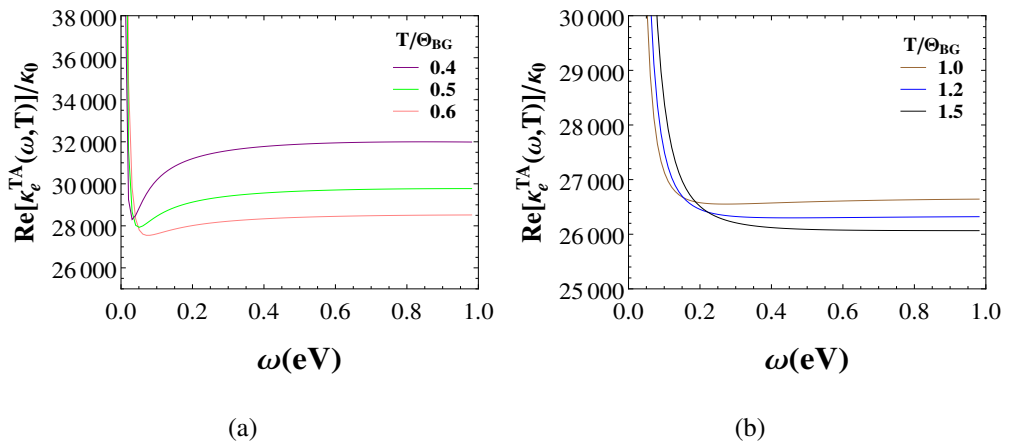


Figure 5.7: The frequency and temperature dependent thermal conductivity for the transverse acoustic phonons is plotted with frequency at different T/Θ_{BG} ratio.

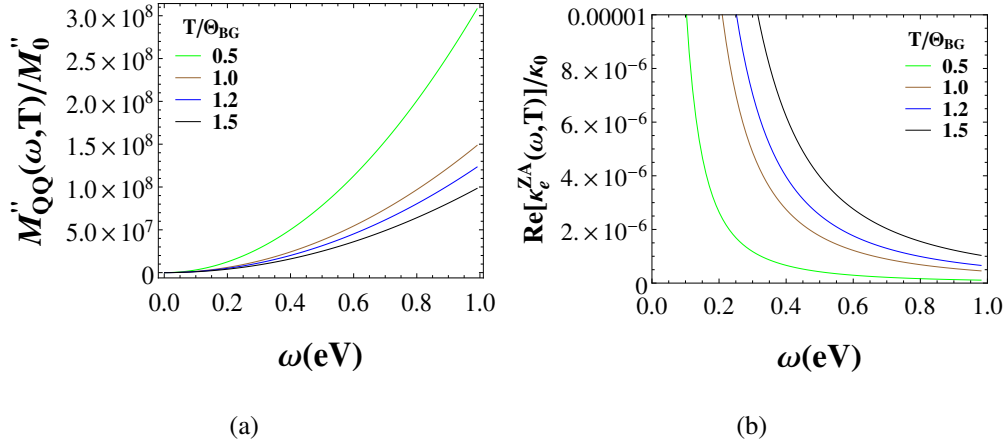


Figure 5.8: (a): The Thermal memory function for the flexural acoustic phonons (ZA) is plotted with frequency T/Θ_{BG} ratio. (b): The corresponding Thermal Conductivity variation of flexural phonons.

case of metal[†]. This gives the signature that the two dimensional scenario modifies the temperature variation of the thermal conductivity but it does not effect the frequency variation of $\kappa(\omega, T)$.

By comparing Fig. 5.3(a), 5.3(b) and 5.4(b), we note that the magnitude of thermal conductivity $\kappa(T)$ is different in all three cases. This is due to the different values such as $v_{\text{LA}} = 21.2 \times 10^3 \text{ ms}^{-1}$, $v_{\text{TA}} = 14.1 \times 10^3 \text{ ms}^{-1}$ and $\alpha = 4.7 \times 10^{-7} \text{ m}^2\text{s}^{-1}$ for the longitudinal, transverse and the flexural phonons respectively. Due to it, the LA phonons contribute more to the electronic thermal conductivity as compared to the TA and ZA phonons. This can also be explained as follows.

According to the Mathiessen's law [3, 5], the total resistivity is the sum of the resistivities due to different interactions separately. And the resistivity is directly proportional to the scattering rate or the memory function. Thus, the memory functions adds up due to the interactions of electrons with longitudinal, transverse and flexural acoustic phonons. Based on that the electronic thermal conductivity, Eq. (5.1.9), is expressed as $1/\kappa_e(T) = 1/\kappa_e^{\text{LA}}(T) + 1/\kappa_e^{\text{TA}}(T) + 1/\kappa_e^{\text{ZA}}(T)$. This shows that at the high temperature $T \gg \Theta_{\text{BG}}$, $1/\kappa_e(T) \approx \text{constant}$ and at the low temperature i.e. $T \ll \Theta_{\text{BG}}$, $1/\kappa_e(T) \approx B \left(\frac{T}{v_{\text{LA}}^5} + \frac{T}{v_{\text{TA}}^5} + \frac{T^{-1/2}}{\alpha^{5/2}} \right)$. Here, we find that at the low temperature, the contribution of the LA phonons to the electronic thermal conductivity due to higher

[†]behavior for metal is discussed in Chapter 3 and Ref. [79].

phonon velocity is more than that from other phonons. Also we observe that the total electronic thermal conductivity decreases approximately linearly with the temperature. Because of the small value of the magnitude of electronic thermal conductivity of ZA phonons, it does not effect much to the total electronic thermal conductivity. Furthermore to understand the whole scenario of the electronic thermal conductivity at the low temperature, one also has to consider the electron-electron interactions which play an opposite role from the electron-phonon interactions [128].

5.3 Conclusion

Graphene is an unique system as it has two dimensional nature, unusual electron dispersion relation, etc. which make its properties different from what is found from the normal three dimensional metal. It also shows unusual phonon modes that do not exist in normal metals. In some sense, these characteristics make the study of graphene novel and more promising. In this connection, we have presented the study of dynamical electronic thermal conductivity of graphene and analyzed its findings.

In a nutshell, the concluding remarks of this chapter are summarized as follows:

1. The electronic thermal conductivity for various acoustic phonons shows different power law behavior due to different phonon dispersion relations.
2. In the zero frequency limit, the electronic thermal conductivity for LA/TA phonons shows T^{-1} and temperature independent behavior in low and high temperature regimes respectively.
3. While for ZA phonons, it shows $T^{1/2}$ and temperature independent behavior in low and high temperature regimes respectively.
4. In the total thermal conductivity, it is found that the LA phonons contribute more to $\kappa(T)$ and the ZA phonons contribute less.
5. For the finite frequency cases, the dynamics of the electronic thermal conductivity due to the electron-phonon interaction is identical to the case of three dimensional system such as a metal [62].

Chapter 6

Moment Expansion to the Memory Function

In the previous chapters, we have discussed the use of the memory function approach to calculate various transport properties of metals and graphene. In addition to these, it has been used extensively in other contexts such as to study the molecular dynamics, thermodynamic properties, etc. [12, 13, 37, 54–56, 61, 62, 96, 129–139]. This wide range of applications make the memory function approach a method of choice in various correlated electronic systems such as strange metal phase of the optimally doped cuprate superconductors where the notion of the electronic quasiparticle breaks down [37, 54]. In a generic electronic system there can be various slow modes such as the charge diffusion, the heat diffusion, etc [37, 54]. In the present study, we consider the electric current as the only relevant slow mode, and then systematically study the effects of other fast degrees of freedom on the current-current correlation with an extension of this formalism. In Ref. [56], the effects of various interactions on the dynamical electrical conductivity (relates to current current correlation function) of a simple metal have been studied previously within the memory function approach in detail. Here, the authors find that the results for electrical conductivity are identical with that of the Boltzmann’s results [3] in the dc limit. However, this formalism is restricted to the lowest order in interaction strength and needs corrections as it increases. In the present work, we make corrections and present a method more accurate than that presented in Ref. [56].

With this motivation, we review the application of the memory function formalism in case of current-current correlation function in metal and propose an expansion of the memory function in terms of its various moments. Then we show that the previously studied Götze-Wölfle [56] formalism and similar other memory function formalism based studies [61, 69, 96, 138] are equivalent to the truncation of our proposed moment expansion at the lowest order. While for the case of higher interaction strength, one has to calculate the contribution from the next order in the moment expansion.

In this chapter, we first introduce the high frequency expansion of the general memory function using the series expansion and the equation of motion methods in Sec. 6.1. Then in Sec. 6.2, we calculate the memory function by considering an example of electron-impurity interaction for a metal. Here we compute the first moment of the memory function. Later in Sec. 6.3, we calculate the memory function with the higher order moments. In Sec. 6.4, we present the results and compare the contribution of different moments to the memory function. Finally, we conclude in Sec. 6.5.

As discussed in Chapter 1, the memory function is expressed as

$$M(z) = \left\langle \dot{A} \left| Q \frac{1}{z - Q\mathcal{L}Q} Q \right| \dot{B} \right\rangle.$$

To discuss the moment expansion of the memory function, we consider one of the application i.e. the electrical conductivity. The latter deals with the current-current correlation function. Hence, we replace the general operators A and B by the current operator J . Thus, the desired memory function becomes

$$M(z) = \left\langle \dot{J} \left| Q \frac{1}{z - Q\mathcal{L}Q} Q \right| \dot{J} \right\rangle. \quad (6.0.1)$$

On expanding $M(z)$ in series expansion, we have

$$M(z) = \frac{1}{z} \left\langle \dot{J} \left| Q \left(1 + \frac{1}{z} Q\mathcal{L}Q + \frac{1}{z^2} Q\mathcal{L}Q\mathcal{L}Q + \dots \right) Q \right| \dot{J} \right\rangle. \quad (6.0.2)$$

Using the fact that $QQ = Q^2 = (1 - P)^2 = Q$ and $\langle J|J \rangle = \langle \dot{J}|\dot{J} \rangle = 0$ (proved in Appendix E), the memory function in series expansion can be written as

$$M(z) = \frac{1}{z} \langle \dot{J}|\dot{J} \rangle + \frac{1}{z^3} \langle \ddot{J}|\ddot{J} \rangle + \dots + \frac{1}{z^{2n-1}} \langle \overset{n}{J}|\overset{n}{J} \rangle. \quad (6.0.3)$$

Here $\overset{n}{J}$ represents the n^{th} time derivative of the current operator. This expression represents the high frequency expansion of the memory function in terms of the equal

time autocorrelation functions [140]. The same scenario for the moment expansion of the memory function can also be proceeded by an alternative way i.e. the equation of motion method, which is widely used in several works for calculating the transport properties [27, 62, 79, 95].

6.1 Equation of motion method

To calculate the memory function using the equation of motion method (EQM), we begin with the expression for response function within the linear response theory by Kubo [59, 60, 97], which is given as,

$$\chi(z) = \langle\langle J; J \rangle\rangle_z = -i \int_0^\infty dt e^{izt} \langle [J(t), J] \rangle. \quad (6.1.1)$$

Using the equation of motion, it can be expressed as (detail is given in Chapter 2)

$$z \langle\langle J; J \rangle\rangle_z = \frac{1}{z} \left(\langle\langle \dot{J}; \dot{J} \rangle\rangle_{z=0} - \langle\langle \dot{J}; \dot{J} \rangle\rangle_z \right). \quad (6.1.2)$$

Here the time derivative of the current operator \dot{J} is equal to the commutator $[J, H]$. Further, this expression is used by Götze and Wölfle [56] to evaluate the memory function for electrons in metal with various interactions. However instead of considering the above expression and evaluating $\langle\langle \dot{J}; \dot{J} \rangle\rangle_z$ perturbatively, we can opt for a higher moment expansion as follows. We apply EQM method again to evaluate the correlation function $\langle\langle J; J \rangle\rangle_z$ in terms of the correlations involving higher time derivatives of \dot{J} . Thus in order to express in second moment, we use the EQM for $\langle\langle \dot{J}; \dot{J} \rangle\rangle_z$, and obtain,

$$z \langle\langle \dot{J}; \dot{J} \rangle\rangle_z = \langle [\dot{J}, \dot{J}] \rangle + \langle\langle [\dot{J}, H]; \dot{J} \rangle\rangle_z. \quad (6.1.3)$$

Using $\langle [\dot{J}, \dot{J}] \rangle = 0$ and $z \langle\langle [\dot{J}, H], \dot{J} \rangle\rangle_z = \langle\langle \ddot{J}; \ddot{J} \rangle\rangle_{z=0} - \langle\langle \ddot{J}; \ddot{J} \rangle\rangle_z$, the above equation can be written as

$$z \langle\langle \dot{J}; \dot{J} \rangle\rangle_z = -\frac{1}{z} \left(\langle\langle \ddot{J}; \ddot{J} \rangle\rangle_{z=0} - \langle\langle \ddot{J}; \ddot{J} \rangle\rangle_z \right). \quad (6.1.4)$$

Substituting above equation in Eq. (6.1.2), we have

$$z \langle\langle J; J \rangle\rangle_z = \frac{1}{z} \langle\langle \dot{J}; \dot{J} \rangle\rangle_{z=0} + \frac{1}{z^3} \left(\langle\langle \ddot{J}; \ddot{J} \rangle\rangle_{z=0} - \langle\langle \ddot{J}; \ddot{J} \rangle\rangle_z \right). \quad (6.1.5)$$

Thus the expression for the response function becomes,

$$z\chi(z) = \frac{1}{z}\langle\langle\dot{J}; \dot{J}\rangle\rangle_{z=0} + \frac{1}{z^3}\left(\langle\langle\ddot{J}; \ddot{J}\rangle\rangle_{z=0} - \langle\langle\ddot{J}; \dot{J}\rangle\rangle_z\right). \quad (6.1.6)$$

By applying EQM recursively, we can obtain a series expansion for $z\chi(z)$ as,

$$\begin{aligned} z\chi(z) &= \frac{1}{z}\langle\langle\dot{J}; \dot{J}\rangle\rangle_{z=0} + \frac{1}{z^3}\langle\langle\ddot{J}; \ddot{J}\rangle\rangle_{z=0} \\ &\quad - \dots + \frac{1}{z^{2n-1}}\langle\langle\overset{n}{J}; \overset{n}{J}\rangle\rangle_{z=0} - \frac{1}{z^{2n-1}}\langle\langle\overset{n}{J}; \overset{n}{J}\rangle\rangle_z. \end{aligned} \quad (6.1.7)$$

In Ref. [56], it is shown that $\chi(z)$ is related to the memory function as

$$M(z) = z\frac{\chi(z)}{\chi_0 - \chi(z)}, \quad (6.1.8)$$

where χ_0 represents the static correlation function ($= N_e/m$, where N_e corresponds to electron density). Here $M(z)$ is the complex memory function, which upon analytic continuation, can be written as a function of real frequency as,

$$M(\omega \pm i0) = M'(\omega) \pm iM''(\omega), \quad (6.1.9)$$

where $M'(\omega)$ and $M''(\omega)$ are real and imaginary part of the memory function and satisfies the symmetry properties $M'(\omega) = -M'(-\omega)$ and $M''(\omega) = M''(-\omega)$ [56].

An approximate form of the memory function can be obtained by assuming that $\chi(z)/\chi_0 \ll 1$. Within this approximation, the expression for the memory function with the leading order term is expressed as,

$$M(z) = z\frac{\chi(z)}{\chi_0}. \quad (6.1.10)$$

The basis of this assumption is the smallness of electron-impurity interaction energy as compared to the electronic kinetic energy [56]. and more details of the validity of the above equation is discussed in Chapter 2. There we have used the current-current correlation function upto the lowest order term i.e. upto first time derivative of the current. Below we go beyond the lowest order result of the correlation function.

Using Eq. (6.1.7), the memory function expansion to general order can be written as,

$$\begin{aligned} M(z) &= \frac{1}{\chi_0}\left(\frac{1}{z}\langle\langle\dot{J}; \dot{J}\rangle\rangle_{z=0} + \frac{1}{z^3}\langle\langle\ddot{J}; \ddot{J}\rangle\rangle_{z=0} + \dots \right. \\ &\quad \left. \dots + \frac{1}{z^{2n-1}}\langle\langle\overset{n}{J}; \overset{n}{J}\rangle\rangle_{z=0} - \frac{1}{z^{2n-1}}\langle\langle\overset{n}{J}; \overset{n}{J}\rangle\rangle_z\right). \end{aligned} \quad (6.1.11)$$

This is an expression of the complex memory function which is equivalent to the Eq. (6.0.3), but under a restrictive condition $\chi(z) \ll \chi_0$ [56, 62]. Here we find that instead of limiting at a perturbative calculation of $\dot{J} - \dot{J}$ correlation, we can include correlations involving higher order time derivatives of \dot{J} . These correlations with higher order time derivatives involves higher order corrections in interaction strength to the scattering rate. We will use this expression with $n = 2$, to evaluate the scattering rate due to the impurity interactions in later sections and will see how the result differs from that of the previously studied lower order corrections.

6.2 Case of electron-impurity scattering

In this section, we review the work discussed in Ref. [56] to calculate the memory function for impurity interactions. We consider a metal where degenerate electrons are interacting with impurities. In this case, the Hamiltonian is

$$H = H_0 + H_{\text{imp}}, \quad (6.2.1)$$

where the unperturbed Hamiltonian H_0 and the perturbed Hamiltonian H_{imp} are defined in Eqs. (2.1.2) and (3.2.1).

We discuss first the memory function, truncating at the first order [56]. In this case, it can be written as

$$M(z, T) = \frac{1}{z\chi_0} \left(\langle\langle \dot{J}; \dot{J} \rangle\rangle_{z=0} - \langle\langle \dot{J}; \dot{J} \rangle\rangle_z \right). \quad (6.2.2)$$

To evaluate the above expression, let us first calculate the time derivative of the electrical current i.e., \dot{J} . The latter is defined as,

$$\dot{J} = -i[J, H] = -i([J, H_0] + [J, H_{\text{imp}}]). \quad (6.2.3)$$

As $[J, H_0] = 0$, thus $\dot{J} = -i[J, H_{\text{imp}}]$. Using Eq. (3.2.1) for perturbed Hamiltonian and defining the current operator $J = \sum_{\mathbf{k}} v_x(\mathbf{k}) c_{\mathbf{k}}^\dagger c_{\mathbf{k}}$, where v_x is the x -component of velocity, the time derivative of J can be written as,

$$\dot{J} = -\frac{i}{N} \sum_{j, \mathbf{k}, \mathbf{k}'} \langle \mathbf{k} | U^j | \mathbf{k}' \rangle \{ v_x(\mathbf{k}) - v_x(\mathbf{k}') \} c_{\mathbf{k}}^\dagger c_{\mathbf{k}'}. \quad (6.2.4)$$

With the above expression, the correlator $\langle\langle \dot{J}; \dot{J} \rangle\rangle_z$ becomes

$$\begin{aligned} \langle\langle \dot{J}; \dot{J} \rangle\rangle_z &= -\frac{1}{N^2} \sum_{j, \mathbf{k}, \mathbf{k}'} \sum_{i, \mathbf{p}, \mathbf{p}'} \langle \mathbf{k} | U^j | \mathbf{k}' \rangle \langle \mathbf{p} | U^i | \mathbf{p}' \rangle \\ &\quad \times \{v_x(\mathbf{k}) - v_x(\mathbf{k}')\} \{v_x(\mathbf{p}) - v_x(\mathbf{p}')\} \langle\langle c_{\mathbf{k}}^\dagger c_{\mathbf{k}'}; c_{\mathbf{p}}^\dagger c_{\mathbf{p}'} \rangle\rangle_z. \end{aligned} \quad (6.2.5)$$

Using the definition of the correlator as defined in Eq. (6.1.1), after performing time integration and thermal average by using $c_{\mathbf{k}}(t) = c_{\mathbf{k}} e^{i\epsilon_{\mathbf{k}} t}$, we get,

$$\langle\langle c_{\mathbf{k}}^\dagger c_{\mathbf{k}'}; c_{\mathbf{p}}^\dagger c_{\mathbf{p}'} \rangle\rangle_z = -\frac{1}{z + \epsilon_{\mathbf{k}} - \epsilon_{\mathbf{k}'}} \{f(\mathbf{k}) - f(\mathbf{k}')\} \delta_{\mathbf{p}', \mathbf{k}} \delta_{\mathbf{p}, \mathbf{k}'}. \quad (6.2.6)$$

We consider the above expression and also the case of dilute impurity and neglecting the interference terms (as done in Chapter 3), thus substitute $i = j$ in Eq. (6.2.5). Performing the summation over impurity sites which contributes N_{imp} , we have

$$\langle\langle \dot{J}; \dot{J} \rangle\rangle_z = 2 \frac{N_{\text{imp}}}{N^2} \sum_{\mathbf{k}, \mathbf{k}'} |\langle \mathbf{k} | U | \mathbf{k}' \rangle|^2 \{v_x(\mathbf{k}) - v_x(\mathbf{k}')\}^2 \frac{f(\mathbf{k}) - f(\mathbf{k}')}{z + \epsilon_{\mathbf{k}} - \epsilon_{\mathbf{k}'}}. \quad (6.2.7)$$

Writing $\mathbf{v} = \mathbf{k}/m$, substituting the above equation in Eq. (6.1.2) and using the Eq. (6.1.10), followed by analytic continuation, i.e. $z \rightarrow \omega + i\zeta$, $\zeta \rightarrow 0^+$, the imaginary part of the memory function becomes,

$$M''(\omega, T) = \frac{2\pi}{3N^2} \frac{N_{\text{imp}}}{mN_e\omega} \sum_{\mathbf{k}, \mathbf{k}'} |\langle \mathbf{k} | U | \mathbf{k}' \rangle|^2 (\mathbf{k} - \mathbf{k}')^2 \{f(\mathbf{k}) - f(\mathbf{k}')\} \delta(\omega + \epsilon_{\mathbf{k}} - \epsilon_{\mathbf{k}'}). \quad (6.2.8)$$

Under the assumption that U is independent of momentum, i.e. for point like impurities [57, 141] the expression further reduces to,

$$M''(\omega, T) = \frac{2\pi}{3N^2} \frac{N_{\text{imp}} U^2}{mN_e\omega} \sum_{\mathbf{k}, \mathbf{k}'} (\mathbf{k} - \mathbf{k}')^2 \{f(\mathbf{k}) - f(\mathbf{k}')\} \delta(\omega + \epsilon_{\mathbf{k}} - \epsilon_{\mathbf{k}'}). \quad (6.2.9)$$

Converting the summation over momentum indices to the energy integrals and performing one integral involving the delta function, the equation further reduces to

$$M''(\omega, T) = \frac{2}{3} \frac{N_{\text{imp}}}{N_e} \frac{U^2 m^3}{\pi^3 \omega} \int_0^\infty d\epsilon \sqrt{\epsilon(\epsilon + \omega)} (2\epsilon + \omega) \{f(\epsilon) - f(\epsilon')\}. \quad (6.2.10)$$

This is the expression of imaginary part of the memory function or the scattering rate of the electronic quasiparticles due to the electron-impurity interactions [56]. Here, for simplicity we replace $\epsilon_{\mathbf{k}}$ and $\epsilon_{\mathbf{k}'}$ by ϵ and ϵ' respectively in rest of the calculations. According to our proposed expansion, this result is equivalent to truncating the Eq. (6.1.11) at $n = 1$ followed by a perturbative evaluation of the $\dot{J} - \dot{J}$ correlation. In the next section we will perform a perturbative calculation at higher order, and will show that this approximation has limited validity.

6.3 The MF with a higher order moment

The memory function with higher order moment can be calculated within the moment expansion method proposed by us using Eq. (6.1.7). One can obtain better result by including higher order moments. Due to mathematical complexity, we restrict ourselves to the evaluation of the memory function $M(z)$ defined in Eq. (6.1.11) at $n = 2$, i.e. by considering upto the $\ddot{J} - \ddot{J}$ correlation. We proceed as follows. We begin with the evaluation of $\langle\langle \ddot{J}; \ddot{J} \rangle\rangle_z$, which is defined as,

$$\begin{aligned} \langle\langle \ddot{J}; \ddot{J} \rangle\rangle_z &= -\langle\langle [\dot{J}, H]; [\dot{J}, H] \rangle\rangle_z \\ &= \langle\langle [[J, H], H]; [[J, H], H] \rangle\rangle_z. \end{aligned} \quad (6.3.1)$$

Now considering the non-interacting and the interacting parts of the Hamiltonian separately the above equation can be rewritten as,

$$\begin{aligned} \langle\langle \ddot{J}; \ddot{J} \rangle\rangle_z &= \langle\langle [[J, H_{\text{imp}}], H_0]; [[J, H_{\text{imp}}], H_0] \rangle\rangle_z \\ &+ \langle\langle [[J, H_{\text{imp}}], H_{\text{imp}}]; [[J, H_{\text{imp}}], H_0] \rangle\rangle_z \\ &+ \langle\langle [[J, H_{\text{imp}}], H_0]; [[J, H_{\text{imp}}], H_{\text{imp}}] \rangle\rangle_z \\ &+ \langle\langle [[J, H_{\text{imp}}], H_{\text{imp}}]; [[J, H_{\text{imp}}], H_{\text{imp}}] \rangle\rangle_z. \end{aligned} \quad (6.3.2)$$

The second term in the above expression is equal to the third term but with an opposite sign (due to the properties of the commutators). Hence they cancel each other and thus we obtain,

$$\begin{aligned} \langle\langle \ddot{J}; \ddot{J} \rangle\rangle_z &= \langle\langle [[J, H_{\text{imp}}], H_0]; [[J, H_{\text{imp}}], H_0] \rangle\rangle_z \\ &+ \langle\langle [[J, H_{\text{imp}}], H_{\text{imp}}]; [[J, H_{\text{imp}}], H_{\text{imp}}] \rangle\rangle_z. \end{aligned} \quad (6.3.3)$$

To find the exact expression for the left hand side of the above equation, calculations can be performed in a way similar to that of the $\langle\langle\dot{J}; \dot{J}\rangle\rangle_z$ as described in Sec. 6.2. The details of which are presented in Appendix F. After several algebraic manipulations, we obtain,

$$\begin{aligned} \langle\langle\ddot{J}; \ddot{J}\rangle\rangle_z &= \frac{2}{3} \frac{N_{\text{imp}} U^2 m^2}{\pi^4} \int_0^\infty d\epsilon \int_0^\infty d\epsilon' \sqrt{\epsilon\epsilon'} (\epsilon + \epsilon') (\epsilon - \epsilon')^2 \frac{f(\epsilon) - f(\epsilon')}{z + \epsilon - \epsilon'} \\ &+ \frac{2}{3} \frac{(N_{\text{imp}} U^2)^2 m^2}{\pi^4} \int_0^\infty d\epsilon \int_0^\infty d\epsilon' \sqrt{\epsilon\epsilon'} (\epsilon + \epsilon') \frac{f(\epsilon) - f(\epsilon')}{z + \epsilon - \epsilon'}. \end{aligned} \quad (6.3.4)$$

Substituting Eq. (6.3.4) and Eq. (6.2.10) into Eq. (6.1.11), the expression for the memory function $M(z, T)$ upto second order becomes,

$$\begin{aligned} M(z, T) &= \frac{2}{3} \frac{m^3}{\pi^4} \frac{1}{N_e} \left\{ -\frac{2}{z} N_{\text{imp}} U^2 \int_0^\infty d\epsilon \int_0^\infty d\epsilon' \epsilon \sqrt{\epsilon\epsilon'} \frac{f(\epsilon) - f(\epsilon')}{\epsilon - \epsilon'} \right. \\ &- \frac{1}{z^2} N_{\text{imp}} U^2 \int_0^\infty d\epsilon \int_0^\infty d\epsilon' \sqrt{\epsilon\epsilon'} (\epsilon + \epsilon') (\epsilon - \epsilon')^2 \frac{f(\epsilon) - f(\epsilon')}{(z + \epsilon - \epsilon')(\epsilon - \epsilon')} \\ &\left. - \frac{1}{z^2} (N_{\text{imp}} U^2)^2 \int_0^\infty d\epsilon \int_0^\infty d\epsilon' \sqrt{\epsilon\epsilon'} (\epsilon + \epsilon') \frac{f(\epsilon) - f(\epsilon')}{(z + \epsilon - \epsilon')(\epsilon - \epsilon')} \right\}. \end{aligned} \quad (6.3.5)$$

After further algebraic manipulations, the expression for the complex memory function $M(z, T)$ reduces to

$$\begin{aligned} M(z, T) &= \frac{2}{3} \frac{m^3}{\pi^4} \frac{1}{N_e} \int_0^\infty d\epsilon \int_0^\infty d\epsilon' \sqrt{\epsilon\epsilon'} \frac{f(\epsilon) - f(\epsilon')}{\epsilon - \epsilon'} \left\{ -N_{\text{imp}} U^2 \frac{\epsilon + \epsilon'}{z + \epsilon - \epsilon'} \right. \\ &\left. - (N_{\text{imp}} U^2)^2 \frac{\epsilon + \epsilon'}{(\epsilon - \epsilon')^2 (z + \epsilon - \epsilon')} + \frac{2}{z} (N_{\text{imp}} U^2)^2 \frac{\epsilon}{(\epsilon - \epsilon')^2} \right\}. \end{aligned} \quad (6.3.6)$$

We are interested in the frequency dependent character of the imaginary part of memory function $M''(\omega, T)$. On performing analytic continuation, i.e. $z \rightarrow \omega + i\zeta$, $\zeta \rightarrow 0$, the expression for $M''(\omega, T)$ becomes,

$$\begin{aligned} M''(\omega, T) &= \frac{2}{3} \frac{m^3}{\pi^3} \frac{1}{N_e} \int_0^\infty d\epsilon \int_0^\infty d\epsilon' \sqrt{\epsilon\epsilon'} \frac{f(\epsilon) - f(\epsilon')}{\epsilon - \epsilon'} \delta(\omega + \epsilon - \epsilon') \\ &\left\{ N_{\text{imp}} U^2 (\epsilon + \epsilon') + (N_{\text{imp}} U^2)^2 \frac{\epsilon + \epsilon'}{(\epsilon - \epsilon')^2} - 2(N_{\text{imp}} U^2)^2 \frac{\epsilon}{(\epsilon - \epsilon')^2} \delta(\omega) \right\}. \end{aligned} \quad (6.3.7)$$

Now performing one of the energy integral, i.e. the integral over ϵ' , the above expression at frequency $\omega > 0$ reduces to,

$$M''(\omega, T) = \frac{2}{3} \frac{m^3}{\pi^3} \frac{1}{N_e} \int_0^\infty d\epsilon \sqrt{\epsilon(\epsilon + \omega)} \frac{f(\epsilon) - f(\epsilon + \omega)}{\omega} (2\epsilon + \omega) \times \left\{ N_{\text{imp}} U^2 + (N_{\text{imp}} U^2)^2 \frac{1}{\omega^2} \right\}. \quad (6.3.8)$$

This is an expression of the imaginary part of memory function for electrons in a metal, within the second order truncation of our proposed moment expansion for correlation function. Here the first term within the braces corresponds to the contribution from the first moment [56] and the second term is the contribution from the second moment to the memory function. The frequency dependent behavior of the above expression with different interaction strength U , impurity concentration N_{imp} and temperature T is discussed in next section.

6.4 Results and Comparison

The equation Eq. (6.3.8), describes the imaginary part of the memory function or the scattering rate as a function of ω , U , N_{imp} and T within a second order in moment expansion. We compare it with the imaginary part of the memory function obtained in Eq. (6.2.9), within first order in moment expansion [56]. The validity of truncating such an expansion at the n -th order is valid when the n -th term in the expansion is smaller than the $(n - 1)$ -th term. In the present work we restrict ourselves to the second order. In this case to check the validity of our results, we define an energy scale ω_0 above which the present high frequency expansion is valid. By taking the ratio of second order term to the first order term, the condition becomes $1/\omega^2 \times \langle \ddot{J} | \ddot{J} \rangle / \langle \dot{J} | \dot{J} \rangle \ll 1$. From Eq. (6.3.8), the above criterion translates to $N_{\text{imp}} U^2 / \omega^2 \ll 1$. This implies that our results are valid if the condition $\omega \geq (N_{\text{imp}} U^2)^{1/2} (= \omega_0)$ is satisfied.

In Fig. 6.1, we plot normalized imaginary part of memory function $M''(\omega)/M_0$ as a function of frequency ω for both the cases (upto the first moment and the second moment), keeping other parameters fixed. In Fig. 6.1(a), the scattering rates are shown at temperature $T = 10\text{K}$. It is observed that at high frequency regime, the result which includes the second moment contribution agrees well with the previous result

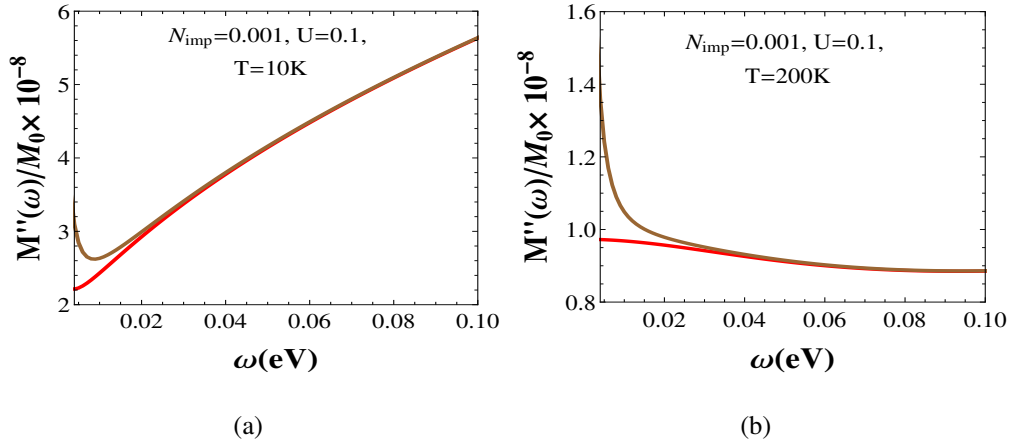


Figure 6.1: Plots of the imaginary part of normalized memory functions at different temperatures (a) at $T = 10\text{K}$ and (b) at $T = 200\text{K}$. Here the red curve corresponds to the case with first moment only and the brown curve corresponds to the case where second moment also considered within the present moment expansion of the memory function. In both cases, there is agreement between the results from the two different approaches at high frequency regimes. However they differ significantly in the low frequency regime.

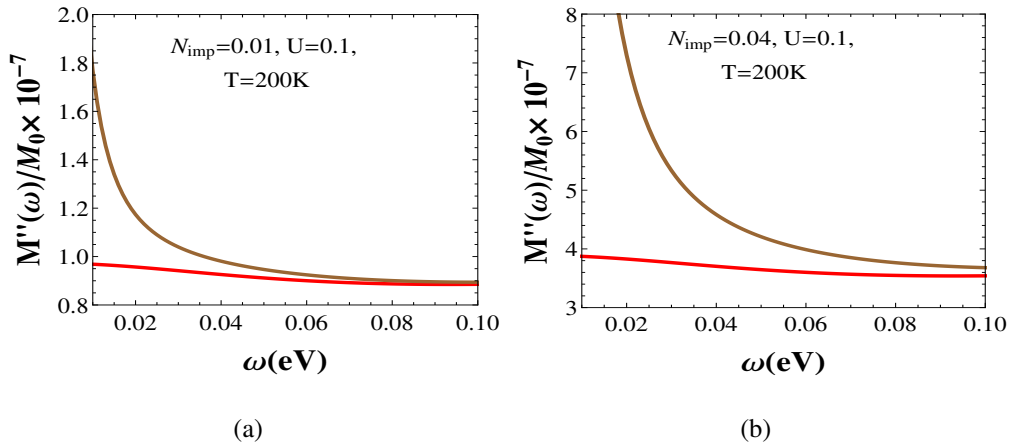


Figure 6.2: Plots of the imaginary part of normalized memory functions at different impurity densities N_{imp} (a) 0.01 and (b) 0.04. Here the red curve corresponds to the case with first moment only and the brown curve corresponds to the case where the second moment is also considered in the moment expansion. Here also a deviation occurs at low frequency regime as in the previous case. The increase in the impurity density enhances the magnitude of the memory function.

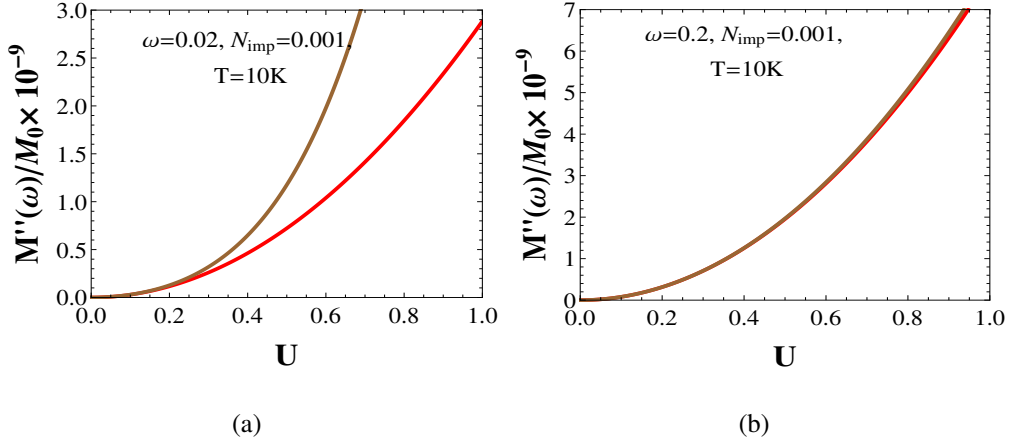


Figure 6.3: Variation of the scattering rates with interaction strength U at different frequencies (a) $\omega = 0.02\text{eV}$ and (b) 0.2eV . Here the red curve represents the scattering rate with the first moment only and the brown curve is with the inclusion of the second moment. It is observed that the deviation is more for higher interaction strength in the low frequency regime, as expected.

(which includes only the first moment) [56]. But above the defined energy scale ω_0 (which is 0.004 in this figure), results deviate from each other. The second moment contributes more in the later deviation and thus increasing the magnitude of the scattering rate compared to the case with only the first moment. We see that the magnitude of the scattering rate in this case is high as compared to the case with $n = 1$ term of $M''(\omega)$. Similarly, the scattering rates are plotted at a different temperature $T = 200\text{K}$ in Fig. 6.1(b). Here we observe that with the increase in temperature, the magnitude of the scattering rate with the inclusion of the second moment term is more as compared to that in the previous figure Fig. 6.1(a).

In Fig. 6.2, again we plot the scattering rates at fixed temperature for different impurity densities $N_{\text{imp}} = 0.01$ and 0.04 . We observe the same trend in both cases similar to the previous figure. Here the increase in the impurity density increases the scattering centers which leads to higher magnitude to the scattering rates. Also, here the results are valid for frequency greater than 0.01 and 0.02 in Figs. 6.2(a) and 6.2(b) respectively. We would like to comment here that our results are valid only for second moment expansion under the condition $\omega > \omega_0 = \sqrt{N_{\text{imp}}U^2}$. Also, one can envisage from Eq. (6.1.11) that higher order terms will be divergent individually in the zero

frequency limit and a more sophisticated resummation of all the higher order terms would be needed to rectify the problem. But we will not undertake this problem in this thesis, and it is beyond the scope of the present work.

Further to elaborate the memory function dependence on the interaction strength U , plot of the scattering rate with U at fixed frequency, N_{imp} and temperature is shown in Fig. 6.3. In Fig. 6.3(a), the scattering rate is shown at a small frequency $\omega = 0.02\text{eV}$ at which earlier we see that there is deviation in the results of memory function with different moment expansions. Here we find that the increase of U increases the scattering rate at low frequency due to the presence of the term $(N_{\text{imp}}U^2)^2$ in the moment expansion of the memory function. In Fig. 6.3(b), we observe that at a higher frequency ($\omega = 0.2\text{eV}$), difference in $M''(\omega)$ with the increase of interaction strength, from two approximations becomes insignificant.

6.5 Conclusion

It is often convenient to express a frequency dependent response function in terms of a memory function [96]. In this work we propose a series expansion for the memory function. We show that, many of the previous works [56,61,62,96], which address the optical conductivity of the metals within the memory function formalism, are equivalent to restricting at the lowest order in the expansion of the memory function. We perform a higher order calculation for the same in the presence of electron-impurity interaction and compare our results with the result from one of the celebrated previous work [56]. In all these approaches, one needs to calculate the current-current correlation function ($\langle\langle JJ \rangle\rangle$), a two particle correlator. In summary, we extend the latter work [56] further by introducing the higher order approximation for the memory function.

In a nutshell, the concluding remarks of this chapter are as follows.

- 1 It is found that there is discrepancy between the results of the imaginary part of memory function computed by including and not including higher order terms.

- 2 These discrepancies have been observed in the low frequency regime and for higher impurity strengths.
- 3 There is an increase in the scattering rate with impurity strength and further the inclusion of higher order contribution leads to higher scattering rates (Fig. 6.3).
- 4 Within the presented systematic memory function expansion, the interaction effects up-to required order depending on the interaction strength can be included. Thus our work goes beyond the GW formalism which is restricted to the lowest order in the interaction strength.

Chapter 7

Summary and Future directions

In this thesis, we have studied theoretically the various transport properties of metals and graphene in the finite frequency and temperature regimes using memory function formalism.

First, we have reviewed the memory function approach where we introduce the projectors and the memory functions, and discuss the application of this to the electronic transport. Further, on applying this approach to the case of metal, we have investigated the behavior of the electrical conductivity in the presence of the gapped density of states. We observe that with the increase of the magnitude of the gap, the suppression in the scattering rate increases. We also find that the memory function and the phenomenological Sharapov-Carbotte approach [64] yield the same results of the scattering rate in the finite frequency regimes. But these approaches show discrepancy in the low frequency regime which is due to the assumptions considered in the Sharapov-Carbotte approach in calculating the scattering rate. The memory function approach, on the other hand, does not make such assumptions.

We have also investigated the dynamical thermal conductivity of metals by considering the electron-impurity and the electron-phonon interactions. Here, we introduce the thermal memory functions and compute them in the zero and finite frequency regimes. We find that in the zero frequency limit, our results agree with that calculated by the traditional Bloch-Boltzmann approach. Also, these results are in qualitative agreement with the experimental findings. In the finite frequency case, we obtain several new results. Some of them are summarized as follows: 1) $T \gg \omega_D$: in this

case, the thermal conductivity as we move from the low frequency regime to the high frequency regime, shows a crossover behavior from the $\kappa \sim T^2/\omega^2$ behavior to the $\kappa \sim T^0/\omega^0$ behavior. 2) On the other hand for $T \ll \omega_D$, we observe that $\kappa \sim T^4/\omega^2$ in the low frequency regime ($\omega \ll \omega_D$), then we find $\kappa \sim T^5 \sinh(\omega/T)/\omega^3$ behavior in the intermediate regime and finally we observe $\kappa \sim T^4(a\omega^{-2} + b)$ behavior in high frequency regime ($\omega \gg \omega_D$).

Further we have computed the thermoelectric response function, Seebeck coefficient, for the case of a metal using the memory function approach. Here, we have studied the role of two different weak interactions such as the electron-impurity and the electron-phonon interactions in the Seebeck coefficient. We have found that in the zero frequency case, $S(T)$ shows temperature independent behavior for the case of electron-impurity interaction and linear temperature dependent behavior in the high temperature regime ($T \gg \Theta_D$) for electron-phonon interaction. These results are in agreement with the previous results calculated by using Mott formula and with the experimental findings. In the finite frequency regimes, we observe that the dynamical Seebeck coefficient saturates at high frequencies in both the interactions.

Then to apply the memory function approach to other class of materials, we have investigated the dynamical thermal conductivity of two dimensional system graphene. We have explored the role of different acoustic phonons in the thermal conductivity and discussed it's power law dependence due to the different dispersion relations of these phonons. We have found that due to the large phonon velocity of the longitudinal phonons, their contribution to the total thermal conductivity is higher than the transverse and flexural phonons.

To extend the memory function approach beyond lowest order perturbative calculation, we have also proposed a systematic expansion of the memory function involving its various moments to account for the case of stronger interaction strengths. We have devoted this study to discuss the general aspects of memory function approach, particularly to discuss the limitations of this approach used by GW [56] to treat weak electron-phonon, electron-impurity interactions. We have calculated the higher order contribution to the generalized Drude scattering rate in the case of electron-impurity interactions in a metal. We have found that the higher moments contribute more in the

low frequency regime and in the case of the large interaction strength.

In this thesis, we have mainly discussed the effects of electron-impurity and electron-phonon interactions in various transport properties under the influence of the electric field. In future work, we plan to study aspects of electron-electron interactions to these properties with memory function technique within the Hubbard model. This model is a simplified model to account the quantum mechanical motion of electrons and to discuss the interaction of electrons with each other through Coulomb interaction. Also, using the memory function approach, the dynamics of the transport properties under the influence of the magnetic field such as Hall effect, Nernst effect can be a topic of future study. Moreover, motivated by the results of the thermal conductivity of metals at low temperature, this formalism can also be employed to investigate the behavior of thermal conductivity by taking the Umklapp scattering process. Further, the effects of charge diffusion in disordered system [54], conserved momentum [54] can also be included.

Appendix A

General formula of GDS for the case of non constant DOS

The imaginary part of memory function Eq. (2.2.17) is

$$M''(\omega, T) = \frac{2\pi}{3} \frac{1}{mN_e} \sum_{\mathbf{k}, \mathbf{k}'} |D(\mathbf{k} - \mathbf{k}')|^2 (\mathbf{k} - \mathbf{k}')^2 f_{\mathbf{k}'} (1 - f_{\mathbf{k}}) n_{\mathbf{k} - \mathbf{k}'}$$

$$\times \left[\frac{e^{\omega/T} - 1}{\omega} \delta(\epsilon - \epsilon' - \omega_{\mathbf{k} - \mathbf{k}'} + \omega) + (\text{terms with } \omega \rightarrow -\omega) \right]. \quad (\text{A.0.1})$$

Converting the summations into energy integrals and inserting the dq integral, we have

$$M''(\omega, T) = \frac{2\pi}{3} \frac{N^2}{mN_e} \int_0^\infty dq \int_{-\infty}^\infty d\epsilon N(\epsilon) \int_{-\infty}^\infty d\epsilon' N(\epsilon') |D(q)|^2 q^2 f'(1 - f) n_q$$

$$\times \int_0^\pi d\theta \sin \theta \delta(q - |\mathbf{k} - \mathbf{k}'|)$$

$$\times \left[\frac{e^{\omega/T} - 1}{\omega} \delta(\epsilon - \epsilon' - \omega_q + \omega) + (\text{terms with } \omega \rightarrow -\omega) \right]. \quad (\text{A.0.2})$$

Here the energy dependent density of states $N(\epsilon)$ has been introduced. Thus on solving the integrals over ϵ' and θ , the above equation reduces to

$$M''(\omega, T) = \frac{2\pi}{3} \frac{N^2}{mN_e k_F^2 \omega} \int_0^\infty dq |D(q)|^2 q^3 \int_{-\infty}^\infty d\epsilon N(\epsilon) \frac{e^{\beta(\epsilon - \epsilon_F)}}{e^{\beta(\epsilon - \epsilon_F)} + 1} \frac{1}{e^{\beta\omega_q} - 1}$$

$$\times \left[N(\epsilon - \omega_q + \omega) \frac{e^{\beta\omega} - 1}{e^{\beta(\epsilon - \epsilon_F - \omega_q + \omega)} + 1} - N(\epsilon - \omega_q - \omega) \frac{e^{-\beta\omega} - 1}{e^{\beta(\epsilon - \epsilon_F - \omega_q - \omega)} + 1} \right]. \quad (\text{A.0.3})$$

This is the general expression for the imaginary part of memory function (called as GDS).

Appendix B

Derivation of static correlation functions

B.1 Thermal-current thermal-current correlation function

The static thermal-current thermal-current correlation is defined as [75]

$$\chi_{QQ}^0(T) = \frac{1}{3T} \sum_{\mathbf{k}} (\epsilon_{\mathbf{k}} - \mu)^2 v_{\mathbf{k}}^2 f_{\mathbf{k}} (1 - f_{\mathbf{k}}). \quad (\text{B.1.1})$$

Converting the summation into energy integral (here the energy is $\mathbf{k}^2/2m$ for the case of three dimensional metal) and substituting $\frac{\epsilon_{\mathbf{k}} - \mu}{T} = \eta$, the above equation reduces to

$$\begin{aligned} \chi_{QQ}^0(T) &= \frac{T^2 k_F^3}{3m} \frac{1}{2\pi^2} \int_0^\infty d\eta \frac{\eta^2 e^\eta}{(e^\eta + 1)^2} \\ &= T^2 \frac{N_e}{m} \frac{\pi^2}{12} \end{aligned} \quad (\text{B.1.2})$$

This shows that the static thermal-current thermal-current correlation varies quadratically in temperature.

B.2 Thermal-current electric-current correlation function

Similarly, the static thermal-current electric-current correlation function is defined as

$$\chi_Q^0(T) = \frac{1}{3T} \sum_{\mathbf{k}} (\epsilon_{\mathbf{k}} - \mu) v_{\mathbf{k}}^2 f_{\mathbf{k}} (1 - f_{\mathbf{k}}). \quad (\text{B.2.1})$$

After simplifications, it can be written as

$$\begin{aligned} \chi_Q^0(T) &= \frac{T k_F^3}{3m} \frac{1}{2\pi^2} \int_0^\infty d\eta \frac{\eta e^\eta}{(e^\eta + 1)^2}. \\ &= T \frac{N_e}{3m} \log 2. \end{aligned} \quad (\text{B.2.2})$$

This shows that the static thermal-current electric-current correlation varies linearly in temperature.

B.3 Thermal-current thermal-current correlation function for two dimensional system

The static thermal-current thermal-current correlation function for the two dimensional system (graphene) can be computed in a similar way as done in Sec. B.1 for three dimensional metals. Here after converting the summation over momentum indices into the energy integral using the linear energy dispersion relation i.e. $\epsilon = v_F |\mathbf{k}|$ for graphene and then simplifying, $\chi_{QQ}^0(T)$ can be expressed as

$$\begin{aligned} \chi_{QQ}^0(T) &= \frac{T^2 k_F^2}{6\pi} \int_0^\infty d\eta \frac{\eta^2 e^\eta}{(e^\eta + 1)^2}. \\ &= T^2 \frac{k_F^2 \pi}{72}. \end{aligned} \quad (\text{B.3.1})$$

Appendix C

Derivation of Eq.(3.1.4) for thermal memory function

In Eq. (3.1.3), we see that the dynamical thermal conductivity $\kappa(z, T)$ depends on the thermal memory function $M_{QQ}(z, T)$. Further the thermal memory function in terms of the correlation function can be expressed in a similar way as the electrical memory function in Eq. (2.2.1) as

$$M_{QQ}(z, T) = z \frac{\chi_{QQ}(z, T)}{\chi_{QQ}^0(T) - \chi_{QQ}(z, T)}, \quad (\text{C.0.1})$$

where $\chi_{QQ}(z, T)$ is the thermal-current thermal-current correlation function, χ_{QQ}^0 corresponds to the static limit of the correlation function. Here $\chi_{QQ}(z, T)$ is defined as

$$\chi_{QQ}(z, T) = \langle\langle J_Q; J_Q \rangle\rangle_z = -i \int_0^\infty dt e^{izt} \langle [J_Q(t), J_Q] \rangle, \quad (\text{C.0.2})$$

where J_Q is the thermal current and defined in Eq. (3.1.2).

Now $\chi_{QQ}(z, T)$ can be obtained by using the equation of motion as done in Chapter 2 to compute $\chi(z, T)$ with replacement of electrical current J by thermal current J_Q . Following the same procedure, the thermal-current thermal-current correlation function can be expressed as

$$\chi_{QQ}(z, T) = \frac{\langle\langle [J_Q, H]; [J_Q, H] \rangle\rangle_{z=0} - \langle\langle [J_Q, H]; [J_Q, H] \rangle\rangle_z}{z^2}. \quad (\text{C.0.3})$$

Further expanding Eq. (C.0.1) and keeping it upto leading order term, the thermal memory function using Eq. (C.0.3) can be expressed as

$$M_{QQ}(z, T) = \frac{\langle\langle [J_Q, H]; [J_Q, H] \rangle\rangle_{z=0} - \langle\langle [J_Q, H]; [J_Q, H] \rangle\rangle_z}{z \chi_{QQ}^0(T)}. \quad (\text{C.0.4})$$

Appendix D

Thermal conductivity using Boltzmann approach

D.1 For electron-impurity interaction

The Boltzmann equation for the semi-classical distribution function $g_k(\mathbf{r}, t)$ is written as

$$v_{\mathbf{k}} \frac{\partial g_k}{\partial r} = \left(\frac{\partial g_k}{\partial t} \right)_{\text{coll}} = \int \frac{d\mathbf{k}'}{2\pi^3} (W(\mathbf{k}' \rightarrow \mathbf{k}) - W(\mathbf{k} \rightarrow \mathbf{k}')). \quad (\text{D.1.1})$$

Here $W(\mathbf{k}' \rightarrow \mathbf{k})$ defines the transition probability of an electron scattering from initial state \mathbf{k}' to final state \mathbf{k} . According to the Fermi-Golden rule, in case of the impurity scattering it can be expressed as

$$W(\mathbf{k}' \rightarrow \mathbf{k}) = 2\pi |\langle \mathbf{k}' | H_{\text{imp}} | \mathbf{k} \rangle|^2 \delta(\epsilon_{\mathbf{k}'} - \epsilon_{\mathbf{k}}). \quad (\text{D.1.2})$$

Considering the impurity interaction Hamiltonian given in Eq. (3.2.1), the transition probability can be expressed as

$$W(\mathbf{k}' \rightarrow \mathbf{k}) = 4\pi \frac{N_{\text{imp}}}{N^2} |U(\mathbf{k}', \mathbf{k})|^2 g_{\mathbf{k}} (1 - g_{\mathbf{k}'}) \delta(\epsilon_{\mathbf{k}'} - \epsilon_{\mathbf{k}}). \quad (\text{D.1.3})$$

Here $U(\mathbf{k}', \mathbf{k}) = \langle \mathbf{k}' | U | \mathbf{k} \rangle$, the matrix element for the impurity interaction. Inserting the above Eq. (D.1.3) in Eq. (D.1.1), we obtain

$$\left(\frac{\partial g_k}{\partial t} \right)_{\text{coll}} = \int d\mathbf{k}' \frac{N_{\text{imp}}}{2\pi^2 N^2} |U(\mathbf{k}', \mathbf{k})|^2 (g_{\mathbf{k}'} - g_{\mathbf{k}}) \delta(\epsilon_{\mathbf{k}'} - \epsilon_{\mathbf{k}}). \quad (\text{D.1.4})$$

Now linearizing the Boltzmann equation using $g_{\mathbf{k}} = f_{\mathbf{k}} + \delta g_{\mathbf{k}}$ and taking equilibrium collision integral terms to zero, the Eq. (D.1.4) can be written as

$$\left(\frac{\partial g_{\mathbf{k}}}{\partial t}\right)_{\text{coll}} = \int d\mathbf{k}' \frac{N_{\text{imp}}}{2\pi^2 N^2} |U(\mathbf{k}', \mathbf{k})|^2 (\delta g_{\mathbf{k}'} - \delta g_{\mathbf{k}}) \delta(\epsilon_{\mathbf{k}'} - \epsilon_{\mathbf{k}}). \quad (\text{D.1.5})$$

In the standard procedure, the collision integral is solved by an iterative procedure [5, 27, 142]. One starts with the relaxation time approximation.

$$g_{\mathbf{k}} = f_{\mathbf{k}} + \delta g_{\mathbf{k}} = f_{\mathbf{k}} + \frac{k_x}{m} \tau(\epsilon_{\mathbf{k}}) \left(\frac{\partial f_{\mathbf{k}}}{\partial T}\right) (\nabla T)_x. \quad (\text{D.1.6})$$

Thus the change in the distribution function is written as

$$\delta g_{\mathbf{k}} = g_{\mathbf{k}} - f_{\mathbf{k}} = \frac{k_x}{m} C(\epsilon_{\mathbf{k}}) \left(\frac{\partial f_{\mathbf{k}}}{\partial \epsilon}\right), \quad (\text{D.1.7})$$

Here $C(\epsilon_{\mathbf{k}})$ is proportional to an energy dependent relaxation time. On substituting the above expression in Eq. (D.1.5) and noticing that $v_{\mathbf{k}}^x \nabla g_{\mathbf{k}} = \frac{k_x}{m} \frac{\partial f_{\mathbf{k}}}{\partial T} \nabla T$, one obtains

$$\frac{1}{\tau(\epsilon_{\mathbf{k}})} = \frac{2N_{\text{imp}} m k_F}{\pi N^2} \int_0^\pi d\theta |U(k_F, \theta)|^2 \sin \theta (1 - \mathbf{k} \cdot \mathbf{k}'). \quad (\text{D.1.8})$$

This shows that the thermal scattering rate due to electron-impurity interaction is independent of the temperature. As the thermal conductivity is defined as

$$\kappa(T) = \frac{2}{T^2} \sum_{\mathbf{k}} \tau(\epsilon_{\mathbf{k}}) (\epsilon_{\mathbf{k}} - \mu)^2 \frac{e^{(\epsilon_{\mathbf{k}} - \mu)/T}}{(e^{(\epsilon_{\mathbf{k}} - \mu)/T} + 1)^2}. \quad (\text{D.1.9})$$

Substituting the Eq. (D.1.8) in the above Eq. (D.1.9), the thermal conductivity due to the electron-impurity interaction shows the temperature dependence as

$$\begin{aligned} \kappa(T) &= \frac{1}{72} \frac{\pi k_F^2}{N_{\text{imp}} U^2 m^2} T \\ \text{i.e. } \kappa(T) &\propto T. \end{aligned} \quad (\text{D.1.10})$$

From this we infer that the results of the thermal conductivity using both the approaches the memory function and the Boltzmann approach agree quantitatively to each other.

D.2 For electron-phonon interaction

Similarly for the electron-phonon interaction case, the Boltzmann equation becomes

$$v_{\mathbf{k}} \frac{\partial g_{\mathbf{k}}}{\partial t} = \left(\frac{\partial g_{\mathbf{k}}}{\partial t}\right)_{\text{coll}} = \int d\mathbf{k}' (W(\mathbf{k} + \mathbf{q} \rightarrow \mathbf{k}) - W(\mathbf{k} \rightarrow \mathbf{k} + \mathbf{q})). \quad (\text{D.2.1})$$

Here $W(i \rightarrow f)$ is the transition probability involving both the emission and absorption of phonons. This, using Fermi Golden rule can be expressed as [17]

$$W(\mathbf{k} + \mathbf{q} \rightarrow \mathbf{k}) = 2\pi |\langle \mathbf{k} | H_{\text{ep}} | \mathbf{k} + \mathbf{q} \rangle|^2 \delta(\epsilon_{\mathbf{k}+\mathbf{q}} - \epsilon_{\mathbf{k}} \pm \omega_q). \quad (\text{D.2.2})$$

Using the Eq. (2.1.3), above expression for the transition probability can be written as

$$W(\mathbf{k} + \mathbf{q} \rightarrow \mathbf{k}) = 4\pi |D(q)|^2 g_{\mathbf{k}+\mathbf{q}} (1 - g_{\mathbf{k}}) (n_{\mathbf{q}} + 1) \delta(\epsilon_{\mathbf{k}} + \omega_q - \epsilon_{\mathbf{k}+\mathbf{q}}). \quad (\text{D.2.3})$$

Considering all possible scattering processes, the collision integral can be written as

$$\left(\frac{\partial g_{\mathbf{k}}}{\partial t} \right)_{\text{coll}} = \int d\mathbf{q} (U(\mathbf{k} + \mathbf{q}; \mathbf{k}) g_{\mathbf{k}+\mathbf{q}} (1 - g_{\mathbf{k}}) - U(\mathbf{k}; \mathbf{k} + \mathbf{q}) g_{\mathbf{k}} (1 - g_{\mathbf{k}+\mathbf{q}})), \quad (\text{D.2.4})$$

where

$$U(\mathbf{k} + \mathbf{q}; \mathbf{k}) = W_{\mathbf{q}}^0 [(n_{\mathbf{q}} + 1) \delta(\epsilon_{\mathbf{k}} + \omega_q - \epsilon_{\mathbf{k}+\mathbf{q}}) + n_{-\mathbf{q}} \delta(\epsilon_{\mathbf{k}} - \omega_q - \epsilon_{\mathbf{k}+\mathbf{q}})], \quad (\text{D.2.5})$$

$$U(\mathbf{k}; \mathbf{k} + \mathbf{q}) = W_{\mathbf{q}}^0 [(n_{-\mathbf{q}} + 1) \delta(\epsilon_{\mathbf{k}+\mathbf{q}} + \omega_q - \epsilon_{\mathbf{k}}) + n_{\mathbf{q}} \delta(\epsilon_{\mathbf{k}+\mathbf{q}} - \omega_q - \epsilon_{\mathbf{k}})], \quad (\text{D.2.6})$$

and $W_{\mathbf{q}}^0 = 4\pi |D(\mathbf{q})|^2$.

The details of the calculation is given in the references ([5, 27, 142]). Here we note that using the relation $U(\mathbf{k} + \mathbf{q}; \mathbf{k}) = e^{\beta \epsilon_{\mathbf{k}+\mathbf{q}}} e^{-\beta \epsilon_{\mathbf{k}}} U(\mathbf{k}; \mathbf{k} + \mathbf{q})$ and linearizing the Boltzmann equation by substituting $g_{\mathbf{k}} = f_{\mathbf{k}} + \delta g_{\mathbf{k}}$ and taking the equilibrium collision integral terms to be zero, the Eq. (D.2.4) can be reduced to,

$$\left(\frac{\partial g_{\mathbf{k}}}{\partial t} \right)_{\text{coll}} = \int d\mathbf{q} U(\mathbf{k}; \mathbf{k} + \mathbf{q}) \left\{ \delta g_{\mathbf{k}+\mathbf{q}} (e^{-\beta(\epsilon_{\mathbf{k}} - \epsilon_{\mathbf{k}+\mathbf{q}})} (1 - f_{\mathbf{k}}) + f_{\mathbf{k}}) - \delta g_{\mathbf{k}} (e^{-\beta(\epsilon_{\mathbf{k}} - \epsilon_{\mathbf{k}+\mathbf{q}})} f_{\mathbf{k}+\mathbf{q}} + (1 - f_{\mathbf{k}+\mathbf{q}})) \right\}. \quad (\text{D.2.7})$$

On further simplifications, the collision integral can be written as

$$\left(\frac{\partial g_{\mathbf{k}}}{\partial t} \right)_{\text{coll}} = \beta \int d\mathbf{q} W_{\mathbf{q}}^0 n_{\mathbf{q}} \left\{ f_{\mathbf{k}+\mathbf{q}} (1 - f_{\mathbf{k}}) \delta(\epsilon_{\mathbf{k}+\mathbf{q}} + \omega_q - \epsilon_{\mathbf{k}}) + f_{\mathbf{k}} (1 - f_{\mathbf{k}+\mathbf{q}}) \delta(\epsilon_{\mathbf{k}+\mathbf{q}} - \omega_q - \epsilon_{\mathbf{k}}) \right\} (\delta\phi(\mathbf{k} + \mathbf{q}) - \delta\phi(\mathbf{k})), \quad (\text{D.2.8})$$

where $\delta\phi(\mathbf{k}) = \frac{\delta g_{\mathbf{k}}}{\beta f_{\mathbf{k}}(1 - f_{\mathbf{k}})}$.

As explained in the impurity scattering case that the calculation is done by an iterative procedure, where one introduces

$$\delta\phi(k) = \frac{k_x}{m} C(\epsilon_k). \quad (\text{D.2.9})$$

From Eqs. (D.2.8) and (D.2.9), we have

$$\begin{aligned} \frac{k_x}{m} \left(\frac{\partial f_k}{\partial T} \right) (\nabla T)_x &= \left(\frac{\partial g_k}{\partial t} \right)_{\text{coll}} \\ &= \frac{4\pi}{mT} \int d\mathbf{q} |D(\mathbf{q})|^2 n_{\mathbf{q}} \{ f_{\mathbf{k}+\mathbf{q}}(1 - f_{\mathbf{k}}) \delta(\epsilon_{\mathbf{k}+\mathbf{q}} + \omega_{-\mathbf{q}} - \epsilon_{\mathbf{k}}) \\ &\quad + f_{\mathbf{k}}(1 - f_{\mathbf{k}+\mathbf{q}}) \delta(\epsilon_{\mathbf{k}+\mathbf{q}} - \omega_{\mathbf{q}} - \epsilon_{\mathbf{k}}) \} \\ &\quad \{ (k_x + q_x) C(\epsilon_{\mathbf{k}+\mathbf{q}}) - k_x C(\epsilon_{\mathbf{k}}) \}. \end{aligned} \quad (\text{D.2.10})$$

On inserting the phonon matrix element, solving the angular integrals and introducing the dimensionless variables $\frac{\epsilon_{\mathbf{k}} - \mu}{T} = \eta$ and $\frac{\omega_{\mathbf{q}}}{T} = y$, the collision integral reduces to

$$\begin{aligned} \left(\frac{\partial g_k}{\partial t} \right)_{\text{coll}} &= -\frac{1}{2\pi m_i N \rho_F^2 (2m)^{1/2}} \epsilon^{-3/2} k_x \frac{\partial f_k}{\partial \epsilon} \left(\frac{T}{\Theta_D} \right)^3 \frac{q_D^4}{\Theta_D} \int_0^{\Theta_D/T} dy \frac{y^2}{e^y - 1} \\ &\quad \left\{ \frac{e^\eta + 1}{e^{\eta-y} + 1} \left[\left(\epsilon - \frac{1}{2} D \left(\frac{T}{\Theta_D} \right)^2 y^2 - \frac{1}{2} T y \right) C(\eta - y) - \epsilon C(\eta) \right] \right. \\ &\quad \left. + \frac{e^y (e^\eta + 1)}{e^{\eta+y} + 1} \left[\left(\epsilon - \frac{1}{2} D \left(\frac{T}{\Theta_D} \right)^2 y^2 + \frac{1}{2} T y \right) C(\eta + y) - \epsilon C(\eta) \right] \right\}. \end{aligned} \quad (\text{D.2.11})$$

Here $D = \frac{q_D^2}{2m}$. On further simplifications, the above expression can be written as

$$\begin{aligned} -\frac{k_x}{m} \eta \left(\frac{\partial f_k}{\partial \epsilon} \right) (\nabla T)_x &= \left(\frac{\partial g_k}{\partial t} \right)_{\text{coll}} \\ &= -\frac{k_x}{2\pi m_i N \rho_F^2 (2m)^{1/2}} \frac{\epsilon^{-3/2}}{\partial \epsilon} \left(\frac{T}{\Theta_D} \right)^3 \frac{q_D^4}{\Theta_D} \int_{-\Theta_D/T}^{\Theta_D/T} dy \frac{y^2}{|e^y - 1|} \\ &\quad \times \frac{e^\eta + 1}{e^{\eta+y} + 1} \left[\left(\epsilon - \frac{1}{2} D \left(\frac{T}{\Theta_D} \right)^2 y^2 + \frac{1}{2} T y \right) C(\eta + y) \right. \\ &\quad \left. - \epsilon C(\eta) \right]. \end{aligned} \quad (\text{D.2.12})$$

In the above Eq. (D.2.12), the contribution from the terms with odd power in z vanishes. Thus on simplification, we have

$$\frac{2\pi m_i N \rho_F^2 \epsilon_F^{1/2} (2m)^{1/2} \Theta_D}{m q_D^4} \left(\frac{\Theta_D}{T}\right)^3 \eta (\nabla T)_x = \int_{-\Theta_D/T}^{\Theta_D/T} dy \frac{y^2}{|e^y - 1|} \frac{e^\eta + 1}{e^{\eta+y} + 1} \left[\left(1 - \frac{D}{2\epsilon_F} \left(\frac{T}{\Theta_D}\right)^2 y^2\right) C(\eta + y) - C(\eta) \right]. \quad (\text{D.2.13})$$

In the high temperature limit i.e. $T \gg \Theta_D$, the term within the bracket in Eq. (D.2.13) with T^2 contributes more than the others terms and in the case $\eta \gg y$, the $C(\eta)$ can be approximated as

$$C(\eta) \approx -\frac{16\pi m_i \rho_F^2 N \epsilon_F^{3/2} (2m)^{1/2} \Theta_D}{m D q_D^4} \left(\frac{\Theta_D}{T}\right) \eta (\nabla T)_x. \quad (\text{D.2.14})$$

The thermal current is defined as

$$\begin{aligned} J_Q &= 2 \int \frac{d\mathbf{k}}{(2\pi)^3} v_{\mathbf{k}} (\epsilon_{\mathbf{k}} - \mu) \delta g_{\mathbf{k}} \\ &= \frac{2k_F^3}{\pi^2} \int d\eta \eta C(\eta) \frac{\partial f_{\mathbf{k}}}{\partial \eta}. \end{aligned} \quad (\text{D.2.15})$$

Substituting the value of $C(\eta)$ and using the relation $J_Q = -\kappa(\nabla T)_x$, we find that the thermal conductivity in high temperature regime becomes

$$\begin{aligned} \kappa(T) &\approx \frac{8\pi k_F^6 m_i \rho_F^2 \Theta_D^2 N}{3 q_D^6 m^2} \\ \text{i.e. } \kappa(T) &= \text{constant}. \end{aligned} \quad (\text{D.2.16})$$

Now in the case of low temperature ($T \ll \Theta_D$), the right hand side of Eq. (D.2.13) can be written as

$$\int_{-\Theta_D/T}^{\Theta_D/T} dy \frac{y^2}{|e^y - 1|} \frac{e^\eta + 1}{e^{\eta+y} + 1} [C(\eta + y) - C(\eta)]. \quad (\text{D.2.17})$$

The above Eq. can be solved by variational method [142]. Following the reference [142], in the low temperature limit, we can write,

$$C(\eta) = -\frac{4\pi \Theta_D \epsilon_F^{1/2} \rho_F^2 m_i N}{3m q_D^4} \left(\frac{\Theta_D}{T}\right)^3 \eta (\nabla T)_x. \quad (\text{D.2.18})$$

Substituting the above Eq. (D.2.18) in (D.2.15), we observe that the thermal conductivity shows a temperature dependence of the following form

$$\begin{aligned} \kappa(T) &\approx \frac{2}{125} \frac{\pi^3 k_F^4 m_i \rho_F^2 \Theta_D^4 N}{m^2 q_D^4} \\ \kappa(T) &\propto T^{-2}. \end{aligned} \quad (\text{D.2.19})$$

Thus, we see that the thermal conductivity in the case of electron-phonon interaction shows inverse square temperature dependence in the low temperature regime and saturates to a constant value in the high temperature regime within the Bloch-Boltzmann approach and this agrees qualitatively with our calculation using the memory function formalism.

Appendix E

Calculation of inner product of the current with its time derivative

To calculate the inner product of the current with its derivative, consider that the ensemble average of current operators at same time argument is represented by

$$\langle J|J \rangle = C \quad (\text{E.0.1})$$

where C is some constant.

Now, differentiate above equation w.r.t. time

$$\begin{aligned} \langle \dot{J}|J \rangle + \langle J|\dot{J} \rangle &= 0 \\ \langle \dot{J}|J \rangle &= -\langle J|\dot{J} \rangle. \end{aligned} \quad (\text{E.0.2})$$

In another way, the ensemble average of J and \dot{J} can be expressed as

$$\begin{aligned} \langle \dot{J}|J \rangle &= \text{tr}(\rho[H, J]J) \\ &= \text{tr}(\rho H J J) - \text{tr}(\rho J H J) \\ &= \text{tr}(\rho J[H, J]) \\ &= \langle J|\dot{J} \rangle. \end{aligned} \quad (\text{E.0.3})$$

From equations (E.0.1) and (E.0.2), we conclude that $\langle J|\dot{J} \rangle = 0$.

Appendix F

Detailed calculation of the higher order contribution

To calculate $\langle\langle \ddot{J}; \ddot{J} \rangle\rangle_z$ we first calculate the first term of Eq. (6.3.3). For this we need $[[J, H_{\text{imp}}], H_0]$ which using Eq. (2.1.2) and (6.2.4) becomes,

$$[[J, H_{\text{imp}}], H_0] = \frac{1}{N} \sum_{j, \mathbf{k}, \mathbf{k}'} \langle \mathbf{k} | U^j | \mathbf{k}' \rangle (v_x(\mathbf{k}) - v_x(\mathbf{k}')) (\epsilon_{\mathbf{k}'} - \epsilon_{\mathbf{k}}) c_{\mathbf{k}}^\dagger c_{\mathbf{k}'}. \quad (\text{F.0.1})$$

Using the above expression, the first term of Eq. (6.3.3) becomes

$$\begin{aligned} &= \frac{1}{N^2} \sum_{j, \mathbf{k}, \mathbf{k}'} \sum_{i, \mathbf{p}, \mathbf{p}'} \langle \mathbf{k} | U^j | \mathbf{k}' \rangle \langle \mathbf{p} | U^i | \mathbf{p}' \rangle (v_x(\mathbf{k}) - v_x(\mathbf{k}')) (v_x(\mathbf{p}) - v_x(\mathbf{p}')) \\ &\quad \times (\epsilon_{\mathbf{k}'} - \epsilon_{\mathbf{k}}) (\epsilon_{\mathbf{p}'} - \epsilon_{\mathbf{p}}) \langle\langle c_{\mathbf{k}}^\dagger c_{\mathbf{k}'}; c_{\mathbf{p}}^\dagger c_{\mathbf{p}'} \rangle\rangle_z. \end{aligned} \quad (\text{F.0.2})$$

Here again we will consider the case of $i = j$ as considered in Eq. (6.2.7) and using Eq. (6.1.1) with performing time integration and ensemble average, the above equation reduces to

$$= \frac{2N_{\text{imp}}}{N^2} \sum_{\mathbf{k}, \mathbf{k}'} |\langle \mathbf{k} | U | \mathbf{k}' \rangle|^2 (v_x(\mathbf{k}) - v_x(\mathbf{k}'))^2 (\epsilon_{\mathbf{k}} - \epsilon_{\mathbf{k}'})^2 \frac{f(\mathbf{k}) - f(\mathbf{k}')}{z + \epsilon_{\mathbf{k}} - \epsilon_{\mathbf{k}'}}. \quad (\text{F.0.3})$$

This expression is further simplified by converting summations into energy integrals and ignoring the momentum dependence of U as

$$= \frac{2}{3} N_{\text{imp}} \frac{U^2 m^2}{\pi^4} \int_0^\infty d\epsilon \int_0^\infty d\epsilon' \sqrt{\epsilon\epsilon'} (\epsilon + \epsilon') (\epsilon - \epsilon')^2 \frac{f(\epsilon) - f(\epsilon')}{z + \epsilon - \epsilon'}. \quad (\text{F.0.4})$$

Now we perform the calculations for the second term of Eq. (6.3.3). First, $[[J, H_{\text{imp}}], H_{\text{imp}}]$ using Eq. (3.2.1) and (6.2.4) is written as

$$\begin{aligned} [[J, H_{\text{imp}}], H_{\text{imp}}] &= \frac{1}{N^2} \sum_{j, \mathbf{k}, \mathbf{k}'} \sum_{i, \mathbf{p}, \mathbf{p}'} \langle \mathbf{k} | U^j | \mathbf{k}' \rangle \langle \mathbf{p} | U^i | \mathbf{p}' \rangle (v_x(\mathbf{k}) - v_x(\mathbf{k}')) \left[c_{\mathbf{k}}^\dagger c_{\mathbf{k}'}, c_{\mathbf{p}}^\dagger c_{\mathbf{p}'} \right] \\ &= \frac{N_{\text{imp}}}{N^2} \sum_{\mathbf{k}, \mathbf{k}', \mathbf{p}} \langle \mathbf{k} | U | \mathbf{k}' \rangle \langle \mathbf{k}' | U | \mathbf{p} \rangle (v_x(\mathbf{k}) - 2v_x(\mathbf{k}') + v_x(\mathbf{p})) c_{\mathbf{k}}^\dagger c_{\mathbf{p}}. \end{aligned} \quad (\text{F.0.5})$$

Using this, $\langle \langle [[J, H_{\text{imp}}], H_{\text{imp}}]; [[J, H_{\text{imp}}], H_{\text{imp}}] \rangle \rangle_z$ can be written as

$$\begin{aligned} &= 2 \frac{N_{\text{imp}}^2}{N^4} \sum_{\mathbf{k}, \mathbf{k}', \mathbf{p}} \sum_{\mathbf{r}, \mathbf{r}', \mathbf{l}} \langle \mathbf{k} | U | \mathbf{k}' \rangle \langle \mathbf{k}' | U | \mathbf{p} \rangle \langle \mathbf{r} | U | \mathbf{r}' \rangle \langle \mathbf{r}' | U | \mathbf{l} \rangle (v_x(\mathbf{k}) - 2v_x(\mathbf{k}') + v_x(\mathbf{p})) \\ &\quad (v_x(\mathbf{r}) - 2v_x(\mathbf{r}') + v_x(\mathbf{l})) \langle \langle c_{\mathbf{k}}^\dagger c_{\mathbf{p}}; c_{\mathbf{r}}^\dagger c_{\mathbf{l}} \rangle \rangle_z. \end{aligned} \quad (\text{F.0.6})$$

After calculating $\langle \langle c_{\mathbf{k}}^\dagger c_{\mathbf{p}}; c_{\mathbf{r}}^\dagger c_{\mathbf{l}} \rangle \rangle_z$ with help of Eq. (6.1.1) and substituting in Eq. (F.0.6) and taking U as independent of momentum, $\langle \langle [[J, H_{\text{imp}}], H_{\text{imp}}]; [[J, H_{\text{imp}}], H_{\text{imp}}] \rangle \rangle_z$ can be expressed as

$$= 2 \frac{N_{\text{imp}}^2 U^4}{N^4 m^2} \sum_{\mathbf{k}, \mathbf{k}', \mathbf{p}, \mathbf{r}'} \frac{1}{z + \epsilon_{\mathbf{k}} - \epsilon_{\mathbf{p}}} (k_x - 2k'_x + p_x) (p_x - 2r'_x + k_x) (f_{\mathbf{k}} - f_{\mathbf{p}}). \quad (\text{F.0.7})$$

After doing algebra, the above expression can be written as

$$= \frac{2 N_{\text{imp}}^2 U^4 m^2}{3 \pi^4} \int_0^\infty d\epsilon \int_0^\infty d\epsilon' \sqrt{\epsilon \epsilon'} (\epsilon + \epsilon') \frac{f(\epsilon) - f(\epsilon')}{z + \epsilon - \epsilon'}. \quad (\text{F.0.8})$$

Substituting Eqs. (F.0.4) and (F.0.8) in Eq. (6.3.3), we have

$$\begin{aligned} \langle \langle \ddot{J}; \ddot{J} \rangle \rangle_z &= \frac{2 N_{\text{imp}} U^2 m^2}{3 \pi^4} \int_0^\infty d\epsilon \int_0^\infty d\epsilon' \sqrt{\epsilon \epsilon'} (\epsilon + \epsilon') (\epsilon - \epsilon')^2 \frac{f(\epsilon) - f(\epsilon')}{z + \epsilon - \epsilon'} \\ &\quad + \frac{2 N_{\text{imp}}^2 U^4 m^2}{3 \pi^4} \int_0^\infty d\epsilon \int_0^\infty d\epsilon' \sqrt{\epsilon \epsilon'} (\epsilon + \epsilon') \frac{f(\epsilon) - f(\epsilon')}{z + \epsilon - \epsilon'}. \end{aligned} \quad (\text{F.0.9})$$

Appendix G

Integrals

The analytic closed form of the integrals mentioned in the different chapters has been calculated by Mathematica and is given as follows with the reference of the equation number(as in the relevant chapter). Here, we have expressed the integral in the form of A(y) and B(x,y) functions which we defined as:

$$A_n(y) = \sum_{m=1}^n (-1)^{m+1} \left(\frac{d^m}{dy^m} y^n \right) \left(\frac{d^{n-m}}{dy^{n-m}} Li_n(e^y) \right). \quad (\text{G.0.1})$$

$$B_n(x, y) = \sum_{m=1}^n (-1)^{m+1} \left(\frac{d^m}{dy^m} y^n \right) \left(\frac{d^{n-m}}{dy^{n-m}} Li_n(e^{x+y}) \right). \quad (\text{G.0.2})$$

$$C_n(y) = \sum_{m=1}^n (-1)^{m+1} \left(\frac{d^m}{dy^m} y^n \right) \left(\frac{d^{n-m}}{dy^{n-m}} Li_n(e^{-1+y}) \right). \quad (\text{G.0.3})$$

1. Eq. (3.2.26)

$$\begin{aligned} I = & \frac{1}{6b^2x} \left[\left\{ -\frac{1}{8}b^2B_8 + \left(a^2 + b^2 \left(\frac{\pi^2}{3} + x^2 \right) \right) B_6 \right. \right. \\ & \left. \left. + \left(\frac{6}{5}a^2x + \frac{2}{5}b^2x(\pi^2 + x^2) \right) B_5 + \text{terms with } x \rightarrow -x \right\} \right. \\ & \left. - \frac{4}{5}x \left\{ 3a^2 + b^2(\pi^2 + x^2) \right\} A_5 \right]. \quad (\text{G.0.4}) \end{aligned}$$

2. Eq. (3.2.27)

$$I = \frac{1}{6} \left\{ \frac{-y^4 e^y}{-1 + e^y} \left(\frac{6a^2}{b^2} + 2\pi^2 + y^2 \right) - \left(\frac{a^2}{b^2} + 2\pi^2 \right) A_4 - A_6 \right\} (\text{G.0.5})$$

3. Eq. (4.2.31)

$$I = b^2 \left\{ \frac{1}{7}(A_7 - C_7) - \frac{1}{3}(A_6 - C_6) + \frac{1}{5}(A_5 - 2C_5) \right\} \\ + a^2 \left\{ \frac{2}{5}(A_5 - C_5) - \frac{1}{2}(A_4 - C_4) \right\}. \quad (\text{G.0.6})$$

4. Eq. (5.1.6)

$$I = \left\{ \frac{1}{9}B_9 + \frac{3}{4}xB_8 + \frac{1}{7}(9x^2 + 4\pi^2 + a^2)B_7 + \frac{x}{6}(4x^2 + 4\pi^2 - a^2)B_6 \right. \\ \left. - \frac{2a^2}{5}(9x^2 + 4\pi^2 + 3a^2)B_5 - \frac{a^2x}{2}(4x^2 + 4\pi^2 - 3a^2)B_4 \right. \\ \left. + (\text{terms with } x \rightarrow -x) \right\} \\ - \frac{3}{2}xA_8 + \frac{1}{3}x(9a^2 - 4\pi^2 - 4x^2)A_6 + a^2x(4x^2 + 4\pi^2 + 3a^2)A_4. \quad (\text{G.0.7})$$

5. Eq. (5.1.7)

$$I = -\frac{1}{24a^2} \left\{ \frac{-y^4(-2a^2 + y^2)(3a^2 + 4\pi^2y^2)}{-1 + e^y} + 2a^2(3a^2 + 4\pi^2) \frac{1}{4} (y^4 + A_4) \right. \\ \left. - (a^2 + 3\pi^2) \frac{1}{6} (y^6 + A_6) - \frac{1}{8} (y^8 + A_8) \right\}. \quad (\text{G.0.8})$$

6. Eq. (5.1.10)

$$I = -\frac{1}{4} (y^4 + A_4) + \frac{1}{12a^2} (y^6 + A_6). \quad (\text{G.0.9})$$

7. Zeta function

$$\zeta(x) = \frac{1}{\Gamma(x)} \int_0^\infty \frac{u^{x-1}}{e^u - 1} du \quad (\text{G.0.10})$$

where $\Gamma(x)$ is the gamma function. If x is an integer n ,

$$\zeta(n) = \frac{1}{\Gamma(n)} \int_0^\infty \frac{u^{n-1}}{e^u - 1} du \\ = \frac{1}{\Gamma(n)} \int_0^\infty \sum_{k=1}^\infty e^{-ku} u^{n-1} du \\ = \sum_{k=1}^\infty \frac{1}{k^n} \quad (\text{G.0.11})$$

Bibliography

- [1] P. Drude, *Annalen der Physik* **308**, 369 (1900).
- [2] D. A. Greenwood, *Proceedings of the Physical Society* **71**, 585 (1958).
- [3] J. M. Ziman, *Electrons and Phonons: the theory of transport phenomenon in solids* (Clarendon Press, Oxford, 1960).
- [4] J. M. Ziman, *Principles of the theory of solids* (Cambridge University Press, Cambridge, 1979).
- [5] A. H. Wilson, *The Theory of Metals* (Cambridge University Press, Cambridge, 1953).
- [6] H. Mori, *Progress of Theoretical Physics* **34**, 399 (1965).
- [7] R. Zwanzig, *Phys. Rev.* **124**, 983 (1961).
- [8] R. Zwanzig, *Lectures in Theoretical Physics*, vol. 3 (Interscience, New York, 1961).
- [9] H. Mori, *Progress of Theoretical Physics* **33**, 423 (1965).
- [10] G. D. Harp and B. J. Berne, *Phys. Rev. A* **2**, 975 (1970).
- [11] R. Zwanzig, *Nonequilibrium Statistical Mechanics* (Oxford University Press, US, 2001).
- [12] D. Forster, *Hydrodynamic Fluctuations, Broken Symmetry and Correlation Functions* (Advanced Book Classics, Addison-Wesley, Boston, 1995).

- [13] P. Fulde, *Correlated Electrons in Quantum Matter* (World Scientific, Singapore, 2012).
- [14] K. Behnia, *Fundamentals of Thermoelectricity* (Oxford University Press, UK, 2015).
- [15] K. Huang, *Statistical Mechanics* (Wiley, New York, 1987).
- [16] D. M. V. Zubarev and R. G., *Statistical Mechanics of Nonequilibrium Processes*, vol. 1: Basic concepts, kinetic theory (Akademie Verlag, Berlin, 1996).
- [17] N. Ashcroft and N. Mermin, *Solid state physics*, Science: Physics (Saunders College, 1976).
- [18] O. Madelung, *Introduction to Solid State Theory* (Springer, Berlin, 1978).
- [19] C. Kittel, *Introduction to Solid State Physics* (John Wiley and Sons, 2005).
- [20] T. M. Tritt, *Thermal Conductivity: theory, properties, and applications* (Kluwer Academic / Plenum Publishers, 2004).
- [21] G. Wiedemann and R. Franz, *Annalen der Physik* **165**, 497 (1853).
- [22] N. Pottier, *Nonequilibrium Statistical Physics, Linear Irreversible Processes* (Oxford University Press, 2010).
- [23] L. D. Landau and E. M. Lifshitz, *Quantum Mechanics* (Addison-Wesley, Reading Mass., 1965).
- [24] G. D. Mahan, *Many-Particle Physics, 2nd ed.* (Plenum, New York/London, 1990).
- [25] W. Kohn and J. M. Luttinger, *Phys. Rev.* **108**, 590 (1957).
- [26] J. M. Luttinger and W. Kohn, *Phys. Rev.* **109**, 1892 (1958).
- [27] N. Singh, *Electronic Transport Theories: From Weakly to Strongly Correlated Materials* (Taylor and Francis Group, CRC Press, Boca Raton, 2016).

- [28] G. D. Mahan, *Condensed Matter in a Nutshell* (Princeton University Press, Princeton, 2010).
- [29] H. M. Rosenberg, *Philosophical Transactions of the Royal Society of London A: Mathematical, Physical and Engineering Sciences* **247**, 441 (1955).
- [30] P. G. Klemens, *Canadian Journal of Physics* **34**, 1212 (1956).
- [31] J. M. Ziman, *Proceedings of the Royal Society of London A: Mathematical, Physical and Engineering Sciences* **226**, 436 (1954).
- [32] E. H. Sondheimer, *Proceedings of the Royal Society A* **203**, 565 (1950).
- [33] E. Grneisen, *Annalen der Physik* **408**, 530 (1933).
- [34] M. Blackman, *Handbook of Physics*, vol. 7/1 (Springer Verlag, Berlin, 1955).
- [35] A. S. T. Pires, *Helvetica Physica Acta* **61**, 988 (1988).
- [36] E. Lange, *Phys. Rev. B* **55**, 3907 (1997).
- [37] A. A. Patel and S. Sachdev, *Phys. Rev. B* **90**, 165146 (2014).
- [38] M. Kubo, R. Toda and H. N., *Statistical Physics II: Nonequilibrium Statistical Mechanics* (Springer Verlag, Berlin, 1978).
- [39] A. A. Khamzin, R. R. Nigmatullin, and I. I. Popov, *Journal of Physics: Conference Series* **394**, 012013 (2012).
- [40] M. D. Buishvili, L. L. Zviadadze and E. K. Khalvashi, *Zh. Éksp. Teor. Fiz.* **91**, 310 (1986).
- [41] A. Pires and M. Gouvêa, *Brazilian Journal of Physics* **34**, 1189 (2004).
- [42] G. Viswanath, V. S. Müller, *The Recursion Method: Application to Many-Body Dynamics* (Springer Verlag, Heidelberg, 1994).
- [43] W. Schimacher, *Theory of Liquids and Other Disordered Media* (Springer, Berlin, 2015).

- [44] A. Rosch and N. Andrei, *Phys. Rev. Lett.* **85**, 1092–1095 (2000).
- [45] E. Shimshoni, N. Andrei, and A. Rosch, *Phys. Rev. B* **68**, 104401 (2003).
- [46] I. Kupčić, *Physica B: Condensed Matter* **344**, 27 (2004).
- [47] S. A. Hartnoll, P. K. Kovtun, M. Müller, and S. Sachdev, *Phys. Rev. B* **76**, 144502 (2007).
- [48] S. A. Hartnoll and C. P. Herzog, *Phys. Rev. D* **77**, 106009 (2008).
- [49] A. Garg, D. Rasch, E. Shimshoni, and A. Rosch, *Phys. Rev. Lett.* **103**, 096402 (2009).
- [50] S. A. Hartnoll and D. M. Hofman, *Phys. Rev. Lett.* **108**, 241601 (2012).
- [51] R. Mahajan, M. Barkeshli, and S. A. Hartnoll, *Phys. Rev. B* **88**, 125107 (2013).
- [52] I. Kupčić, *Phys. Rev. B* **95**, 035403 (2017).
- [53] M. W. Evans, G. J. Evans, W. T. Coffey, and P. Grigolini, *Molecular Dynamics* (Wiley, New York, 1982).
- [54] A. Lucas, *Journal of High Energy Physics* **2015**, 1 (2015).
- [55] A. Lucas and S. Sachdev, *Phys. Rev. B* **91**, 195122 (2015).
- [56] W. Götze and P. Wölfle, *Phys. Rev. B* **6**, 1226 (1972).
- [57] N. Das, P. Bhalla, and N. Singh, *Int. J. Mod. Phys. B* **30**, 1630015 (2016).
- [58] A. Hartnoll, Sean A. Lucas and S. Sachdev (2016).
- [59] L. P. Kadanoff and P. C. Martin, *Annals of Physics* **24**, 419 (1963).
- [60] D. N. Zubarev, *Physics-Uspekhi* **3**, 320 (1960).
- [61] B. Arfi, *Phys. Rev. B* **45**, 2352 (1992).
- [62] P. Bhalla and N. Singh, *The European Physical Journal B* **89**, 1 (2016).
- [63] P. B. Allen, *Phys. Rev. B* **3**, 305 (1971).

- [64] S. G. Sharapov and J. P. Carbotte, *Phys. Rev. B* **72**, 134506 (2005).
- [65] S. Shulga, O. Dolgov, and E. Maksimov, *Physica C: Superconductivity* **178**, 266 (1991).
- [66] B. Mitrović and M. A. Fiorucci, *Phys. Rev. B* **31**, 2694 (1985).
- [67] J. Hwang, *Phys. Rev. B* **83**, 014507 (2011).
- [68] J. Hwang and J. P. Carbotte, *Phys. Rev. B* **86**, 094502 (2012).
- [69] P. Bhalla and N. Singh, *The European Physical Journal B* **87**, 1 (2014).
- [70] Y. M. Dai, B. Xu, P. Cheng, H. Q. Luo, H. H. Wen, X. G. Qiu, and R. P. S. M. Lobo, *Phys. Rev. B* **85**, 092504 (2012).
- [71] Y. S. Lee, K. Segawa, Z. Q. Li, W. J. Padilla, M. Dumm, S. V. Dordevic, C. C. Homes, Y. Ando, and D. N. Basov, *Phys. Rev. B* **72**, 054529 (2005).
- [72] T. Holstein, *Phys. Rev.* **96**, 535 (1954).
- [73] R. R. Joyce and P. L. Richards, *Phys. Rev. Lett.* **24**, 1007 (1970).
- [74] D. Cao, F. Bridges, G. R. Kowach, and A. P. Ramirez, *Phys. Rev. Lett.* **89**, 215902 (2002).
- [75] A. L. Chernyshev and W. Brenig, *Phys. Rev. B* **92**, 054409 (2015).
- [76] A. Jain and A. J. H. McGaughey, *Phys. Rev. B* **93**, 081206 (2016).
- [77] G. Romano, K. Esfarjani, D. A. Strubbe, D. Broido, and A. M. Kolpak, *Phys. Rev. B* **93**, 035408 (2016).
- [78] S. G. Volz, *Phys. Rev. Lett.* **87**, 074301 (2001).
- [79] P. Bhalla, P. Kumar, N. Das, and N. Singh, *Phys. Rev. B* **94**, 115114 (2016).
- [80] Y. K. Koh and D. G. Cahill, *Phys. Rev. B* **76**, 075207 (2007).
- [81] B. S. Shastry, *Phys. Rev. B* **73**, 085117 (2006).
- [82] B. S. Shastry, *Reports on Progress in Physics* **72**, 016501 (2009).

- [83] A. Dhar, O. Narayan, A. Kundu, and K. Saito, *Phys. Rev. E* **83**, 011101 (2011).
- [84] Y. Ezzahri and K. Joulain, *Journal of Applied Physics* **112**, 083515 (2012).
- [85] F. Yang and C. Dames, *Phys. Rev. B* **91**, 165311 (2015).
- [86] P. G. Klemens, *Thermal Conductivity of Solids at Low Temperatures*, vol. 14 (Springer-Verlag, Berlin, 1956).
- [87] F. Seitz and D. Turnbull, *Solid State Physics, Advances in Research and Applications*, vol. 4 (Academic Press, New York, 1957).
- [88] E. S. Snyder, G. J. Toberer, *Nature Materials* **7**, 105 (2008).
- [89] J.-C. Zheng, *Frontiers of Physics in China* **3**, 269 (2008).
- [90] D. G. Bulusu A, Walker, *Superlattices and Microstructures* **44**, 1 (2008).
- [91] D. M. Rowe, *Thermoelectrics Handbook: Macro to nano* (CRC, Boca Raton, FL, USA, 2006).
- [92] A. Shakouri, *Annual Review of Materials Research* **41**, 399 (2011).
- [93] M. Zebarjadi, K. Esfarjani, M. S. Dresselhaus, Z. F. Ren, and G. Chen, *Energy Environ. Sci.* **5**, 5147 (2012).
- [94] Y. Ezzahri and K. Joulain, *Journal of Applied Physics* **115**, 223703 (2014).
- [95] P. Bhalla, N. Das, and N. Singh, *Physics Letters A* **380**, 2000 (2016).
- [96] N. Das and N. Singh, *Int. J. Mod. Phys. B* **30**, 1650071 (2016).
- [97] R. Kubo, *Journal of the Physical Society of Japan* **12**, 570 (1957).
- [98] K. S. Geim, A. K. Novoselov, *Nature Materials* **6**, 183 (2007).
- [99] A. H. Castro Neto, F. Guinea, N. M. R. Peres, K. S. Novoselov, and A. K. Geim, *Rev. Mod. Phys.* **81**, 109 (2009).
- [100] Y.-W. Tan, Y. Zhang, K. Bolotin, Y. Zhao, S. Adam, E. H. Hwang, S. Das Sarma, H. L. Stormer, and P. Kim, *Phys. Rev. Lett.* **99**, 246803 (2007).

- [101] E. H. Hwang, B. Y.-K. Hu, and S. Das Sarma, *Phys. Rev. B* **76**, 115434 (2007).
- [102] E. H. Hwang, S. Adam, and S. D. Sarma, *Phys. Rev. Lett.* **98**, 186806 (2007).
- [103] S. Adam, E. H. Hwang, V. M. Galitski, and S. D. Sarma, *Proceedings of the National Academy of Sciences of the United States of America* **104**, 18392 (2007).
- [104] S. Adam and S. Das Sarma, *Phys. Rev. B* **77**, 115436 (2008).
- [105] E. H. Hwang and S. Das Sarma, *Phys. Rev. B* **77**, 195412 (2008).
- [106] E. H. Hwang, E. Rossi, and S. Das Sarma, *Phys. Rev. B* **80**, 235415 (2009).
- [107] S. D. Sarma and K. Yang, *Solid State Communications* **149**, 1502 (2009).
- [108] E. H. Hwang and S. Das Sarma, *Phys. Rev. B* **79**, 165404 (2009).
- [109] N. M. R. Peres, *Rev. Mod. Phys.* **82**, 2673 (2010).
- [110] D. Abergel, V. Apalkov, J. Berashevich, K. Ziegler, and T. Chakraborty, *Advances in Physics* **59**, 261 (2010).
- [111] D. R. Cooper, B. D'Anjou, N. Ghattamaneni, B. Harack, M. Hilke, A. Horth, N. Majlis, M. Massicotte, L. Vandsburger, E. Whiteway, and V. Yu, *ISRN Condensed Matter Physics* (2012).
- [112] T. Zhu and E. Ertekin, *Phys. Rev. B* **91**, 205429 (2015).
- [113] T. Zhu and E. Ertekin, *Phys. Rev. B* **93**, 155414 (2016).
- [114] S. Das Sarma, S. Adam, E. H. Hwang, and E. Rossi, *Rev. Mod. Phys.* **83**, 407 (2011).
- [115] A. A. Balandin, S. Ghosh, W. Bao, I. Calizo, D. Teweldebrhan, F. Miao, and C. N. Lau, *Nano Letters* **8**, 902 (2008).
- [116] D. L. Nika and A. A. Balandin, *Journal of Physics: Condensed Matter* **24**, 233203 (2012).

- [117] D. L. Nika, E. P. Pokatilov, A. S. Askerov, and A. A. Balandin, *Phys. Rev. B* **79**, 155413 (2009).
- [118] S. Ghosh, I. Calizo, D. Teweldebrhan, E. P. Pokatilov, D. L. Nika, A. A. Balandin, W. Bao, F. Miao, and C. N. Lau, *Applied Physics Letters* **92**, 151911 (2008).
- [119] T. Y. Kim, C.-H. Park, and N. Marzari, *Nano Letters* **16**, 2439 (2016).
- [120] D. K. Efetov and P. Kim, *Phys. Rev. Lett.* **105**, 256805 (2010).
- [121] E. Munoz, *Journal of Physics: Condensed Matter* **24**, 195302 (2012).
- [122] E. H. Hwang and S. Das Sarma, *Phys. Rev. B* **77**, 115449 (2008).
- [123] T. Ando, *NPG Asia Mater* **1**, 17 (2009).
- [124] G. D. Sanders, A. R. T. Nugraha, K. Sato, J.-H. Kim, J. Kono, R. Saito, and C. J. Stanton, *Journal of Physics: Condensed Matter* **25**, 144201 (2013).
- [125] K. Kaasbjerg, K. S. Thygesen, and K. W. Jacobsen, *Phys. Rev. B* **85**, 165440 (2012).
- [126] B. Amorim and F. Guinea, *Phys. Rev. B* **88**, 115418 (2013).
- [127] R. Verma, S. Bhattacharya, and S. Mahapatra, *Semiconductor Science and Technology* **28**, 015009 (2013).
- [128] A. Principi and G. Vignale, *Phys. Rev. Lett.* **115**, 056603 (2015).
- [129] W. Götze and P. Wölfle, *Journal of Low Temperature Physics* **5**, 575 (1971).
- [130] N. Plakida, *Journal of the Physical Society of Japan* **65**, 3964 (1996).
- [131] N. Plakida, *Zeitschrift für Physik B Condensed Matter* **103**, 383 (1997).
- [132] A. A. Vladimirov, D. Ihle, and N. M. Plakida, *Phys. Rev. B* **85**, 224536 (2012).
- [133] I. Sega, P. Prelovšek, and J. Bonča, *Phys. Rev. B* **68**, 054524 (2003).
- [134] P. Prelovšek, I. Sega, and J. Bonča, *Phys. Rev. Lett.* **92**, 027002 (2004).

-
- [135] I. Sega and P. Prelovšek, Phys. Rev. B **79**, 140504 (2009).
- [136] I. Sega and P. Prelovšek, Phys. Rev. B **73**, 092516 (2006).
- [137] P. Prelovšek and I. Sega, Phys. Rev. B **74**, 214501 (2006).
- [138] P. F. Maldague, Phys. Rev. B **16**, 2437 (1977).
- [139] P. Grigolini, G. Grosso, G. P. Parravicini, and M. Sparpaglione, Phys. Rev. B **27**, 7342 (1983).
- [140] M. Dupuis, Progress of Theoretical Physics **37**, 502 (1967).
- [141] K. H. Bennemann and J. B. Ketterson, *Superconductivity*, vol. 1,2 (Heidelberg: Springer, 2008).
- [142] T. Kasuya, Progress of Theoretical Physics **13**, 561 (1955).

List of Publications

Publications in refereed journals

1. **Pankaj Bhalla**, Pradeep Kumar, Nabyendu Das and Navinder Singh:
Finite frequency Seebeck coefficient of metals: A memory function approach,
Journal of Physics and Chemistry of Solids, **109**, 31 (2017).
2. **Pankaj Bhalla**:
Role of acoustic phonons in frequency dependent thermal conductivity of graphene,
Phys. Lett. A **381**, 924 (2017).
3. **Pankaj Bhalla**, Pradeep Kumar, Nabyendu Das and Navinder Singh:
Theory of the Dynamical Thermal conductivity of Metals,
Phys. Rev. B, **94**, 115114 (2016).
4. Nabyendu Das, **Pankaj Bhalla** and Navinder Singh:
Memory Function Approach to Correlated Electron Transport: A Comprehensive Review,
International Journal of Modern Physics B, **30**, 1630015 (2016).
5. **Pankaj Bhalla**, Nabyendu Das and Navinder Singh:
Moment Expansion to the Memory Function for Generalized Drude Scattering rate,
Phys. Lett. A, **380**, 2000 (2016).
6. **Pankaj Bhalla** and Navinder Singh:
Generalized Drude Scattering rate from the memory function formalism: an independent verification of the Sharapov-Carbotte result,
Eur. Phys. J. B, **89**, 49 (2016).
7. **Pankaj Bhalla** and Navinder Singh:
Infrared properties of cuprates in the pseudogap state: A study of Mitrovic-

Fiorucci and Sharapov-Carbotte scattering rates,
Eur. Phys. J. B, **87**, 213 (2014).

Publications attached with thesis

1. **Pankaj Bhalla:**

Role of acoustic phonons in frequency dependent thermal conductivity of graphene,
Phys. Lett. A **381**, 924 (2017). doi: [10.1016/j.physleta.2017.01.006](https://doi.org/10.1016/j.physleta.2017.01.006)

2. **Pankaj Bhalla**, Pradeep Kumar, Nabyendu Das and Navinder Singh:

Theory of the Dynamical Thermal conductivity of Metals,
Phys. Rev. B, **94**, 115114 (2016). doi: [10.1103/PhysRevB.94.115114](https://doi.org/10.1103/PhysRevB.94.115114)

3. Nabyendu Das, **Pankaj Bhalla** and Navinder Singh:

Memory Function Approach to Correlated Electron Transport: A Comprehensive Review , International Journal of Modern Physics B, **30**, 1630015 (2016).
doi: [10.1142/S0217979216920028](https://doi.org/10.1142/S0217979216920028)

4. **Pankaj Bhalla**, Nabyendu Das and Navinder Singh:

Moment Expansion to the Memory Function for Generalized Drude Scattering rate, Phys. Lett. A, **380**, 2000 (2016). doi: [10.1016/j.physleta.2016.04.010](https://doi.org/10.1016/j.physleta.2016.04.010)

5. **Pankaj Bhalla** and Navinder Singh:

Generalized Drude Scattering rate from the memory function formalism: an independent verification of the Sharapov-Carbotte result, Eur. Phys. J. B, **89**, 49 (2016). doi: [10.1140/epjb/e2016-60799-9](https://doi.org/10.1140/epjb/e2016-60799-9)

Memory function approach to correlated electron transport: A comprehensive review

Nabyendu Das^{*,†,§}, Pankaj Bhalla^{†,‡,¶} and Navinder Singh^{†,||}

**Department of Physics, The LNM-Institute of Information Technology,
 Jaipur 302032, India*

*†Theoretical Physics Division, Physical Research Laboratory,
 Ahmedabad 380009, India*

‡Indian Institute of Technology, Gandhinagar-382355, India

§nabyendu@prl.res.in

¶pankajbhalla66@gmail.com

||navinder@prl.res.in

Received 17 March 2016

Accepted 27 June 2016

Published 25 August 2016

Memory function formalism or projection operator technique is an extremely useful method to study the transport and optical properties of various condensed matter systems. A recent revival of its uses in various correlated electronic systems is being observed. It is being used and discussed in various contexts, ranging from nonequilibrium dynamics to the optical properties of various strongly correlated systems such as high temperature superconductors. However, a detailed discussion on this method, starting from its origin to its present day applications at one place is lacking. In this paper, we attempt a comprehensive review of the memory function approach focusing on its uses in studying the dynamics and the transport properties of correlated electronic systems.

Keywords: Electronic conduction in metals; theory of electronic transport; scattering mechanisms; memory function formalism.

PACS numbers: 72.10.-d, 72.15.-v

1. Motivation

Condensed matter physics deals with the collective phenomena that emerge out of the mutual interactions between a large number of particles. Many of them are novel, i.e., are beyond the realm of pre-existent theories and almost none of them can have first principle microscopic explanations. Understanding such novel complex cooperative phenomena requires new physical ideas such as spontaneous symmetry breaking, Goldstone modes, renormalization of physical parameters etc.¹

[§]Corresponding author.

The basic principle of all such descriptions is adapting an effective description by separating the low energy slow degrees of freedom from the high energy faster degrees of freedom in a system of macroscopically large number of particles to study its low energy and long wavelength properties. Successes of such theories depend on how accurately one can develop an effective description of the effects of a large number of faster degrees of freedom on a few slower degrees of freedom which are experimentally probed in a certain physical system. As a result, these theories are dependent on some common aspects of the various systems, e.g., energy and each of them works well for a certain class of physical systems.²

Advent of the memory function formalism is a major theoretical progress in this line of thought. It was developed and is being used to study the dynamics and the transport properties of various complex many body systems.³⁻⁸ This technique relies on the idea of separating the slow and the faster degrees of freedom in a physical system and to systematically calculate the effects of the latter on the former. Separation of scales is a very familiar and essential concept in studying various physical systems. It is suitable in systems having finite number of slow modes related to the dynamics of conserved variables and/or the broken symmetry variables. Their studies are often termed as hydrodynamics and those slow modes are called hydrodynamic modes and soft modes, respectively.¹⁰

To illustrate the idea of separating the scales, we can choose a simple example, a particle moving in a fluid. In this case, when the particle moves, the fluid particles oppose its motion as depicted in Fig. 1. An attempt to build up a microscopic theory for this motion will require a Hamiltonian that describes the Coulomb interactions between all the atoms and electrons present in the total system. Then one can try to solve Poisson or Schrödinger equation respectively depending on whether the system is classical or quantum in nature. Such a microscopic attempt is not only impossible, also it is too complicated to capture the essential physical description of the system.¹ On the other hand, we can build up a simple description without compromising with the basic physics as follows. If the moving particle is macroscopically large and if the velocity of the center-of-mass is small compared to the

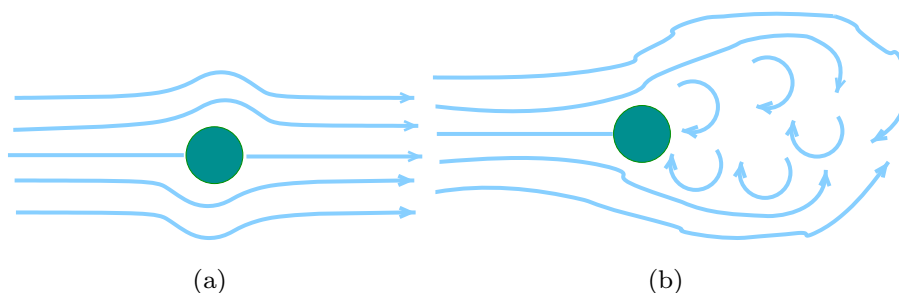


Fig. 1. (Color online) (a) We see viscous drag from the fluid molecules during a streamline flow, i.e., when an external particle of macroscopic size moves slowly inside the fluid. In this case, the time scales corresponding to the macro-particle and the fluid particles are nicely separable, (b) a turbulence sets in during a faster motion of a particle within fluid where such separation of scales is not possible.

velocity of the fluid molecules, we can separate or project out the center-of-mass coordinates from the rest of the degrees of freedom of the total system. In such a situation, we can write its effective equation of motion where the effects of the rest of the degrees of freedom can be termed as “molecular drag” on its motion. The latter can be incorporated through a drag force. This leads to a very simple and well known equation of motion of the dragged particle of the form,⁹

$$\ddot{\mathbf{R}} - \gamma \dot{\mathbf{R}} + \mathbf{F} = 0. \quad (1)$$

Here, \mathbf{R} is the position vector of the center-of-mass of the macroscopic particle of unit mass, $\dot{\mathbf{R}}$ and $\ddot{\mathbf{R}}$ represent its time derivative or the velocity and the acceleration respectively and \mathbf{F} is the external force. This is indeed a major simplification of a very complex system. The parameter γ is termed as friction coefficient, viscous coefficient, etc. depending on the contexts. It describes dissipation or the flow of energy and or momentum from the coherent to the incoherent degrees of freedom in a system. It can also be space and time dependent. However, when the velocity of the particle becomes comparable to that of the fluid molecules, as seen in part B of Fig. 1, turbulence sets in and the idea of separation of scales does not remain obvious.

Many such examples can be found in the vast literature on complex systems both in the classical and quantum domains. It is to be noted that there is no concept of dissipation in the microscopic principles. In an effective description of a physical system, we observe the system within our desired or convenient time scale and length scale. We thus ignore the complete distribution of energy which occurs over a larger time and length scales. Hence, we effectively observe dissipation of the momentum or energy of the particle as a result of the interaction with other fast degrees of freedom. The same picture emerges in various effective descriptions of interacting systems and the study of the low energy properties becomes synonymous to finding out the generalized dissipative constant or the scattering rates of the collective excitations. We will see in the later sections that the *Memory function approach* deals with systematic evaluations of the generalized dissipative constant (γ in Eq. (1)) related to the dynamics of generalized slow variables.

In this paper, we will first address the general aspects of the Memory function formalism in Sec. 2. We elaborate it further in Sec. 3 and in Sec. 4. In those sections, we present derivation of the generalized Langevin equation within this formalism and present a continued fraction representation of the dynamic correlation, respectively. In Sec. 5, we discuss its applications in various electronic systems. Finally in Sec. 6, we conclude.

2. Projectors and Memory Functions

Memory function technique was introduced by Zwanzig and Mori.³⁻⁷ The mathematical formalism used for systematic calculation of the memory function is also called projection operator method. Following Refs. 10 and 11, we summarize the

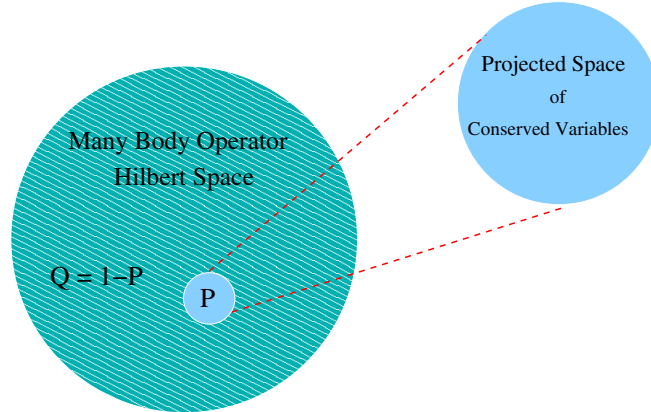


Fig. 2. (Color online) A schematic representation of the idea of projection in the memory function formalism. Here, the full big circle is the total many body operator Hilbert Space and is equivalent to identity. The projection of the full many body states defined by few operators representing conserved variables residing in the region P . On the other hand, the incoherent degrees of freedom lives in the part of the Hilbert space defined by $I - Q$.

idea of using projectors and the general mathematical setup for calculating the memory function. Let us start with a many body system having macroscopically large number, i.e., an Avogadro number ($\sim 10^{23}/cc$) of degrees of freedom and look for its macroscopic properties. Our system can be both classical and quantum in nature. A classical system is described by a set of variables comprising of the particles position and momentum variables. Such a set of position and momentum variables is called phase space. In the systems obeying quantum mechanics, a set of linearly independent operators do the same job. In that case, a mathematical space containing the set of operators forms a Hilbert space as depicted pictorially in the big green circle in Fig. 2. Now understanding the low energy consequences of the interactions between such a large number of variables or operators is extremely complicated, if not impossible. We need methods which eliminate the technical difficulties but capture the correct low energy physics.

Basic principle of the memory function formalism is as follows. Suppose we are interested in studying the center-of-mass motion of a system of N number of particles. Then we separate or project out the center-of-mass variable from the others. Here, the center-of-mass variable is a macroscopic variable and is defined as a linear combination of the microscopic variables. Now in memory function formalism, it is shown that the effects of the rest of the microscopic variables on the dynamics of the macroscopic variable can be estimated systematically and is cast in a so-called *Memory function* in different systems.^{12–16} The reason behind the use of the term “memory” will be discussed in detail in the next section. The above discussion is applicable to the quantum systems also, except the fact that the classical variables will be replaced by operators. Since we discuss this formalism in context of the electronic systems, we invoke quantum mechanics from the very beginning and work with operator language, henceforth.

Let us consider an observable represented by an operator A obeying the Hamiltonian dynamics. To determine its dynamics, we define the Liouville operator associated with the Hamiltonian. Mathematically, the latter is called a super-operator as it acts on operators and produces a new operator. For a system with a given Hamiltonian H , it is defined as,

$$\mathcal{L}A = [H, A] = -i\frac{dA}{dt}. \quad (2)$$

Here, $[,]$ is the commutator between two operators. From Eq. (2), we see that an operator evolves with time as,

$$A(t) = e^{i\mathcal{L}t}A(0). \quad (3)$$

In a many body system, we need to quantify the correlation between various physical quantities represented by various operators A_i . We can express their correlation in terms of a correlation function matrix $\mathcal{R}(z)$, defined in frequency space with matrix elements as,

$$\begin{aligned} R_{ij}(z) &= i \int dt e^{izt} \langle A_i(t) | A_j \rangle = i \int dt e^{i(z-\mathcal{L})t} \langle A_i(t) | A_j \rangle \\ &= \left\langle A_i \left| \frac{1}{z-\mathcal{L}} A_j \right. \right\rangle, \quad z = \omega + i\eta. \end{aligned} \quad (4)$$

Here, $\eta \rightarrow 0^+$ is a small positive number, which assures causality. Evaluation of $R_{ij}(z)$ is a many body problem and is in general complicated. To simplify the evaluation of the above expression, we invoke the principle of memory function formalism and introduce a projection operator defined as follows,^{10,11}

$$\begin{aligned} P &= \sum_{ij} |A_i\rangle \chi_{ij}^{-1} \langle A_j|, \quad \chi_{ij} = \langle A_i | A_j \rangle, \\ &= \mathbb{I} - Q. \end{aligned} \quad (5)$$

Here, P separates the operator A_i s, corresponding to the observed macroscopic quantity, from the rest of the microscopic degrees of freedom and the act of Q is just the opposite. A generic projection operator should have the following properties.

$$P^2 = P, \quad PQ = QP = 0, \quad \text{etc.} \quad (6)$$

We also introduce a decomposition $\mathcal{L} = \mathcal{L}P + \mathcal{L}Q$ and introduce the identity

$$\frac{1}{X+Y} = \frac{1}{X} - \frac{1}{X}Y\frac{1}{X+Y}. \quad (7)$$

Using the above identity, the expression for the time dependent correlation function becomes

$$R_{ij}(z) = \langle A_i | \left\{ \frac{1}{z-\mathcal{L}Q} + \frac{1}{z-\mathcal{L}Q} \mathcal{L}P \frac{1}{z-\mathcal{L}} \right\} | A_j \rangle. \quad (8)$$

Since $Q|A_j\rangle = 0$, we can simplify the first term in the right-hand side of the above expression as,

$$\left\langle A_i \left| \frac{1}{z - \mathcal{L}Q} \right| A_j \right\rangle = \frac{1}{z} \langle A_i | A_j \rangle = \frac{1}{z} \chi_{ij}. \quad (9)$$

Therefore, the expression for the correlator can be re-written as,

$$R_{ij}(z) = \frac{1}{z} \chi_{ij} + \sum_{lm} \left\langle A_i \left| \frac{1}{z - \mathcal{L}Q} \mathcal{L}A_l \right\rangle \chi_{lm}^{-1} R_{mj}. \quad (10)$$

Above expression can be cast in a matrix notation as follows:

$$(z\mathbb{I} - \mathcal{K}\chi^{-1}) \mathcal{R} = \chi. \quad (11)$$

The matrix \mathcal{K} has the elements defined as,

$$K_{il} = \left\langle A_i \left| \frac{z}{z - \mathcal{L}Q} \mathcal{L}A_l \right\rangle. \quad (12)$$

Elements of \mathcal{K} can be decomposed as,

$$K_{il} = \langle A_i | \mathcal{L}A_l \rangle + \left\langle A_i \left| \mathcal{L}Q \frac{1}{z - \mathcal{L}Q} \mathcal{L}A_l \right\rangle. \quad (13)$$

The first part of the above expression is called the frequency matrix and is given as,

$$\mathcal{L}_{il} = \langle A_i | \mathcal{L}A_l \rangle. \quad (14)$$

Remaining part contains the effects of the faster degrees of freedom residing in the unprojected part of the Hilbert space and is termed as the memory matrix. It is defined as

$$M_{il} = \left\langle A_i \left| \mathcal{L}Q \frac{1}{z - Q\mathcal{L}Q} Q\mathcal{L}A_l \right\rangle. \quad (15)$$

The relation $Q^2 = Q$ is used to write it in a symmetric form. This form is very instructive. The above expression tells that the memory function is defined in terms of the unprojected part of the $|\dot{A}\rangle = \mathcal{L}|A\rangle$ and the unprojected part of the Liouville operator \mathcal{L} , i.e., $Q\mathcal{L}Q$. The projected degrees of freedom during their slow dynamics, cannot keep track of the movements of the fast unprojected part and treat the later as incoherent excitations. Since the memory function consists of the unprojected degrees of freedom only, it describes the effects of the incoherent excitations on the low energy excitations in a system and accounts for the dissipation in the slow degrees of freedom. Using the above expressions, the correlator between different components of A can be written in a compact notation as,

$$\mathcal{R}(z) = \frac{1}{z\mathbb{I} - [\mathcal{L} + M(z)]\chi^{-1}} \chi. \quad (16)$$

Writing in terms of the matrix elements, it takes the form,

$$\sum_l \left(z\delta_{il} - \sum_s [\mathcal{L}_{is} + M_{is}] \chi_{sl}^{-1} \right) R_{lj}(z) = \chi_{ij}. \quad (17)$$

Here, we see that any given correlation function can be written in terms of the corresponding memory matrix. This completes the general description of the memory function formalism. The use of it to study the electronic transport will be discussed in later sections.

3. Generalized Langevin Equation

Before using this formalism in the case of electronic transport, let us elaborate its physical contents in more detail in context of an well-known physical system. Consider the dynamics of a system where few macroscopic slow degrees of freedom are immersed in and interacting with a soup of fast microscopic degrees of freedom. The famous Brownian motion is such an example.^{17,10} Here, a particle is suspended in a fluid and it collides with the fluid molecules. As a result, it follows a zigzag trajectory as shown in Fig. 3.

To explain such a phenomena, in the classical limit a scenario that the particle is experiencing “some random force”, is adopted. As a result, for the particle a Newtonian equation of motion with phenomenological random force, mimicking the kicks from the fluid particles can be written. Such an equation of motion is called Langevin equation¹⁸ and for the simplest case, in one dimension it takes the following form.

$$\frac{d^2}{dt^2}R(t) = \gamma \frac{d}{dt}R(t) + f(t). \quad (18)$$

Here, $f(t)$ is a random force of “white noise” type, i.e., with correlation $\langle f(t)f(t') \rangle = \gamma k_B T \delta(t - t')$ and the mass of the particle is assumed to be unity. This correlation has a delta function in time structure and thus it is frequency independent. Such a random force description is used quite often and is highly successful in explaining various complex phenomena. How such a probabilistic picture emerges from the microscopic interactions which are deterministic in nature, can be addressed within the memory function formalism.¹⁹

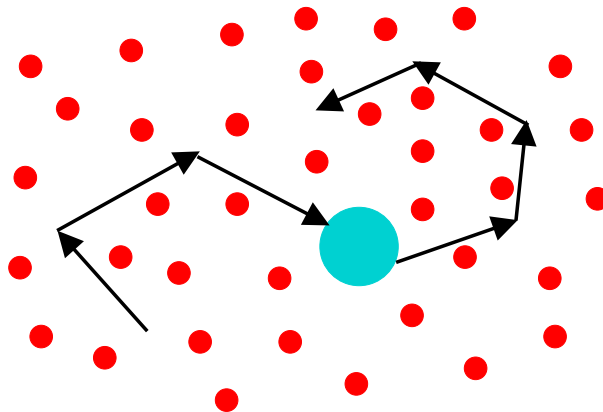


Fig. 3. (Color online) Motion of a Brownian particle (Big circle) moving in a fluid. Red dots represents small fluid molecules and they exhibit faster movements. The Brownian particle collides with the fluid particles and follows a zigzag path.

Let us consider a time dependent operator $A(t)$ which mimic the velocity of a Brownian particle and consider its time evolution. The corresponding Liouville equation is given as,²⁰

$$\frac{d}{dt}A(t) = i\mathcal{L}A(t), \quad A(t) = e^{i\mathcal{L}t}A(0). \quad (19)$$

The time derivative of the operator $A(t)$ can be written in terms of its initial value $A(0)$ as,

$$\frac{d}{dt}A(t) = i\mathcal{L}e^{i\mathcal{L}t}A(0). \quad (20)$$

Now we introduce the projection operator acting on an operator B as,

$$PB = \frac{\langle A, B \rangle}{\langle A, A \rangle}A, \quad P^2 = P. \quad (21)$$

We insert the identity $\mathbb{I} = P + Q$ in Eq. (19), and get,

$$\frac{d}{dt}A(t) = ie^{i\mathcal{L}t}(P + Q)\mathcal{L}A(0). \quad (22)$$

Now onwards, we drop the argument 0 from $A(0)$ for convenience and thus the first term in the above expression can be evaluated as,

$$e^{i\mathcal{L}t}P\mathcal{L}A = \frac{\langle \mathcal{L}A, A \rangle}{\langle A, A \rangle}e^{i\mathcal{L}t}A = \Omega e^{i\mathcal{L}t}A. \quad (23)$$

Here, $\Omega = \frac{\langle \mathcal{L}A, A \rangle}{\langle A, A \rangle}$ is the frequency matrix. To evaluate the second term, we introduce the identity,

$$\begin{aligned} e^{i\mathcal{L}t} &= e^{i(P+Q)\mathcal{L}t} \\ &= e^{iQ\mathcal{L}t} + \int_0^t d\tau e^{i\mathcal{L}(t-\tau)}iP\mathcal{L}e^{iQ\mathcal{L}\tau}. \end{aligned} \quad (24)$$

Applying it to the second term of Eq. (22), we get,

$$\begin{aligned} e^{i\mathcal{L}t}iQ\mathcal{L}A &= e^{iQ\mathcal{L}t}iQ\mathcal{L}A \\ &+ \int_0^t d\tau e^{i\mathcal{L}(t-\tau)}iP\mathcal{L}e^{iQ\mathcal{L}\tau}iQ\mathcal{L}A. \end{aligned} \quad (25)$$

We call the first term of the above equation a ‘‘force’’ which is given as,

$$f(t) = e^{iQ\mathcal{L}t}iQ\mathcal{L}A = e^{iQ\mathcal{L}t}f(0). \quad (26)$$

Here, $f(0)$ is a ‘‘force’’ inserted on the slow variable by the incoherent degrees of freedom and $f(t)$ is formers time propagation. The other term can be evaluated as follows,

$$\begin{aligned} I_2 &= \int_0^t d\tau e^{i\mathcal{L}(t-\tau)}iP\mathcal{L}e^{iQ\mathcal{L}\tau}iQ\mathcal{L}A \\ &= \int_0^t d\tau e^{i\mathcal{L}(t-\tau)}iP\mathcal{L}f(t) \end{aligned}$$

$$\begin{aligned}
 &= \int_0^t d\tau e^{i\mathcal{L}(t-\tau)} i \frac{\langle \mathcal{L}f(t), A \rangle}{\langle A, A \rangle} A \\
 &= \int_0^t d\tau e^{i\mathcal{L}(t-\tau)} i \frac{\langle \mathcal{L}Qf(t), A \rangle}{\langle A, A \rangle} A.
 \end{aligned} \tag{27}$$

Since both Q and \mathcal{L} are Hermitian, the above integral can be written as

$$\begin{aligned}
 I_2 &= - \int_0^t d\tau e^{i\mathcal{L}(t-\tau)} i \frac{\langle f(t), \mathcal{L}QA \rangle}{\langle A, A \rangle} A \\
 &= - \int_0^t d\tau e^{i\mathcal{L}(t-\tau)} \frac{\langle f(t), f(0) \rangle}{\langle A, A \rangle} A \\
 &= - \int_0^t d\tau \kappa(t) A(t - \tau).
 \end{aligned} \tag{28}$$

This term relates the dissipation in A with the fluctuations in other fast incoherent degrees of freedom. Such a relation is often termed as *fluctuation dissipation theorem*.^{21,22} It leads to the generalized Langevin equation which can be written as

$$\frac{d}{dt} A(t) = i\Omega A(t) - \int_0^t d\tau \gamma(t) A(t - \tau) + f(t). \tag{29}$$

The force-force correlator $\gamma(t)$ and its Fourier transform have in general, complicated time and hence frequency dependence, respectively. Thus, it carries the information of the memory or the history of the past scattering events and are termed as non-Markovian processes. This is why, the kernel describing the effects of the unprojected or incoherent degrees of freedom is termed as *memory function*. For a specific case when $\gamma(t) = \gamma_0 \delta(t)$, i.e., when its Fourier transform is constant, the dynamics becomes memory less and are called Markovian process in statistical mechanics literature.²³ Let us now compare the above expression which is obtained from the exact microscopic description, with that of the Langevin equation used from a phenomenological consideration. In the later case, the force $f(t)$ is considered as random with a variance assumed phenomenologically. In principle, $f(t)$ follows deterministic equation of motion and its exact evolution requires solutions of infinite set of equations as we will discuss in the next section. This is computationally impossible as no system is completely isolated and thus the “total system” implies the whole universe! To a good approximation, it is justified to consider force of some suitable order as random variables and solving the above equation to get an effective understanding about the system dynamics. Findings from such probabilistic description fits nicely with experimental findings. This is how an effective random or probabilistic description out of deterministic microscopic principles can emerge in a complex system. However, the origin of randomness in a purely deterministic system is a subtle issue. For more discussions interested readers can consult Ref. 5.

4. Continued Fraction Description

To elaborate on the memory function description further, we discuss how any dynamical correlation function can be expressed in terms of the static correlations in a continued fraction form. It was first shown by Mori, in his seminal work.⁷ From Eq. (29), we see that, the time dependence of a general dynamical variable say $A(t)$ is dictated by the correlations of its time derivative $\dot{A}(t)$. Same should hold true for $\dot{A}(t)$ and its higher time derivatives also.²⁴ This leads to a new type of moment expansion as follows. We can rewrite the generalized Langevin equation [Eq. (29)] as

$$\frac{d}{dt}A(t) = i\Omega_0 A(t) - \int_0^t d\tau \kappa_1(t) A(t - \tau) + A_1(t). \quad (30)$$

Here, A_1 is termed as the random force and has the same symmetry as \dot{A} . If we write its equation of motion, it will also follow a generalized Langevin equation involving higher time derivative of \dot{A} . The equation of motion for a n th order “force” A_n becomes,

$$\dot{A}_n(t) = i\Omega_n A_n(t) - \int_0^t d\tau \kappa_{n+1}(t) A_n(t - \tau) + A_{n+1}(t) \quad (31)$$

with n th order frequency and the $(n + 1)$ th order memory kernel

$$\Omega_n = \frac{\langle \mathcal{L}A_n, A_n \rangle}{\langle A_n, A_n \rangle}, \quad \kappa_{n+1}(t) = \frac{\langle A_{n+1}(t), A_{n+1} \rangle}{\langle A_n, A_n \rangle}, \quad (32)$$

respectively. This recurrence formula can be cast in a single continued fraction form of the correlation function as follows,

$$\int_0^\infty dt e^{-izt} \langle A(t); A \rangle = \frac{\langle A; A \rangle}{i(z - \Omega_0) + \frac{\Delta_1}{i(z - \Omega_1) + \frac{\Delta_2}{i(z - \Omega_2) + \dots}}}. \quad (33)$$

In the above expression $\Delta_n = \kappa_n(0)$. Here, the dynamic property of a system is completely described by its static correlations. The above result is in principle exact. But the exact evaluation needs the knowledge of the static correlations upto infinite order.²⁵ However, depending on the situation one can truncate the continued fraction at some suitable order and get sensible results.²⁶ A detailed discussions of its use in various systems are beyond the scope of this paper. Interested readers may look at Refs. 27–29, where dynamic correlations in the case of simple metal, Hubbard Model and spin $\frac{1}{2}$ -XYZ model respectively are cast in the continued fraction form.

5. Application to the Electronic Transport

In the previous sections, we described various aspects of the memory function approach. Thus, we set up the stage for using it to study the dynamical transport properties of various electronic systems. Here our focus is on the time evolution of the current operator and the correlation of its various components in a generic

many body system. In our discussions on electronic systems, first we assume that the momentum is the only nearly conserved quantity in the system.^a Thus there is only one slow mode associated with this conservation law. We study the momentum relaxation of a charged particle under external perturbation. In this case, the projector operator is defined solely in terms of the current operator. This assumption holds good if there is no other slow modes associated with any other conservation law or broken symmetry that couples to the charge degrees of freedom.^{30–33} However, for simplicity, we stick to this picture for the time being and will generalize it in the later subsections.

Now, we can start with the expression for memory function as defined in Eq. (15). In certain situations, we can evaluate the expression in the spirit of perturbation theory. Memory function can be viewed as “the self-energy” of the current–current correlation function. It has an added advantage that such “self-energy” calculation does not require vertex correction. The latter is extremely important and problematic when the current–current correlation is expressed through the renormalized single particle propagators.³⁴ Now, for further simplicity, we consider the case of an one component current operator J and replace $|A\rangle$ by $|J\rangle$. To clarify more, in an electronic system $|J\rangle \equiv J|\Phi_0\rangle$, where $|\Phi_0\rangle$ is the electronic ground state. The correlation denoted by $\langle J(t)|J\rangle$, can be used to represent correlation of the form $\langle [J(t), J] \rangle$ without changing the form of Eq. (16). We choose the latter form, as it is used to describe the response function. We focus on the response of an electronic system under an external electric field and the relevant quantity is dynamic conductivity $\sigma(z)$ and is given in terms of a commutator correlation of the current operators. In this case, Eq. (16) can be written as,

$$\sigma(z) = \frac{1}{z - M(z)/\chi} \chi. \quad (34)$$

It is to be noted that, we assume time reversal invariance so that $\langle J|\mathcal{L}|J\rangle = \langle \dot{J}|J\rangle = 0$, i.e., the generalized frequency vanishes. Here, we see that using memory function formalism, the dynamic susceptibility can be written in an Extended Drude form, frequently used by the experimentalists³⁵ to explain any non-Drude dynamic conductivity. Here, we see that the memory function or the generalized many particle (two particle in this case) self-energy defined by Eq. (15) is the most important quantity to determine the dynamic conductivity. Within our simplified picture, it takes the following form,

$$M(z) = \left\langle J \left| \mathcal{L} Q \frac{1}{z - Q \mathcal{L} Q} Q \mathcal{L} J \right. \right\rangle = \left\langle \dot{J} \left| Q \frac{1}{z - Q \mathcal{L} Q} Q J \right. \right\rangle. \quad (35)$$

To get some qualitative idea, we can opt for a “high frequency expansion” of the above expression. We consider an energy scale $z_0 = \langle \dot{J}|Q\mathcal{L}Q\dot{J}\rangle/\chi$. As long as $z_0 \ll$

^aIt means that the related correlation function has a very slow decay, e.g., of the form $e^{-\frac{t}{\tau}}$, with the relaxation time $\tau \rightarrow \infty$.

$|z|$, we can expand inverse operator $\frac{1}{z-Q\mathcal{L}Q}$ in a series and can rewrite the memory function as follows,

$$\begin{aligned} M &= \frac{1}{z} \left\langle \dot{J} \left| Q \left(1 + \frac{1}{z} Q\mathcal{L}Q + \frac{1}{z^2} Q\mathcal{L}Q\mathcal{L}Q + \dots \right) Q \dot{J} \right. \right\rangle \\ &= \frac{1}{z} \langle \dot{J} | Q \dot{J} \rangle + \frac{1}{z^2} \langle \dot{J} | Q\mathcal{L}Q \dot{J} \rangle + \frac{1}{z^3} \langle \dot{J} | Q\mathcal{L}Q\mathcal{L}Q \dot{J} \rangle + \dots \end{aligned} \quad (36)$$

Here we use the fact $Q^2 = Q$ and the above expansion can be termed as a high frequency expansion. Its validity will depend on how small or large the $z_0/|z|$ is. Since the time derivative of two different orders are uncorrelated in a system having time reversal symmetry, i.e., $\langle \dot{J} | \dot{J} \rangle, \langle \dot{J} | \ddot{J} \rangle = 0$, as proved in Appendix A,

$$M(z) = \frac{1}{z} \langle \dot{J} | \dot{J} \rangle + \frac{1}{z^3} \langle \ddot{J} | \ddot{J} \rangle + \dots \quad (37)$$

Clearly this expansion will hold good in high frequencies and will breakdown below certain energy scale set by the incoherent part of the Hamiltonian. Here, J is the current operator. Now, its time derivative $\dot{J} = [J, H = H_0 + H'] = [J, H']$ is proportional to the coupling strength g (say) with the dimension of energy of different interactions. Thus, the above expansion can be viewed as an expansion in terms of $\frac{g^2}{z^2}$. For very weak interactions, one can truncate the above expression at the first term itself and calculate the conductivity. However, this perturbation theory is different from the diagrammatic perturbation theory that incorporates interaction effects through single particle self energy and vertex corrections.³⁶

5.1. Weak coupling theory

The memory function formalism was first used in a systematic way to calculate the electrical conductivity in the case of simple metals with various interactions by Götze and Wölfle.³⁶ Similar approach is used by many others in this context.³⁷⁻⁴³ Their approach can be summarized as follows. According to the linear response theory, the dynamical conductivity is defined as,^{34,44-46}

$$\sigma(z) = -i \frac{1}{z} \chi(z) + i \frac{\omega_p^2}{4\pi z}. \quad (38)$$

Here, $\omega_p^2 = 4\pi N_e e^2 / m$ is the square of plasma frequency where e electronic charge, m electron mass and N_e is the electron density, z is the complex frequency and $\chi(z)$ is the current-current correlation function defined as,

$$\chi(z) = \langle\langle J; J \rangle\rangle_z = i \int_0^\infty e^{izt} \langle [J(t), J] \rangle, \quad (39)$$

where $J = \sum_{\mathbf{k}} ev(\mathbf{k})c_{\mathbf{k},\sigma}^\dagger c_{\mathbf{k},\sigma}$ is the current density and $v(\mathbf{k})$ is the velocity dispersion. Here, $[J(t), J]$ denotes the commutator, $\langle \dots \rangle$ denotes the ensemble average at temperature T and $\langle\langle \dots \rangle\rangle$ denotes the Laplace transform of the ensemble average.

According to the Götze and Wölfle approach,³⁶ the memory function is defined as

$$M(z) = z \frac{\chi(z)}{\chi_0 - \chi(z)}, \quad (40)$$

where χ_0 corresponds to the static limit of correlation function (i.e., $\chi_0 = N_e/m$).³⁶ Using this, the expression for dynamical conductivity in Eq. (38) can be cast in an extended Drude form as,

$$\sigma(z) = \frac{i}{4\pi} \frac{\omega_p^2}{z + M(z)}. \quad (41)$$

In Ref. 36, an expansion for $M(z) = \frac{z\chi(z)}{\chi_0} (1 + \frac{\chi(z)}{\chi_0} - \dots)$ is used. Basis of this assumption is the smallness of the contribution from the interaction part as compared to the kinetic energy of free electrons. Using this expansion and on keeping the leading order term, the memory function $M(z)$ can be written as

$$M(z) = z \frac{\chi(z)}{\chi_0} = z \frac{\langle\langle J; J \rangle\rangle_z}{\chi_0}. \quad (42)$$

To compute memory function, we need $\langle\langle J; J \rangle\rangle_z$ which by using equation of motion is

$$z \langle\langle J; J \rangle\rangle_z = \langle[J, J]\rangle + \langle\langle [J, H']; J \rangle\rangle_z. \quad (43)$$

As the first term of right-hand side is zero, hence the above expression is equivalent to second term which can be further calculated by applying equation of motion.

$$z \langle\langle [J, H']; J \rangle\rangle_z = \langle\langle [[J, H'], J] \rangle\rangle - \langle\langle [J, H']; [J, H'] \rangle\rangle_z. \quad (44)$$

For $z = 0$, $\langle\langle [J, H'], J \rangle\rangle = \langle\langle [J, H']; [J, H'] \rangle\rangle_{z=0}$. Thus, the memory function $M(z)$ becomes

$$M(z) = \frac{\phi(0) - \phi(z)}{z\chi_0}. \quad (45)$$

Here, $\phi(z)$ (called as correlation function) is defined as

$$\phi(z) = \langle\langle [J, H']; [J, H'] \rangle\rangle_z. \quad (46)$$

Here, the current operator $J_i = \sum v_i(\mathbf{k}) c_{\mathbf{k}\sigma}^\dagger c_{\mathbf{k}\sigma}$ and its derivative or “force” $A = \dot{J} = [J, H]$. Here, the total Hamiltonian has two parts, H_0 the free part or the kinetic part and an interaction part. While the first part commutes with the current operator, the later part does not. Thus, $A = \dot{J} = [J, H_0 + H'] = [J, H']$ is determined by the interaction part only and is different for different types of interactions. Within this approach, they calculated the frequency dependent conductivity with various interactions such as electron–phonon, electron-impurity, electron-magnetic impurity, scattering with localized modes, etc. To illustrate their work further, we will discuss the simplest case of electron-impurity interaction.

In this case, the interaction part of the Hamiltonian is given as

$$H' = \frac{1}{N} \sum_j \langle \mathbf{k} | U | \mathbf{k}' \rangle c_{\mathbf{k}\sigma}^\dagger c_{\mathbf{k}'\sigma}. \quad (47)$$

Here, U denotes the impurity potential. In this case, the j th component of the force operator A is given as

$$A_j = \frac{1}{N} \sum \langle \mathbf{k} | U | \mathbf{k}' \rangle [v_j(\mathbf{k}) - v_j(\mathbf{k}')] c_{\mathbf{k}\sigma}^\dagger c_{\mathbf{k}'\sigma}. \quad (48)$$

Here, $v_j(\mathbf{k})$ is the velocity of the particle with momentum \mathbf{k} in the j th direction. The force-force correlation in the case of free electron is estimated as

$$\phi(z) = \langle \langle A | A \rangle \rangle_z = (2c/3m^2N) \sum_{\mathbf{k}\mathbf{k}'} |\langle \mathbf{k} | U | \mathbf{k}' \rangle|^2 (\mathbf{k} - \mathbf{k}')^2 \frac{f(\epsilon_k) - f(\epsilon_{k'})}{z - \epsilon_k + \epsilon_{k'}}. \quad (49)$$

From this expression, the imaginary or the absorptive part of the memory function can be estimated as

$$M''(\omega) = \mathcal{C} \times \frac{1}{N^2} \sum_{\mathbf{k}\mathbf{k}'} |\langle \mathbf{k} | U | \mathbf{k}' \rangle|^2 (\mathbf{k} - \mathbf{k}')^2 \times [f(\epsilon_k) - f(\epsilon_{k'})] \delta(\omega - \epsilon_k + \epsilon_{k'}) / \omega. \quad (50)$$

For momentum independent U , i.e., point impurity

$$M''(\omega) = \mathcal{C}' (U \rho_F)^2 \epsilon_F, \quad (51)$$

where ρ_F and ϵ_F are the density of states at the Fermi surface and the Fermi energy, respectively. For $\omega \ll \epsilon_F$, the imaginary part of the memory function is independent of the frequency and the result is identical to the Drude result. On the other hand, if the impurities are spatially extended,

$$M''(\omega) \equiv \frac{1}{\tau} \sim v_F \iint d\Omega \sigma_{sc} (1 - \cos \theta). \quad (52)$$

In the above expression, the differential scattering cross-section is defined as

$$\sigma_{sc}(\Omega) = (\pi k_F)^2 |\rho_F U(\mathbf{k}_F - \mathbf{k}'_F)|^2. \quad (53)$$

For interactions with nonmagnetic impurity, we see that the results are identical to the single particle calculations with vertex corrections. This is indeed a benchmark and major success of this formalism. In other cases, there are deviations from the Drude formula. They argued that these discrepancies are because of spin-flip scattering in a magnetic field, because of resonance scattering, because of phonon creation at low temperatures, and because of breaking of the screening cloud attached to charged impurities, respectively. However, this version of the memory function approach to calculate the dynamic conductivity is somewhat limited. It is designed for simple metal, i.e., for weakly-interacting electrons with very weak electron-phonon or electron-impurity or other interactions and nonexpandable to the cases of strong interactions. Lifting these limitations, as required for more exotic systems like strange metal phase in cuprates near optimal doping, and others need substantial improvements.

5.2. Strong coupling extension

A large volume of works^{47–59} on the applications of the memory function in the case of strongly interacting electronic systems is being done by Plakida and his collaborators based on the mathematical formalism developed by Tserkovnikov.⁶⁰ We see in the Götze and Wölfle formalism, that the dynamical conductivity or the current–current correlation $\langle J; J \rangle$ can be calculated with the knowledge of $\langle \dot{J}; \dot{J} \rangle$ which is calculated by simple perturbation theory. However, it will be seen in this section that, their approach misses some subtle points which may not affect the results in the perturbative limit but can be problematic in the case of strongly correlated systems. Plakida *et al.* refined the relation between the memory function and the \dot{J} – \dot{J} correlation as follows. First, a relation between two time retarded Green’s function and the Kubo–Mori relaxation function can be established as follows. The two time retarded Green’s function for two Heisenberg operators A and B are defined as

$$\begin{aligned} G_{AB}^r(t-t') &\equiv \langle\langle A(t)|B(t') \rangle\rangle \\ &= -i\Theta(t-t') \langle A(t)B(t') - \eta B(t')A(t) \rangle. \end{aligned} \quad (54)$$

Here the step function $\Theta(t) = 1$ for $t > 0$ and $\Theta(t) = 0$ for $t < 0$. The $\langle \dots \rangle$ represents the thermal average, i.e., $Tr e^{-\beta H}(\dots)$ with β as the inverse temperature and $\eta = \pm$ for Bosons and Fermions, respectively. The above Green’s function follows an equation of motion,

$$i \frac{d}{dt} \langle\langle A(t)|B(t') \rangle\rangle = \delta(t-t') \langle [A, B]_{\eta} \rangle + \langle\langle \dot{A}(t)|B(t') \rangle\rangle. \quad (55)$$

On the other hand, Kubo–Mori relaxation function is defined as

$$\Phi_{AB}(t-t') \equiv ((A(t)|B(t'))) = -i\Theta(t-t') (A(t)|B(t')). \quad (56)$$

The last expression is called the Kubo–Mori scalar product and is defined as,⁹

$$(A(t)|B) = \int_0^{\beta} d\lambda \langle A(t-i\lambda)B \rangle. \quad (57)$$

It can be shown that,⁶⁰

$$\begin{aligned} \omega((A|B))_{\omega} &= (A|B) + \langle\langle A|B \rangle\rangle_{\omega} \\ &= -\langle\langle A|B \rangle\rangle_0 + \langle\langle A|B \rangle\rangle_{\omega}. \end{aligned} \quad (58)$$

Now, we apply projection operator technique to the Green’s function,

$$G_{k,k'}(t-t') = \langle\langle A_k(t)|A_{k'}^{\dagger}(t') \rangle\rangle. \quad (59)$$

It has an equation of motion

$$i \frac{d}{dt} \langle\langle A_k(t)|A_{k'}^{\dagger}(t') \rangle\rangle = \delta(t-t') \langle [A_k, B_{k'}]_{\eta} \rangle + \langle\langle \dot{A}_k(t)|A_{k'}^{\dagger}(t') \rangle\rangle. \quad (60)$$

Here, $\dot{A}_k(t) = [A_k(t), H]$. Now, we extract the linear term in the equation of motion as

$$i\dot{A}_k(t) = [A_k(t), H] = \sum_q E_{k,q} A_q + Z_k^{ir}. \quad (61)$$

The irreducible part Z_k^{ir} is defined by the orthogonality condition

$$\langle [Z_k^{ir}, A_{k'}^\dagger]_\eta \rangle = 0. \quad (62)$$

This defines the frequency matrix

$$E_{kq} = \sum_{k'} \langle [[A_k(t), H], A_{k'}]_\eta \rangle I_{k'q}^{-1}, \quad I_{k'q} = \langle [A_k, A_{k'}]_\eta \rangle. \quad (63)$$

Upon Fourier transform, Eq. (60) gives,

$$G_{k,k'}(\omega) = G_{k,k'}^0(\omega) + \sum_{qq'} G_{k,k'}^0(\omega) I_{qq'}^{-1} \langle \langle Z_{q'}^{ir} | A_{k'}^\dagger \rangle \rangle. \quad (64)$$

Here, the zeroth-order Green's function is given as,

$$G_{k,k'}^0(\omega) = \sum_q \frac{I_{qk'}}{\omega \delta_{kq} - E_{kq}}. \quad (65)$$

This defines the excitation spectrum in the mean field approximations. In order to determine the many body part of the Green's function $\langle \langle Z_{q'}^{ir}(t) | A_{k'}^\dagger(t') \rangle \rangle$, one needs to differentiate it with respect to t' and after taking Fourier transform one obtains,

$$G_{k,k'}(\omega) = G_{k,k'}^0(\omega) + \sum_{qq'} G_{k,q}^0(\omega) T_{qq'}(\omega) G_{q',k'}^0(\omega). \quad (66)$$

The scattering matrix appeared above is defined as

$$T_{kk'}(\omega) = \sum_{qq'} I_{k,q}^{-1} \langle \langle Z_q^{ir} | (Z_{q'}^{ir})^\dagger \rangle \rangle I_{q'k'}^{-1}. \quad (67)$$

Now, if we define the self-energy as

$$T_{kk'}(\omega) = \Sigma_{kk'}(\omega) + \sum_{qq'} \Sigma_{kq}(\omega) G_{q,q'}^0(\omega) T_{q'k'}(\omega). \quad (68)$$

Then the Green's function can be cast in a Dyson form as,

$$G_{k,k'}(\omega) = G_{k,k'}^0(\omega) + \sum_{qq'} G_{k,q}^0(\omega) \Sigma_{qq'}(\omega) G_{q',k'}(\omega). \quad (69)$$

This tells that the generalized self-energy or the memory function is given by the proper part of the scattering matrix. Thus it can be written as,

$$\Sigma_{kk'}(\omega) = \sum_{qq'} I_{k,q}^{-1} \langle \langle Z_q^{ir} | (Z_{q'}^{ir})^\dagger \rangle \rangle^{\text{proper}} I_{q'k'}^{-1}. \quad (70)$$

If we recall the Dyson equations in the electronic Green's function,³⁴ we can easily identify that the $T(\omega)$ is the generalized many body or multi-particle scattering matrix while the memory function or the generalized multi-particle self-energy $\Sigma(\omega)$

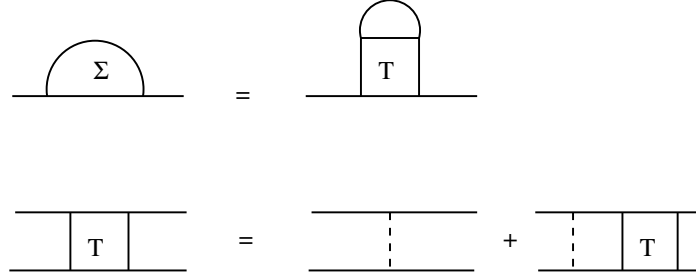


Fig. 4. A diagrammatic description of the relation between the single particle self-energy and the T-matrix for electron-Boson interaction is shown here. The solid lines represent the electron propagator while the dashed lines represent Bosonic propagators.

is given by the proper part of $T(\omega)$. Diagrammatically, it means that the part of the scattering matrix is not connected by a single relaxation function. To clarify this statement, a diagrammatic description for the same in case of single particle electronic Green's function or propagator in a coupled electron-Boson system is presented in Fig. 4.

Now to calculate the conductivity, we need to focus on the current-current correlations. In this case, the relevant response function $\Phi_{JJ}(\omega)$ and the memory function or the corresponding multi-particle self-energy $M(\omega)$ is related to each other as

$$\Phi_{JJ}(\omega) = ((J|J))_{\omega} = \frac{\chi_0}{\omega + M(\omega)}. \quad (71)$$

Here, $\chi_0 = \chi_{JJ}(0)$ and the memory function has both real and imaginary parts, i.e., $M(\omega + i\delta) = M'(\omega) + iM''(\omega)$. Again following the general procedure as discussed earlier, the time derivative of the response function,

$$\Phi_{JJ}(t - t') = ((J(t)|J(t'))), \quad (72)$$

followed by the Fourier transform gives,

$$\Phi_{JJ}(\omega) = \Phi_{JJ}^0(\omega) + \Phi_{JJ}^0(\omega)T_{JJ}(\omega)\Phi_{JJ}^0(\omega). \quad (73)$$

Here, $\Phi_{JJ}^0(\omega) = \frac{\chi_0}{\omega}$ and in this case the scattering matrix is given as

$$T_{JJ}(\omega) = \frac{1}{\chi_0}((\dot{J}|\dot{J}))_{\omega} \frac{1}{\chi_0}. \quad (74)$$

In order to express Eq. (73) in the form of Eq. (71), we need the following relation between the memory function and the scattering matrix.

$$T_{JJ}(\omega) = -\frac{1}{\chi_0}[M(\omega) + M(\omega)\Phi_{JJ}^0(\omega)T_{JJ}(\omega)]. \quad (75)$$

The above equation tells that the memory function for the electrical conductivity is equivalent to the irreducible or the proper part of the force-force correlator, i.e.,

$$M(\omega) = \frac{1}{\chi_0}((\dot{J}|\dot{J}))_{\omega}^{\text{proper}} \frac{1}{\chi_0}. \quad (76)$$

These authors use this improved definition of the memory function to calculate dynamical quantities in various system such as t - J model in context of high temperature superconductors and many others in the references cited at the beginning of this subsection.

As we see, the evaluation of memory function requires evaluation of $\dot{J} = [J, H']$ and its correlation. Thus any scheme based on the memory function depends on the interaction part of the Hamiltonian and the algebra followed by the operators corresponding to the observables in a system. Also an evaluation of correlator of the form shown in Eq. (76) needs some approximations with suitable justifications.

Plakida *et al.* consider the t - J model^{61,62} for the strongly correlated normal phase of the cuprate superconductors to apply their formalism. The authors use it to calculate both the optical conductivity and the dynamic spin susceptibility in this model. Due to the involved mathematical complexity, the detail description of the application in this model is beyond the scope of this review. However, the findings from this approach are comparable with the other analytical methods and also comparable with the experiments. Interested reader can look at Refs. 52 and 57, where Plakida has nicely reviewed the related works.

Similar approach is also used by some other researchers to calculate the spin susceptibility in strongly correlated electronic systems.⁶³⁻⁷⁰ Since we focus on the electrical conductivity here, we skip those discussions here.

5.3. *Effects of additional slow modes*

Until now, we consider systems where the electrical current of the momentum was the only slow mode. However, in many systems we need to consider many other slow modes which couple to the electrical current. For example in a system where there is charge conservation, along with the drift current (related to the momentum of the charge particles), there is another slow mode namely charge diffusion or diffusion current mode.³⁰⁻³³ The latter is also a slow mode and couples to the electric current. In such a system, the projected space along with the electrical current also contains density fluctuation operators. Following Ref. 30, we define,

$$J_0(\mathbf{q}) = \rho(\mathbf{q}) \quad \text{and} \quad \mathbf{J}_1(\mathbf{q}) = \mathbf{J}(\mathbf{q}). \quad (77)$$

Due to the charge conservation, the density and the longitudinal part of the current operator are related as

$$\mathcal{L}J_0 = -q\mathbf{J}^L. \quad (78)$$

Since the number of slow modes is more than one, in this case, the memory function takes a matrix form as shown in Eq. (15). Here, we consider two slow modes, hence the memory matrix has a 2×2 structure and is defined by four correlation functions, namely $R_{00} = \rho - \rho$, $R_{01} = \rho - \mathbf{J}$, $R_{10} = \mathbf{J} - \rho$ and $R_{11} = \mathbf{J} - \mathbf{J}$. However, the density fluctuations couple only to the longitudinal part of the current and thus in

this case Eq. (17) can be written in a set of two decoupled equations as follows,

$$\sum_{l=0}^1 \left[z\delta_{il} - \sum_s [\mathcal{L}_{is} + M_{is}^L] \chi_{sl}^{-1} \right] R_{ij}^L(z) = \chi_{ij}, \quad (79)$$

$$[z - [\mathcal{L}_{11} + M_{11}^T] \chi_{11}^{-1}] R_{11}^T(z) = \chi_{11}^T.$$

Here, $\chi_{ij} = \langle J_i | J_j \rangle$ is the static correlation function. Now the continuity equation (78) and the time reversal invariance in the system tell that $\langle J_0 | J_1^L \rangle \sim \langle J_0 | \dot{J}_0 \rangle = 0$. Moreover, since $\mathcal{L}J_0 \propto J_1^L$, the first component of the “four force” lies within the projected space and thus its unprojected part, i.e., $Q\mathcal{L}J_0$ is identically zero. This simplifies this picture drastically as it leads to

$$M_{00} = M_{01}^L = M_{10}^L = 0. \quad (80)$$

Thus, only $M_{11} = M$ survives and it can be calculated using Eq. (15) and assuming $Q \approx 1$.^{30,31} Once the memory function is determined suitably, the coupled equation can be solved and the effects of charge diffusion can be discussed in varieties of systems as done in references cited in this section.

In this connection, we can mention the works of Lucas and Sachdev.^{31,33} In their work, they focus on the magneto-transport in strange metals. Their system is a 2D quantum critical metal under an external magnetic field. They consider systems where electronic quasi-particles are absent. Thus, they use memory formalism instead of standard perturbation theory to determine the relevant response functions. In their approach, they include the effects of other slow modes such as charge diffusions and heat diffusions in their formalism. Within this formalism, they present some explanation of recently observed anomalous behavior in the hall angle in the strange metal phase.⁷¹ In summary, this approach contains the essential complexity of a typical non-Fermi liquid. It provides a systematic way of including various slow modes within this approach and thus very promising.

5.4. Comments on few recent works

In this section, we will qualitatively discuss few of the present day activities based on memory function formalism. We aim to give a flavor of the present day importance of this formalism and keep the discussion very brief. For details, readers are advised to look at the articles cited in appropriate paragraphs.

Holographic approach: Since the memory function formalism does not invoke single particle picture to calculate electrical transport. In principle, it can be used to calculate transport properties even when quasi-particle picture is not valid. Recently many researchers used both the holographic ADS-CFT principle to study electronic transport in a similar situation, namely $2d$ metals near quantum critical point.³¹ These models include the coupling between various slow modes and thus produces various non-Fermi liquid transport behavior. To check the consistency, results are often compared with the complimentary memory function calculations and interestingly they have very good agreements.

Nonequilibrium steady state: Some of the present authors⁷² used memory function formalism to study electronic transport in nonequilibrium steady state, where the electron and the phonon temperatures are different. They consider nonequilibrium relaxation of electrons due to their coupling with phonons in a simple metal. In their model, electrons are living at a higher temperature than that of the phonon bath, mimicking a nonequilibrium steady state situation. They show that the dc scattering rate at high temperatures and optical scattering rate at high frequencies, are independent of the temperature difference between the electrons and the phonons is found in this work. The present formalism forms a basis which can also be extended to study hot-electron relaxation in more complex situations.

Scattering rates in the gapped system: In an another work, two of the present authors⁷³ calculated generalized Drude scattering (GDS) rate for the case of electron-phonon scattering in metals with a gap in the electronic density of states at the Fermi energy. The resulting GDS is compared with a recent one by Sharapov and Carbotte⁷⁴ obtained through a different setup. They find good agreement between the two at finite frequencies. However, there are discrepancies in the dc scattering rate which are severe at high temperature which they attribute to some assumptions made in the Sharapov and Carbotte formalism.

High frequency expansion: Most of the studies within the memory function formalism suffers from the lowest order perturbative evaluation of the required two particle correlation function. This is done without much justifications, particularly in case of strong correlations. One needs to improve upon by considering higher order terms in the continued fraction representation [Eq. (33)] or the high frequency expansion [Eq. (37)] as shown in the previous sections. Present authors recently proposed⁷⁵ a systematic expansion of the memory function involving its various moments. They calculate the higher order contribution to the GDS rate in case of electron-impurity interactions. They find larger contributions from the higher moments in the low frequency regime and also in the case of larger interaction strength.

5.5. Future directions

As mentioned by Lucas and Sachdev in their work,^{31,33} a lot of work is needed in incorporating various slow modes in a generic electronic system which often lead to non-Fermi liquid behavior. Depending on the systems under consideration, one needs to include slow modes occurring from various broken symmetries related to spin density wave, charge density wave, superconductor, nematic transitions in a systematic way.

Also the same formalism can be used to explore the response of a physical system due to the external fields other than the electric field. Present authors are involved in calculating thermal coefficient and thermoelectric coefficients (Seebeck coefficient and Peltier coefficient, respectively) and magneto-thermoelectric effects or Nernst effects within this approach.

6. Discussions

As discussed in this paper, though the memory function formalism originated in context of nonequilibrium statistical mechanics, it is being used recently as an important tool to calculate various dynamic transport quantities in various interacting systems. From a theorists point of view, this formalism directly deals with the two particle correlations and thus the existence of electronic quasiparticle is not an essential ingredient here. This is the main advantage of this formalism compared to the single particle perturbation theories which fails in making good predictions in these systems.³⁴ Moreover, in this formalism dynamical conductivity can be cast in an extended Drude form. The latter has a structure as predicted by Drude in case of noninteracting electrons, but with a frequency dependent scattering rate and mass enhancement factor. This form becomes very convenient for experimentalists to estimate the deviation of their data from the simple Drude expression for metals. Thus, this method is becoming popular to both the communities. In this paper, we summarize the foundation of the memory function formalism. We review its applications in transport studies of various electronic systems in detail. Also we critically examine the approximations used within this formalism in various works and discuss the possible improvements. This review brings all the necessary details of the memory function formalism together at one place. We hope that the present review will be useful to whoever works in this area, particularly the newcomers.

Acknowledgment

We thank Pradeep Kumar Soam for many helpful discussions.

Appendix A. Some Useful Relations

Here, we mention few useful relations. The detailed derivation of them can be found in Ref. 60. First, we define the Kubo–Mori scalar product as

$$(A(t), B) = \int_0^\beta d\lambda \langle A(t - i\lambda) B \rangle. \quad (\text{A.1})$$

Here $\langle \dots \rangle$ represents an equilibrium thermal average. Next, we define Greens function for the above scalar product as follows,

$$((A(t), B))_z = \int_0^\infty dt e^{izt} (A(t), B). \quad (\text{A.2})$$

The commutator Green’s function is defined as,

$$\langle\langle A(t), B \rangle\rangle_z = \int_0^\infty dt e^{izt} \langle [A(t), B] \rangle. \quad (\text{A.3})$$

These two Green’s functions are related as,

$$z((A(t), B))_z = \langle\langle A(t), B \rangle\rangle_z - \langle\langle A(t), B \rangle\rangle_{z=0}. \quad (\text{A.4})$$

We also have the following relations,

$$((i\dot{A}, B))_z = ((A(t), -i\dot{B}))_z = \langle\langle A, B \rangle\rangle_z. \quad (\text{A.5})$$

$$(i\dot{A}, B) = (A(t), -i\dot{B}) = \langle[A, B]\rangle. \quad (\text{A.6})$$

Here we see, if $B = A$,

$$(i\dot{A}, A) = (A(t), -i\dot{A}) = \langle[A, A]\rangle = 0. \quad (\text{A.7})$$

References

1. P. W. Anderson, *Science* **177**, 393 (1972).
2. P. W. Anderson, *Basic Notions of Condensed Matter Physics* (Addison-Wesley, Reading, MA, 1997).
3. R. Zwanzig, *Phys. Rev.* **124**, 983 (1961).
4. R. Zwanzig, *Lectures in Theoretical Physics*, Vol. 3, eds. W. E. Brittin, B. W. Downs and J. Downs (Interscience, New York, 1961), p. 135.
5. R. Zwanzig, *Nonequilibrium Statistical Mechanics* (Oxford University Press, US, 2001).
6. H. Mori, *Progr. Theor. Phys.* **33**, 423 (1965).
7. H. Mori, *Progr. Theor. Phys.* **34**, 399 (1965).
8. G. D. Harp and B. J. Berne, *Phys. Rev. A* **2**, 975 (1970).
9. R. Kubo, M. Toda and N. Hashitsume, *Statistical Physics II: Nonequilibrium Statistical Mechanics* (Springer-Verlag, Berlin, 1978).
10. D. Forster, *Hydrodynamic Fluctuations, Broken Symmetry and Correlation Functions* (Advanced Books Classics, New York, 1995).
11. P. Fulde, *Correlated Electrons in Quantum Matter* (World Scientific, Singapore, 2012).
12. A. S. T. Pires and M. E. Gouvêa, *Braz. J. Phys.* **34**, 1189 (2004).
13. A. A. Khamzin, R. R. Nigmatullin and I. I. Popov, *J. Phys. Conf. Ser.* **394**, 012013 (2012).
14. V. S. Viswanath and G. Müller, *The Recursion Method: Application to Many-Body Dynamics*, Chap. 3 (Springer-Verlag, Heidelberg, 1994).
15. W. Schimacher, *Theory of Liquids and Other Disordered Media*, Chap. 8 (Springer, Berlin, 2015), pp. 111–120.
16. L. L. Buishvili, M. D. Zviadadze and É. Kh. Khalvashi, *Zh. Eksp. Teor. Fiz.* **91**, 310 (1986).
17. B. Robert, *Philos. Mag.* **4**, 161 (1828).
18. P. C. R. Langevin, *Acad. Sci. (Paris)* **146**, 530 (1908).
19. E. Darve, J. Solomon and A. Kia, *Proc. Natl. Acad. Sci. USA* **106**, 10884 (2009).
20. T. Karasudani *et al.*, *Prog. Theor. Phys.* **61**, 850 (1979).
21. H. Nyquist, *Phys. Rev.* **32**, 110 (1928).
22. H. B. Callen and T. A. Welton, *Phys. Rev.* **83**, 34 (1951).
23. N. G. Van Kampen, *Stochastic Processes in Physics and Chemistry*, 3rd edn. (North-Holland Publishers, Netherlands, 2007).
24. J. Okada, I. Sawada and Y. Kuroda, *J. Phys. Soc. Jpn.* **64**, 4092 (1995).
25. M. Dupis, *Prog. Theor. Phys.* **37**, 502 (1967).
26. A. S. T. Pires, *Helv. Phys. Acta* **61**, 988 (1988).
27. J. Y. Sug *et al.*, *Phys. Rev. E* **51**, 929 (1995).
28. P. Grigolini, G. Grosso and G. Pastori Parravicini, *Phys. Rev. B* **27**, 7342 (1983).
29. E. Sardella, *Phys. Rev. B* **43**, 13653 (1991).
30. C. A. Ullrich and G. Vignale, *Phys. Rev. B* **65**, 245102 (2002).

31. A. Lucas, *J. High Energy Phys.* **2015**(3), 071 (2015).
32. A. A. Patel and S. Sachdev, *Phys. Rev. B* **90**, 165146 (2014).
33. A. Lucas and S. Sachdev, *Phys. Rev. B* **91**, 195122 (2015).
34. G. D. Mahan, *Many-Particle Physics* (Springer, US, 1995).
35. D. N. Basov *et al.*, *Rev. Mod. Phys.* **83**, 471 (2011).
36. W. Götze and P. Wölfle, *Phys. Rev. B* **6**, 1226 (1972).
37. W. Götze and P. Wölfle, *J. Low Temp. Phys.* **5**, 575 (1971).
38. V. K. Jindal, H. B. Singh and K. N. Pathak, *Phys. Rev. B* **15**, 252 (1977).
39. J. S. Helman and W. Baltensperger, *Phys. Rev. B* **17**, 2427 (1978).
40. V. Čápek and I. Barvík, *J. Phys. C, Solid State Phys.* **18**, 6149 (1985).
41. P. N. Argyres and D. G. Resendes, *J. Phys., Condens. Matter* **1**, 7001 (1989).
42. P. Jung, Transport and approximate conservation laws in low dimensional systems, Ph.D. Thesis (University of Cologne, 2007).
43. F. V. Kyrychenko and C. A. Ullrich, arXiv:0704.2061.
44. L. P. Kadanoff and P. C. Martin, *Ann. Phys.* **24**, 419 (1963).
45. D. N. Zubarev, *Usp. Fiz. Nauk* **71**, 71 (1960).
46. B. Arfi, *Phys. Rev. B* **45**, 2352 (1992).
47. D. Ihle and N. M. Plakida, *Z. Phys. B* **96**, 159 (1994).
48. N. Plakida, *J. Phys. Soc. Jpn.* **65**, 12 (1996).
49. N. M. Plakida, *Z. Phys. B* **103**, 383 (1997).
50. N. M. Plakida, arXiv:1110.6715.
51. G. Jackeli and N. M. Plakida, *Theor. Math. Phys.* **114**, 335 (1998).
52. N. M. Plakida, *Correlations, Coherence, and Order*, eds. D. V. Shopova and D. I. Uzunov (Springer Science and Business Media, New York, 1999).
53. G. Jackeli and N. M. Plakida, *Phys. Rev. B* **60**, 5266 (1999).
54. A. A. Vladimirov, D. Ihle and N. M. Plakida, *Theor. Math. Phys.* **145**, 1576 (2005).
55. A. A. Vladimirov, D. Ihle and N. M. Plakida, *Phys. Rev. B* **80**, 104425 (2009).
56. N. M. Plakida, *High Temperature Cuprate Superconductors*, Chap. 5 (Springer, Heidelberg, 2010).
57. N. M. Plakida, *Strongly Correlated Systems*, Vol. 171, Springer Series in Solid-State Sciences, p. 173 (2011).
58. A. A. Vladimirov, D. Ihle and N. M. Plakida, *Phys. Rev. B* **83**, 024411 (2011).
59. A. A. Vladimirov, D. Ihle and N. M. Plakida, *Phys. Rev. B* **85**, 224536 (2012).
60. Yu. A. Tserkovnikov, *Theor. Math. Phys.* **50**, 171 (1982).
61. J. Spalek and A. M. Oleś, preprint of Jagiellonian University, SSPJU-6/76 (1976); *Physica B* **86–88**, 375 (1977).
62. P. Fazekas, *Lecture Notes on Electron Correlation and Magnetism* (World Scientific, Singapore, 1999).
63. P. F. Maldague, *Phys. Rev. B* **16**, 2437 (1977).
64. R. Kilian and G. Khaliullin, *Phys. Rev. B* **58**, R11841 (1998).
65. P. Prelovšek and A. Ramšak, *Phys. Rev. B* **65**, 174529 (2001).
66. I. Sega, P. Prelovšek and J. Bonča, *Phys. Rev. B* **68**, 054524 (2003).
67. P. Prelovšek, I. Sega and J. Bonča, *Phys. Rev. Lett.* **92**, 027002 (2004).
68. I. Sega and P. Prelovšek, *Phys. Rev. B* **73**, 092516 (2006).
69. P. Prelovšek and I. Sega, *Phys. Rev. B* **74**, 214501 (2006).
70. I. Sega and P. Prelovšek, *Phys. Rev. B* **79**, 140504 (2009).
71. T. R. Chien, Z. Z. Wang and N. P. Ong, *Phys. Rev. Lett.* **67**, 2088 (1991).
72. N. Das and N. Singh, *Int. J. Mod. Phys. B* **30**, 1650071 (2016).
73. P. Bhalla and N. Singh, *Eur. Phys. J. B* **89**, 49 (2016).
74. S. G. Sharapov and J. P. Carbotte, *Phys. Rev. B* **72**, 134506 (2005).
75. P. Bhalla, Nabyendu Das and N. Singh, *Phys. Lett. A* **380**, 2000 (2016).

EPJ B

Condensed Matter
and Complex Systems

EPJ.org
your physics journal

Eur. Phys. J. B (2016) 89: 49

DOI: [10.1140/epjb/e2016-60799-9](https://doi.org/10.1140/epjb/e2016-60799-9)

Generalized Drude scattering rate from the memory function formalism: an independent verification of the Sharapov-Carbotte result

Pankaj Bhalla and Navinder Singh

edp sciences



 Springer

Generalized Drude scattering rate from the memory function formalism: an independent verification of the Sharapov-Carbotte result

Pankaj Bhalla^{1,2,a} and Navinder Singh¹

¹ Physical Research Laboratory, Navrangpura, 380009 Ahmedabad, India

² Indian Institute of Technology 382424 Gandhinagar, India

Received 8 October 2015 / Received in final form 15 December 2015

Published online 17 February 2016 – © EDP Sciences, Società Italiana di Fisica, Springer-Verlag 2016

Abstract. An explicit perturbative computation of the Mori's memory function was performed by Götze and Wölfle (GW) to calculate generalized Drude scattering (GDS) rate for the case of electron-impurity and electron-phonon scattering in metals by assuming constant electronic density of states at the Fermi energy. In the present investigation, we go beyond this assumption and extend the GW formalism to the case in which there is a gap around the Fermi surface in electron density of states. The resulting GDS is compared with a recent one by Sharapov and Carbotte (SC) obtained through a different route. We find good agreement between the two at finite frequencies. However, we find discrepancies in the dc scattering rate. These are due to a crucial assumption made in SC namely $\omega \gg |\Sigma(\epsilon + \omega) - \Sigma^*(\epsilon)|$. No such high frequency assumption is made in the memory function based technique.

1 Introduction

The study of transport properties like optical conductivity is very important to understand the electronic interactions in complex many body systems like cuprates [1,2]. The electronic interactions comprises of electron-phonon, electron-boson (spin-fluctuations), electron-impurity, electron-electron interactions. Experimentally, the signatures of these interactions can be grasped by using optical data ($\sigma(\omega, T)$) [3,4] which includes the deduction of the generalized Drude scattering (GDS) rate and mass enhancement factor using the standard form

$$\sigma(\omega, T) = \frac{\omega_p^2}{4\pi} \frac{1}{1/\tau(\omega, T) + i\omega(1 + \lambda(\omega, T))}. \quad (1)$$

Here $1/\tau(\omega, T)$ is the frequency and temperature dependent scattering rate, $\lambda(\omega, T)$ is the frequency and temperature dependent mass enhancement factor and ω_p is the plasma frequency. On theory side, the derivation of the analytical formulae for these quantities (like $1/\tau(\omega, T)$ and $\lambda(\omega, T)$) is very complicated.

Generally, the optical conductivity is calculated using Boltzmann's equation by assuming relaxation time approximation [5–7]. In that picture, scattering rate is considered as constant (independent of frequency and temperature) and the resulting behaviour corresponds to the Drude behaviour. In systems such as cuprates where the

electron-boson, electron-electron interactions are important, this approach is inadequate as experiments show that scattering rate *does* depend on frequency and temperature [8,9]. The complete solution of the transport problem in cuprates and other strongly correlated materials is complicated as there are no controlled perturbation parameters. For example, in simple metals where, as first shown by Holstein [10], the perturbation parameter is v_s/v_F (sound speed/Fermi velocity) which is a small parameter and perturbative calculations are justified. Building upon Holstein's work on metals [10], Allen [11] has derived a relation for frequency dependent scattering rate. This has been further generalized by Mitrović and Fiorucci [12] by considering the effects of non-constant density of states. Further this has been extended recently for the finite temperature case by Sharapov and Carbotte [13]. All these approaches are based on some assumptions such as neglecting vertex corrections. To go beyond this assumption, we have developed a formula for frequency and temperature dependent scattering rate using memory function technique [14,15] which includes the effect of vertex corrections [16] (where the current-current correlators are directly computed without writing them in terms of single-particle Green's function). This technique is a generalization of Zwanzig projection operator technique [17,18]. Physically, this approach is very appealing, because the conductivity $\sigma(\omega, T)$ can be cast into the generalized Drude form with frequency and temperature dependent scattering rate. Recently, it has also been used by several

^a e-mail: pankaj@prl.res.in

authors to study the transport properties of different systems [19–27].

The paper is organized as follows. In Section 2, we have elaborated the Götze-Wölfle memory function formalism [16]. In Section 3, we go beyond the constant electronic density of states assumption and introduce the gapped density of states and calculate the imaginary part of memory function. Here we also discuss the dc and ac imaginary part of memory function in different temperature regimes and in appropriate limits we reproduce GW results. In Section 4, we compare our findings with SC result [13] and finally we conclude with a brief discussion in Section 5.

2 Götze-Wölfle formalism for electron-phonon scattering

In this section, a short introduction to GW formalism is presented [16]. The Hamiltonian used for electron-phonon interaction is given by

$$H = H_0 + H_{\text{ep}} + H_{\text{p}}, \quad (2)$$

where H_0 is the Hamiltonian for *non-interacting electrons* and is represented as:

$$H_0 = \sum_{\mathbf{k}, \sigma} \epsilon(\mathbf{k}) c_{\mathbf{k}, \sigma}^\dagger c_{\mathbf{k}, \sigma}, \quad (3)$$

where $\epsilon(\mathbf{k})$ is the band dispersion and $c_{\mathbf{k}, \sigma}^\dagger$, $c_{\mathbf{k}, \sigma}$ are creation and annihilation operators with wave vector \mathbf{k} and spin σ . The Hamiltonian H_{ep} represents the electron-phonon interaction and is given by

$$H_{\text{ep}} = \sum_{\mathbf{k}, \mathbf{k}', \sigma} \left[D(\mathbf{k} - \mathbf{k}') c_{\mathbf{k}', \sigma}^\dagger c_{\mathbf{k}, \sigma} b_{\mathbf{k} - \mathbf{k}'} + \text{h.c.} \right]. \quad (4)$$

Here $b_{\mathbf{k} - \mathbf{k}'}$, $b_{\mathbf{k} - \mathbf{k}'}^\dagger$ are the annihilation and creation operators for phonons and $D(\mathbf{k} - \mathbf{k}')$ is the electron-phonon matrix element. Here the symbol *h.c.* corresponds to the Hermitian conjugate of first term. The third part of equation (2) represents the free phonon Hamiltonian

$$H_{\text{p}} = \sum_q \omega_q \left(b_q^\dagger b_q + \frac{1}{2} \right), \quad (5)$$

where ω_q is the phonon frequency.

According to the linear response theory, the dynamical conductivity is defined as [28–31]

$$\sigma(z) = -i \frac{1}{z} \chi(z) + i \frac{\omega_p^2}{4\pi z}. \quad (6)$$

Here $\omega_p^2 = 4\pi N_e e^2 / m$ is the square of plasma frequency where e electronic charge, m electron mass and N_e is the electron density, z is the complex frequency and $\chi(z)$ is the current-current correlation function defined as:

$$\chi(z) = \langle \langle J; J \rangle \rangle_z = i \int_0^\infty e^{izt} \langle [J(t), J] \rangle, \quad (7)$$

where $J = \sum_{\mathbf{k}} e v(\mathbf{k}) c_{\mathbf{k}, \sigma}^\dagger c_{\mathbf{k}, \sigma}$ is the current density and $v(\mathbf{k})$ is the velocity dispersion. Here $[J(t), J]$ denotes the commutator, $\langle \dots \rangle$ denotes the ensemble average at temperature T and $\langle \langle \dots \rangle \rangle$ denotes the Laplace transform of the ensemble average.

According to the Götze and Wölfle approach [16], the memory function is defined as

$$M(z) = z \frac{\chi(z)}{\chi_0 - \chi(z)} \quad \text{or} \quad \chi(z) = \chi_0 \frac{M(z)}{z + M(z)}, \quad (8)$$

where χ_0 corresponds to the static limit of correlation function (i.e. $\chi_0 = N_e / m$) [16]. Using this, the conductivity from equation (6) in terms of memory function can be written as

$$\sigma(z) = \frac{i}{4\pi} \frac{\omega_p^2}{z + M(z)}. \quad (9)$$

In reference [16], an expansion for

$$M(z) = \frac{z\chi(z)}{\chi_0} \left(1 + \frac{\chi(z)}{\chi_0} - \dots \right)$$

is used. Basis of this assumption is the smallness of electron-phonon interaction energy as compared to the Fermi energy of free electrons. Using this expansion and on keeping the leading order term, the memory function $M(z)$ can be written as:

$$M(z) = z \frac{\chi(z)}{\chi_0} = z \frac{\langle \langle J; J \rangle \rangle_z}{\chi_0}. \quad (10)$$

To compute memory function, we need $\langle \langle J; J \rangle \rangle_z$ which by using equation of motion is:

$$z \langle \langle J; J \rangle \rangle_z = \langle [J, J] \rangle + \langle \langle [J, H_{\text{ep}}]; J \rangle \rangle_z. \quad (11)$$

As the first term of r.h.s is zero, hence the above expression is equivalent to second term which can be further calculated by applying equation of motion.

$$z \langle \langle [J, H_{\text{ep}}]; J \rangle \rangle_z = \langle \langle [J, H_{\text{ep}}], J \rangle \rangle - \langle \langle [J, H_{\text{ep}}]; [J, H_{\text{ep}}] \rangle \rangle_z. \quad (12)$$

For $z = 0$, $\langle \langle [J, H_{\text{ep}}], J \rangle \rangle = \langle \langle [J, H_{\text{ep}}]; [J, H_{\text{ep}}] \rangle \rangle_{z=0}$. Thus, the memory function $M(z)$ becomes

$$M(z) = \frac{\phi(0) - \phi(z)}{z\chi_0}. \quad (13)$$

Here $\phi(z)$ (called as correlation function) is defined as

$$\phi(z) = \langle \langle [J, H_{\text{ep}}]; [J, H_{\text{ep}}] \rangle \rangle_z. \quad (14)$$

For the present case of electron-phonon interaction, the correlation function from equations (4) and (14) is

$$\begin{aligned} \phi(z) &= \sum_{\mathbf{k}, \mathbf{k}'} \sum_{\mathbf{p}, \mathbf{p}'} \sum_{\sigma, \sigma'} [v_1(\mathbf{k}) - v_1(\mathbf{k}')] [v_1(\mathbf{p}) - v_1(\mathbf{p}')] \\ &\times \left\langle \left\langle D(\mathbf{k} - \mathbf{k}') c_{\mathbf{k}, \sigma}^\dagger c_{\mathbf{k}', \sigma} b_{\mathbf{k} - \mathbf{k}'} - D^*(\mathbf{k} - \mathbf{k}') b_{\mathbf{k} - \mathbf{k}'}^\dagger c_{\mathbf{k}', \sigma}^\dagger c_{\mathbf{k}, \sigma}; \right. \right. \\ &\left. \left. D(\mathbf{p} - \mathbf{p}') c_{\mathbf{p}, \sigma'}^\dagger c_{\mathbf{p}', \sigma'} b_{\mathbf{p} - \mathbf{p}'} - D^*(\mathbf{p} - \mathbf{p}') b_{\mathbf{p} - \mathbf{p}'}^\dagger c_{\mathbf{p}', \sigma'}^\dagger c_{\mathbf{p}, \sigma'} \right\rangle \right\rangle \end{aligned} \quad (15)$$

$$\begin{aligned} \phi(z) &= - \sum_{\mathbf{k}, \mathbf{k}'} \sum_{\mathbf{p}, \mathbf{p}'} \sum_{\sigma, \sigma'} [v_1(\mathbf{k}) - v_1(\mathbf{k}')] [v_1(\mathbf{p}) - v_1(\mathbf{p}')] \\ &\times [D(\mathbf{k} - \mathbf{k}') D^*(\mathbf{p} - \mathbf{p}')] \\ &\times \left(\left\langle \left\langle c_{\mathbf{k}, \sigma}^\dagger c_{\mathbf{k}', \sigma} b_{\mathbf{k} - \mathbf{k}'}; b_{\mathbf{p} - \mathbf{p}'}^\dagger c_{\mathbf{p}', \sigma'}^\dagger c_{\mathbf{p}, \sigma'} \right\rangle \right\rangle \right. \\ &\left. + \left\langle \left\langle c_{\mathbf{k}, \sigma} c_{\mathbf{k}', \sigma}^\dagger b_{\mathbf{k} - \mathbf{k}'}^\dagger; b_{\mathbf{p} - \mathbf{p}'} c_{\mathbf{p}', \sigma'} c_{\mathbf{p}, \sigma'}^\dagger \right\rangle \right\rangle \right). \end{aligned} \quad (16)$$

To evaluate the $\phi(z)$, we need to calculate

$$\left\langle \left\langle c_{\mathbf{k}, \sigma}^\dagger c_{\mathbf{k}', \sigma} b_{\mathbf{k} - \mathbf{k}'}; b_{\mathbf{p} - \mathbf{p}'}^\dagger c_{\mathbf{p}', \sigma'}^\dagger c_{\mathbf{p}, \sigma'} \right\rangle \right\rangle$$

which can be calculated as (using definition (7))

$$\begin{aligned} &\left\langle \left\langle c_{\mathbf{k}, \sigma}^\dagger c_{\mathbf{k}', \sigma} b_{\mathbf{k} - \mathbf{k}'}; b_{\mathbf{p} - \mathbf{p}'}^\dagger c_{\mathbf{p}', \sigma'}^\dagger c_{\mathbf{p}, \sigma'} \right\rangle \right\rangle \\ &= i \int_0^\infty dt e^{izt} \langle [c_{\mathbf{k}, \sigma}^\dagger(t) c_{\mathbf{k}', \sigma}(t) b_{\mathbf{k} - \mathbf{k}'}(t); b_{\mathbf{p} - \mathbf{p}'}^\dagger(t) c_{\mathbf{p}', \sigma'}^\dagger(t) c_{\mathbf{p}, \sigma'}(t)] \rangle. \end{aligned} \quad (17)$$

Using $c_{\mathbf{k}, \sigma}(t) = c_{\mathbf{k}, \sigma} e^{-i\epsilon_{\mathbf{k}} t}$ and performing the integration over time and ensemble average, we have

$$\begin{aligned} &\left\langle \left\langle c_{\mathbf{k}, \sigma}^\dagger c_{\mathbf{k}', \sigma} b_{\mathbf{k} - \mathbf{k}'}; b_{\mathbf{p} - \mathbf{p}'}^\dagger c_{\mathbf{p}', \sigma'}^\dagger c_{\mathbf{p}, \sigma'} \right\rangle \right\rangle \\ &= - \frac{[f(1 - f')(1 + n) - f'(1 - f)n] \delta_{\mathbf{k}, \mathbf{p}} \delta_{\mathbf{k}', \mathbf{p}'} \delta_{\sigma, \sigma'}}{z - \epsilon_{\mathbf{k}'} + \epsilon_{\mathbf{k}} - \omega_{\mathbf{k} - \mathbf{k}'}}. \end{aligned} \quad (18)$$

Here $f \equiv f(\epsilon_{\mathbf{k}}) = (e^{\beta \epsilon_{\mathbf{k}}} + 1)^{-1}$ and $n \equiv n(\omega_{\mathbf{k} - \mathbf{k}'}) = (e^{\beta \omega_{\mathbf{k} - \mathbf{k}'}} - 1)^{-1}$ represent the Fermi and Bose distribution functions and β corresponds to inverse of temperature. Inserting this equation in equation (16) and hence in equation (13) and then by taking the limit $z \rightarrow \omega + i\eta$, $\eta \rightarrow 0^+$, the imaginary part of the memory function can be expressed as

$$\begin{aligned} M''(\omega, T) &= \frac{2\pi}{3} \frac{1}{mN_e} \sum_{\mathbf{k}, \mathbf{k}'} |D(\mathbf{k} - \mathbf{k}')|^2 (\mathbf{k} - \mathbf{k}')^2 f'(1 - f)n \\ &\times \left[\frac{e^{\beta \omega} - 1}{\omega} \delta(\epsilon_{\mathbf{k}} - \epsilon_{\mathbf{k}'} - \omega_{\mathbf{k} - \mathbf{k}'} + \omega) \right. \\ &\left. + (\text{terms with } \omega \rightarrow -\omega) \right]. \end{aligned} \quad (19)$$

Convert the summations over \mathbf{k} and \mathbf{k}' into integrations and assuming that \mathbf{k} is pointing along the z -direction

and \mathbf{k}' subtends an angle θ with it (at the end \mathbf{k} integration over all directions and magnitudes is to be performed). Insert an integral $\int dq \delta(q - |\mathbf{k} - \mathbf{k}'|)$ over q to stratify the calculation as given below. Thus equation (19) becomes

$$\begin{aligned} M''(\omega, T) &= \frac{2}{3} \pi \frac{2N^2}{(2\pi)^4 mN_e} \int_0^\infty dq q^2 |D(q)|^2 \int_0^\infty dk k^2 \\ &\times \int_0^\infty dk' k'^2 \int_0^\pi d\theta \sin \theta \delta(q - |\mathbf{k} - \mathbf{k}'|) \\ &\times f'(1 - f)n \left[\frac{e^{\beta \omega} - 1}{\omega} \delta(\epsilon_{\mathbf{k}} - \epsilon_{\mathbf{k}'} - \omega_{\mathbf{k} - \mathbf{k}'} + \omega) \right. \\ &\left. + (\text{terms with } \omega \rightarrow -\omega) \right]. \end{aligned} \quad (20)$$

Here due to the presence of Fermi factors $f'(1 - f)$ the integrand has finite value only around the Fermi surface and vanishes outside the strip of width $2/\beta$ ($\omega \ll \epsilon_F$). Thus \mathbf{k} and \mathbf{k}' can be approximately replaced by \mathbf{k}_F . With this the θ integral can be simplified as:

$$\int_0^\pi d\theta \sin \theta \delta(q - \sqrt{2}k_F \sqrt{1 - \cos \theta})$$

which will yield the result $\frac{q}{k_F^2}$. Using this and converting \mathbf{k} integrals into energy integrals, the above equation reduces to

$$\begin{aligned} M''(\omega, T) &= \frac{4}{3} \frac{N^2 m^2 \epsilon_F}{(2\pi)^3 N e k_F^2} \int_0^{q_D} dq q^3 |D(q)|^2 \\ &\times \int_{-\infty}^\infty d\epsilon \frac{n}{e^{-\beta(\epsilon - \epsilon_F)} + 1} \\ &\times \left[\frac{1}{e^{\beta(\epsilon - \epsilon_F + \omega - \omega_q)} + 1} \frac{e^{\beta \omega} - 1}{\omega} \right. \\ &\left. + (\text{terms with } \omega \rightarrow -\omega) \right]. \end{aligned} \quad (21)$$

This is an expression for the imaginary part of memory function as deduced by Götze-Wölfle [16]. It can be simplified by using electron-phonon matrix element for acoustic phonons which is defined as [5]

$$D(\mathbf{q}) = \left(\frac{1}{2m_i N \omega_q} \right)^{-1/2} q C(q); \quad \omega_q = c_s q, \quad (22)$$

where $C(q)$ is the slowly varying function of q , m_i is the ion mass, N is the total number of unit cells and c_s is the sound velocity. To analyze equation (21), various limiting cases using equation (22) were discussed in reference [16].

3 Memory function with gapped density of states

In this section we go beyond the assumption of constant electronic density of states and we consider a system with

a gap around the Fermi surface. In this case, density of states is zero in energy region $(-\Delta, \Delta)$. Thus the energy integration in equation (21) has to be

$$I = \int_{-\infty}^{\epsilon_F - \Delta} d\epsilon \frac{e^{\beta(\epsilon - \epsilon_F)}}{e^{\beta(\epsilon - \epsilon_F)} + 1} \frac{1}{e^{\beta(\epsilon - \epsilon_F + \omega - \omega_q)} + 1} + \int_{\epsilon_F + \Delta}^{\infty} d\epsilon \frac{e^{\beta(\epsilon - \epsilon_F)}}{e^{\beta(\epsilon - \epsilon_F)} + 1} \frac{1}{e^{\beta(\epsilon - \epsilon_F + \omega - \omega_q)} + 1}. \quad (23)$$

After simplification we have

$$I = \frac{1}{\beta} \frac{1}{e^{\beta(\omega - \omega_q)} - 1} \times \log \left(\frac{(1 + e^{\beta(-\Delta + \omega - \omega_q)})(1 + e^{\beta\Delta})e^{\beta(\omega - \omega_q)}}{(1 + e^{\beta(\Delta + \omega - \omega_q)})(1 + e^{-\beta\Delta})} \right). \quad (24)$$

Using this, the imaginary part of memory function can be written as:

$$M''(\omega, T) = \frac{\pi^3 N^2 \rho_F^2}{4mk_F^5} \int_0^{q_D} dq q^3 |D(q)|^2 \frac{1}{\beta} n \times \left[\frac{e^{\beta\omega} - 1}{\omega} \frac{1}{e^{\beta(\omega - \omega_q)} - 1} \times \log \left[\left(\frac{1 + e^{\beta\Delta}}{1 + e^{-\beta\Delta}} \right) \left(\frac{1 + e^{-\beta(\Delta - \omega + \omega_q)}}{e^{\beta\Delta} + e^{\beta(\omega_q - \omega)}} \right) \right] + (\text{terms with } \omega \rightarrow -\omega) \right]. \quad (25)$$

This is the desired expression for the frequency and temperature dependent imaginary part of memory function. For $\Delta = 0$ and using phonon matrix element (Eq. (22)), this expression reduces to the expression (refer Eq. (54a)) given in original GW work [16], as it should. In actual practise (i.e. for an arbitrary form of gap around the Fermi surface), the general expression of the imaginary part of memory function is complicated and is difficult to proceed analytically. A general formulae is given in Appendix. Thus for the simplicity of calculation, we have discussed the specific system in this article. Further to write $M''(\omega, T)$ in compact form, change the variable ω_q to Ω in above equation which can be rewritten as:

$$M''(\omega, T) = \frac{2\pi}{\omega} \int_0^{\omega_D} d\Omega \alpha^2 F(\Omega) \frac{1}{\beta} \left[\frac{e^{\beta\omega} - 1}{e^{\beta(\omega - \Omega)} - 1} \times \frac{1}{e^{\beta\Omega} - 1} \log \left(\frac{1 + e^{-\beta(\Delta - \omega + \Omega)}}{1 + e^{-\beta(\Delta + \omega - \Omega)}} \right) - (\text{terms with } \omega \rightarrow -\omega) \right], \quad (26)$$

where $\alpha^2 F(\Omega)$ is defined as

$$\alpha^2 F(\Omega) = \frac{\pi^2 N^2 \rho_F^2}{8mk_F^5 c_s^4} \Omega^3 |D(\Omega)|^2. \quad (27)$$

This is known as phonon spectral function [11]. In the case of cuprates, it is replaced by $I^2 \chi(\Omega)$ which represents the

boson spectral function [13]. This form is same as given by Allen [11]

$$\left(\alpha^2 F(\Omega) = \frac{N(0)}{4v_F^2} \langle \langle |M_{\mathbf{k}\mathbf{k}'}|^2 (v(\mathbf{k}) - v(\mathbf{k}'))^2 \times \delta(\hbar\Omega_{\mathbf{Q}} - \hbar\Omega) \rangle \rangle \right).$$

Equation (26) is our main result. To discuss it in various temperature and frequency regimes, we use the phonon matrix element equation (22) and calculate $M''(\omega, T)$ in next sections.

3.1 DC memory function

In the zero frequency limit and assuming $C(q)$ as a constant i.e. $C(q) = 1/\rho_F$ [5], the imaginary part of the memory function (Eq. (25)) becomes

$$M''(0, T) = \frac{1}{8} \pi^3 \frac{N}{mm_i k_F^5} \int_0^{q_D} dq q^5 \frac{1}{(e^{\beta\omega_q} - 1)(e^{-\beta\omega_q} - 1)} \times \frac{1}{\omega_q} \log \left[\frac{1 + e^{\beta\Delta}}{1 + e^{-\beta\Delta}} \frac{1 + e^{-\beta(\Delta + \omega_q)}}{e^{\beta\Delta} + e^{\beta\omega_q}} \right]. \quad (28)$$

Now consider the case of $T \gg \omega_D, \Delta$, the above equation reduces to

$$M''(0, T) = \frac{1}{8} \pi^3 \frac{N}{mm_i k_F^5} \int_0^{q_D} dq q^5 \frac{1}{\omega_q} \frac{-1 + \beta\omega_q}{(\beta\omega_q)^2} \times \log \left[\frac{2 - \beta\Delta - \beta\omega_q}{2 - \beta\Delta + \beta\omega_q} \right]. \quad (29)$$

On substituting $x = \frac{q\Theta_D}{q_D T}$ (i.e. $\beta\omega_q = x$) where Θ_D is the Debye temperature, the dc memory function reduces to

$$M''(0, T) = \frac{1}{8} \pi^3 \frac{N}{mm_i k_F^5 \Theta_D} q_D^6 \left(\frac{T}{\Theta_D} \right)^5 \times \int_0^{\beta\Theta_D} dx x^2 (x - 1) \log \left[\frac{2 - \beta\Delta - x}{2 - \beta\Delta + x} \right]. \quad (30)$$

This expression under case $T \gg \omega_D, \Delta$ is equivalent to

$$M''(0, T) \simeq A \left\{ \frac{T}{\Theta_D} + \frac{\Delta}{\Theta_D} + \frac{1}{T} \left(\frac{\Delta^2}{8\Theta_D} + \frac{8\Delta}{5} - \frac{\Theta_D}{6} \right) \dots \right\}, \quad (31)$$

where A refers for constant numerical factor. Similarly for $T \ll \omega_D, \Delta$, equation (28) becomes

$$M''(0, T) = -\frac{1}{8} \pi^3 \frac{N}{mm_i k_F^5 \Theta_D} q_D^6 \left(\frac{T}{\Theta_D} \right)^5 \times \int_0^{\beta\Theta_D} dx x^4 e^{-x} \log \left[\frac{e^{\beta\Delta} + e^{-x}}{e^{\beta\Delta} + e^x} \right]. \quad (32)$$

This expression can also be simplified as:

$$M''(0, T) \simeq A e^{-\beta\Delta} \left\{ \frac{1}{5} - \frac{3}{4} \left(\frac{T}{\Theta_D} \right)^5 \dots \right\}. \quad (33)$$

Substituting equation (32) in equation (8) and hence in equation (6), leads to the expression of dc conductivity for the electron-phonon interaction. Here if we insert gap $\Delta = 0$ in equation (28), we obtain equation (54b) as given in reference [16], as expected.

3.2 AC memory function

We proceed again with equation (25) to study frequency dependent behaviour of memory function in different regimes. In the high frequency regime i.e. for $\omega \gg \omega_D$ and using same approximation ($C(q) = 1/\rho_F$) as considered for the dc case, the imaginary part of memory function becomes

$$M''(\omega, T) = \frac{1}{8} \pi^3 \frac{N}{mm_i k_F^5} \int_0^{q_D} dq q^5 \frac{1}{\beta \omega q} \frac{n}{\omega} \times \left[\log \left(\frac{1 + e^{-\beta(\Delta-\omega)}}{1 + e^{-\beta(\Delta+\omega)}} \right) - e^{\beta\omega q} \log \left(\frac{1 + e^{-\beta(\Delta+\omega)}}{1 + e^{-\beta(\Delta-\omega)}} \right) \right]. \quad (34)$$

When the gap is smaller than the $|\omega - \omega_D|$ i.e. $\Delta < |\omega - \omega_D|$, the above equation reduces to¹

$$M''(\omega, T) = \frac{1}{8} \pi^3 \frac{N}{mm_i k_F^5 \Theta_D} q_D^6 \left(\frac{T}{\Theta_D} \right)^5 \times \int_0^{\beta\Theta_D} dx x^4 \coth \left(\frac{x}{2} \right). \quad (35)$$

From this we identify that at high temperature, the imaginary part of memory function becomes temperature and frequency independent. This means the saturation behaviour of $M''(\omega, T)$ for $\omega \gg \omega_D$. The reason is that under this condition, the integral approaches to $(\Theta_D/T)^5$ and it cancels with prefactor $(T/\Theta_D)^5$ in equation (35). At low temperature, it varies linearly with temperature as the integral approaches to $(\Theta_D/T)^4$.

In the next section we compare our findings (Eq. (26)) with the Sharapov-Carbotte [13].

4 Comparison with Sharapov-Carbotte results

Sharapov and Carbotte have deduced a relation for the generalized Drude scattering rate [13] taking electron-boson interaction and non constant electronic density of states. Using Kubo formula [32] and calculating the self

energy under certain assumptions (as discussed below), they derived the following expression

$$\frac{1}{\tau(\omega, T)} = \frac{\pi}{\omega} \int_0^\infty d\Omega I^2 \chi(\Omega) \int_{-\infty}^\infty d\omega' \times \left[\frac{\tilde{N}(\omega' - \Omega)}{N(0)} + \frac{\tilde{N}(-\omega' + \Omega)}{N(0)} \right] \times [n(\Omega) + f(\Omega - \omega')] \times [f(\omega' - \omega) - f(\omega' + \omega)], \quad (36)$$

where $I^2 \chi(\omega)$ is the boson spectral function and $\tilde{N}(\omega)$ is the quasiparticle electronic density of states and $N(0)$ is for normalization. In deriving the above formula, the following assumptions were made: (1) vertex corrections were neglected, (2) energy independent character of plasma frequency in the vicinity of Fermi level and (3) $|\Sigma(\epsilon + \omega) - \Sigma^*(\epsilon)| \ll \omega$ where $\Sigma(\epsilon)$ is the electronic self energy.

To compare our approach (Eq. (26)) with SC approach (Eq. (36)), we have done calculations using models for electronic density of states and the boson spectral function. First in SC approach, for the electronic density of states, we use a square well type model with center at Fermi energy and considered a gap of 2Δ around it. Same gap is taken in our approach (Eq. (26)). Second, for the boson spectral function, $I^2 \chi(\Omega)$, we modelled it as Lorentzian of the type $\frac{\Gamma \Omega}{(\Omega - \Omega_E)^2 + (\Gamma)^2}$ where Ω_E represents the boson peak frequency and Γ is the width of the Lorentzian (this form has been used extensively in Refs. [33–35]). Thus for comparison, we use the same form of $I^2 \chi(\Omega)$ in SC approach and our approach. In the whole analysis, we have fixed the value of Ω_E and Γ as 0.02 eV and 0.04 eV, respectively in both approaches. The value of Debye frequency (the upper limit of phonon frequency integration Eq. (26)) is very much high as compared to the Lorentzian width, hence ω_D does not give any effect in whole calculation. To compare the results from both the approaches, the frequency dependent scattering rate has been plotted at different temperatures. In Figure 1, we can observe an excellent agreement between both the approaches. As the gap magnitude is increased, the scattering rate shows suppression upto the frequency $\omega \sim \Delta$ as expected (compare Figs. 1a and 1c). These results qualitatively agree with experimental results [8,9].

In Figure 2, we plot $1/\tau(\omega \rightarrow 0, T)$ as a function of temperature T . Here we can observe that the memory function approach yields more magnitude over the SC approach. In Figure 2a i.e. in zero frequency limit, the ratio $|\frac{1/\tau_{MF} - 1/\tau_{SC}}{1/\tau_{MF}}|_{100K}$, where $1/\tau_{MF}$ and $1/\tau_{SC}$ represents the scattering rate by memory function technique and SC technique respectively, is 0.7 which becomes 0.4 at $\omega = 0.05$ eV (as shown in Fig. 2b) and at $\omega = 0.5$ eV it further reduces to 0.031 (as shown in Fig. 2c). This shows that the difference between scattering rates using memory function approach and SC approach reduces as we go from dc limit to finite frequency limit. Also both approaches explain the Holstein's mechanism at $T = 0$ K [36,37] (as shown in Figs. 2b and 2c). Thus we notice that there are

¹ In the opposite case $|\omega - \omega_D| < \Delta$, equation (25) leads to vanishing scattering rate.

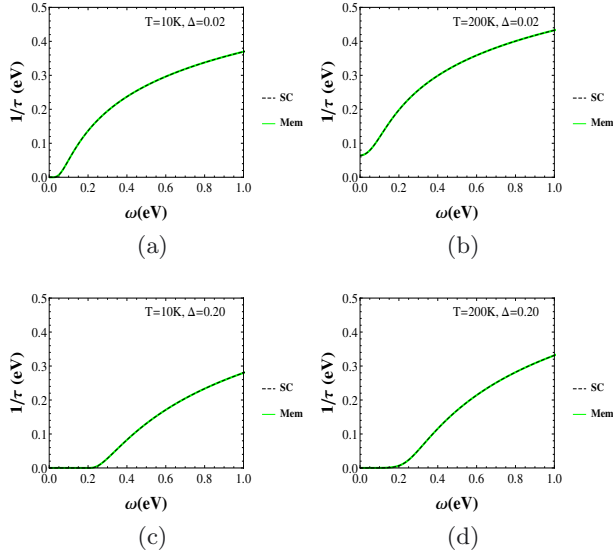


Fig. 1. Comparison plot of scattering rate $1/\tau(\omega, T)$ ($=M''(\omega, T)$) calculated using Memory function approach (Mem, solid, green) and Sharapov-Carbotte approach (SC, dashed, black) at temperature $T = 10$ K and 200 K and at gap $\Delta = 0.02$ eV and 0.20 eV. The agreement is excellent.

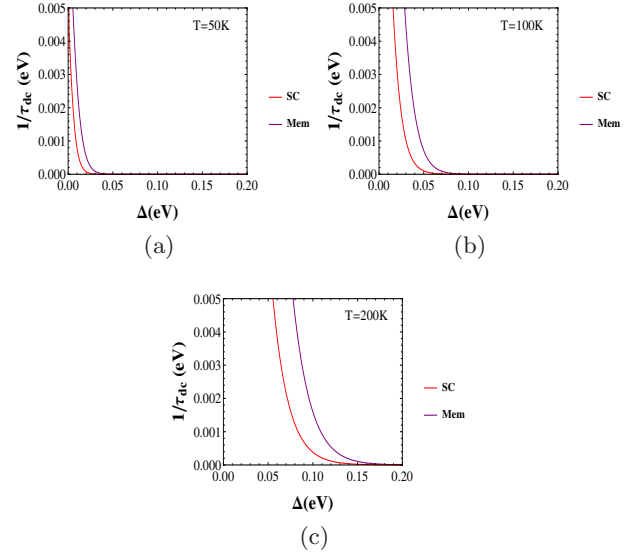


Fig. 3. Comparison of dc scattering rate ($1/\tau_{dc}$) as a function of Δ using Memory function approach (Mem, Purple) and Sharapov-Carbotte approach (SC, Red) at various temperatures 50 K, 100 K and 200 K.

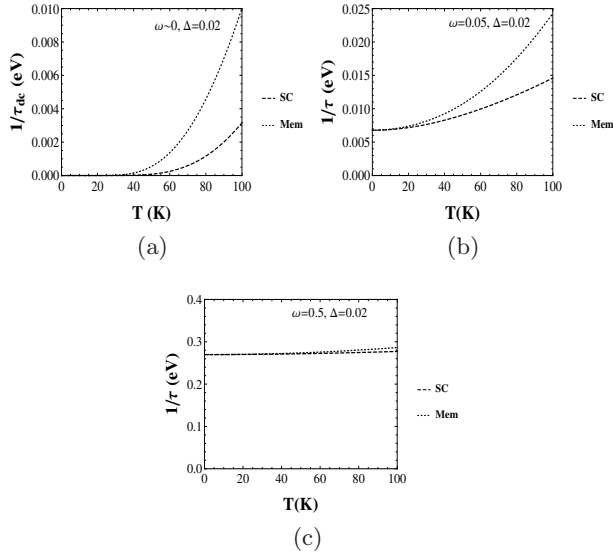


Fig. 2. Temperature variation of scattering rate with two different approaches namely memory function (Mem, dotted) and Sharapov-Carbotte (SC, dashed) at gap 0.02 eV; (a) dc case (b) at $\omega = 0.05$ eV (c) at $\omega = 0.5$ eV.

discrepancies between the two approaches in the d.c. limit. The reasons are discussed in next section.

Next, we have plotted $1/\tau_{dc}$ at different temperatures as a function of Δ and compare the both approaches. Here we observe that $1/\tau_{dc}$ decreases with the increase of gap energy Δ . Also, we find that the difference between the $1/\tau_{SC}$ and $1/\tau_{MF}$ is not much dependent on Δ , but it does

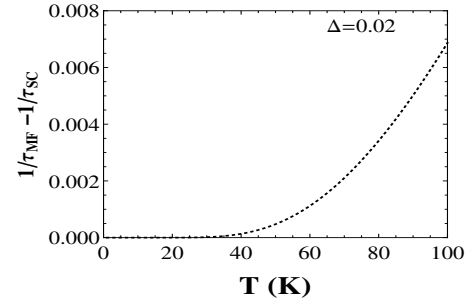


Fig. 4. Variation of difference $(1/\tau_{MF} - 1/\tau_{SC})$ of dc scattering rate with temperature calculated by two different approaches MF and SC at $\Delta = 0.02$ eV.

increase with increasing temperature. These discrepancies observed in the dc limit are discussed in the next section.

5 Discussion

It is observed that the finite frequency scattering rate using memory function formula is in excellent agreement with the same obtained from SC formula as shown in Figure 1. This shows that the assumptions made in these two different approaches are consistent at finite frequencies. However, while discussing dc scattering rate, we observe significant discrepancy between the two approaches (Figs. 2a and 3). To illustrate it further, we have plotted the difference in the magnitudes of scattering rates calculated by both approaches. The difference $(1/\tau_{MF} - 1/\tau_{SC})$ at $\Delta = 0.02$ eV is plotted in Figure 4. Here we find that

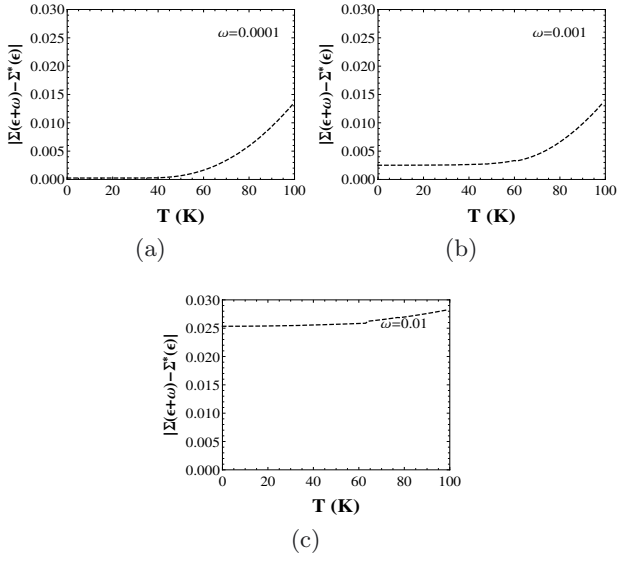


Fig. 5. Plot of $|\Sigma(\epsilon+\omega) - \Sigma^*(\epsilon)|$ with temperature at different frequencies such as (a) $\omega = 0.0001$ eV, (b) $\omega = 0.001$ eV and (c) $\omega = 0.01$ eV. Here $\Sigma(\omega)$ represents the self energy and * corresponds to the conjugate.

this difference increases with the rise of temperature. The reason behind this difference in the dc case is the assumption made by SC i.e. $\omega \gg |\Sigma(\epsilon + \omega) - \Sigma^*(\epsilon)|$ which becomes more severe in high temperature regime. To clarify this fact, we plot the quantity $|\Sigma(\epsilon + \omega) - \Sigma^*(\epsilon)|$ as a function of temperature in Figure 5 (where the expression used for $\Sigma(\omega)$ has been given in Ref. [13]). It shows that the magnitude of the difference of self energy increases with the temperature. This shows the stronger violation of the condition $\omega \gg |\Sigma(\epsilon + \omega) - \Sigma^*(\epsilon)|$ in high temperature limit. It implies that SC formalism is not appropriate to study the dc behavior and the disagreement is severe at high temperature, but it is quite reasonable for the finite frequency case.

Regime of validity of Memory function: It is important to recognize that memory function calculation of $1/\tau(\omega)$ presented here is also perturbative in character and has its own limitations. Here in calculation, we have used the expansion for $M(z)$ which is given below equation (9) where $M(z) = (z\chi(z)/\chi_0) (1 + \chi(z)/\chi_0 + \dots)$. In the leading order approximation, we took $\chi(z)/\chi_0 \ll 1$, which implies that the magnitude of memory function is smaller than z ($M(z)/z = \chi(z)/\chi_0$). Thus to ensure this point we have plotted the frequency dependent scattering rate for temperature 10 K and 200 K at $\Delta = 0.02$ eV and 0.20 eV in Figure 6 and compared with the linear variation $f(\omega) = \omega$. From Figure 6, we find that our approach is valid for regime where $\Delta \gg T$ (as shown in Figs. 6a, 6c and 6d). Thus it is quite suited to study the pseudogap phase of cuprates when Δ is greater than the T . But our approach is not good *in the low frequency regime* to discuss the case where $\Delta \sim T$ (as shown in Fig. 6b). Such small gap scenarios occur in spin/charge density systems [38–40].

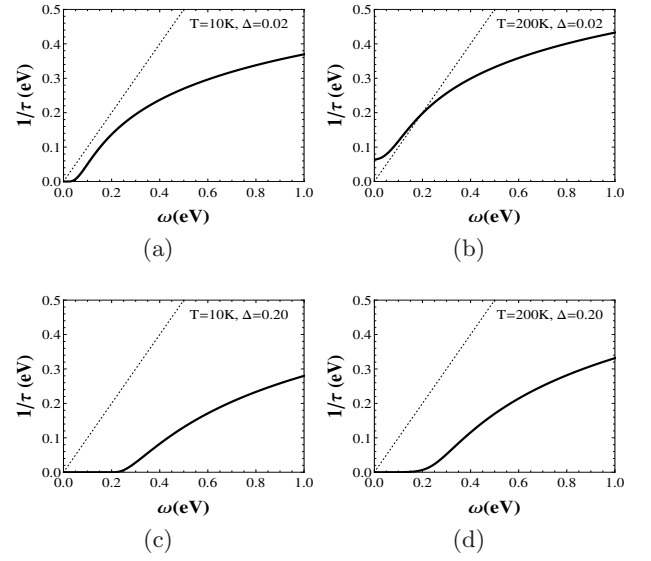


Fig. 6. Solid line: variation of scattering rate with frequency at different temperature and Δ (in eV). Dotted line: plot of $f(\omega) = \omega$ to check the validity of memory function approach.

Authors contribution statement

Both authors contributed equally to the paper.

The authors are thankful to Nabyendu Das for helpful discussions.

Appendix

The imaginary part of memory function (Eq. (19)) is

$$M''(\omega, T) = \frac{2\pi}{3} \frac{1}{mN_e} \sum_{\mathbf{k}, \mathbf{k}'} |D(\mathbf{k} - \mathbf{k}')|^2 (\mathbf{k} - \mathbf{k}')^2 f'(1-f)n \times \left[\frac{e^{\omega/T} - 1}{\omega} \delta(\epsilon - \epsilon' - \omega_{\mathbf{k}-\mathbf{k}'} + \omega) + (\text{terms with } \omega \rightarrow -\omega) \right]. \quad (\text{A.1})$$

Converting the summations into energy integrals and inserting the dq integral as before, we have

$$M''(\omega, T) = \frac{2\pi}{3} \frac{N^2}{mN_e} \int_0^\infty dq \int_{-\infty}^\infty d\epsilon N(\epsilon) \int_{-\infty}^\infty d\epsilon' N(\epsilon') \times \int_0^\pi d\theta \sin \theta \delta(q - |\mathbf{k} - \mathbf{k}'|) |D(q)|^2 q^2 f'(1-f)n \times \left[\frac{e^{\omega/T} - 1}{\omega} \delta(\epsilon - \epsilon' - \omega_q + \omega) + (\text{terms with } \omega \rightarrow -\omega) \right]. \quad (\text{A.2})$$

Here the energy dependent density of states $N(\epsilon)$ has been introduced. Thus on solving the integrals over ϵ' and θ ,

the above equation reduces to

$$M''(\omega, T) = \frac{2\pi}{3} \frac{N^2}{mN_e k_F^2 \omega} \int_0^\infty dq |D(q)|^2 q^3 \\ \times \int_{-\infty}^\infty d\epsilon N(\epsilon) \frac{e^{\beta(\epsilon - \epsilon_F)} - 1}{e^{\beta(\epsilon - \epsilon_F)} + 1} \frac{1}{e^{\beta\omega_q} - 1} \\ \times \left[N(\epsilon - \omega_q + \omega) \frac{e^{\beta\omega} - 1}{e^{\beta(\epsilon - \epsilon_F - \omega_q + \omega)} + 1} \right. \\ \left. - N(\epsilon - \omega_q - \omega) \frac{e^{-\beta\omega} - 1}{e^{\beta(\epsilon - \epsilon_F - \omega_q - \omega)} + 1} \right]. \quad (\text{A.3})$$

This is the general expression for the imaginary part of memory function (called as GDS).

References

1. D.N. Basov, T. Timusk, *Rev. Mod. Phys.* **77**, 721 (2005)
2. D.N. Basov, R.D. Averitt, D. van der Marel, M. Dressel, K. Haule, *Rev. Mod. Phys.* **83**, 471 (2011)
3. T. Timusk, *Solid State Commun.* **127**, 337 (2003)
4. A.V. Puchkov, D.N. Basov, T. Timusk, *J. Phys.: Condens. Matter* **8**, 10049 (1996)
5. J.M. Ziman, *Electrons and Phonons* (Clarendon Oxford, 1960)
6. D. Pines, P. Nozieres, *The Theory of Quantum Liquids* (Benjamin, New York, 1966)
7. N.W. Ashcroft, N.D. Mermin, *Solid State Physics* (Saunders College, 1976)
8. Y.M. Dai, B. Xu, P. Cheng, H.Q. Luo, H.H. Wen, X.G. Qiu, R.P.S.M. Lobo, *Phys. Rev. B* **85**, 092504 (2012)
9. Y.S. Lee, K. Segawa, Z.Q. Li, W.J. Padilla, M. Dumm, S.V. Dordevic, C.C. Homes, Y. Ando, D.N. Basov, *Phys. Rev. B* **72**, 054529 (2005)
10. T. Holstein, *Ann. Phys.* **29**, 410 (1964)
11. P.B. Allen, *Phys. Rev. B* **3**, 305 (1971)
12. B. Mitrović, M.A. Fiorucci, *Phys. Rev. B* **31**, 2694 (1985)
13. S.G. Sharapov, J.P. Carbotte, *Phys. Rev. B* **72**, 134506 (2005)
14. H. Mori, *Prog. Theor. Phys.* **33**, 423 (1965)
15. W. Götze, P. Wölfle, *J. Low Temp. Phys.* **5**, 575 (1971)
16. W. Götze, P. Wölfle, *Phys. Rev. B* **6**, 1226 (1972)
17. R. Zwanzig, *Phys. Rev.* **124**, 983 (1961)
18. R. Zwanzig, in *Lectures in Theoretical Physics*, edited by W.E. Brittin, B.W. Downs, J. Downs (Interscience, New York, 1961), Vol. 3, p. 135
19. N. Plakida, *J. Phys. Soc. Jpn* **65**, 12 (1996)
20. N.M. Plakida, *Z. Phys. B* **103**, 383 (1997)
21. A.A. Vladimirov, D. Ihle, N.M. Plakida, *Phys. Rev B* **85**, 224536 (2012)
22. D. Forster, *Hydrodynamic Fluctuations, Broken Symmetry And Correlation Functions* (Advanced Books Classics, 1995)
23. P. Fulde, *Correlated electrons in Quantum Matter* (World Scientific, 2012)
24. A. Lucas, *J. High Energy Phys.* **2015**, 1 (2015)
25. A. Lucas, S. Sachdev, *Phys. Rev. B* **91**, 195122 (2015)
26. A.A. Patel, S. Sachdev, *Phys. Rev. B* **90**, 165146 (2014)
27. N. Das, N. Singh, [arXiv:1509.03418](https://arxiv.org/abs/1509.03418) (2015)
28. L.P. Kadanoff, P.C. Martin, *Ann. Phys.* **24**, 419 (1963)
29. D.N. Zubarev, *Usp. Fiz. Nauk* **71**, 71 (1960)
30. G.D. Mahan, *Many-Particle Physics*, 2nd edn. (Plenum, New York, London, 1990)
31. B. Arfi, *Phys. Rev. B*, **45**, 2352 (1992)
32. R. Kubo, *J. Phys. Soc. Jpn* **12**, 570 (1957)
33. J. Hwang, *Phys. Rev. B* **83**, 014507 (2011)
34. J. Hwang, J.P. Carbotte, *Phys. Rev. B*, **86**, 094502 (2012)
35. P. Bhalla, N. Singh, *Eur. Phys. J. B* **87**, 213 (2014)
36. T. Holstein, *Phys. Rev.* **96**, 535 (1954)
37. R.R. Joyce, P.L. Richards, *Phys. Rev. Lett.* **24**, 1007 (1970)
38. G. Grüner, *Rev. Mod. Phys.* **60**, 1129 (1988)
39. G. Grüner, *Rev. Mod. Phys.* **60**, 1 (1994)
40. G. Grüner, *Density Waves in Solids* (Addison-Wesley Publishing Company, 1994)

Theory of the dynamical thermal conductivity of metals

Pankaj Bhalla,^{1,2,*} Pradeep Kumar,^{1,2} Nabyendu Das,¹ and Navinder Singh¹

¹Physical Research Laboratory, Navrangpura, Ahmedabad-380009, India

²Indian Institute of Technology, Gandhinagar-382424, India

(Received 13 June 2016; revised manuscript received 22 August 2016; published 7 September 2016)

The Mori's projection method, known as the memory function method, is an important theoretical formalism to study various transport coefficients. In the present work, we calculate the dynamical thermal conductivity in the case of metals using the memory function formalism. We introduce thermal memory functions for the first time and discuss the behavior of thermal conductivity in both the zero frequency limit and in the case of nonzero frequencies. We compare our results for the zero frequency case with the results obtained by the Bloch-Boltzmann kinetic approach and find that both approaches agree with each other. Motivated by some recent experimental advancements, we obtain several new results for the ac or the dynamical thermal conductivity.

DOI: [10.1103/PhysRevB.94.115114](https://doi.org/10.1103/PhysRevB.94.115114)

I. INTRODUCTION

There have been significant advancements in the study of the thermal transport coefficients for complex systems [1–5]. In such systems, the transport coefficients can be understood via the transport lifetime which captures the role of different interactions such as electron-impurity, electron-phonon, and electron-electron interactions. Several methods [6–8] based on the Kubo formalism and the Bloch-Boltzmann method have been applied to compute the effects of such interactions on various transport coefficients such as thermal conductivity. The commonly used method is the Bloch-Boltzmann transport method [9]. Within this approach, it is found that the thermal conductivity $\kappa(T)$ is proportional to the temperature T both in high and low temperature regimes in the case of impurity interactions. While in the case of electron-phonon interactions, it varies as T^{-2} in the low temperature limit ($T \ll \Theta_D$, where Θ_D is the Debye temperature) and saturates to a constant value in the high temperature limit ($T \gg \Theta_D$) [9]. These signatures are predicted long ago and are well verified. However, the notion of frequency dependent (dynamical) thermal conductivity was not previously known and hence was not addressed in theoretical discussions.

Recently, the notion of the dynamical thermal conductivity is introduced by Volz *et al.* [10]. With this idea, the recent experiments access frequency in which ω dependence cannot be ignored. There it is introduced in the context of its usefulness for the thermal design of microsystems and nanosystems which operates at several GHz clock frequency. Cooling of the Joule heating in such systems is an important issue [10] and it requires detailed understanding of the frequency dependence of the thermal conductivity. In Ref. [10], the dynamical thermal conductivity is introduced in the context of phonon mediated thermal transport in Si crystals. However, in the case of metals, and particularly at certain frequency, the electronic contributions to the thermal conductivity may predominate. We consider that scenario and present the paper to a careful theoretical analysis of the frequency dependent electronic thermal conductivity of metals in various regimes of interest. In a recent computer simulation using the molecular dynamics technique,

it is found that the phononic thermal conductivity reduces its magnitude at high frequencies [10]. Experimentally, it is also studied in the context of semiconductor alloys and it is found that the magnitude of the phononic thermal conductivity reduces as the frequency increases [11].

Theoretically, the electronic and the phononic dynamical thermal conductivity is discussed in the recent past by Shastri [12] and others [13–16] in different contexts such as in open systems, strongly correlated systems, semiconductor crystals, etc. In the present work, we *explicitly* derive the various expressions for the electronic thermal conductivity in case of metal with electron-impurity and electron-phonon interaction.

We use the memory function formalism which was introduced by Mori and Zwanzig [17–19]. It is formulated in several renditions. The commonly used version named projection operator formalism is the most fascinating regarding the physical aspects of the systematic approximations. The main motivation of this approach is the determination of the time correlation function in quantum or classical many body systems in a systematic way [20–29].

We calculate for the first time, *the dynamical thermal memory functions* for the case of electron-impurity and electron-phonon interactions. It is directly related to the dynamical thermal conductivity viz. $\kappa(z, T) \sim \frac{1}{z + M_{QQ}(z, T)}$, where $M_{QQ}(z, T)$ is the thermal memory function and z is the complex frequency. The details of $M_{QQ}(z, T)$ will be discussed in the next section. The results in the zero frequency limit are consistent with the results predicted using the Bloch-Boltzmann approach. We also calculate the dynamical thermal memory functions in different frequency regimes and discuss the effects of the impurity and the phonon scattering on it.

This paper is organized as follows: We review the basics of the memory function formalism in Sec. II. Later in Sec. III, we introduce the model Hamiltonian and then calculate the thermal memory functions for the case of electron-impurity and electron-phonon interactions. Then, we discuss its behavior in different frequency and temperature regimes. Here we also calculate the asymptotic behavior of the thermal conductivity in the presence of these interactions. The results for the zero frequency case is compared with the results previously obtained by the Boltzmann approach and we find good agreement. We make several predictions in frequency dependence cases in Sec. IV. Finally, in Sec. V, we conclude.

*pankajbhalla66@gmail.com

II. MEMORY FUNCTION FORMALISM

Before embarking into the detailed calculation of the thermal memory function, let us first briefly review the general framework of the memory function formalism in this section.

Consider two operators A and B corresponding to two different physical observables. Their correlation function is defined as [30–32]

$$\chi_{AB}(t) = \langle A(t); B(0) \rangle, \quad (1)$$

where $\langle \dots \rangle$ denotes the thermal average and t is the time variable. The Laplace transform of the correlation function in the complex frequency domain can be expressed as

$$\chi_{AB}(z) = \langle \langle A; B \rangle \rangle_z = -i \int_0^\infty e^{izt} \langle [A(t), B] \rangle dt. \quad (2)$$

Here $[\cdot, \cdot]$ represents the commutator between two operators, z is the complex frequency variable, and the outer angular bracket $\langle \dots \rangle$ in $\langle \langle A; B \rangle \rangle_z$ refers to the Laplace transform.

In frequency space, the equation of motion of this correlation function can be cast in the following form:

$$z \langle \langle A; B \rangle \rangle_z = \langle [A, B] \rangle + \langle \langle [A, H]; B \rangle \rangle_z. \quad (3)$$

Here H represents the total Hamiltonian of the system. In the present work, we are interested in calculating the thermal current-thermal current correlation function. Thus we replace both the general operators A and B by the thermal current operator J_Q and Eq. (3) takes the form,

$$z \langle \langle J_Q; J_Q \rangle \rangle_z = \langle [J_Q, J_Q] \rangle + \langle \langle [J_Q, H]; J_Q \rangle \rangle_z. \quad (4)$$

Here the first term in the right-hand side contains equal time commutator $[J_Q, J_Q]$ which identically vanishes. Thus, $z \langle \langle J_Q; J_Q \rangle \rangle_z = \langle \langle [J_Q, H]; J_Q \rangle \rangle_z$. Again applying equation of motion on $\langle \langle [J_Q, H]; J_Q \rangle \rangle_z$, one obtains

$$z \langle \langle J_Q; J_Q \rangle \rangle_z = \frac{\langle \langle [J_Q, H]; [J_Q, H] \rangle \rangle_{z=0} - \langle \langle [J_Q, H]; [J_Q, H] \rangle \rangle_z}{z}. \quad (5)$$

Finally, the correlation function can be expressed as

$$\chi_{QQ}(z, T) = \frac{\langle \langle [J_Q, H]; [J_Q, H] \rangle \rangle_{z=0} - \langle \langle [J_Q, H]; [J_Q, H] \rangle \rangle_z}{z^2}. \quad (6)$$

Following the Refs. [33,34], the correlation function $\chi_{QQ}(z, T)$ and the memory function $M_{QQ}(z)$ are related as

$$M_{QQ}(z, T) = z \frac{\chi_{QQ}(z, T)}{\chi_{QQ}^0(T) - \chi_{QQ}(z, T)}, \quad (7)$$

where $\chi_{QQ}^0(T)$ is the static thermal current-thermal current correlation function. This above expression is identical to that in the case of electrical transport.

On considering the assumption that $\chi_{QQ}(z, T)/\chi_{QQ}^0(T)$ is smaller than one, the above expression with the leading order term can be expressed as

$$M_{QQ}(z, T) \approx z \frac{\chi_{QQ}(z, T)}{\chi_{QQ}^0(T)}. \quad (8)$$

The validity of this approximation is discussed in detail in Refs. [35,36] for the electrical transport and the same should follow to the case of thermal transport.

Using Eqs. (6) and (8), the thermal memory function can be written as

$$M_{QQ}(z, T) = \frac{\langle \langle [J_Q, H]; [J_Q, H] \rangle \rangle_{z=0} - \langle \langle [J_Q, H]; [J_Q, H] \rangle \rangle_z}{z \chi_{QQ}^0(T)}. \quad (9)$$

This is an expression for the complex thermal memory function in terms of the thermal force-thermal force correlation. Further the thermal conductivity can be written in terms of the thermal memory function as follows,

$$\kappa(z, T) = i \frac{1}{T} \frac{\chi_{QQ}^0(T)}{z + M_{QQ}(z, T)}. \quad (10)$$

This is a general expression for the thermal conductivity in a memory function formalism (proof is given in Appendix A). Here $M_{QQ}(z, T)$ is the thermal memory function which provides the information about the effects of various interactions such as electron-impurity and electron-phonon interactions on the thermal conductivity $\kappa(z, T)$. The specific cases are discussed in detail in the next section.

III. THERMAL CONDUCTIVITY

A. Model Hamiltonian

In this work, we consider a system in which electrons interact with impurities and phonons. The total Hamiltonian of such a system takes the form,

$$H = H_0 + H_{\text{imp}} + H_{\text{ep}} + H_{\text{ph}}. \quad (11)$$

Here the first term in the right-hand side of the above equation corresponds to the unperturbed part which is expressed as

$$H_0 = \sum_{\mathbf{k}\sigma} \epsilon_{\mathbf{k}} c_{\mathbf{k}\sigma}^\dagger c_{\mathbf{k}\sigma}, \quad (12)$$

where $\epsilon_{\mathbf{k}}$ is the energy dispersion for free electrons, and $c_{\mathbf{k}\sigma}$ and $c_{\mathbf{k}\sigma}^\dagger$ are annihilation and creation operators having crystal momentum \mathbf{k} and spin σ . The second term is the perturbed Hamiltonian for the electron-impurity interactions which is described as

$$H_{\text{imp}} = N^{-1} \sum_i \sum_{\mathbf{k}\mathbf{k}'\sigma} \langle \mathbf{k} | U^i | \mathbf{k}' \rangle c_{\mathbf{k}\sigma}^\dagger c_{\mathbf{k}'\sigma}. \quad (13)$$

Here N represents the number of lattice cells, U^i refers for impurity interaction strength, and sum over i index refers to the number of impurity sites. Here the unit cell volume is taken as unity. The third term of Eq. (11) describes the interacting Hamiltonian for electron-phonon interactions which is defined as

$$H_{\text{ep}} = \sum_{\mathbf{k}\mathbf{k}'\sigma} [D(\mathbf{k} - \mathbf{k}') c_{\mathbf{k}\sigma}^\dagger c_{\mathbf{k}'\sigma} b_{\mathbf{k}-\mathbf{k}'} + \text{H.c.}]. \quad (14)$$

Here $b_{\mathbf{q}}(b_{\mathbf{q}}^\dagger)$ is the phonon annihilation(creation) operator having momentum \mathbf{q} . The electron-phonon matrix element

$D(\mathbf{q})$ can be considered in the following form [9]:

$$D(\mathbf{q}) = \frac{1}{\sqrt{2m_i N \omega_q}} q C(q), \quad (15)$$

where m_i is the ion mass, and ω_q is the phonon dispersion. $C(q)$ is a slowly varying function of the phonon momentum which in the case of metal is considered as $1/\rho_F$, where ρ_F is the density of the states (DOS) at the Fermi surface [9]. The last term of the Hamiltonian represents free phonons and is given by

$$H_{\text{ph}} = \sum_q \omega_q \left(b_q^\dagger b_q + \frac{1}{2} \right). \quad (16)$$

With this Hamiltonian, we proceed to the calculation of the thermal memory functions.

B. Thermal memory functions

To compute the thermal memory functions, we need to define the heat current [37] which is the energy current where energy is measured with respect to the electronic chemical potential μ . In an operator form, it can be written as

$$J_Q = \frac{1}{m} \sum_{\mathbf{k}} \mathbf{k} \hat{n}(\epsilon_{\mathbf{k}} - \mu) c_{\mathbf{k}}^\dagger c_{\mathbf{k}}, \quad (17)$$

where \hat{n} is the unit vector parallel to the direction of heat current and m is the electron mass.

Using this definition, let us focus on the calculation of the thermal memory function and hence thermal conductivity. In general, the $M_{QQ}(z, T)$ is a complex valued function of frequency having both real and imaginary parts. Its imaginary part describes the scattering rate due to the presence of different interactions such as electron-impurity and electron-phonon interactions. On the other hand, the real part describes mass enhancement.

1. Electron-impurity interaction

In the presence of only electron-impurity interactions, the thermal memory function defined in Eq. (9) is computed by considering the total Hamiltonian $H = H_0 + H_{\text{imp}}$.

To compute it, we first evaluate the commutator of J_Q and H . Since J_Q commutes with the free part of the Hamiltonian H_0 , then $[J_Q, H] = [J_Q, H_{\text{imp}}]$. Thus using Eqs. (13) and (17), the commutator becomes

$$[J_Q, H] = \frac{1}{mN} \sum_i \sum_{\mathbf{k}\mathbf{k}'\sigma} \langle \mathbf{k} | U^i | \mathbf{k}' \rangle, \quad (18)$$

$$(\mathbf{k}(\epsilon_{\mathbf{k}} - \mu) - \mathbf{k}'(\epsilon_{\mathbf{k}'} - \mu)) \hat{n} c_{\mathbf{k}\sigma}^\dagger c_{\mathbf{k}'\sigma}.$$

Using the above expression, the Laplace transform and the thermal average of the inner product $\langle\langle [J_Q, H]; [J_Q, H] \rangle\rangle_z$ becomes

$$= \frac{1}{m^2 N^2} \sum_{ij} \sum_{\mathbf{k}\mathbf{k}'\sigma} \sum_{\mathbf{p}\mathbf{p}'\tau} \langle \mathbf{k} | U^i | \mathbf{k}' \rangle \langle \mathbf{p} | U^j | \mathbf{p}' \rangle$$

$$\times (\mathbf{k}(\epsilon_{\mathbf{k}} - \mu) - \mathbf{k}'(\epsilon_{\mathbf{k}'} - \mu)) \hat{n},$$

$$(\mathbf{p}(\epsilon_{\mathbf{p}} - \mu) - \mathbf{p}'(\epsilon_{\mathbf{p}'} - \mu)) \hat{n},$$

$$\langle\langle c_{\mathbf{k}\sigma}^\dagger c_{\mathbf{k}'\sigma}; c_{\mathbf{p}'\tau}^\dagger c_{\mathbf{p}\tau} \rangle\rangle_z. \quad (19)$$

By considering the case of dilute impurity, i.e., $i = j$ and performing the ensemble average using Eq. (2) followed by integration over time, Eq. (19) takes the following form:

$$= \frac{2N_{\text{imp}}}{m^2 N^2} \sum_{\mathbf{k}\mathbf{k}'} |\langle \mathbf{k} | U | \mathbf{k}' \rangle|^2 [(\mathbf{k}(\epsilon_{\mathbf{k}} - \mu) - \mathbf{k}'(\epsilon_{\mathbf{k}'} - \mu)) \hat{n}]^2$$

$$\times \frac{f_{\mathbf{k}} - f_{\mathbf{k}'}}{z + \epsilon_{\mathbf{k}} - \epsilon_{\mathbf{k}'}}. \quad (20)$$

Here N_{imp} represents the impurity concentration, the factor 2 is due to the electronic spin degeneracy and $f_{\mathbf{k}} = \frac{1}{e^{\beta(\epsilon_{\mathbf{k}} - \mu)} + 1}$ is the Fermi distribution function, and β is the inverse of the temperature.

Substituting the above equation in Eq. (9) and on performing the analytic continuation $z \rightarrow \omega + i\eta$, $\eta \rightarrow 0^+$, the imaginary part of the thermal memory function becomes

$$M''_{QQ}(\omega, T) = \frac{2\pi}{N^2} \frac{N_{\text{imp}}}{\chi_{QQ}^0(T) m^2} \sum_{\mathbf{k}\mathbf{k}'} |\langle \mathbf{k} | U | \mathbf{k}' \rangle|^2$$

$$\times [(\mathbf{k}(\epsilon_{\mathbf{k}} - \mu) - \mathbf{k}'(\epsilon_{\mathbf{k}'} - \mu)) \hat{n}]^2$$

$$\times \frac{f_{\mathbf{k}} - f_{\mathbf{k}'}}{\omega} \delta(\omega + \epsilon_{\mathbf{k}} - \epsilon_{\mathbf{k}'}). \quad (21)$$

To reduce the equation further, it is convenient to assume that the system has cubic symmetry. Then on averaging over all directions, we obtain

$$[(\mathbf{k}(\epsilon_{\mathbf{k}} - \mu) - \mathbf{k}'(\epsilon_{\mathbf{k}'} - \mu)) \hat{n}]^2$$

$$= \frac{1}{3} |\mathbf{k}(\epsilon_{\mathbf{k}} - \mu) - \mathbf{k}'(\epsilon_{\mathbf{k}'} - \mu)|^2. \quad (22)$$

Using the above equation along with the assumption that U is independent of momentum, Eq. (21) can be written in the integral form,

$$M''_{QQ}(\omega, T) = \frac{U^2 N_{\text{imp}}}{3(2\pi)^5 m^2 \chi_{QQ}^0(T)} \int \frac{d\epsilon_{\mathbf{k}}}{v_{\mathbf{k}}} k^2 \sin \theta d\theta d\phi,$$

$$\int \frac{d\epsilon_{\mathbf{k}'}}{v_{\mathbf{k}'}} k'^2 \sin \theta' d\theta' d\phi',$$

$$|\mathbf{k}(\epsilon_{\mathbf{k}} - \mu) - \mathbf{k}'(\epsilon_{\mathbf{k}'} - \mu)|^2,$$

$$\frac{f_{\mathbf{k}} - f_{\mathbf{k}'}}{\omega} \delta(\omega + \epsilon_{\mathbf{k}} - \epsilon_{\mathbf{k}'}). \quad (23)$$

For our convenience, we drop the subscript \mathbf{k} from all $\epsilon_{\mathbf{k}}$ in further calculations and solve one of the energy integrals using the property of delta function. In a typical metal, the Fermi energy is very large (of the order of 10^4 K). On the other hand the experiments are usually performed at temperature of the order of 10^2 K. Thus, electrons from a small region of width $k_B T$ (in the present case $k_B = 1$) around the Fermi surface participate in the scattering events. Hence, we assume that the magnitudes of \mathbf{k} and \mathbf{k}' are equal to k_F , the Fermi wave vector. Thus, the imaginary part of the thermal memory function takes the following form:

$$M''_{QQ}(\omega, T) = \frac{N_{\text{imp}} U^2 k_F^4}{6\pi^3 \chi_{QQ}^0(T)} \int d\epsilon ((\epsilon - \mu)^2 + (\epsilon - \mu + \omega)^2)$$

$$\times \frac{f(\epsilon - \mu) - f(\epsilon - \mu + \omega)}{\omega}. \quad (24)$$

Substituting $\frac{\epsilon - \mu}{T} = \eta$ and $\frac{\omega}{T} = x$, the above expression can be written in simpler form as

$$M''_{QQ}(\omega, T) = \frac{N_{\text{imp}} U^2 k_F^4 T^2}{6\pi^3 \chi_{QQ}^0(T)} \int_0^\infty d\eta \frac{\eta^2 + (\eta + x)^2}{x} \left[\frac{1}{e^\eta + 1} - \frac{1}{e^{\eta+x} + 1} \right]. \quad (25)$$

This is the final expression for the imaginary part of the thermal memory function due to the impurity interactions. Here we assume that the electronic kinetic energy is higher than the temperature T . Further in various frequency and temperature limits, its behavior can be discussed as follows:

Case I. In the dc limit, i.e., $\omega \rightarrow 0$.

In this limit, Eq. (25) reduces to

$$M''_{QQ}(T) = \frac{N_{\text{imp}} U^2 k_F^4 T^2}{3\pi^3 \chi_{QQ}^0(T)} \int_0^\infty d\eta \eta^2 \frac{e^\eta}{(e^\eta + 1)^2}. \quad (26)$$

This concludes that the temperature dependent imaginary part of the thermal memory function, also known as thermal scattering rate, $1/\tau_{\text{th}}$ varies with temperature as $T^2/\chi_{QQ}^0(T)$, since the static correlation function $\chi_{QQ}^0(T)$ is directly proportional to the square of temperature (proof is given in Appendix B). Thus, $1/\tau_{\text{th}}$ in the zero frequency limit is independent of the temperature. This result agrees with the Bloch-Boltzmann result. On the other hand, due to the symmetry relations of the thermal memory function [33], its real part becomes identically zero in the dc limit. On substituting this in the expression for the thermal conductivity [Eq. (10)], we find that the real part of the thermal conductivity depends on the temperature as

$$\text{Re}[\kappa(T)] = \frac{1}{T} \frac{\chi_{QQ}^0(T)}{M''_{QQ}(T)}. \quad (27)$$

Using Eqs. (26) and (B2) (mentioned in Appendix B), the above equation for the thermal conductivity reduces to

$$\text{Re}[\kappa(T)] = \frac{1}{72} \frac{\pi k_F^2}{N_{\text{imp}} U^2 m^2} T, \quad \text{i.e., } \text{Re}[\kappa(T)] \propto T. \quad (28)$$

This result is in accord with the result predicted earlier using Boltzmann's equation approach [Eq. (C10) in Appendix C 1].

Case II. In the finite frequency limit.

In the high frequency limit, i.e., $\omega \gg T$, the imaginary part of the thermal memory function becomes

$$M''_{QQ}(\omega, T) \approx \frac{N_{\text{imp}} U^2 k_F^4 T^2}{6\pi^3 \chi_{QQ}^0(T)} \int_0^\infty d\eta x \left[\frac{1}{e^\eta + 1} - \frac{1}{e^{\eta+x} + 1} \right] \approx \frac{N_{\text{imp}} U^2 k_F^4 T^2}{6\pi^3 \chi_{QQ}^0(T)} \int_0^\infty d\eta \frac{1}{e^\eta + 1} \frac{\omega}{T}. \quad (29)$$

This yields that the thermal memory function or the thermal scattering rate approximately varies linearly with the frequency and inversely with the temperature. While in the opposite case $\omega \ll T$, the leading order term in Eq. (29) becomes

$$M''_{QQ}(T) \approx \frac{N_{\text{imp}} U^2 k_F^4 T^2}{6\pi^3 \chi_{QQ}^0(T)} \int_0^\infty d\eta \frac{\eta^2}{e^\eta + 1} \left(2 - \frac{\omega}{T} \right). \quad (30)$$

These results are summarized in Table I.

TABLE I. The thermal scattering rate due to the electron-impurity interaction in different frequency and temperature domains.

$\omega = 0$	$\omega \neq 0$	
	$\omega \gg T$	$\omega \ll T$
$1/\tau_{\text{th}} \sim T^0$	$1/\tau_{\text{th}} \sim \frac{\omega}{T}$	$1/\tau_{\text{th}} \sim (2 - \frac{\omega}{T})$

2. Electron-phonon interaction

Now consider that the system has only electron-phonon interaction. Then, the thermal memory function can be calculated in a similar fashion as is done in the case of the impurity interaction. Here the total Hamiltonian is considered as $H = H_0 + H_{\text{ep}} + H_{\text{ph}}$. The thermal current commutes with the free electron and the free phonon parts of the Hamiltonian. Thus, we are left with the commutator of the thermal current J_Q and the interaction term H_{ep} which is expressed as

$$[J_Q, H_{\text{ep}}] = \frac{1}{m} \sum_{\mathbf{k}\mathbf{k}'\sigma} (\mathbf{k}(\epsilon_{\mathbf{k}} - \mu) - \mathbf{k}'(\epsilon_{\mathbf{k}'} - \mu)) \cdot \hat{n}, \quad (D(\mathbf{k} - \mathbf{k}') c_{\mathbf{k}\sigma}^\dagger c_{\mathbf{k}'\sigma} b_{\mathbf{k}-\mathbf{k}'} - \text{H.c.}). \quad (31)$$

Using the above commutation relation, $\langle\langle [J_Q, H_{\text{ep}}]; [J_Q, H_{\text{ep}}] \rangle\rangle_z$ can be cast in the following form:

$$= \frac{1}{m^2} \sum_{\mathbf{k}\mathbf{k}'\sigma} \sum_{\mathbf{p}\mathbf{p}'\tau} (\mathbf{k}(\epsilon_{\mathbf{k}} - \mu) - \mathbf{k}'(\epsilon_{\mathbf{k}'} - \mu)) \cdot \hat{n}, \quad (\mathbf{p}(\epsilon_{\mathbf{p}} - \mu) - \mathbf{p}'(\epsilon_{\mathbf{p}'} - \mu)) \cdot \hat{n}, \quad (D(\mathbf{k} - \mathbf{k}') D^*(\mathbf{p} - \mathbf{p}') \langle\langle c_{\mathbf{k}\sigma}^\dagger c_{\mathbf{k}'\sigma} b_{\mathbf{k}-\mathbf{k}'}; c_{\mathbf{p}'\tau}^\dagger c_{\mathbf{p}\tau} b_{\mathbf{p}-\mathbf{p}'} \rangle\rangle_z - D^*(\mathbf{k} - \mathbf{k}') D(\mathbf{p} - \mathbf{p}') \langle\langle c_{\mathbf{k}'\sigma}^\dagger c_{\mathbf{k}\sigma} b_{\mathbf{k}-\mathbf{k}'}; c_{\mathbf{p}\tau}^\dagger c_{\mathbf{p}'\tau} b_{\mathbf{p}-\mathbf{p}'} \rangle\rangle_z). \quad (32)$$

On further simplifications, the above expression reduces to

$$= \frac{2}{m^2} \sum_{\mathbf{k}\mathbf{k}'} [(\mathbf{k}(\epsilon_{\mathbf{k}} - \mu) - \mathbf{k}'(\epsilon_{\mathbf{k}'} - \mu)) \cdot \hat{n}]^2 |D(\mathbf{k} - \mathbf{k}')|^2, \quad (f_{\mathbf{k}}(1 - f_{\mathbf{k}'})(1 + n) - (1 - f_{\mathbf{k}})f_{\mathbf{k}'}n), \quad \left\{ \frac{1}{z + \epsilon_{\mathbf{k}} - \epsilon_{\mathbf{k}'} - \omega_{\mathbf{k}-\mathbf{k}'}} - \frac{1}{z + \epsilon_{\mathbf{k}'} - \epsilon_{\mathbf{k}} + \omega_{\mathbf{k}-\mathbf{k}'}} \right\}, \quad (33)$$

where $n = \frac{1}{e^{\beta\omega_{\mathbf{k}-\mathbf{k}'}} - 1}$ is the Boson distribution function at a temperature $1/\beta$.

On substituting the above equation in the thermal memory function Eq. (9) and then performing the analytic continuation $z \rightarrow \omega + i\eta$, $\eta \rightarrow 0^+$, the imaginary part of the thermal memory function can be written as

$$M''_{QQ}(\omega, T) = \frac{2\pi}{\chi_{QQ}^0(T) m^2} \sum_{\mathbf{k}\mathbf{k}'} [(\mathbf{k}(\epsilon_{\mathbf{k}} - \mu) - \mathbf{k}'(\epsilon_{\mathbf{k}'} - \mu)) \cdot \hat{n}]^2, \quad |D(\mathbf{k} - \mathbf{k}')|^2 (1 - f_{\mathbf{k}}) f_{\mathbf{k}'} n, \quad \left\{ \frac{e^{\omega/T} - 1}{\omega} \delta(\epsilon_{\mathbf{k}} - \epsilon_{\mathbf{k}'} - \omega_{\mathbf{k}-\mathbf{k}'} + \omega) \right. \quad \left. + (\text{terms with } \omega \rightarrow -\omega) \right\}. \quad (34)$$

To evaluate the above equation, we use the law of conservation of energy $\epsilon_{\mathbf{k}} = \epsilon_{\mathbf{k}'} - \omega_q$ and conservation of momentum $\mathbf{q} = \mathbf{k}' - \mathbf{k}$ which simplify a factor appearing in Eq. (34) as follows:

$$[(\mathbf{k}(\epsilon_{\mathbf{k}} - \mu) - \mathbf{k}'(\epsilon_{\mathbf{k}'} - \mu)) \cdot \hat{n}]^2 = [(\omega_q \mathbf{k}' + (\epsilon_{\mathbf{k}} - \mu) \mathbf{q}) \cdot \hat{n}]^2. \quad (35)$$

For simplicity, we consider that the system has cubic symmetry as considered in the case of impurity. Then on averaging over all directions, we obtain

$$[(\omega_q \mathbf{k}' + (\epsilon_{\mathbf{k}} - \mu) \mathbf{q}) \cdot \hat{n}]^2 = \frac{1}{3} \{ \omega_q^2 k'^2 + q^2 (\epsilon_{\mathbf{k}} - \mu)^2 + \omega_q (\epsilon_{\mathbf{k}} - \mu) q^2 \}. \quad (36)$$

Substituting Eq. (36) in (34) and on converting the summations to integrals, we get

$$M''_{QQ}(\omega, T) = \frac{N^2}{3\chi_{QQ}^0(T)m^2(2\pi)^5} \int \frac{d\epsilon_{\mathbf{k}}}{v_{\mathbf{k}}} k^2 \sin \theta d\theta d\phi, \\ \int \frac{d\epsilon_{\mathbf{k}'}}{v_{\mathbf{k}'}} k'^2 \sin \theta' d\theta' d\phi' \int dq |D(q)|^2, \\ \delta(q - |\mathbf{k} - \mathbf{k}'|)(1 - f_{\mathbf{k}})f_{\mathbf{k}'}, \\ \{ \omega_q^2 k'^2 + q^2 (\epsilon_{\mathbf{k}} - \mu)^2 + \omega_q (\epsilon_{\mathbf{k}} - \mu) q^2 \}, \\ \left\{ \frac{e^{\omega/T} - 1}{\omega} \delta(\epsilon_{\mathbf{k}} - \epsilon_{\mathbf{k}'} - \omega_{\mathbf{k}-\mathbf{k}'} + \omega) \right. \\ \left. + (\text{terms with } \omega \rightarrow -\omega) \right\}. \quad (37)$$

Following the argument as quoted in the impurity case, for low energy scattering, we consider the magnitudes of \mathbf{k} and \mathbf{k}' of the order of k_F . With these facts and solving one of the energy integrals, the above equation reduces to

$$M''_{QQ}(\omega, T) = \frac{N^2}{12\pi^3} \frac{1}{\chi_{QQ}^0(T)} \int_0^\infty d\eta \int_0^{q_D} dq q |D(q)|^2, \\ \frac{1}{e^y - 1} \frac{1}{e^{-\eta} + 1} \{ \omega_q^2 k_F^2 + q^2 \eta^2 T^2 + \omega_q \eta T q^2 \}, \\ \left[\frac{1}{e^{\eta-y-x} + 1} \frac{e^y - 1}{x} + (\text{terms with } \omega \rightarrow -\omega) \right]. \quad (38)$$

Here we introduce new dimensionless variables $\frac{\epsilon_{\mathbf{k}} - \mu}{T} = \eta$, $\frac{\omega_q}{T} = y$, and $\frac{\omega}{T} = x$. Now integrating over η , we obtain

$$M''_{QQ}(\omega, T) = \frac{N^2 T^6}{12\pi \chi_{QQ}^0(T)} \left(\frac{q_D}{\Theta_D} \right)^4 \int_0^{\Theta_D/T} dy y^3 |D(y)|^2, \\ \left[\frac{(x-y)}{e^{x-y} - 1} \frac{e^x - 1}{x(e^y - 1)} \left\{ \frac{k_F^2}{\pi^2} \left(\frac{\Theta_D}{q_D T} \right)^2 \right. \right. \\ \left. \left. + \frac{1}{3} + \frac{(x-y)^2}{\pi^2} + \frac{1}{2\pi^2} y(x-y) \right\} \right. \\ \left. + (\text{terms with } \omega \rightarrow -\omega) \right]. \quad (39)$$

Substituting the phonon matrix element using Eq. (15), the thermal memory function is simplified to

$$M''_{QQ}(\omega, T) = \frac{N}{24\pi m_i \rho_F^2} \frac{T^7}{\chi_{QQ}^0(T)} \left(\frac{q_D}{\Theta_D} \right)^6 \int_0^{\Theta_D/T} dy y^4, \\ \left[\frac{(x-y)}{e^{x-y} - 1} \frac{e^x - 1}{x(e^y - 1)} \left\{ \frac{k_F^2}{\pi^2} \left(\frac{\Theta_D}{q_D T} \right)^2 \right. \right. \\ \left. \left. + \frac{1}{3} + \frac{(x-y)^2}{3\pi^2} + \frac{1}{2\pi^2} y(x-y) \right\} \right. \\ \left. + (\text{terms with } \omega \rightarrow -\omega) \right]. \quad (40)$$

This is the frequency and the temperature dependent thermal memory function for the case of electron-phonon interaction. In certain regimes of temperature and frequency, this can be solved analytically and is discussed as follows:

Case I. In the dc limit, i.e., $\omega \rightarrow 0$.

In this limit, Eq. (40) reduces to

$$M''_{QQ}(T) = \frac{N}{12\pi m_i \rho_F^2} \frac{T^7}{\chi_{QQ}^0(T)} \left(\frac{q_D}{\Theta_D} \right)^6 \int_0^{\Theta_D/T} dy, \\ \frac{y^5 e^y}{(e^y - 1)^2} \left\{ \frac{k_F^2}{\pi^2 T^2} \left(\frac{\Theta_D}{q_D} \right)^2 + \frac{1}{3} - \frac{1}{6\pi^2} y^2 \right\}. \quad (41)$$

In the high temperature limit, i.e., when the temperature is much more than the Debye temperature ($T \gg \Theta_D$), the second term within the curly brackets contributes more as compared to the other terms. Because the other terms vary inversely as square of the temperature, they contribute less than the second term (i.e., $1/3$). Hence, the thermal memory function $M''_{QQ}(T)$ with leading term can be approximated as

$$M''_{QQ}(T) \approx \frac{N}{36\pi m_i \rho_F^2} \frac{T^7}{\chi_{QQ}^0(T)} \left(\frac{q_D}{\Theta_D} \right)^6, \\ \int_0^{\Theta_D/T} dy \frac{y^5 e^y}{(e^y - 1)^2}. \\ M''_{QQ}(T) = \frac{N \Theta_D^4}{144\pi m_i \rho_F^2} \left(\frac{q_D}{\Theta_D} \right)^6 \frac{T^3}{\chi_{QQ}^0(T)}. \quad (42)$$

Thus on considering the temperature variation of the static thermal correlation function, we find that the imaginary part of the dc thermal memory function varies linearly with the temperature in the high temperature regime. On substituting this in Eq. (10), we find that the real part of the thermal conductivity varies as

$$\text{Re}[\kappa(T)] = \text{constant}. \quad (43)$$

In the low temperature limit, i.e., when the temperature is much less than the Debye temperature ($T \ll \Theta_D$), the first term and the third term in Eq. (41) contributes more to the thermal memory function as compared to the second term. If we consider q_D to be smaller than the k_F , then the first term dominates over the third term. Thus using this fact $M''_{QQ}(T)$

becomes

$$M''_{QQ}(T) \approx \frac{Nk_F^2}{12\pi^3 m_i \rho_F^2} \left(\frac{q_D}{\Theta_D} \right)^6 \frac{T^5}{\chi_{QQ}^0(T)} \int_0^\infty dy y^5 \frac{e^y}{(e^y - 1)^2}. \quad (44)$$

The above equation tells that the imaginary part of the thermal memory function or the thermal scattering rate varies as T^3 ($1/\tau_{th} \propto T^3$). As argued in the impurity case, the mass renormalization is zero. Thus, we find that the real part of the thermal conductivity [Eq. (10)] which varies inversely as square of the temperature, i.e.,

$$\text{Re}[\kappa(T)] \propto T^{-2}. \quad (45)$$

These results in different temperature regimes are in accord with the results obtained by the Boltzmann equation approach [8,9] and with the experimental results [38–40]. In Appendix C 2, we compare these results with the results from the Bloch-Boltzmann equation and we observe agreement.

Case II. In the finite frequency case.

In the high frequency limit, i.e., when frequency is much higher than the Debye frequency ($\omega \gg \omega_D$), the thermal memory function [Eq. (40)] becomes

$$M''_{QQ}(\omega, T) \approx \frac{N}{12\pi m_i \rho_F^2} \frac{T^7}{\chi_{QQ}^0(T)} \left(\frac{q_D}{\Theta_D} \right)^6 \int_0^{\Theta_D/T} dy, \quad (46)$$

$$\frac{y^4}{e^y - 1} \left\{ \frac{k_F^2}{\pi^2} \left(\frac{\Theta_D}{q_D T} \right)^2 + \frac{1}{3} + \frac{1}{3\pi^2} \frac{\omega^2}{T^2} \right\}.$$

In the high temperature limit, i.e., $T \gg \Theta_D$ and $\omega \ll T$, the second term of Eq. (46) contributes more over the other terms. Thus, the imaginary part of the thermal memory function becomes

$$M''_{QQ}(\omega, T) \approx \frac{N}{36\pi m_i \rho_F^2} \left(\frac{q_D}{\Theta_D} \right)^6 \frac{T^7}{\chi_{QQ}^0(T)} \times \int_0^{\Theta_D/T} dy \frac{y^4}{e^y - 1}. \quad (47)$$

On solving the integral in the above limits, we obtain

$$M''_{QQ}(\omega, T) \propto T. \quad (48)$$

In the case, when $T \gg \Theta_D$ and $\omega \gg T$, the third term of Eq. (46) contributes to the thermal memory function as

$$M''_{QQ}(\omega, T) \approx \frac{N}{36\pi^3 m_i \rho_F^2} \frac{T^7}{\chi_{QQ}^0(T)} \left(\frac{q_D}{\Theta_D} \right)^6 \times \frac{\omega^2}{T^2} \int_0^{\Theta_D/T} dy \frac{y^4}{e^y - 1}. \quad (49)$$

In the above mentioned frequency and temperature regime, the thermal memory function varies as $\frac{\omega^2}{T}$.

In the low temperature limit, i.e., $T \ll \Theta_D$, the first term and the third term are the leading order terms in the thermal

memory function. Further in the limit $\omega \gg T$,

$$M''_{QQ}(\omega, T) \approx \frac{N}{12\pi m_i \rho_F^2} \frac{T^7}{\chi_{QQ}^0(T)} \left(\frac{q_D}{\Theta_D} \right)^6 \times \left\{ \frac{k_F^2}{\pi^2} \left(\frac{\Theta_D}{q_D T} \right)^2 + \frac{1}{3\pi^2} \frac{\omega^2}{T^2} \right\} \int_0^\infty dy \frac{y^4}{e^y - 1}. \quad (50)$$

Similarly in the low frequency limit, i.e., when frequency is much smaller than the Debye frequency ($\omega \ll \omega_D$), Eq. (40) is written as

$$M''_{QQ}(\omega, T) \approx \frac{N}{24\pi m_i \rho_F^2} \frac{T^7}{\chi_{QQ}^0(T)} \left(\frac{q_D}{\Theta_D} \right)^6 \frac{\sinh(\omega/T)}{\omega/T}, \quad (51)$$

$$\int_0^{\Theta_D/T} dy \frac{y^5 e^y}{(e^y - 1)^2},$$

$$\left\{ \frac{k_F^2}{\pi^2} \left(\frac{\Theta_D}{q_D T} \right)^2 + \frac{1}{3} - \frac{y^2}{6\pi^2} \right\}.$$

In the limit $T \gg \Theta_D$ and $\omega \ll T$,

$$M''_{QQ}(\omega, T) \approx \frac{N}{36\pi m_i \rho_F^2} \frac{T^7}{\chi_{QQ}^0(T)} \left(\frac{q_D}{\Theta_D} \right)^6 \times \int_0^{\Theta_D/T} dy \frac{y^5 e^y}{(e^y - 1)^2}. \quad (52)$$

This shows the linear temperature variation and frequency independent character of the thermal scattering rate.

In the case when $T \ll \Theta_D$ and $\omega \ll T$, Eq. (51) becomes

$$M''_{QQ}(\omega, T) \approx \frac{Nk_F^2}{12\pi^3 m_i \rho_F^2} \frac{T^5}{\chi_{QQ}^0(T)} \left(\frac{q_D}{\Theta_D} \right)^4 \times \int_0^\infty dy \frac{y^5 e^y}{(e^y - 1)^2}. \quad (53)$$

From the above equation, we find that $M''_{QQ}(\omega, T)$ varies as T^3 and frequency independent behavior.

In the limit $T \ll \Theta_D$ and $\omega \gg T$,

$$M''_{QQ}(\omega, T) \approx \frac{Nk_F^2}{24\pi^3 m_i \rho_F^2} \frac{T^5}{\chi_{QQ}^0(T)} \left(\frac{q_D}{\Theta_D} \right)^4 \frac{\sinh(\omega/T)}{\omega/T} \times \int_0^\infty dy \frac{y^5 e^y}{(e^y - 1)^2}. \quad (54)$$

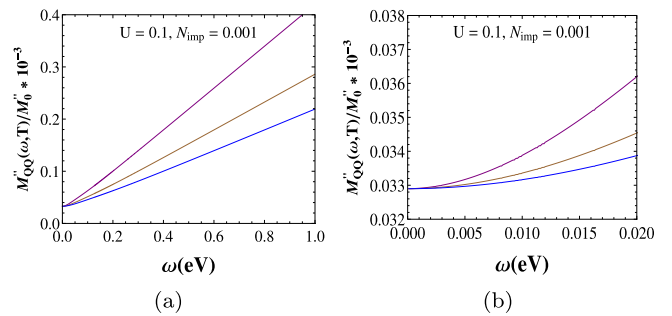


FIG. 1. (a) The imaginary part of the thermal memory function for the case of electron-impurity interaction is plotted with frequency at different temperatures such as 200 (purple), 300 (brown), and 400 K (blue) at fixed interaction strength U and impurity concentration N_{imp} . (b) The low frequency regime of Fig. 1(a) is elaborated.

TABLE II. The thermal scattering rate due to the electron-phonon interaction in different frequency and temperature domains.

$\omega = 0$		$\omega \gg \omega_D$		$\omega \ll \omega_D$	
$T \gg \Theta_D$	$T \ll \Theta_D$	$\omega \gg T$	$\omega \ll T$	$\omega \gg T$	$\omega \ll T$
$1/\tau_{\text{th}} \sim T$	$1/\tau_{\text{th}} \sim T^3$	$T \gg \Theta_D$	$T \ll \Theta_D$	$T \gg \Theta_D$	$T \ll \Theta_D$
		$1/\tau_{\text{th}} \sim \frac{\omega^2}{T}$	$1/\tau_{\text{th}} \sim T^3 \left(\frac{k_F^2 \Theta_D^2}{\pi^2 q_D^2} + \frac{\omega^2}{3\pi^2} \right)$	$1/\tau_{\text{th}} \sim T$	$1/\tau_{\text{th}} \sim T^3$
				$1/\tau_{\text{th}} \sim T^4 \frac{\sinh(\omega/T)}{\omega}$	$1/\tau_{\text{th}} \sim T$

These analytical predictions of the dynamical behavior of the thermal memory functions in different temperature and frequency domains are supplemented by numerical calculation in the next section. We summarize the above results in Table II.

IV. RESULTS AND DISCUSSION

In this section, we have plotted the imaginary part of the dynamical thermal memory functions $M''_{QQ}(\omega, T)$ for the case of the electron-impurity and electron-phonon interactions. To extract the characteristic frequency dependent and temperature dependent behavior of $M''_{QQ}(\omega, T)$, we suitably normalize it in various cases.

First for the impurity interaction, we plot $M''_{QQ}(\omega, T)/M''_0$ where M''_0 is the frequency and temperature independent constant ($= \frac{2k_F^4 m}{\pi^3 N_e}$), as a function of frequency using Eq. (25) in Fig. 1. Here we consider impurity concentration $N_{\text{imp}} = 0.001$ and interaction strength $U = 0.1$ eV. It is found that the normalized thermal scattering rate increases linearly with the frequency in the range where the frequency is very high as compared to the temperature (as shown in Fig. 1(a)). This linear feature becomes more prominent as the temperature is lowered. For example in Fig. 1(b), the purple curve drawn at $T = 200$ K starts showing a linear behavior above a frequency lower than that of the other two curves drawn at higher temperatures such as 300 and 400 K. The low frequency regime $\omega \ll T$ of the plot is more elaborated in Fig. 1(b) which shows deviations from linearity. Also in both the regimes, the thermal scattering rate due to the impurity interaction decreases with the rise in temperature. These features are in accord with our asymptotic analytical predictions (Table I).

In the zero frequency limit, the thermal scattering rate [Eq. (26)] becomes temperature independent. The same result

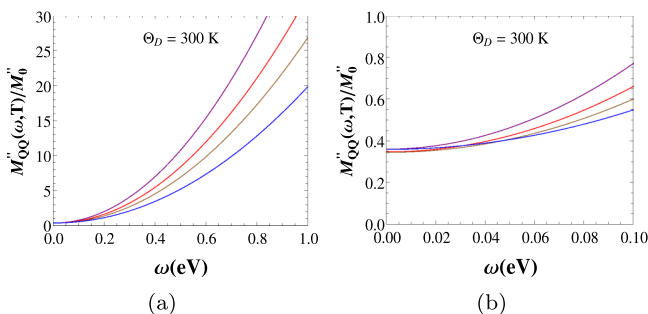


FIG. 2. (a) The imaginary part of the thermal memory function for electron-phonon interaction is plotted with frequency at different temperatures such as 200 (purple), 250 (red), 300 (brown), and 400 K (blue) at fixed Debye temperature $\Theta_D = 300$ K. (b) The low frequency regime of Fig. 2(a) is elaborated.

can be obtained using the Boltzmann approach as mentioned in Appendix C 1. This feature is also in accord with the experimental findings [8,9].

For the electron-phonon interaction, the frequency dependent behavior of the normalized thermal scattering rate [Eq. (40)] is shown in Fig. 2 at different temperatures. Here the Debye temperature Θ_D is kept fixed at 300 K. In Fig. 2(a), we observe that in the high frequency regime ($\omega \gg \Theta_D$), M''_{QQ}/M''_0 ($M''_0 = \frac{Nm q_D^6}{6\pi^3 m_i \rho_F^2 N_e \Theta_D}$) increases as the frequency increases. While in the low frequency regime, it becomes constant. To see the zoomed low frequency behavior, we replot the same curves within a small frequency regime (as shown in Fig. 2(b)). We also observe that the magnitude of the thermal memory function reduces with the increase in temperature. However, the exact temperature dependence in the low frequency regime depends on whether the temperature is greater or lower than the Debye temperature. The detail asymptotic behaviors are obtained analytically in the previous section (Sec. III) and given in Table II.

In Fig. 3, the real part of the thermal conductivity in the case of electron-phonon interaction using Eq. (10) is plotted as a function of frequency at a fixed Debye temperature Θ_D and at different temperatures. Here we assume that the leading frequency dependence of the thermal conductivity is coming from the thermal scattering rate. Thus to make our discussion simpler, we neglect the frequency dependence of the mass renormalization factor in the thermal conductivity coming from the real part of the thermal memory function. Here we have scaled the frequency with parameter ω_0 ($= \frac{Nm q_D^6}{6\pi^3 m_i \rho_F^2 N_e \Theta_D}$), which has the dimension of energy and normalized the real part of the thermal conductivity $\text{Re}[\kappa(\omega, T)]$ with κ_0 ($= \frac{\pi^2 N_e}{4m\omega_0}$). It is

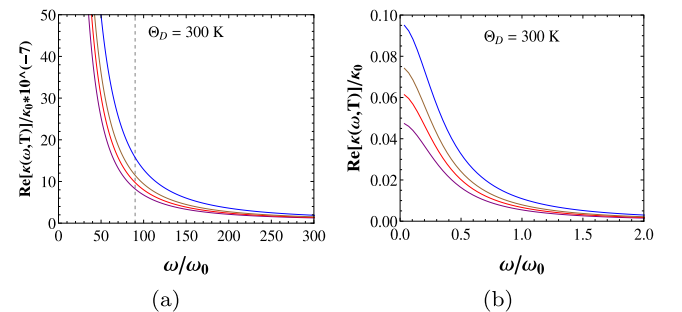


FIG. 3. (a) The normalized frequency dependent thermal conductivity is plotted with the ratio ω/ω_0 for electron-phonon interaction at different temperatures such as 200 (purple), 250 (red), 300 (brown), and 400 K (blue) and at Debye temperature $\Theta_D = 300$ K. Here ω_0 is a constant having dimensions of energy and the dashed line corresponds to the scale for Debye frequency cutoff, i.e., ω_D/ω_0 . (b) The low frequency regime of Fig. 3(a) is elaborated.

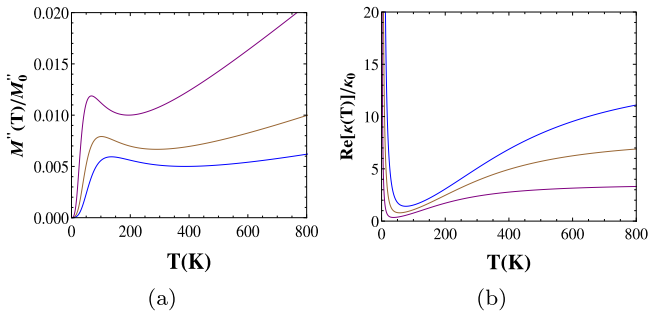


FIG. 4. (a) Plot of temperature dependent normalized dc imaginary part of the thermal memory function for electron-phonon interaction at different Debye temperatures such as 200 (purple), 300 (brown), and 400 K (blue). (b) The variation of the normalized thermal conductivity with T at the same Debye temperatures.

observed that the thermal conductivity decays with the increase in frequency in a nonlinear manner. Also with the increase of temperature, the thermal conductivity increases. This detail behavior can be understood as follows. Since our calculation is limited to a perturbative regime, i.e., $M''_{QQ}(\omega, T) \ll \omega$, then $\text{Re}[\kappa(\omega, T)] \sim \frac{\chi_{QQ}^0}{T} \frac{M''_{QQ}(\omega, T)}{\omega^2}$. As $\chi_{QQ}^0(T) \sim T^2$, thus the real part of the thermal conductivity becomes $\text{Re}[\kappa(\omega, T)] \sim \frac{TM''_{QQ}(\omega, T)}{\omega^2}$. Under this condition, the increase in the thermal conductivity due to the increase in temperature is governed by the factor $TM''_{QQ}(\omega, T)$ which is an increasing function of temperature. Using this relation and Table II, various regimes of Fig. 4 can be understood. For example, (1) in the regime $T \ll \omega \ll \omega_D$, $\text{Re}[\kappa(\omega, T)] \sim T^5 \frac{\sinh(\omega/T)}{\omega^3}$, (2) in regime $T \gg \omega \gg \omega_D$, $\text{Re}[\kappa(\omega, T)] \sim \frac{T^2}{\omega^2}$, (3) for $\omega \gg \omega_D$, $\omega \gg T$, and $T \ll \Theta_D$, $\text{Re}[\kappa(\omega, T)] \sim T^4(\frac{a}{\omega^2} + b)$, where a and b are constants, etc. The detail asymptotic results of the thermal conductivity due to the electron-phonon and the electron impurity is given in Tables III and IV. These signatures are new predictions from our formalism and can be verified in future experiments.

Now in the dc limit, we plot $M''_{QQ}(T)/M_0$ as a function of temperature T at different Debye's temperatures in Fig. 4(a). Here we find three important features. One is the increase of the nonlinear thermal scattering rate with temperature in the low temperature regime ($\sim T^3$, refer to Table II). Second, it increases linearly with the temperature at the high temperature regime. Third in the intermediate regime around the Debye temperature, there is a minima in the thermal scattering rate. These features (at high and low temperatures namely T^3 at $T \ll \Theta_D$ and T at $T \gg \Theta_D$) are in agreement with experiments [38–40]. In Fig. 4(b), using Eq. (10) the normalized thermal conductivity has been plotted with temperature T . This shows that it decreases as T^{-2}

TABLE IV. The real part of the thermal conductivity due to the electron-impurity interaction in different frequency and temperature domains.

$\omega = 0$	$\omega \neq 0$	
$\kappa \sim T$	$\omega \gg T$ $\kappa \sim \frac{1}{\omega}$	$\omega \ll T$ $\kappa \sim \frac{T}{\omega^2}$

in the low temperature regime and becomes constant in the high temperature regime. These results are consistent with the results derived using the Boltzmann approach in Appendix C 2. In the intermediate temperature regime, it passes through a minimum. This minimum in the thermal conductivity plot is an artifact of neglecting contributions from the Umklapp process in the memory function. Such minima occurs near the Debye temperature where the Umklapp process becomes important. The same peculiarity is also found in the Bloch-Boltzmann theory when the Umklapp processes are neglected [9,41]. Such a minima is purely a theoretical artifact and is not observed in any experiments [42].

V. CONCLUSION

Traditionally, the dc transport of a metallic system is discussed in several contexts using the Boltzmann equation approach with much success [8,34,43]. However within this approach, the calculation of the dynamical thermal conductivity is lacking. Also, the Boltzmann approach is solved using relaxation time approximation [29]. On the other hand, the memory function approach is beyond the relaxation time approximation. So, it is a better choice to study the dynamical transport properties in various electronic systems. Also, this approach does not require the quasiparticle picture, hence has a broader range of applicability [44–46]. Thus, the memory function formalism is a better choice to study the dynamical transport properties in various electronic systems. However, in the present work, we deal with the system having well-defined quasiparticles, i.e., metals.

In this work, we perform analytical calculation of the dynamical thermal conductivity of metal for electron-impurity and electron-phonon interactions. We discuss the results in different frequency and temperature domains. Since in the zero frequency limit thermal conductivity of the metal is well known, we consider the results from the Bloch-Boltzmann approach and the experimental findings as a benchmark and compare our results with them.

According to the memory function formalism, the total thermal memory function is the thermal current-thermal current correlation function which captures the role of the impurity and the electron-phonon interactions. This leads

TABLE III. The real part of the thermal conductivity due to the electron-phonon interaction in different frequency and temperature domains.

$\omega = 0$		$\omega \gg \omega_D$			$\omega \ll \omega_D$		
$T \gg \Theta_D$ $\kappa \sim T^0$	$T \ll \Theta_D$ $\kappa \sim T^{-2}$	$\omega \gg T$ $T \gg \Theta_D$ $\kappa \sim \omega^0 T^0$	$\omega \ll T$ $T \ll \Theta_D$ $\kappa \sim T^4(\frac{a}{\omega^2} + b)$	$\omega \ll T$ $T \gg \Theta_D$ $\kappa \sim \frac{T^2}{\omega^2}$	$\omega \gg T$ $T \ll \Theta_D$ $\kappa \sim T^5 \frac{\sinh(\omega/T)}{\omega^3}$	$\omega \ll T$ $T \ll \Theta_D$ $\kappa \sim \frac{T^4}{\omega^2}$	$\omega \ll T$ $T \gg \Theta_D$ $\kappa \sim \frac{T^2}{\omega^2}$

the thermal memory function as the sum of the memory functions due to the electron-impurity interactions and the electron-phonon interactions which further result to the total thermal conductivity. We found that at the low temperature, the thermal memory function due to the impurity interaction shows the temperature independent behavior [Eq. (26)]. While due to the electron-phonon interaction, it shows T^3 behavior [Eq. (44)]. On the other hand, at the high temperature, the thermal memory function gives linear temperature behavior [Eq. (42)].

Now, in the dc limit, the thermal conductivity can be written as

$$\kappa(T) \approx \frac{T}{M''_{QQ}(T)}, \quad (55)$$

which shows that it varies with an inverse of the memory function. According to the Matthiessen's rule [9,47], resistivities add up. Hence, the memory function also adds up which is the sum of the memory function due to the electron-impurity and the electron-phonon interactions. Based on that the thermal conductivity can be explained as follows. At very low temperature regime, the conductivity comes mainly due to the impurity interactions which gives the linear temperature dependence behavior. As the temperature increases, the population of the phonon starts increasing, resulting in the increase of the memory function due to the electron-phonon interaction and the corresponding thermal conductivity decreases. But as the temperature becomes more than the Debye temperature Θ_D , the population of the phonon saturates and thus the memory function gives linear temperature dependent behavior and hence the thermal conductivity becomes constant.

In other words, if we consider the impurity and phonon contribution together, we see that the total thermal conductivity can be expressed in an empirical form as

$$\begin{aligned} \frac{1}{\kappa_{\text{total}}(T)} &= \frac{1}{\kappa_{\text{imp}}(T)} + \frac{1}{\kappa_{\text{ep}}(T)} \\ &\sim \begin{cases} \frac{A}{T} + BT^2, & \text{at } T \ll \Theta_D \\ \frac{A}{T} + C, & \text{at } T \gg \Theta_D. \end{cases} \end{aligned} \quad (56)$$

Here, the first term and the second term are due to the electron-impurity interaction and the electron-phonon interaction, respectively and A , B , and C are material dependent constants. These results are in accord with the results calculated using the Bloch-Boltzmann approach [8,9] and also with the experimental findings [38–40].

In a general theory of electrical and/or thermal conductivity within the memory function(matrix) theory one must consider the slow relaxation of the conserved total momentum. In principle, one should consider all the relevant slow modes to construct the “full memory matrix.” The mode with the slowest relaxation rate is the most relevant in studying the dynamics. First, to keep our discussion simple we neglect the inclusion of the conserved total momentum. However, we see good agreement between our results with that of the previous theories and experiments as well. This is possible because we have confined our discussions on metals with a well-defined Fermi surface.

In the finite frequency cases we have several predictions depending on the relative values of the frequency ω , tem-

perature T , and the Debye frequency ω_D . Few of them can be summarized as follows: (1) $T \gg \omega_D$: in this case, as we move from the low frequency regime to the high frequency regime we see a crossover from the $\kappa \sim \frac{T^2}{\omega^2}$ behavior to the $\kappa \sim T^0/\omega^0$ behavior. (2) On the other hand for $T \ll \omega_D$, we observe that $\kappa \sim \frac{T^4}{\omega^2}$ in the low frequency regime, then we see $\kappa \sim T^5 \frac{\sinh \omega/T}{\omega^3}$ behavior in the intermediate regime, and finally see $\kappa \sim T^4(\frac{a}{\omega^2} + b)$ behavior. These predictions can be verified in future experiments. Moreover, the present approach can also be used to study other transport properties such as thermoelectric coefficients, etc.

APPENDIX A: THERMAL CONDUCTIVITY AND MEMORY FUNCTION RELATION

In the linear response theory, the thermal conductivity is expressed as [30–32]

$$\kappa_{\mu\nu}(z) = \frac{1}{T} \int_0^\infty dt e^{izt} \int_0^\beta d\lambda \langle J_{\nu Q}(-i\hbar\lambda) J_{\mu Q}(t) \rangle. \quad (A1)$$

Here $\mu, \nu = x, y, z$ and represent special directions.

In the classical limit, i.e., $\hbar \rightarrow 0$, the above equation reduces to

$$\kappa_{\mu\nu}(z) = \frac{1}{T^2} \int_0^\infty dt e^{izt} \langle J_{\nu Q}(0) J_{\mu Q}(t) \rangle. \quad (A2)$$

The time evolution of a dynamical variable f follows the Liouville equation which is given as

$$\frac{\partial f}{\partial t} = -\mathcal{L}f, \quad (A3)$$

where \mathcal{L} is the Liouvillian operator. The solution of the above equation yields

$$f(t) = e^{i\mathcal{L}t} f(0). \quad (A4)$$

Using the above relation, the Kubo formula for the thermal conductivity can be written as

$$\kappa_{\mu\nu}(z) = \frac{1}{T^2} \int_0^\infty dt e^{izt} \langle J_{\nu Q}(0) e^{i\mathcal{L}t} J_{\mu Q}(0) \rangle. \quad (A5)$$

On further simplification, it becomes

$$\kappa_{\mu\nu}(z) = \frac{1}{T^2} \left\langle J_{\nu Q} \left| \frac{i}{z + \mathcal{L}} \right| J_{\mu Q} \right\rangle. \quad (A6)$$

Now we introduce the projection operator \mathcal{P} which is defined as follows:

$$\mathcal{P} = \sum_{\nu, \mu} \frac{|J_{\nu Q}\rangle \langle J_{\mu Q}|}{\langle J_{\nu Q} | J_{\mu Q} \rangle} = \mathcal{I} - \mathcal{Q}, \quad (A7)$$

where \mathcal{I} is an identity matrix and $\mathcal{Q} = \mathcal{I} - \mathcal{P}$ is an unprojected part. Then replace \mathcal{L} by $\mathcal{L}(\mathcal{P} + \mathcal{Q})$ in Eq. (A6), and $\kappa_{\mu\nu}(z)$ becomes

$$\begin{aligned} \kappa_{\mu\nu}(z) &= i \frac{1}{T^2} \left\langle J_{\nu Q} \left| \frac{i}{z + \mathcal{L}Q} \right| J_{\mu Q} \right\rangle \\ &\quad - i \frac{1}{T^2} \left\langle J_{\nu Q} \left| \frac{i}{z + \mathcal{L}Q} \mathcal{L} \mathcal{P} \frac{1}{z + \mathcal{L}} \right| J_{\mu Q} \right\rangle. \end{aligned} \quad (A8)$$

On expanding the above equation, the first term is $i \frac{1}{zT^2} \langle J_{\nu Q} | J_{\mu Q} \rangle$ which can be written as $i \frac{\chi_{\mu\nu}^0(T)}{Tz}$ where $\chi_{\mu\nu}^0(T)$

is the static thermal current-thermal current correlation function. Inserting the projection operator into the second term, the latter becomes

$$\frac{1}{T^2} \left\langle J_{\nu Q} \left| \frac{i}{z + \mathcal{L}Q} \mathcal{L} \sum_{\mu'Q} |J_{\mu'Q}\rangle \langle J_{\mu'Q}| \frac{1}{z + \mathcal{L}} \right| J_{\mu Q} \right\rangle. \quad (\text{A9})$$

Inserting the above expressions of the first and second terms in Eq. (A8), the thermal conductivity in the isotropic case can be written as

$$\kappa(z, T) = i \frac{1}{T} \frac{\chi_{QQ}^0(T)}{z + M_{QQ}(z, T)}, \quad (\text{A10})$$

where $M_{QQ}(z, T)$ is the thermal memory function,

$$M_{QQ}(z, T) = \frac{1}{T \chi_{QQ}^0(T)} \left\langle J_Q \left| \frac{z}{z + \mathcal{L}Q} \mathcal{L} \right| J_Q \right\rangle. \quad (\text{A11})$$

APPENDIX B: DERIVATION OF STATIC CORRELATION FUNCTION

The static thermal current-thermal current correlation is defined as [3]

$$\chi_{QQ}^0(T) = \frac{1}{3T} \sum_{\mathbf{k}} (\epsilon_{\mathbf{k}} - \mu)^2 v_{\mathbf{k}}^2 f_{\mathbf{k}} (1 - f_{\mathbf{k}}). \quad (\text{B1})$$

Converting the summation into the energy integral and substituting $\frac{\epsilon_{\mathbf{k}} - \mu}{T} = \eta$, the above equation reduces to

$$\begin{aligned} \chi_{QQ}^0(T) &= \frac{T^2 k_F^3}{3m} \frac{1}{2\pi^2} \int_0^\infty d\eta \frac{\eta^2 e^\eta}{(e^\eta + 1)^2} \\ &= T^2 \frac{N_e}{m} \frac{\pi^2}{12}. \end{aligned} \quad (\text{B2})$$

This shows that the static thermal current-thermal current correlation varies quadratically in temperature.

APPENDIX C: THERMAL CONDUCTIVITY USING BOLTZMANN APPROACH

1. For impurity interaction

The Boltzmann equation for the semiclassical distribution function $g_{\mathbf{k}}(\mathbf{r}, t)$ is written as

$$v_{\mathbf{k}} \frac{\partial g_{\mathbf{k}}}{\partial r} = \left(\frac{\partial g_{\mathbf{k}}}{\partial t} \right)_{\text{coll}} = \int \frac{d\mathbf{k}'}{2\pi^3} (W(\mathbf{k}' \rightarrow \mathbf{k}) - W(\mathbf{k} \rightarrow \mathbf{k}')). \quad (\text{C1})$$

Here $W(\mathbf{k}' \rightarrow \mathbf{k})$ defines the transition probability of an electron scattering from initial state \mathbf{k}' to final state \mathbf{k} . According to the Fermi golden rule, in the case of the impurity scattering it can be expressed as

$$W(\mathbf{k}' \rightarrow \mathbf{k}) = 2\pi |\langle \mathbf{k}' | H_{\text{imp}} | \mathbf{k} \rangle|^2 \delta(\epsilon_{\mathbf{k}'} - \epsilon_{\mathbf{k}}). \quad (\text{C2})$$

Considering the impurity interaction Hamiltonian given in Eq. (13), the transition probability can be expressed as

$$W(\mathbf{k}' \rightarrow \mathbf{k}) = 4\pi \frac{N_{\text{imp}}}{N^2} |U(\mathbf{k}', \mathbf{k})|^2 g_{\mathbf{k}} (1 - g_{\mathbf{k}'}) \delta(\epsilon_{\mathbf{k}'} - \epsilon_{\mathbf{k}}). \quad (\text{C3})$$

Here $U(\mathbf{k}', \mathbf{k}) = \langle \mathbf{k}' | U | \mathbf{k} \rangle$, the matrix element for the impurity interaction. Inserting the above equation in Eq. (C1), we obtain

$$\left(\frac{\partial g_{\mathbf{k}}}{\partial t} \right)_{\text{coll}} = \int d\mathbf{k}' \frac{N_{\text{imp}}}{2\pi^2 N^2} |U(\mathbf{k}', \mathbf{k})|^2 (g_{\mathbf{k}'} - g_{\mathbf{k}}) \delta(\epsilon_{\mathbf{k}'} - \epsilon_{\mathbf{k}}). \quad (\text{C4})$$

Now linearizing the Boltzmann equation using $g_{\mathbf{k}} = f_{\mathbf{k}} + \delta g_{\mathbf{k}}$ and taking equilibrium collision integral terms to zero, Eq. (C4) can be written as

$$\left(\frac{\partial g_{\mathbf{k}}}{\partial t} \right)_{\text{coll}} = \int d\mathbf{k}' \frac{N_{\text{imp}}}{2\pi^2 N^2} |U(\mathbf{k}', \mathbf{k})|^2 (\delta g_{\mathbf{k}'} - \delta g_{\mathbf{k}}) \delta(\epsilon_{\mathbf{k}'} - \epsilon_{\mathbf{k}}). \quad (\text{C5})$$

In the standard procedure, the collision integral is solved by an iterative procedure [8,34,43]. One starts with the relaxation time approximation.

$$g_{\mathbf{k}} = f_{\mathbf{k}} + \delta g_{\mathbf{k}} = f_{\mathbf{k}} + \frac{k_x}{m} \tau(\epsilon_{\mathbf{k}}) \left(\frac{\partial f_{\mathbf{k}}}{\partial T} \right) (\nabla T)_x. \quad (\text{C6})$$

Thus the change in the distribution function is written as

$$\delta g_{\mathbf{k}} = g_{\mathbf{k}} - f_{\mathbf{k}} = \frac{k_x}{m} C(\epsilon_{\mathbf{k}}) \left(\frac{\partial f_{\mathbf{k}}}{\partial \epsilon} \right). \quad (\text{C7})$$

Here $C(\epsilon_{\mathbf{k}})$ is proportional to an energy dependent relaxation time. On substituting the above expression in Eq. (C5) and noticing that $v_{\mathbf{k}}^x \nabla g_{\mathbf{k}} = \frac{k_x}{m} \frac{\partial f_{\mathbf{k}}}{\partial T} \nabla T$, one obtains

$$\frac{1}{\tau(\epsilon_{\mathbf{k}})} = \frac{2N_{\text{imp}} m k_F}{\pi N^2} \int_0^\pi d\theta |U(k_F, \theta)|^2 \sin \theta (1 - \mathbf{k} \cdot \mathbf{k}'). \quad (\text{C8})$$

This shows that the thermal scattering rate due to the impurity interaction is independent of the temperature. The thermal conductivity is defined as

$$\kappa(T) = \frac{2}{T^2} \sum_{\mathbf{k}} \tau(\epsilon_{\mathbf{k}}) (\epsilon_{\mathbf{k}} - \mu)^2 \frac{e^{(\epsilon_{\mathbf{k}} - \mu)/T}}{(e^{(\epsilon_{\mathbf{k}} - \mu)/T} + 1)^2}. \quad (\text{C9})$$

Substituting Eq. (C8) in the above equation, the thermal conductivity due to the electron-impurity interaction shows the temperature dependence as

$$\begin{aligned} \kappa(T) &= \frac{1}{72} \frac{\pi k_F^2}{N_{\text{imp}} U^2 m^2} T, \\ \text{i.e., } \kappa(T) &\propto T. \end{aligned} \quad (\text{C10})$$

From this we infer that the results of the thermal conductivity using both approaches, the memory function and the Boltzmann approach, agree quantitatively with each other.

2. For electron-phonon interaction

Similarly for the electron-phonon interaction case, the Boltzmann equation becomes

$$\begin{aligned} v_{\mathbf{k}} \frac{\partial g_{\mathbf{k}}}{\partial r} &= \left(\frac{\partial g_{\mathbf{k}}}{\partial t} \right)_{\text{coll}} \\ &= \int d\mathbf{k} (W(\mathbf{k} + \mathbf{q} \rightarrow \mathbf{k}) - W(\mathbf{k} \rightarrow \mathbf{k} + \mathbf{q})). \end{aligned} \quad (\text{C11})$$

Here $W(i \rightarrow f)$ is the transition probability involving both the emission and absorption of phonons. This, using the Fermi

golden rule, can be expressed as [47]

$$W(\mathbf{k} + \mathbf{q} \rightarrow \mathbf{k}) = 2\pi |\langle \mathbf{k} | H_{\text{ep}} | \mathbf{k} + \mathbf{q} \rangle|^2 \delta(\epsilon_{\mathbf{k}+\mathbf{q}} - \epsilon_{\mathbf{k}} \pm \omega_q). \quad (\text{C12})$$

Using Eq. (14), the above expression for the transition probability can be written as

$$W(\mathbf{k} + \mathbf{q} \rightarrow \mathbf{k}) = 4\pi |D(q)|^2 g_{\mathbf{k}+\mathbf{q}} (1 - g_{\mathbf{k}}) (n_{\mathbf{q}} + 1), \quad \delta(\epsilon_{\mathbf{k}} + \omega_q - \epsilon_{\mathbf{k}+\mathbf{q}}). \quad (\text{C13})$$

Considering all possible scattering processes, the collision integral can be written as

$$\left(\frac{\partial g_{\mathbf{k}}}{\partial t} \right)_{\text{coll}} = \int d\mathbf{q} U(\mathbf{k} + \mathbf{q}; \mathbf{k}) g_{\mathbf{k}+\mathbf{q}} (1 - g_{\mathbf{k}}) - U(\mathbf{k}; \mathbf{k} + \mathbf{q}) g_{\mathbf{k}} (1 - g_{\mathbf{k}+\mathbf{q}}), \quad (\text{C14})$$

where

$$U(\mathbf{k} + \mathbf{q}; \mathbf{k}) = W_{\mathbf{q}}^0 [(n_{\mathbf{q}} + 1) \delta(\epsilon_{\mathbf{k}} + \omega_q - \epsilon_{\mathbf{k}+\mathbf{q}}) + n_{-\mathbf{q}} \delta(\epsilon_{\mathbf{k}} - \omega_q - \epsilon_{\mathbf{k}+\mathbf{q}})], \quad (\text{C15})$$

$$U(\mathbf{k}; \mathbf{k} + \mathbf{q}) = W_{\mathbf{q}}^0 [(n_{-\mathbf{q}} + 1) \delta(\epsilon_{\mathbf{k}+\mathbf{q}} + \omega_q - \epsilon_{\mathbf{k}}) + n_{\mathbf{q}} \delta(\epsilon_{\mathbf{k}+\mathbf{q}} - \omega_q - \epsilon_{\mathbf{k}})], \quad (\text{C16})$$

and $W_{\mathbf{q}}^0 = 4\pi |D(\mathbf{q})|^2$.

The details of the calculation is given in the references ([8,34,43]). Here we note that using the relation $U(\mathbf{k} + \mathbf{q}; \mathbf{k}) = e^{\beta\epsilon_{\mathbf{k}+\mathbf{q}}} e^{-\beta\epsilon_{\mathbf{k}}} U(\mathbf{k}; \mathbf{k} + \mathbf{q})$ and linearizing the Boltzmann equation by substituting $g_{\mathbf{k}} = f_{\mathbf{k}} + \delta g_{\mathbf{k}}$ and taking the equilibrium collision integral terms to be zero, Eq. (C14) can be reduced to

$$\left(\frac{\partial g_{\mathbf{k}}}{\partial t} \right)_{\text{coll}} = \int d\mathbf{q} U(\mathbf{k}; \mathbf{k} + \mathbf{q}) \{ \delta g_{\mathbf{k}+\mathbf{q}} (e^{-\beta(\epsilon_{\mathbf{k}} - \epsilon_{\mathbf{k}+\mathbf{q}})}, (1 - f_{\mathbf{k}}) + f_{\mathbf{k}}) - \delta g_{\mathbf{k}} (e^{-\beta(\epsilon_{\mathbf{k}} - \epsilon_{\mathbf{k}+\mathbf{q}})} f_{\mathbf{k}+\mathbf{q}} + (1 - f_{\mathbf{k}+\mathbf{q}})) \}. \quad (\text{C17})$$

On further simplifications, the collision integral can be written as

$$\left(\frac{\partial g_{\mathbf{k}}}{\partial t} \right)_{\text{coll}} = \beta \int d\mathbf{q} W_{\mathbf{q}}^0 n_{\mathbf{q}} (f_{\mathbf{k}+\mathbf{q}} (1 - f_{\mathbf{k}}) \delta(\epsilon_{\mathbf{k}+\mathbf{q}} + \omega_{-q} - \epsilon_{\mathbf{k}}) + f_{\mathbf{k}} (1 - f_{\mathbf{k}+\mathbf{q}}) \delta(\epsilon_{\mathbf{k}+\mathbf{q}} - \omega_q - \epsilon_{\mathbf{k}}), (\delta\phi(\mathbf{k} + \mathbf{q}) - \delta\phi(\mathbf{k})), \quad (\text{C18})$$

where $\delta\phi(\mathbf{k}) = \frac{\delta g_{\mathbf{k}}}{\beta f_{\mathbf{k}} (1 - f_{\mathbf{k}})}$.

As explained in the impurity scattering case the calculation is done by an iterative procedure, where one introduces

$$\delta\phi(k) = \frac{k_x}{m} C(\epsilon_{\mathbf{k}}). \quad (\text{C19})$$

From Eqs. (C18) and (C19), we have

$$\begin{aligned} \frac{k_x}{m} \left(\frac{\partial f_{\mathbf{k}}}{\partial T} \right) (\nabla T)_x &= \left(\frac{\partial g_{\mathbf{k}}}{\partial t} \right)_{\text{coll}} \\ &= \frac{4\pi}{mT} \int d\mathbf{q} |D(\mathbf{q})|^2 n_{\mathbf{q}} \\ &\quad \{ f_{\mathbf{k}+\mathbf{q}} (1 - f_{\mathbf{k}}) \delta(\epsilon_{\mathbf{k}+\mathbf{q}} + \omega_{-q} - \epsilon_{\mathbf{k}}) \end{aligned}$$

$$+ f_{\mathbf{k}} (1 - f_{\mathbf{k}+\mathbf{q}}) \delta(\epsilon_{\mathbf{k}+\mathbf{q}} - \omega_q - \epsilon_{\mathbf{k}}), \quad \{ (k_x + q_x) C(\epsilon_{\mathbf{k}+\mathbf{q}}) - k_x C(\epsilon_{\mathbf{k}}) \}. \quad (\text{C20})$$

On inserting the phonon matrix element, solving the angular integrals and introducing the dimensionless variables $\frac{\epsilon_{\mathbf{k}} - \mu}{T} = \eta$ and $\frac{\omega_q}{T} = z$, the collision integral reduces to

$$\begin{aligned} \left(\frac{\partial g_{\mathbf{k}}}{\partial t} \right)_{\text{coll}} &= - \frac{1}{2\pi m_i N \rho_F^2 (2m)^{1/2}} \epsilon^{-3/2} k_x \frac{\partial f_{\mathbf{k}}}{\partial \epsilon} \left(\frac{T}{\Theta_D} \right)^3 \frac{q_D^4}{\Theta_D}, \\ &\quad \int_0^{\Theta_D/T} dz \frac{z^2}{e^z - 1}, \\ &\quad \left\{ \frac{e^\eta + 1}{e^{\eta-z} + 1} \left[\left(\epsilon - \frac{1}{2} D \left(\frac{T}{\Theta_D} \right)^2 z^2 - \frac{1}{2} Tz \right), \right. \right. \\ &\quad \left. \left. C(\eta - z) - \epsilon C(\eta) \right] + \frac{e^z (e^\eta + 1)}{e^{\eta+z} + 1}, \right. \\ &\quad \left. \left[\left(\epsilon - \frac{1}{2} D \left(\frac{T}{\Theta_D} \right)^2 z^2 + \frac{1}{2} Tz \right), \right. \right. \\ &\quad \left. \left. C(\eta + z) - \epsilon C(\eta) \right] \right\}. \quad (\text{C21}) \end{aligned}$$

Here $D = \frac{q_D^2}{2m}$. On further simplifications, the above expression can be written as

$$\begin{aligned} - \frac{k_x}{m} \eta \left(\frac{\partial f_{\mathbf{k}}}{\partial \epsilon} \right) (\nabla T)_x &= \left(\frac{\partial g_{\mathbf{k}}}{\partial t} \right)_{\text{coll}} \\ &= - \frac{k_x}{2\pi m_i N \rho_F^2 (2m)^{1/2}} \frac{\epsilon^{-3/2}}{\partial \epsilon} \frac{\partial f_{\mathbf{k}}}{\partial \epsilon} \left(\frac{T}{\Theta_D} \right)^3 \\ &\quad \times \frac{q_D^4}{\Theta_D} \int_{-\Theta_D/T}^{\Theta_D/T} dz \frac{z^2}{|e^z - 1|} \frac{e^\eta + 1}{e^{\eta+z} + 1}, \\ &\quad \left[\left(\epsilon - \frac{1}{2} D \left(\frac{T}{\Theta_D} \right)^2 z^2 + \frac{1}{2} Tz \right), \right. \\ &\quad \left. C(\eta + z) - \epsilon C(\eta) \right]. \quad (\text{C22}) \end{aligned}$$

In the above equation, the contribution from the terms with odd power in z vanishes. Thus on simplification, we have

$$\begin{aligned} &\frac{2\pi m_i N \rho_F^2 \epsilon_F^{1/2} (2m)^{1/2}}{m} \frac{\Theta_D}{q_D^4} \left(\frac{\Theta_D}{T} \right)^3 \eta (\nabla T)_x \\ &= \int_{-\Theta_D/T}^{\Theta_D/T} dz \frac{z^2}{|e^z - 1|} \frac{e^\eta + 1}{e^{\eta+z} + 1}, \\ &\quad \left[\left(1 - \frac{D}{2\epsilon_F} \left(\frac{T}{\Theta_D} \right)^2 z^2 \right) C(\eta + z) - C(\eta) \right]. \quad (\text{C23}) \end{aligned}$$

In the high temperature limit, i.e., $T \gg \Theta_D$, the term within the bracket in Eq. (C23) with T^2 contributes more than the others terms and in the case $\eta \gg z$, the $C(\eta)$ can be approximated as

$$C(\eta) \approx - \frac{16\pi m_i \rho_F^2 N \epsilon_F^{3/2} (2m)^{1/2} \Theta_D}{m D q_D^4} \left(\frac{\Theta_D}{T} \right) \eta (\nabla T)_x.$$

The thermal current is defined as

$$J_Q = 2 \int \frac{d\mathbf{k}}{(2\pi)^3} v_{\mathbf{k}}(\epsilon_{\mathbf{k}} - \mu) \delta g_{\mathbf{k}} \\ = \frac{2k_F^3}{\pi^2} \int d\eta \eta C(\eta) \frac{\partial f_{\mathbf{k}}}{\partial \eta}. \quad (\text{C24})$$

Substituting the value of $C(\eta)$ and using the relation $J_Q = -\kappa(\nabla T)_x$, we find that the thermal conductivity in high temperature regime becomes

$$\kappa(T) \approx \frac{8 \pi k_F^6 m_i \rho_F^2 \Theta_D^2 N}{3 q_D^6 m^2}, \\ \text{i.e., } \kappa(T) = \text{constant}. \quad (\text{C25})$$

Now in the case of low temperature ($T \ll \Theta_D$), the right-hand side of Eq. (C23) can be written as

$$\int_{-\Theta_D/T}^{\Theta_D/T} dz \frac{z^2}{|e^z - 1|} \frac{e^\eta + 1}{e^{\eta+z} + 1} [C(\eta + z) - C(\eta)]. \quad (\text{C26})$$

The above equation can be solved by the variational method [43]. Following the Ref. [43], in the low temperature limit, we

can write

$$C(\eta) = -\frac{4\pi \Theta_D \epsilon_F^{1/2} \rho_F^2 m_i N}{3m q_D^4} \left(\frac{\Theta_D}{T}\right)^3 \eta (\nabla T)_x. \quad (\text{C27})$$

Substituting the above equation in (C24), we observe that the thermal conductivity shows a temperature dependence of the following form,

$$\kappa(T) \approx \frac{2 \pi^3 k_F^4 m_i \rho_F^2 \Theta_D^4 N}{125 m^2 q_D^4}, \\ \kappa(T) \propto T^{-2}. \quad (\text{C28})$$

Thus, we see that the thermal conductivity in the case of electron-phonon interaction shows inverse square temperature dependence in the low temperature regime and saturates to a constant value in the high temperature regime within the Bloch-Boltzmann approach and this agrees qualitatively with our calculation using the memory function formalism. Because of the approximate results of the thermal conductivity, the numeric factors are different in the thermal conductivity expressions in both the approaches.

-
- [1] D. Cao, F. Bridges, G. R. Kowach, and A. P. Ramirez, *Phys. Rev. Lett.* **89**, 215902 (2002).
- [2] P. Bhalla and N. Singh, *Eur. Phys. J. B* **87**, 213 (2014).
- [3] A. L. Chernyshev and W. Brenig, *Phys. Rev. B* **92**, 054409 (2015).
- [4] A. Jain and A. J. H. McGaughey, *Phys. Rev. B* **93**, 081206 (2016).
- [5] G. Romano, K. Esfarjani, D. A. Strubbe, D. Broido, and A. M. Kolpak, *Phys. Rev. B* **93**, 035408 (2016).
- [6] C. C. Bidwell, *Phys. Rev.* **58**, 561 (1940).
- [7] B. Deo and S. N. Behera, *Phys. Rev.* **141**, 738 (1966).
- [8] A. H. Wilson, *The Theory of Metals* (Cambridge University Press, Cambridge, 1953).
- [9] J. M. Ziman, *Electrons and Phonons* (Clarendon, Oxford, 1960).
- [10] S. G. Volz, *Phys. Rev. Lett.* **87**, 074301 (2001).
- [11] Y. K. Koh and D. G. Cahill, *Phys. Rev. B* **76**, 075207 (2007).
- [12] B. S. Shastry, *Phys. Rev. B* **73**, 085117 (2006).
- [13] B. S. Shastry, *Rep. Prog. Phys.* **72**, 016501 (2009).
- [14] A. Dhar, O. Narayan, A. Kundu, and K. Saito, *Phys. Rev. E* **83**, 011101 (2011).
- [15] Y. Ezzahri and K. Joulain, *J. Appl. Phys.* **112**, 083515 (2012).
- [16] F. Yang and C. Dames, *Phys. Rev. B* **91**, 165311 (2015).
- [17] R. Zwanzig, *Phys. Rev.* **124**, 983 (1961).
- [18] R. Zwanzig, in *Lectures in Theoretical Physics*, edited by W. E. Brittin, B. W. Downs, and J. Downs (Interscience, New York, 1961), Vol. 3, p. 135.
- [19] H. Mori, *Prog. Theor. Phys.* **33**, 423 (1965).
- [20] D. Forster, *Hydrodynamic Fluctuations, Broken Symmetry and Correlation Functions* (Advanced Books Classics, Addison-Wesley, Boston, 1995).
- [21] P. Fulde, *Correlated Electrons in Quantum Matter* (World Scientific, Singapore, 2012).
- [22] A. S. T. Pires, *Helv. Phys. Acta* **61**, 988 (1988).
- [23] B. J. Berne, J. P. Boon, and S. A. Rice, *J. Chem. Phys.* **45**, 1086 (1966).
- [24] G. D. Harp and B. J. Berne, *Phys. Rev. A* **2**, 975 (1970).
- [25] B. J. Berne and G. D. Harp, *Adv. Chem. Phys.* **17**, 63 (1970).
- [26] B. Arfi, *Phys. Rev. B* **45**, 2352 (1992).
- [27] P. F. Maldague, *Phys. Rev. B* **16**, 2437 (1977).
- [28] N. Das and N. Singh, *Int. J. Mod. Phys. B* **30**, 1650071 (2016).
- [29] N. Das, P. Bhalla, and N. Singh, *Int. J. Mod. Phys. B* **30**, 1630015 (2016).
- [30] L. P. Kadanoff and P. C. Martin, *Ann. Phys.* **24**, 419 (1963).
- [31] R. Kubo, *J. Phys. Soc. Jpn.* **12**, 570 (1957).
- [32] D. N. Zubarev, *Usp. Fiz. Nauk* **71**, 71 (1960).
- [33] W. Götze and P. Wölfle, *Phys. Rev. B* **6**, 1226 (1972).
- [34] N. Singh, *Electronic Transport Theories: From Weakly to Strongly Correlated Materials* (Taylor and Francis Group, CRC Press, Boca Raton, 2016).
- [35] P. Bhalla and N. Singh, *Eur. Phys. J. B* **89**, 49 (2016).
- [36] P. Bhalla, N. Das, and N. Singh, *Phys. Lett. A* **380**, 2000 (2016).
- [37] G. D. Mahan, *Many-Particle Physics*, 2nd ed. (Plenum, New York/London, 1990).
- [38] J. M. Ziman, *Proc. R. Soc. London A* **226**, 436 (1954).
- [39] H. M. Rosenberg, *Philos. Trans. R. Soc. London A* **247**, 441 (1955).
- [40] P. G. Klemens, *Thermal Conductivity of Solids at Low Temperatures* (Springer-Verlag, Berlin, 1956), Vol. 14.
- [41] F. Seitz and D. Turnbull, *Solid State Physics, Advances in Research and Applications* (Academic Press, New York, 1957), Vol. 4.
- [42] A calculation based on the memory function formalism including both the N-process and the U-process is planned for a future investigation.
- [43] T. Kasuya, *Prog. Theor. Phys.* **13**, 561 (1955).
- [44] A. A. Patel and S. Sachdev, *Phys. Rev. B* **90**, 165146 (2014).
- [45] A. Lucas, *J. High Energy Phys.* **03** (2015) 071.
- [46] A. Lucas and S. Sachdev, *Phys. Rev. B* **91**, 195122 (2015).
- [47] N. W. Ashcroft and N. D. Mermin, *Solid State Physics*, Science: Physics (Saunders College, Rochester, 1976).



Contents lists available at ScienceDirect

Physics Letters A

www.elsevier.com/locate/pla

Role of acoustic phonons in frequency dependent electronic thermal conductivity of graphene

Pankaj Bhalla^{a,b}^a Physical Research Laboratory, Navrangpura, Ahmedabad-380009, India^b Indian Institute of Technology, Gandhinagar-382355, India

ARTICLE INFO

Article history:

Received 3 October 2016
Received in revised form 10 November 2016
Accepted 6 January 2017
Available online xxxx
Communicated by R. Wu

Keywords:

Electronic transport in graphene
Scattering mechanisms
Thermal conductivity
Phonon scattering

ABSTRACT

We study the effect of the electron–phonon interaction on the finite frequency dependent electronic thermal conductivity of two dimensional graphene. We calculate it for various acoustic phonons present in graphene and characterized by different dispersion relations using the memory function approach. It is found that the electronic thermal conductivity $\kappa_e(T)$ in the zero frequency limit follows different power law for the longitudinal/transverse and the flexural acoustic phonons. For the longitudinal/transverse phonons, $\kappa_e(T) \sim T^{-1}$ at the low temperature and saturates at the high temperature. These signatures qualitatively agree with the results calculated by solving the Boltzmann equation analytically and numerically. Similarly, for the flexural phonons, we find that $\kappa_e(T)$ shows $T^{1/2}$ law at the low temperature and then saturates at the high temperature. In the finite frequency regime, we observe that the real part of the electronic thermal conductivity, $\text{Re}[\kappa_e(\omega, T)]$ follows ω^{-2} behavior at the low frequency and becomes frequency independent at the high frequency.

© 2017 Elsevier B.V. All rights reserved.

In recent times, Graphene [1–3] has attracted a lot of attention both in the fundamental and applied research due to its unique electronic and optical properties. These properties include anomalous high electrical conductivity, high thermal conductivity, quantum Hall effect, effect of impurities on the electric properties, etc. [4–17] which make the use of this material quite promising for the fabrication or design of the electronic devices. Among these properties, electrical conductivity, Hall effect have been discussed several times in literature, while there is lack of discussions in the electronic contribution to the thermal conductivity. Thus, in the present work, we focus on the electronic thermal conductivity of graphene.

In the literature, it is argued that the unusual high thermal conductivity of graphene [18,19] is mainly contributed by the phonons and the electronic contribution is small, hence neglected. However, in real systems, the total thermal conductivity is expressed as the sum of the electronic and the phononic thermal conductivity. In different temperature limits, these thermal conductivities show different temperature behavior. In the high temperature limit, due to larger number of phonons the electronic thermal conductivity shows temperature independent behavior [20–22] due to the scattering by electron–phonon interactions. On the other hand, the phononic thermal conductivity shows T^{-1} behavior due

to the dominating scattering mechanism by phonon–phonon interactions. In the opposite limit i.e. the low temperature limit, the electronic and the phononic thermal conductivities are due to the interactions of electrons and phonons with impurities, boundaries, defects. These different scenarios of the electronic thermal conductivity in both low and high temperature limits make this study important.

In case of metals, it has been depicted that at the low temperature i.e. $T \ll \Theta_D$, Θ_D being the Debye temperature, only the acoustic phonons within the phonon sphere of radius k_{ph} with $k_{\text{ph}} \ll k_D$, where k_D is the radius of Debye sphere, play a role in the electronic thermal conductivity [20–22]. In these three dimensional systems, it leads to T^{-2} behavior of the electronic thermal conductivity. In such systems, the radius of the Fermi sphere is larger than the radius of the Debye sphere i.e. $2k_F \gg k_D$. Thus all phonons can scatter off the electrons. But in the systems where $k_F \ll k_D$, only small number of phonons can scatter off the electrons. These phonons are restricted within the energy range $v_s k_{\text{ph}} \leq 2v_s k_F$. This can be explained by introducing the new temperature scale known as Bloch Grüneisen (BG) temperature which is smaller than the Debye temperature [23]. This scale defines two regimes i.e. low temperature ($T \ll \Theta_{\text{BG}}$) and high temperature ($T \gg \Theta_{\text{BG}}$) regimes for the electron–phonon interaction in graphene. In the low temperature regime ($T \ll \Theta_{\text{BG}}$), the acoustic phonons with linear dispersion relation yield inverse temperature behavior to the electronic thermal conductivity (i.e.

E-mail address: pankajbhalla66@gmail.com.

<http://dx.doi.org/10.1016/j.physleta.2017.01.006>

0375-9601/© 2017 Elsevier B.V. All rights reserved.

$\kappa_e \sim T^{-1}$) and then change to the temperature independent behavior in the high temperature regime ($T \gg \Theta_{BG}$) [24,25]. However, because of the two dimensional nature of the graphene, there are also other acoustic phonons known as flexural phonons or out of plane phonons which obey quadratic dispersion relation and hence give different power law behavior to the electronic thermal conductivity. Thus the role of the different acoustic phonons is very important to understand the transport or the electronic thermal conductivity of graphene. However most of the studies have considered only the zero frequency limit. But for the generation of the integrated circuits, high frequency communication devices, the study of the electronic thermal conductivity in the dynamical regime is important as it may degrade the issue of the heat dissipation within the systems [26–29].

With this motivation, we have examined the electronic thermal conductivity both in the zero frequency and the finite frequency regime using the memory function approach [30–34]. The advantage of using memory function approach is that it directly deals with the dynamics of the transport [35]. Here we discuss the dynamical behavior of the electronic thermal conductivity due to the interactions of electrons with different acoustic phonons and also its difference with the behavior in normal metals. In the zero frequency limit, our findings for the electronic thermal conductivity of graphene agrees qualitatively with the results calculated by solving the Boltzmann equation analytically and numerically [40,24,25]. In the finite frequency regime, our findings may be important from both the fundamental and the application points of view and may inspire important experimental studies in future.

This paper is organized as follows. In Sec. 1, first we discuss the basic idea of the thermal conductivity and its relation with the memory function. Then the model Hamiltonian considering only the electron–phonon interactions in graphene is discussed. Later, we discuss the phonon dispersion relation of different acoustic phonons. With these descriptions, we calculate the finite frequency and temperature dependent electronic thermal conductivity for different acoustic phonons. In Sec. 2, the results are presented in the two subsections. In one subsection, we discuss the electronic thermal conductivity in the zero frequency limit. In other subsection, the results for the finite frequency in different BG regimes has been discussed. Finally, in Sec. 3, we conclude.

1. Theoretical framework

1.1. Thermal conductivity

The thermal conductivity is defined as the rate of flow of heat across a unit area of cross section in a unit temperature gradient [36]. Mathematically, this can be depicted from the following expression

$$J_Q = -\kappa \nabla T. \quad (1)$$

Here J_Q is the thermal current density and is defined as,

$$J_Q = \frac{1}{m} \sum_{\mathbf{k}} \mathbf{k} \hat{n} (\epsilon_{\mathbf{k}} - \mu) c_{\mathbf{k}}^{\dagger} c_{\mathbf{k}}, \quad (2)$$

where $c_{\mathbf{k}}$ ($c_{\mathbf{k}}^{\dagger}$) is the annihilation (creation) operator having momentum \mathbf{k} , $\epsilon_{\mathbf{k}}$ is the electron energy dispersion of graphene, μ is the chemical potential, m is the electron mass and \hat{n} is the unit vector parallel to the direction of heat current. And in Eq. (1) ∇T is the temperature gradient and κ is the thermal conductivity. The latter is known as response due to the change in the temperature gradient and is generally analyzed by various approaches [20,21] where the gradient of the temperature is considered as static. But in the present work, we assume that ∇T is not static, while

it oscillates with the external driving frequency ω . This oscillation leads to the dynamical variation of the thermal conductivity. Here we set $\hbar = 1$ and $k_B = 1$ in our calculations.

To compute it, we employ the memory function approach. Following the latter approach, the dynamical thermal conductivity at complex frequency z and temperature T is defined as [22]

$$\kappa(z, T) = \frac{i}{T} \frac{\chi_{QQ}^0(T)}{z + M_{QQ}(z, T)}, \quad (3)$$

where $\chi_{QQ}^0(T)$ is the static thermal current–thermal current correlation function i.e. $\chi_{QQ}^0(T) = \frac{\pi}{24} \frac{k_F^3}{m^2 v_F} T^2$, where k_F is the Fermi wave vector and v_F is the Fermi velocity, $M_{QQ}(z, T)$ is the thermal memory function.

It is known that within the perturbation theory, the thermal memory function can be expressed to the leading order in the electron–phonon coupling, as [37,35,22]

$$M_{QQ}(z, T) = \frac{\langle\langle [J_Q, H]; [J_Q, H] \rangle\rangle_{z=0} - \langle\langle [J_Q, H]; [J_Q, H] \rangle\rangle_z}{z \chi_{QQ}^0(T)}. \quad (4)$$

This is the complex memory function in which the imaginary part of the memory function describes the thermal scattering rate and the real part describes the mass enhancement factor. In the present work, we focus on the thermal scattering rate which leads to the real part of the thermal conductivity. Here for simplicity, we have ignored the mass enhancement contribution to the thermal conductivity. To calculate it, we require the total Hamiltonian that is discussed in the next subsection.

1.2. Model Hamiltonian

We consider a two dimensional graphene with only electron–phonon interactions. The Hamiltonian of such a system is described as

$$H = H_0 + H_{ep} + H_{ph}, \quad (5)$$

where $H_0 = \sum_{\mathbf{k}\sigma} \epsilon_{\mathbf{k}} c_{\mathbf{k}\sigma}^{\dagger} c_{\mathbf{k}\sigma}$ and $H_{ph} = \sum_q \omega_q (b_q^{\dagger} b_q + \frac{1}{2})$ corresponds to the Hamiltonians of the free electrons and phonons respectively. Here ω_q is the phonon energy dispersion, b_q (b_q^{\dagger}) is the phonon annihilation (creation) operator having phonon wave vector $\mathbf{q} = \mathbf{k} - \mathbf{k}'$ and σ is the electron spin. H_{ep} describes the electron–phonon interactions and is given as $H_{ep} = \sum_{\mathbf{k}\mathbf{k}'\sigma} [D(\mathbf{k} - \mathbf{k}') c_{\mathbf{k}\sigma}^{\dagger} c_{\mathbf{k}'\sigma} b_{\mathbf{k}-\mathbf{k}'} + H.c.]$, where $D(q)$ is the electron–phonon matrix element. The latter is usually written in the following form [38,39]

$$D(\mathbf{q}) = \frac{D_0 q}{\sqrt{2\rho_m \omega_q}} \left(1 - \left(\frac{q}{2k_F} \right)^2 \right)^{1/2}. \quad (6)$$

Here D_0 is the deformation potential coupling constant, ρ_m is the graphene mass density and ω_q is the phonon energy dispersion.

1.3. Phonon dispersions

Before proceeding to compute the thermal scattering rate and the corresponding electronic thermal conductivity for the sake of completeness, we will first discuss the phonon dispersion relations in this subsection.

The thermal transport due to the electron–phonon interactions significantly depends on the characteristics of the phonon which are further determined by the two dimensional structure of the graphene. In graphene, there are two carbon atoms per hexagonal

unit cell which gives six phonon branches in the dispersion spectrum. These are three acoustic and three optical branches namely LA (Longitudinal Acoustic), TA (Transverse Acoustic), LO (Longitudinal Optical), TO (Transverse Optical), ZA (Flexural Acoustic) and ZO (Flexural Optical). The detailed description of these phonons are discussed in Refs. [16,17,40,41]. Among these, the optical phonons usually have higher energies than the acoustic phonons. And in the present work our main focus is on the low temperature behavior (i.e. below the Debye temperature) of the electronic thermal conductivity. Thus, for the time being we ignore the contribution of optical phonons and consider only acoustic phonons henceforth.

From the phonon dispersion spectra, it has been found that these modes follow different dispersion relations. The LA and TA modes follow the linear dispersion relations [41,42] i.e.

$$\begin{aligned}\omega_{LA} &\approx v_{LA}q \\ \omega_{TA} &\approx v_{TA}q,\end{aligned}\quad (7)$$

where v_{LA} and v_{TA} are the longitudinal and transverse phonon velocities and $v_{LA} = 21.3 \times 10^3 \text{ m s}^{-1}$, $v_{TA} = 14.1 \times 10^3 \text{ m s}^{-1}$ [42].

The other acoustic phonon ZA approximately follows the quadratic dispersion relation as [41,43]

$$\omega_{\text{flex}} \approx \alpha q^2. \quad (8)$$

Here the parameter $\alpha = \left(\frac{s}{\rho_m}\right)^{1/2}$, where s is the bending stiffness of the graphene, ρ_m is the graphene mass density and $\alpha = 4 \times 10^{-7} \text{ m}^2 \text{ s}^{-1}$ [44].

1.4. Calculation of $\kappa_e(\omega, T)$

As discussed earlier, the electronic thermal conductivity can be computed using Eq. (3) and (4). Thus with the definitions of the thermal current (Eq. (2)) and the model Hamiltonian (Eq. (5)), the imaginary part of the thermal memory function or the thermal scattering rate can be expressed as

$$\begin{aligned}M''_{QQ}(\omega, T) &= \frac{4\pi}{\chi_{QQ}^0(T)m^2} \\ &\times \sum_{\mathbf{k}\mathbf{k}'} [(\mathbf{k}(\epsilon_{\mathbf{k}} - \mu) - \mathbf{k}'(\epsilon_{\mathbf{k}'} - \mu)) \cdot \hat{n}]^2 |D(\mathbf{k} - \mathbf{k}')|^2 \\ &(1 - f_{\mathbf{k}})f_{\mathbf{k}'}n \left\{ \frac{e^{\omega/T} - 1}{\omega} \delta(\epsilon_{\mathbf{k}} - \epsilon_{\mathbf{k}'} - \omega_{\mathbf{k}-\mathbf{k}'} + \omega) \right. \\ &\left. + (\text{terms with } \omega \rightarrow -\omega) \right\}.\end{aligned}\quad (9)$$

Here $f_{\mathbf{k}} = \frac{1}{e^{\beta(\epsilon_{\mathbf{k}} - \mu)} + 1}$ and $n = \frac{1}{e^{\beta\omega_{\mathbf{q}}} - 1}$ are the Fermi and the Bose distribution functions, β is the inverse of the temperature and factor 4 is for the two spin and two valley degeneracies.

To simplify Eq. (9), we convert the summations over momentum indices into the two dimensional energy integrals using the linear electron energy dispersion relation $\epsilon_{\mathbf{k}} = v_F k$ and $\epsilon_{\mathbf{k}'} = v_F k'$, where v_F is the Fermi velocity. This linear dispersion relation distinguish the characteristics of the graphene from those of the three dimensional normal metals which follows the quadratic dispersion relation. Further these simplifications along with integrations over the angular parts yield

$$M''_{QQ}(\omega, T) = \frac{\epsilon_F^2 D_0^2}{4\pi^2 m^2 \rho_m v_F^4 k_F \chi_{QQ}^0(T)} \int d\epsilon_{\mathbf{k}} \int_0^\lambda dq \frac{q^2}{\omega_q} \sqrt{1 - \left(\frac{q}{2k_F}\right)^2}$$

$$\left(\omega_q^2 k_F^2 + (\epsilon_{\mathbf{k}} - \mu)^2 q^2 + \frac{\omega_q(\epsilon_{\mathbf{k}} - \mu)}{2} q^2 \right) (1 - f(\epsilon_{\mathbf{k}}))n \left\{ \frac{e^{\omega/T} - 1}{\omega} f(\epsilon_{\mathbf{k}} - \omega_q + \omega) + (\text{terms with } \omega \rightarrow -\omega) \right\}. \quad (10)$$

Here we use the expression for the electron-phonon matrix element given in Eq. (6) and the symbol λ corresponds to the upper cut off value of the phonon momentum. Since in normal metals, the Fermi sphere is very large as compared to the Debye sphere, the phonons residing in the Debye sphere participate in scattering events and we restrict λ to q_D , q_D being the Debye momentum. While in the case of graphene, this does not remain the same due to the smaller Fermi surface than the Debye surface. This allows only phonons residing below the Fermi surface to participate in the scattering phenomenon, hence restrict the upper cut off value of q integral to $2k_F$. Further the above Eq. (10) for graphene can be solved for various acoustic phonons in the following subsections.

1.4.1. Longitudinal/Transverse acoustic phonons (LA/TA)

To compute $M_{QQ}(z, T)$ for the Longitudinal and the Transverse acoustic phonons (having linear dispersion relation), we define few dimensionless quantities such as $\frac{\epsilon_{\mathbf{k}} - \mu}{T} = \eta$, $\frac{\omega_q}{T} = y$ and $\frac{\omega}{T} = x$, where $\omega_q = v_s q$, $v_s \equiv (v_{LA}, v_{TA})$. Using these variables and then performing the integral over the energy, Eq. (10) becomes

$$\begin{aligned}M''_{QQ}(\omega, T) &= \frac{\epsilon_F^2 D_0^2}{4\pi^2 m^2 \rho_m v_F^4 v_s^5 k_F} \frac{T^6}{\chi_{QQ}^0(T)} \int_0^{\Theta_{BG}/T} dy \frac{y^3}{e^y - 1} \left(1 - \frac{y^2 T^2}{2\Theta_{BG}^2} \right) \\ &\left\{ \frac{x - y}{e^{x-y} - 1} \frac{e^x - 1}{x} \left(\frac{\Theta_{BG}^2}{4T^2} + \frac{\pi^2}{3} + \frac{(x - y)^2}{3} + \frac{y(x - y)}{4} \right) \right. \\ &\left. + (\text{terms with } \omega \rightarrow -\omega) \right\}.\end{aligned}\quad (11)$$

Here Θ_{BG} is the Bloch-Grüneisen temperature and is equal to $2k_F v_s$. Further, the above expression in different frequency and temperature domains can be discussed or analyzed as follows:

Case-I: The zero frequency limit i.e. $\omega \rightarrow 0$

In this limit in Eq. (11), $M''_{QQ}(T)$ becomes

$$\begin{aligned}M''_{QQ}(T) &= \frac{\epsilon_F^2 D_0^2}{2\pi^2 m^2 \rho_m A v_F^4 v_s^5 k_F} \frac{T^6}{\chi_{QQ}^0(T)} \\ &\times \int_0^{\Theta_{BG}/T} dy \frac{y^4 e^y}{(e^y - 1)^2} \left(1 - \frac{y^2 T^2}{2\Theta_{BG}^2} \right) \\ &\times \left(\frac{\Theta_{BG}^2}{4T^2} + \frac{\pi^2}{3} + \frac{y^2}{12} \right).\end{aligned}\quad (12)$$

Here, we find that $M''_{QQ}(\omega, T)$ for the case of interaction of the electrons with the longitudinal or transverse phonons leads to the linear and the quadratic temperature dependence in the high ($T \gg \Theta_{BG}$) and low ($T \ll \Theta_{BG}$) temperature regimes respectively.

Now the electronic thermal conductivity Eq. (3) in the zero frequency limit can be written as [22]

$$\kappa_e(T) = \frac{1}{T} \frac{\chi_{QQ}^0(T)}{M''_{QQ}(T)} \approx \frac{T}{M''_{QQ}(T)}. \quad (13)$$

Thus the electronic thermal conductivity depends inversely on the thermal memory function. From Eqs. (12) and (13), we find that $\kappa_e(T)$ for the case of LA and TA phonons varies inversely with the

Table 1
The results of thermal memory function and the electronic thermal conductivity for the interaction of electrons with LA/TA and ZA phonons in different frequency and temperature domains.

Regimes	LA/TA phonons		ZA phonons	
	Thermal memory function $1/\tau_{th}$ or M''_{QQ}	Electronic thermal conductivity, $\kappa_e^{LA/TA}$	Thermal memory function $1/\tau_{th}$ or M''_{QQ}	Electronic thermal conductivity, κ_e^{ZA}
$\omega = 0, T \gg \Theta_{BG}$	T^1	T^0	T^1	T^0
$\omega = 0, T \ll \Theta_{BG}$	T^2	T^{-1}	$T^{1/2}$	$T^{1/2}$
$\omega \ll T \ll \Theta_{BG}$	T^2	$T^3 \omega^{-2}$	$T^{1/2}$	$T^{3/2} \omega^{-2}$
$\omega \ll \Theta_{BG} \ll T$	T^1	$T^2 \omega^{-2}$	T^1	$T^2 \omega^{-2}$
$T \ll \omega \ll \Theta_{BG}$	$T^3 \omega^{-1} e^{\omega/T}$	$T^4 \omega^{-3} e^{\omega/T}$	$T^{5/2} \omega^{-1} e^{\omega/T}$	$T^{7/2} \omega^{-3} e^{\omega/T}$
$\Theta_{BG} \ll \omega \ll T$	T^1	$T^2 \omega^{-2}$	T^1	$T^2 \omega^{-2}$
$\Theta_{BG} \ll T \ll \omega$	$T^{-1} \omega^2$	$T^0 \omega^0$	$T^{-1} \omega^2$	$T^0 \omega^0$
$T \ll \Theta_{BG} \ll \omega$	$T^2 \omega^2$	T^3	$\omega^2 T^{-1/2}$	$T^{1/2}$

temperature and becomes saturate at the low and the high temperature regimes respectively (as shown in Table 1). These are in accordance with the results existed in the literature [24,25].

Case-II: Finite frequency regimes

In finite frequency regimes, the asymptotic results of the thermal memory function and the corresponding electronic thermal conductivity in different temperature and the frequency regimes are shown in Table 1. Here, we observe that $M''_{QQ}(\omega, T)$ shows frequency independent behavior at extremely low frequency (or dc limit) and then in the intermediate regimes, the complicated behavior is observed. In the high frequency regime, due to more excitations, it varies quadratically with the increase in the frequency.

Now from Eq. (3), the real part of the electronic thermal conductivity is expressed as

$$Re[\kappa_e(\omega, T)] = \frac{\chi_{QQ}^0(T)}{T} \frac{M''_{QQ}(\omega, T)}{\omega^2 + (M''_{QQ}(\omega, T))^2}, \tag{14}$$

where $M''_{QQ}(\omega, T)$ for different regimes are given in Table 1. In the perturbative regime of small electron-phonon couplings, we assume that the frequency dependent thermal memory function is small. Using this assumption, Eq. (14) can be written as [22,37]

$$Re[\kappa_e(\omega, T)] \approx \frac{\chi_{QQ}^0(T)}{T} \frac{M''_{QQ}(\omega, T)}{\omega^2} \approx \frac{TM''_{QQ}(\omega, T)}{\omega^2}. \tag{15}$$

Here we use the temperature variation of the static correlation function. On substituting the variation of the temperature and the frequency dependent thermal memory function, we conclude that the electronic thermal conductivity at high frequency shows frequency independent behavior. While at the low frequency, it gives large conductivity due to the weakly frequency dependent behavior of the thermal memory function. These behaviors are summarized in Table 1.

1.4.2. Flexural acoustic phonons (ZA)

Now, in the case of the flexural acoustic phonons having quadratic dispersion [43] i.e. $\omega_q = \alpha q^2$, the thermal memory function can be computed in a similar fashion as done in the case of the LA/TA phonons.

Following the same procedure, the Eq. (10) for ZA phonons is written as

$$M''_{QQ}(\omega, T) = \frac{\epsilon_F^2 D_0^2}{8\pi^2 m^2 \rho_m v_F^4 \alpha^{3/2} k_F} \frac{T^{7/2}}{\chi_{QQ}^0(T)} \int_0^{\Theta_{BG}/T} dy \frac{y^{1/2}}{e^y - 1} \left(1 - \frac{yT}{8\Theta_{BG}}\right) \times \left\{ \frac{x-y}{e^{x-y} - 1} \frac{e^x - 1}{x} \left(\frac{\Theta_{BG}}{4T} y + \frac{\pi^2}{3} + \frac{(x-y)^2}{3} + \frac{y(x-y)}{4} \right) \right.$$

$$\left. + (\text{terms with } \omega \rightarrow -\omega) \right\}. \tag{16}$$

This is analyzed in different frequency and temperature domains as follows.

Case-I: The zero frequency limit i.e. $\omega \rightarrow 0$

Using this limit in Eq. (16), we have

$$M''_{QQ}(\omega, T) = \frac{\epsilon_F^2 D_0^2}{4\pi^2 m^2 \rho_m v_F^4 \alpha^{3/2} k_F} \frac{T^{7/2}}{\chi_{QQ}^0(T)} \times \int_0^{\Theta_{BG}/T} dy \frac{y^{3/2} e^y}{(e^y - 1)^2} \left(1 - \frac{yT}{8\Theta_{BG}}\right) \times \left(\frac{\Theta_{BG}}{4T} y + \frac{\pi^2}{3} + \frac{y^2}{12} \right). \tag{17}$$

Further in the high and the low temperature regimes, Eq. (17) shows that the thermal memory function $M''_{QQ}(T)$ varies as a square root and linearly with temperature at $T \gg \Theta_{BG}$ and $T \ll \Theta_{BG}$ respectively (shown in Table 1). Accordingly, the electronic thermal conductivity (Eq. (13)) leads to the $T^{1/2}$ power law behavior at the low temperature and temperature independent behavior in the high temperature.

Case-II: Finite frequency regimes

In this case, we have shown the asymptotic results in Table 1. It is observed that the frequency variation for $M''_{QQ}(\omega, T)$ and the corresponding $\kappa_e(\omega, T)$ is the same as the case for the longitudinal or the transverse phonons. But the temperature variations are different. At the temperature higher than the BG temperature, the ZA phonons show identical temperature dependent behavior as the LA/TA phonons. On the other hand, at the low temperature then the BG temperature, the temperature dynamics of ZA phonons is different from the LA/TA phonons.

2. Results

In this section, we present our findings for the thermal scattering rate and the electronic thermal conductivity for different cases.

2.1. Electronic thermal conductivity in zero frequency limit

In Fig. 1, $M''_{QQ}(T)$ is plotted as a function of T for LA and TA phonons at different Θ_{BG} which depends on the carrier density n . Here we separately plot it by setting $\Theta_{BG} \approx 57\sqrt{n}$ and $\Theta_{BG} \approx 38\sqrt{n}$ for the LA and the TA phonons respectively. Also, we have scaled the $M''_{QQ}(\omega, T)$ with $M''_0 (= \frac{6\epsilon_F^2 D_0^2}{\pi^3 \rho_m v_F^3 v_s^5 k_F})$. It is ob-

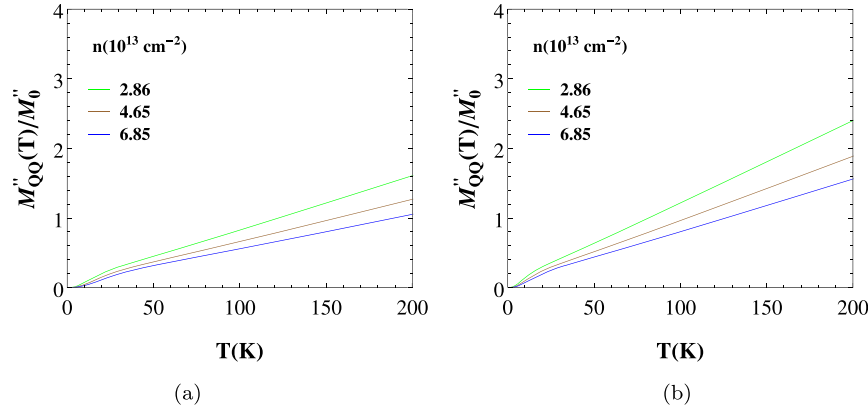


Fig. 1. The imaginary part of the thermal memory function for the longitudinal and transverse acoustic phonons are plotted with temperature at different $\Theta_{BG} \propto \sqrt{n}$. (a): For the longitudinal acoustic (LA) phonons and (b): for the transverse acoustic (TA) phonons.

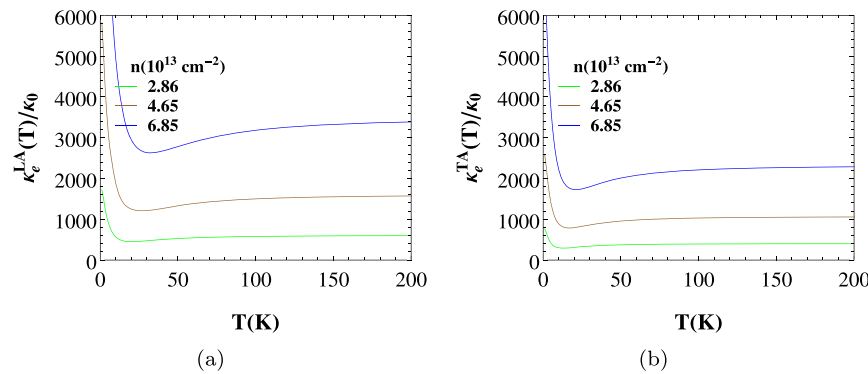


Fig. 2. The electronic thermal conductivity for the longitudinal and transverse acoustic phonons are plotted with temperature at different $\Theta_{BG} \propto \sqrt{n}$. (a): For the longitudinal acoustic (LA) phonons and (b): for the transverse acoustic (TA) phonons.

served that the thermal memory function increases linearly with increase in the temperature in the high temperature $T \gg \Theta_{BG}$ and non-linearly in the low temperature $T \ll \Theta_{BG}$ regimes. Also, it decreases with the increase in the carrier density or Θ_{BG} . This decrease is due to the linear density of states which provides more phase space to phonons to scatter. This results in the less electron-phonon scattering rate. On comparing the Fig. 1(a) and 1(b), it is found that the magnitude of the thermal memory function for the TA phonons is more than the LA phonons. This is due to the low phonon velocity of the TA phonons.

The corresponding electronic thermal conductivity for LA and TA phonons is shown in Fig. 2. Here for $T \ll \Theta_{BG}$, the electronic thermal conductivity reduces with the increase in T and at $T \gg \Theta_{BG}$, it saturates. These observed features are in accordance with the results existed in the literature [24,25]. In the intermediate regime i.e. around Θ_{BG} , the small dip is observed which is due to the consideration of the normal process scattering in the system.

For the flexural (ZA) phonons, $M''_{QQ}(T)$ is shown with the variation in the temperature in Fig. 3. Here we have set $\Theta_{BG} \approx 0.1n$. This small Θ_{BG} ensures that these phonons play significant role in the low temperature behavior of the electronic thermal conductivity of graphene. Here the value of M''_0 is $\frac{3\epsilon_F^2 D_0^2}{\pi^3 \rho_m v_F^2 k_B^4 \alpha^{5/2}}$. It is observed that the thermal memory function increases with the increase in the temperature by power law $T^{1/2}$ which further results the increase in the electronic thermal conductivity as $T^{1/2}$ law. But at the high temperature, it increases linearly similar to the case of LA/TA phonons and hence results in the temperature independent electronic thermal conductivity.

2.2. Electronic thermal conductivity in finite frequency regime

To discuss our results at the finite frequency, we plot $M''_{QQ}(\omega, T)/M''_0$ and $\text{Re}[\kappa_e(\omega, T)]/\kappa_0$ with the variation in the frequency at different temperature ratio i.e. T/Θ_{BG} .

In Figs. 4 and 7(a), we find that in the high frequency regime, the thermal memory function increases with the increase in the frequency. While at the low frequency, it shows saturation behavior. Next, using this variation, we plot the real part of the electronic thermal conductivity (14) in Figs. 5, 6 and 7(b). From the frequency behavior of the electronic thermal conductivity, we observe that it is suppressed by the factor $1/\omega^2$ in the high frequency regime. While in the low frequency regime, the frequency variations are observed. This frequency dependent behavior of $\kappa_e(\omega, T)$ is identical to the case of the metal. This gives the signature that the two dimensional scenario modifies the temperature variation of the electronic thermal conductivity and does not give effect on the frequency variation of $\kappa_e(\omega, T)$.

By comparing Figs. 2(a), 2(b) and 3(b), we note that the magnitude of electronic thermal conductivity $\kappa_e(T)$ is different in all three cases. This is due to the different values such as $v_{LA} = 21.2 \times 10^3 \text{ m s}^{-1}$, $v_{TA} = 14.1 \times 10^3 \text{ m s}^{-1}$ and $\alpha = 4.7 \times 10^{-7} \text{ m}^2 \text{ s}^{-1}$ for the longitudinal, transverse and the flexural phonons respectively. Due to it, the LA phonons contribute more to the electronic thermal conductivity as compared to the TA and ZA phonons. This can also be explained as follows.

According to the Mathiessen's law [20,21], the total resistivity is the sum of the resistivities due to different interactions separately. And the resistivity is directly proportional to the scattering

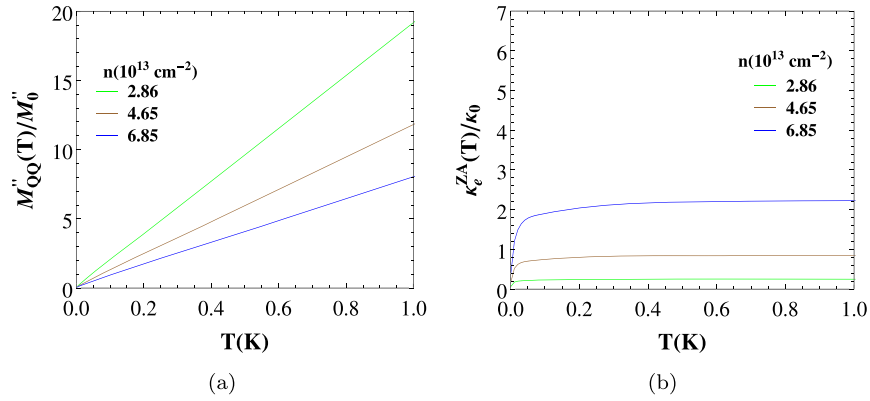


Fig. 3. (a): The thermal memory function for the flexural acoustic phonons (ZA) is plotted with temperature at different $\Theta_{BG} \propto n$ and (b): the corresponding electronic thermal conductivity.

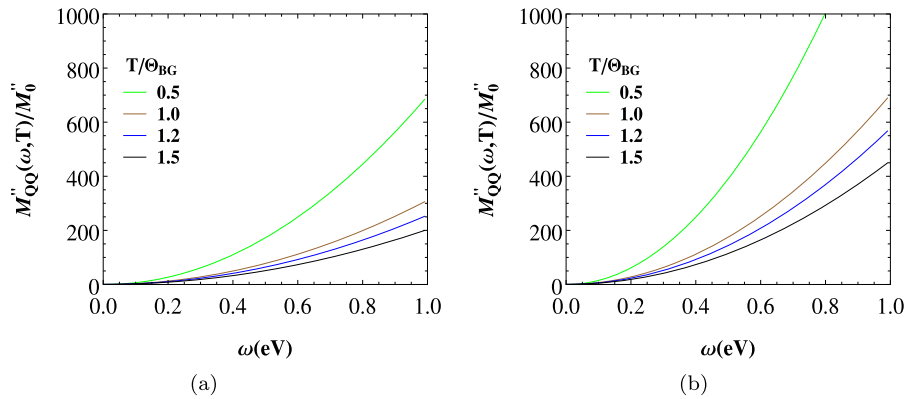


Fig. 4. The frequency and temperature dependent thermal memory function or the thermal scattering rate for the longitudinal and transverse acoustic phonons are plotted with frequency at different T/Θ_{BG} ratios. (a): For the longitudinal acoustic (LA) phonons and (b): for the transverse acoustic (TA) phonons.

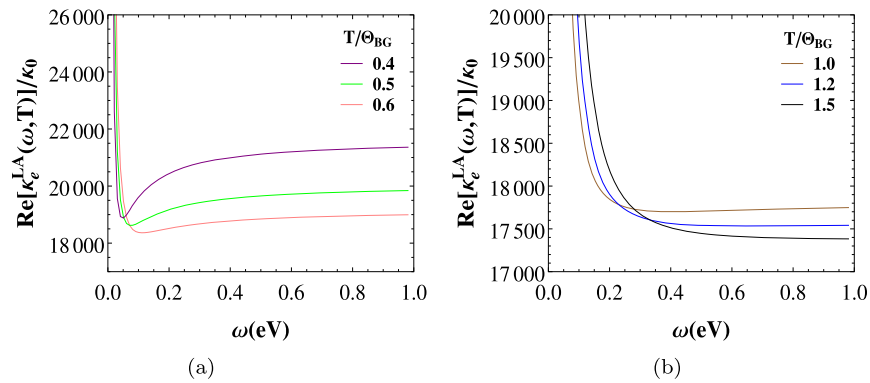


Fig. 5. The frequency and temperature dependent electronic thermal conductivity for the longitudinal acoustic phonons is plotted with frequency at different T/Θ_{BG} ratios.

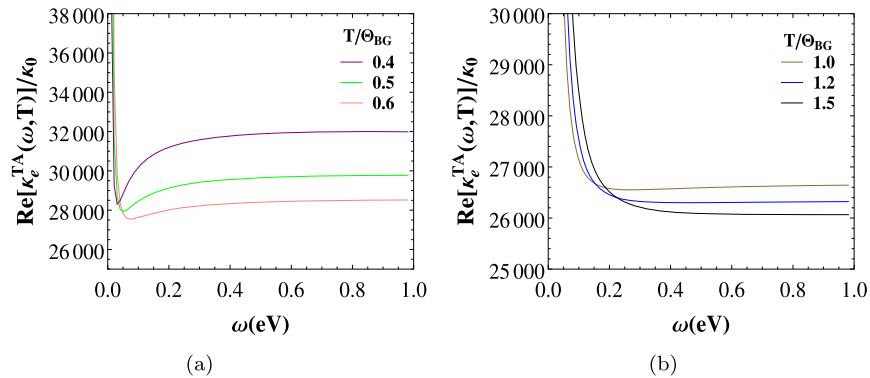


Fig. 6. The frequency and temperature dependent electronic thermal conductivity for the transverse acoustic phonons is plotted with frequency at different T/Θ_{BG} ratios.

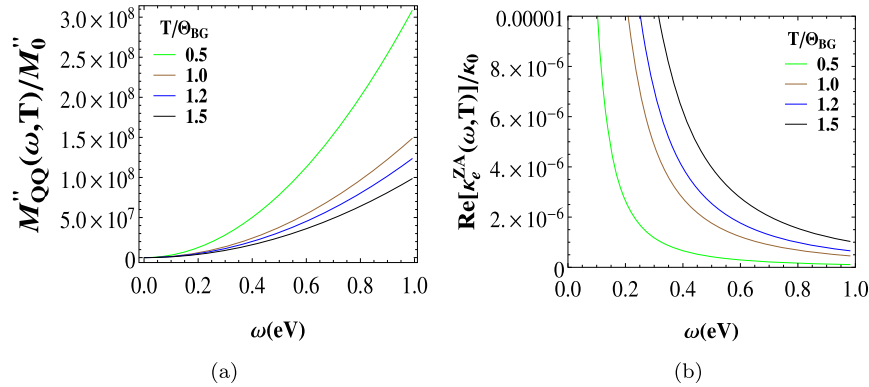


Fig. 7. (a): The thermal memory function for the flexural acoustic phonons (ZA) is plotted with frequency T/Θ_{BG} ratio. (b): The corresponding electronic thermal conductivity variation of flexural phonons.

rate or the memory function. Thus, the memory functions adds up due to the interactions of electrons with longitudinal, transverse and flexural acoustic phonons. Based on that the electronic thermal conductivity, Eq. (13), is expressed as $1/\kappa_e(T) = 1/\kappa_e^{LA}(T) + 1/\kappa_e^{TA}(T) + 1/\kappa_e^{ZA}(T)$. This shows that at the high temperature $T \gg \Theta_{BG}$, $1/\kappa_e(T) \approx \text{constant}$ and at the low temperature i.e. $T \ll \Theta_{BG}$, $1/\kappa_e(T) \approx B \left(\frac{T}{v_{LA}^3} + \frac{T}{v_{TA}^3} + \frac{T^{-1/2}}{\alpha^{5/2}} \right)$. Here, we find that at the low temperature, the contribution of the LA phonons is more than others. And the total electronic thermal conductivity decreases approximately linearly with the temperature. Because of the small value of the magnitude of electronic thermal conductivity of ZA phonons, it does not effect much to the total electronic thermal conductivity. Furthermore to understand the whole scenario of the electronic thermal conductivity at the low temperature, one also has to consider the electron–electron interactions which play reverse role from the electron–phonon interactions [45].

3. Conclusion

In the present study, the effect of the electron–acoustic phonon interactions to the electronic thermal conductivity is analyzed in detail. These analytic calculations for $\kappa_e(\omega, T)$ have been performed by using the memory function formalism which is beyond the relaxation time approximation. We find that the electronic thermal conductivity for various acoustic phonons shows different power law behavior due to the linear and quadratic phonon dispersion relations. These power law predictions are in agreement with the existing results in the literature [24,25]. It is also showed that in the total electronic thermal conductivity, the contribution of the ZA phonons is extremely small.

For the finite frequency cases, we have studied the dynamics of the electronic thermal conductivity due to the electron–phonon interaction which is identical to the case of three dimensional system such as metal [22]. But due to the semi-metallic character of the graphene, its' dynamical study may give information about the heat control for the reliable use of electronic devices.

Acknowledgements

The author is thankful to N. Singh, N. Das, S. K. Haldar and A. Atreya for helpful suggestions and discussions.

References

- [1] A.K. Geim, K.S. Novoselov, Nat. Matters 6 (2007) 183.
- [2] S.D. Sarma, A.K. Geim, P. Kim, A.H. MacDonald, Solid State Commun. 143 (2007) (special issue).
- [3] A.H. Castro Neto, F. Guinea, N.M.R. Peres, K.S. Novoselov, A.K. Geim, Rev. Mod. Phys. 81 (2009) 109.
- [4] S. Adam, E.H. Hwang, V.M. Galitski, S.D. Sarma, Proc. Natl. Acad. Sci. USA 104 (2007) 18392.
- [5] E.H. Hwang, S. Adam, S.D. Sarma, Phys. Rev. Lett. 98 (2007) 186806.
- [6] Y-W. Tan, Y. Zhang, K. Bolotin, Y. Zhao, S. Adam, E.H. Hwang, S. Das Sarma, H.L. Stormer, P. Kim, Phys. Rev. Lett. 99 (2007) 246803.
- [7] E.H. Hwang, Yu-Kuang Ben, S. Das Sarma, Phys. Rev. B 76 (2007) 115434.
- [8] E.H. Hwang, S. Das Sarma, Phys. Rev. B 77 (2008) 195412.
- [9] S. Adam, S. Das Sarma, Phys. Rev. B 77 (2008) 115436.
- [10] E.H. Hwang, S. Das Sarma, Phys. Rev. B 79 (2009) 165404.
- [11] E.H. Hwang, E. Rossi, S. Das Sarma, Phys. Rev. B 80 (2009) 235415.
- [12] S.D. Sarma, K. Yang, Solid State Commun. 149 (2009) 1502.
- [13] N.M.R. Peres, Rev. Mod. Phys. 82 (2010) 2673.
- [14] D.S. Abergel, V. Apalkov, J. Berashevich, K. Ziegler, T. Chakraborty, Adv. Phys. 59 (2010) 261.
- [15] D.R. Cooper, B. D'Anjou, N. Ghattamaneni, B. Harack, M. Hilke, A. Horth, N. Majlis, M. Massicotte, L. Vandsburger, E. Whiteway, V. Yu, ISRN Condens. Matter Phys. 2012 (2012) 501686.
- [16] T. Zhu, E. Ertekin, Phys. Rev. B 91 (2015) 205429.
- [17] T. Zhu, E. Ertekin, Phys. Rev. B 93 (2016) 155414.
- [18] A.A. Balandin, S. Ghosh, W. Bao, I. Calizo, D. Teweldebrhan, F. Miao, C.N. Lau, Nano Lett. 8 (2008) 902.
- [19] D.L. Nika, A.A. Balandin, J. Phys. Condens. Matter 24 (2012) 233203.
- [20] A.H. Wilson, The Theory of Metals, Cambridge University Press, 1953.
- [21] J.M. Ziman, Electrons and Phonons, Clarendon, Oxford, 1960.
- [22] P. Bhalla, P. Kumar, N. Das, N. Singh, Phys. Rev. B 94 (2016) 115114.
- [23] D.K. Efetov, P. Kim, Phys. Rev. Lett. 105 (2010) 256805.
- [24] E. Muñoz, J. Phys. Condens. Matter 24 (2012) 195302.
- [25] T.Y. Kim, C.H. Park, N. Marzari, Nano Lett. 16 (2016) 2439.
- [26] S.G. Volz, Phys. Rev. Lett. 87 (2001) 074301.
- [27] B.S. Shastry, Phys. Rev. B 73 (2006) 085117.
- [28] Y.K. Koh, D.G. Cahill, Phys. Rev. B 76 (2007) 075207.
- [29] B.S. Shastry, Rep. Prog. Phys. 72 (2009) 016501.
- [30] R. Zwanzig, Phys. Rev. 124 (1961) 983.
- [31] R. Zwanzig, in: W.E. Brittin, B.W. Downs, J. Downs (Eds.), Lectures in Theoretical Physics, vol. 3, Interscience, New York, 1961, p. 135.
- [32] H. Mori, Prog. Theor. Phys. 33 (1965) 423.
- [33] D. Forster, Hydrodynamic Fluctuations, Broken Symmetry and Correlation Functions, Advanced Books Classics, 1995.
- [34] P. Fulde, Correlated Electrons in Quantum Matter, World Scientific, 2012.
- [35] N. Das, P. Bhalla, N. Singh, Int. J. Mod. Phys. B 30 (2016) 1630015.
- [36] G.D. Mahan, Many-Particle Physics, 2nd ed., Plenum, New York and London, 1990.
- [37] P. Bhalla, N. Singh, Eur. Phys. J. B 89 (2016) 49.
- [38] E.H. Hwang, S. Das Sarma, Phys. Rev. B 77 (2008) 115449.
- [39] S.D. Sarma, S. Adam, E.H. Hwang, E. Rossi, Rev. Mod. Phys. 83 (2011) 407.
- [40] J.K. Viljas, T.T. Heikkilä, Phys. Rev. B 81 (2010) 245404.
- [41] G.D. Sanders, A.R.T. Nugraha, K. Sato, J.-H. Kim, J. Kono, R. Saito, C.J. Stanton, J. Phys. Condens. Matter 25 (2013) 144201.
- [42] K. Kaasbjerg, K.S. Thygesen, K.W. Jacobsen, Phys. Rev. B 85 (2012) 165440.
- [43] B. Amorim, F. Guinea, Phys. Rev. B 88 (2013) 115418.
- [44] R. Verma, S. Bhattacharya, S. Mahapatra, Semicond. Sci. Technol. 28 (2013) 015009.
- [45] A. Principi, G. Vignale, Phys. Rev. Lett. 115 (2015) 056603.



Moment expansion to the memory function for generalized Drude scattering rate



Pankaj Bhalla^{a,b,*}, Nabyendu Das^a, Navinder Singh^a

^a Physical Research Laboratory, Navrangpura, Ahmedabad 380009, India

^b Indian Institute of Technology Gandhinagar, 382355, India

ARTICLE INFO

Article history:

Received 17 March 2016

Accepted 7 April 2016

Available online 12 April 2016

Communicated by R. Wu

Keywords:

Electronic transport in metal

Scattering mechanisms

Impurity scattering

Memory function formalism

ABSTRACT

The memory function formalism is an important tool to evaluate the frequency dependent electronic conductivity. It is previously used within some approximations in the case of electrons interacting with various other degrees of freedom in metals with great success. However, one needs to go beyond those approximations as the interaction strengths become stronger. In this work, we propose a systematic expansion of the memory function involving its various moments. We calculate the higher order contribution to the generalized Drude scattering rate in case of electron–impurity interactions. Further we compare our results with the results from previously studied lowest order calculations. We find larger contributions from the higher moments in the low frequency regime and also in the case of larger interaction strength.

© 2016 Elsevier B.V. All rights reserved.

1. Introduction

The study of frequency dependent conductivity or optical conductivity is very important for understanding various interactions in the electronic systems [1,2]. In case of non-interacting electrons (neglecting Coulomb interactions) colliding with ions, it can be cast in the simple Drude formula, where the optical conductivity $\sigma(\omega)$ is expressed as $\sigma(\omega) = \frac{\sigma_0}{1-i\omega\tau}$ [3]. Here $\sigma_0 = \frac{ne^2\tau}{m}$ is the DC conductivity, where n is the electron density, m is the electron mass and $1/\tau$ refers to the scattering rate. Strictly speaking, the above Drude expression for optical conductivity is valid when $\omega \ll 1/\tau$. Thus we see that the frequency regime over which the Drude theory is valid depends on the smallness of the scattering rate $1/\tau$. The latter increases with the increase of interaction strength and the validity regime shrinks. In presence of interactions, a modified form of the Drude conductivity with frequency dependent scattering rate is often used and the resulting expression is known as the generalized Drude conductivity [4–6]. Within the linear response theory, the frequency dependent scattering rate ($1/\tau(\omega)$) is related to the current–current correlation which is equivalent to the two particle correlation functions [7]. It captures the effects of different interactions within an electronic system.

The correlation functions can be calculated by several ways such as Mori's formalism [8], within Pade approximation [9], Ru-

elle response theory [10], generalized methods for recursion relations [11–14], etc. In general any formalism based on standard quantum many body perturbation theory, expresses two particle correlators in terms of single particle correlations [7]. Thus the current–current correlator is expressed in terms of single particle correlators or single particle spectral function and the formalism depends on the existence of the quasiparticle. On the other hand the Mori–Zwanzig memory function formalism [8,15,16] deals with the two particle correlators. It is based on the existence of few slow modes (e.g. conserved or nearly conserved electric current) related to certain conservation laws in the system. Hence the existence of quasiparticles is not a necessity here and this approach has a wider range of applicability. The detailed discussions on its application in correlated electronic system can be found in a recent review by the present authors [17]. In this method, the generalized scattering rate $1/\tau(\omega)$ can be expressed as an imaginary part of a memory function ($ImM(\omega)$). The latter will be defined in the next section.

In literature, the memory function approach has been used in various systems, such as to study the molecular dynamics, thermodynamic properties, transport properties, etc. [18–22,24–42]. It becomes a method of choice in various strongly correlated electronic systems such as strange metal phase of the optimally doped cuprate superconductors where the very notion of the electronic quasiparticle breaks down [38,40], but the translational invariance is present. In a generic electronic system there can be various slow modes such as the charge diffusion, the heat diffusion etc. [38,40]. In the present study, we consider the electric current as the only

* Corresponding author.

E-mail address: pankajbhalla66@gmail.com (P. Bhalla).

relevant slow mode. We then systematically study the effects of other fast degrees of freedom on the current–current correlation within this formalism. In the present case, our main focus will be only on the role of electron–impurity interactions on the current–current correlation. The effects of the impurity interactions on the dynamical conductivity of a simple metal have been studied previously within the memory function in Ref. [22] in detail. These authors yield identical results for electrical conductivity with that of the Boltzmann’s results [23] in the dc limit. However the formalism is restricted to the lowest order in interaction strength and needs corrections as the latter increases.

With this motivation, we review the application of the memory function (MF) formalism in case of current–current correlation in metals and propose an expansion in terms of its various moments. Then we show that the previously studied Götze–Wölfle [24] formalism and similar other studies [6,25,36,41] are equivalent to the truncation our proposed moment expansion at the lowest order. We look for the case of higher interaction strength and calculate the contribution from the next order in the moment expansion.

This paper is organized as follows: In Sec. 2, we present the memory function formalism for electrical conductivity. In Sec. 3, the memory function is derived using equation of motion approach. Then in Sec. 4 the scattering rate has been calculated for impurity interactions with first moment expansion as done in literature. Then, we derive the second moment expansion of scattering rate and give the expression of scattering rate up-to second moment in our expansion of the memory function in Sec. 5. In Sec. 6, we compare our results with the former results. In Sec. 7, we conclude with discussion.

2. Memory function formalism

The memory function method, also known as projection operator method is first introduced by Zwanzig [15,16] to study the time evolution of correlation functions. Later, the method was generalized by Mori [8] and the Laplace transform of an autocorrelation function was cast into a continued fraction form. In this section, we will review the mathematical description of the memory function formalism [29].

Let us consider a system with a given Hamiltonian H in which Liouville operator \mathcal{L} is defined by its action on any operator A as,

$$\mathcal{L}A = [H, A] = -i \frac{dA}{dt}. \quad (1)$$

Here A is an operator representing some observable and $[\dots, \dots]$ represents the commutator between two such operators and we use units in which $\hbar = 1$ and $k_B = 1$. The above equation yields the time evolution of the operator as,

$$A(t) = e^{i\mathcal{L}t} A(0). \quad (2)$$

To understand the dynamic property of certain observable in many body systems, the time evolutions of related operators are needed. Let A_i represent such operators. Their correlation is expressed in terms of the correlation function matrix $\mathcal{R}(t)$. The latter, in terms of its matrix elements is defined as,

$$R_{ij}(t) = \langle A_i(t) | A_j(0) \rangle. \quad (3)$$

Here the inner product of such operators is defined as canonical ensemble average. Using eqn. (2) and performing the Laplace transform, the above equation can be expressed as,

$$R_{ij}(z) = \int_0^\infty dt e^{izt} \langle A_i(t) | A_j(0) \rangle = \left\langle A_i \left| \frac{i}{z - \mathcal{L}} \right| A_j \right\rangle. \quad (4)$$

Here z is a complex frequency and $z = \omega + i\eta$ with $\eta \rightarrow 0^+$. To express the correlation function in terms of the memory function, we

introduce a projector operator P which projects onto an operator A and is defined as,

$$P = \sum_{i,j} \frac{|A_i\rangle\langle A_j|}{\langle A_i | A_j \rangle} = \mathcal{I} - Q. \quad (5)$$

Replacing the operator \mathcal{L} by $\mathcal{L}(P + Q)$ in eqn. (4) and using the identity

$$\frac{1}{X + Y} = \frac{1}{X} - \frac{1}{X} Y \frac{1}{X + Y}, \quad (6)$$

the matrix elements of correlation function (eqn. (4)) becomes,

$$R_{ij} = \left\langle A_i \left| \left\{ \frac{1}{z - \mathcal{L}Q} + \frac{1}{z - \mathcal{L}Q} \mathcal{L}P \frac{1}{z - \mathcal{L}} \right\} \right| A_j \right\rangle. \quad (7)$$

On simplification, the above expression can be rewritten as,

$$R_{ij} = \frac{1}{z} \chi_{ij} + \sum_{lm} \left\langle A_i \left| \frac{1}{z - \mathcal{L}Q} \mathcal{L} \right| A_l \right\rangle \chi_{lm}^{-1} R_{mj}, \quad (8)$$

where $\chi_{ij} = \langle A_i | A_j \rangle$. In matrix notation, this can be written as,

$$(z\mathcal{I} - \mathcal{K}\chi^{-1})\mathcal{R} = \chi. \quad (9)$$

Here the elements of matrix \mathcal{K} are defined as,

$$\begin{aligned} K_{il} &= \left\langle A_i \left| \frac{z}{z - \mathcal{L}Q} \mathcal{L} \right| A_l \right\rangle \\ &= \langle A_i | \mathcal{L} | A_l \rangle + \left\langle A_i \left| \mathcal{L}Q \frac{1}{z - \mathcal{L}Q} \mathcal{L} \right| A_l \right\rangle. \end{aligned} \quad (10)$$

The first part of the right hand side of the above equation is known as frequency matrix and is defined as,

$$\mathcal{L}_{il} = \langle A_i | \mathcal{L} | A_l \rangle. \quad (11)$$

The other part is known as memory matrix and is defined as follows,

$$M_{il}(z) = \left\langle A_i \left| \mathcal{L}Q \frac{1}{z - \mathcal{L}Q} \mathcal{L} \right| A_l \right\rangle. \quad (12)$$

Using the fact $Q^2 = Q$, the above expression can be written in a symmetric form as,

$$M(z) = \left\langle A \left| \mathcal{L}Q \frac{1}{z - Q\mathcal{L}Q} Q\mathcal{L} \right| B \right\rangle. \quad (13)$$

Now, on applying the Liouvillian operator on both the operators A and B , the above equation reduces to

$$M(z) = \left\langle \dot{A} \left| Q \frac{1}{z - Q\mathcal{L}Q} Q \right| \dot{B} \right\rangle. \quad (14)$$

We focus on the electrical conductivity and thus our concern is the current–current correlation. Hence, we replace both A and B operators by the current operator J . Thus the desired memory function for the electrical conductivity becomes,

$$M(z) = \left\langle J \left| Q \frac{1}{z - Q\mathcal{L}Q} Q \right| J \right\rangle. \quad (15)$$

On expanding $M(z)$ in series expansion, we have

$$\begin{aligned} M(z) &= \frac{1}{z} \left\langle J \left| Q \left(1 + \frac{1}{z} Q\mathcal{L}Q \right. \right. \right. \\ &\quad \left. \left. \left. + \frac{1}{z^2} Q\mathcal{L}Q Q\mathcal{L}Q + \dots \right) Q \right| J \right\rangle. \end{aligned} \quad (16)$$

Using the fact that $Q Q = Q^2 = (1 - P)^2 = Q$ and $\langle J | \dot{J} \rangle, \langle \dot{J} | \dot{J} \rangle = 0$ (proved in Appendix A), the memory function in series expansion can be written as

$$M(z) = \frac{1}{z} \langle \dot{J} | \dot{J} \rangle + \frac{1}{z^3} \langle \ddot{J} | \ddot{J} \rangle + \cdots + \frac{1}{z^{2n-1}} \langle \overset{n}{J} | \overset{n}{J} \rangle. \quad (17)$$

Here $\overset{n}{J}$ represents the n th time derivative of the current operator. This expression represents the high frequency expansion of the memory function in terms of the equal time autocorrelation function [45]. With this motivation, we will derive a similar expression for the memory function by an alternative way in the next section.

3. Equation of motion method

In an alternative way, the memory function can also be calculated using the equation of motion method (EQM) as follows. Let us start with the expression for response function within the linear response theory by Kubo [46–48], which is given as,

$$\chi_{AB}(z) = \langle \langle A; B \rangle \rangle_z = -i \int_0^{\infty} e^{izt} \langle [A(t), B(0)] \rangle dt. \quad (18)$$

Here A and B are two operators and correspond to two physical variables, $[A, B]$ denotes their commutator and the inner $\langle \cdots \rangle$ represents statistical ensemble average at temperature T . The outer $\langle \cdots \rangle$ represents the Laplace transform at a complex frequency z . Using the equation of motion, $\langle \langle A; B \rangle \rangle_z$ can be written as,

$$z \langle \langle A; B \rangle \rangle_z = \langle [A, B] \rangle + \langle \langle [A, H]; B \rangle \rangle_z. \quad (19)$$

Here H is the total Hamiltonian of the system. According to the Heisenberg equation of motion, an operator evolves as,

$$i \frac{dA}{dt} = i \dot{A} = [A, H]. \quad (20)$$

Using the above expression, eqn. (19) can be expressed as,

$$z \langle \langle A; B \rangle \rangle_z = \langle [A, B] \rangle + i \langle \langle \dot{A}; B \rangle \rangle_z. \quad (21)$$

In the present case, we are interested in current–current correlation function. Hence, we replace both A and B by current operator J . Thus, the above equation becomes

$$z \langle \langle J; J \rangle \rangle_z = \langle [J, J] \rangle + i \langle \langle \dot{J}; J \rangle \rangle_z. \quad (22)$$

As the commutator $[J, J] = 0$, the above equation reduces to

$$z \langle \langle J; J \rangle \rangle_z = i \langle \langle \dot{J}; J \rangle \rangle_z. \quad (23)$$

Again from the equation of motion (using eqn. (19)),

$$z \langle \langle \dot{J}; J \rangle \rangle_z = \langle [\dot{J}, J] \rangle + i \langle \langle \ddot{J}; J \rangle \rangle_z. \quad (24)$$

For $z = 0$, $\langle [\dot{J}, J] \rangle = -i \langle \langle \dot{J}; J \rangle \rangle_{z=0}$. Using these, eqn. (23) can be written as,

$$z \langle \langle J; J \rangle \rangle_z = \frac{1}{z} (\langle \langle \dot{J}; J \rangle \rangle_{z=0} - \langle \langle \dot{J}; J \rangle \rangle_z). \quad (25)$$

This expression is used in the well cited work by Götze and Wölfle [24] to evaluate the memory function for electrons in metal with various interactions. However instead of considering the above expression and evaluating $\langle \langle \dot{J}; J \rangle \rangle_z$ perturbatively, we can opt for a higher moment expansion as follows. We apply EQM method again to evaluate the correlation function $\langle \langle J; J \rangle \rangle$ in terms of the correlations involving higher time derivatives of \dot{J} . Thus in order to express the correlation function in terms of the next moment, i.e. second moment, we use the EQM for $\langle \langle \dot{J}; J \rangle \rangle_z$, and obtain,

$$z \langle \langle \dot{J}; J \rangle \rangle_z = \langle [\dot{J}, J] \rangle + \langle \langle [\dot{J}, H]; J \rangle \rangle_z. \quad (26)$$

Using $\langle [\dot{J}, J] \rangle = 0$ and $z \langle \langle [\dot{J}, H]; J \rangle \rangle = \langle \langle \ddot{J}; J \rangle \rangle_{z=0} - \langle \langle \ddot{J}; J \rangle \rangle_z$, the above equation can be written as

$$z \langle \langle \dot{J}; J \rangle \rangle_z = -\frac{1}{z} (\langle \langle \ddot{J}; J \rangle \rangle_{z=0} - \langle \langle \ddot{J}; J \rangle \rangle_z). \quad (27)$$

Substitute this equation in eqn. (25), we have

$$z \langle \langle J; J \rangle \rangle_z = \frac{1}{z} \langle \langle \dot{J}; J \rangle \rangle_{z=0} + \frac{1}{z^3} (\langle \langle \ddot{J}; J \rangle \rangle_{z=0} - \langle \langle \ddot{J}; J \rangle \rangle_z). \quad (28)$$

Thus the expression for the response function becomes,

$$z \chi(z) = \frac{1}{z} \langle \langle \dot{J}; J \rangle \rangle_{z=0} + \frac{1}{z^3} (\langle \langle \ddot{J}; J \rangle \rangle_{z=0} - \langle \langle \ddot{J}; J \rangle \rangle_z). \quad (29)$$

By applying EQM again and again, we can obtain a series expansion for $z \chi(z)$ as,

$$z \chi(z) = \frac{1}{z} \langle \langle \dot{J}; J \rangle \rangle_{z=0} + \frac{1}{z^3} \langle \langle \ddot{J}; J \rangle \rangle_{z=0} - \cdots + \frac{1}{z^{2n-1}} \langle \langle \overset{n}{J}; J \rangle \rangle_{z=0} - \frac{1}{z^{2n-1}} \langle \langle \overset{n}{J}; J \rangle \rangle_z. \quad (30)$$

In Ref. [24], it is shown that $\chi(z)$ is related to the memory function as

$$M(z) = z \frac{\chi(z)}{\chi_0 - \chi(z)}, \quad (31)$$

where χ_0 represents the static correlation function ($= N_e/m$, where N_e corresponds to electron density). Here $M(z)$ is the complex memory function, which upon analytic continuation, can be written as a function of real frequency,

$$M(\omega \pm i0) = M'(\omega) \pm M''(\omega), \quad (32)$$

where $M'(\omega)$ and $M''(\omega)$ are real and imaginary part of the memory function and satisfy the symmetry properties $M'(\omega) = -M'(-\omega)$ and $M''(\omega) = M''(-\omega)$ [24].

An approximate form of the memory function can be obtained by assuming that $\chi(z)/\chi_0$ is smaller than one. Within this approximation, the expression for the memory function becomes,

$$M(z) = \frac{z \chi(z)}{\chi_0} \left(1 + \frac{\chi(z)}{\chi_0} - \cdots \right). \quad (33)$$

Keeping only the leading order term, the memory function can be expressed as

$$M(z) = z \frac{\chi(z)}{\chi_0}. \quad (34)$$

This expression is valid under the approximation discussed before and works well in high frequency regime and shows valid/invalid results in low frequency regime depending upon the parameters chosen to calculate the $\chi(z)$. More details of its validity are discussed in our recent work [42].

Using eqn. (30), the memory function to general order can be written as,

$$M(z) = \frac{1}{\chi_0} \left(\frac{1}{z} \langle \langle \dot{J}; J \rangle \rangle_{z=0} + \frac{1}{z^3} \langle \langle \ddot{J}; J \rangle \rangle_{z=0} + \cdots + \frac{1}{z^{2n-1}} \langle \langle \overset{n}{J}; J \rangle \rangle_{z=0} - \frac{1}{z^{2n-1}} \langle \langle \overset{n}{J}; J \rangle \rangle_z \right). \quad (35)$$

This is an expression of the complex memory function which is equivalent to eqn. (17), but under a restrictive condition $\chi(z) \ll \chi_0$ [42]. Here we see that instead of limiting at a perturbative calculation of \dot{J} - J correlation, we can include correlations involving higher order time derivatives of \dot{J} . Since the correlations with higher order time derivatives involve higher order corrections in interaction strength to the scattering rate. We will use this expression with $n = 2$, to evaluate the scattering rate due to the impurity interactions in later sections and will see how the result differs from that of the previously studied lower order corrections.

4. Case of electron–impurity scattering

In this section, we review the work discussed in Ref. [24] to calculate the memory function for impurity interactions. We consider a metal where degenerate electrons are interacting with impurities. In this case, the Hamiltonian is described as

$$H = H_0 + H_{\text{imp}}. \quad (36)$$

Here H_0 is the unperturbed Hamiltonian and in second quantized notation can be written as [7]

$$H_0 = \sum_{\mathbf{p}} \epsilon_{\mathbf{p}} c_{\mathbf{p}}^{\dagger} c_{\mathbf{p}}. \quad (37)$$

Here $c_{\mathbf{p}}^{\dagger}$ and $c_{\mathbf{p}}$ are electron creation and annihilation operators respectively and $\epsilon_{\mathbf{p}}$ is the energy of free electrons with momenta \mathbf{p} . The other part of Hamiltonian describes the electron–impurity interaction and is given as,

$$H_{\text{imp}} = \frac{1}{N} \sum_{j=1}^{N_{\text{imp}}} \sum_{\mathbf{k}, \mathbf{k}', \sigma} (\mathbf{k}|U^j|\mathbf{k}') c_{\mathbf{k}, \sigma}^{\dagger} c_{\mathbf{k}' \sigma}, \quad (38)$$

where N represents the number of lattice cells, N_{imp} corresponds to number of impurity sites and U^j is the scattering potential from j th impurity.

Computation of the memory function in Ref. [24] is restricted to the first moment only. First we discuss it. Truncating at the first order, the memory function can be written as,

$$M(z) = \frac{1}{z\chi_0} (\langle\langle \dot{J}; \dot{J} \rangle\rangle_{z=0} - \langle\langle \ddot{J}; \ddot{J} \rangle\rangle_z). \quad (39)$$

To evaluate the above expression, let us first calculate \dot{J} . It is defined as,

$$\dot{J} = -i[J, H] = -i([J, H_0] + [J, H_{\text{imp}}]). \quad (40)$$

As $[J, H_0] = 0$, thus $\dot{J} = -i[J, H_{\text{imp}}]$. Using eqn. (38) and defining the current operator $J = \sum_{\mathbf{k}} v_x(\mathbf{k}) c_{\mathbf{k}}^{\dagger} c_{\mathbf{k}}$, where v_x is the x -component of velocity, the time derivative of J can be written as,

$$\dot{J} = -\frac{i}{N} \sum_{j, \mathbf{k}, \mathbf{k}'} (\mathbf{k}|U^j|\mathbf{k}') (v_x(\mathbf{k}) - v_x(\mathbf{k}')) c_{\mathbf{k}}^{\dagger} c_{\mathbf{k}'}. \quad (41)$$

With the above expression, the correlator $\langle\langle \dot{J}; \dot{J} \rangle\rangle$ becomes

$$\begin{aligned} \langle\langle \dot{J}; \dot{J} \rangle\rangle_z &= -\frac{1}{N^2} \sum_{j, \mathbf{k}, \mathbf{k}'} \sum_{i, \mathbf{p}, \mathbf{p}'} (\mathbf{k}|U^j|\mathbf{k}') (\mathbf{p}|U^i|\mathbf{p}') \\ &\quad \times (v_x(\mathbf{k}) - v_x(\mathbf{k}')) (v_x(\mathbf{p}) - v_x(\mathbf{p}')) \langle\langle c_{\mathbf{k}}^{\dagger} c_{\mathbf{k}'}; c_{\mathbf{p}}^{\dagger} c_{\mathbf{p}'} \rangle\rangle. \end{aligned} \quad (42)$$

Using the definition of the correlator as defined in eqn. (18), $\langle\langle c_{\mathbf{k}}^{\dagger} c_{\mathbf{k}'}; c_{\mathbf{p}}^{\dagger} c_{\mathbf{p}'} \rangle\rangle$ after doing time integration and thermal average by using $c_{\mathbf{k}}(t) = c_{\mathbf{k}} e^{i\epsilon_{\mathbf{k}} t}$, we get,

$$-\frac{1}{z + \epsilon_{\mathbf{k}} - \epsilon_{\mathbf{k}'}} (f(\mathbf{k}) - f(\mathbf{k}')) \delta_{\mathbf{p}', \mathbf{k}} \delta_{\mathbf{p}, \mathbf{k}'}. \quad (43)$$

We consider the above expression and also the case of dilute impurity and neglecting the interference terms, thus substitute $i = j$ in eqn. (42). Performing the summation over impurity sites which contributes N_{imp} , we have

$$\begin{aligned} \langle\langle \dot{J}; \dot{J} \rangle\rangle_z &= 2 \frac{N_{\text{imp}}}{N^2} \sum_{\mathbf{k}, \mathbf{k}'} |(\mathbf{k}|U|\mathbf{k}')|^2 (v_x(\mathbf{k}) - v_x(\mathbf{k}'))^2 \frac{f(\mathbf{k}) - f(\mathbf{k}')}{z + \epsilon_{\mathbf{k}} - \epsilon_{\mathbf{k}'}}. \end{aligned} \quad (44)$$

Here factor 2 is due to the spin degeneracy. After simplification considering isotropic free electron case and writing $\mathbf{v} = \mathbf{k}/m$,

$$\langle\langle \dot{J}; \dot{J} \rangle\rangle_z = \frac{2}{3} \frac{N_{\text{imp}}}{m^2 N^2} \sum_{\mathbf{k}, \mathbf{k}'} |(\mathbf{k}|U|\mathbf{k}')|^2 (\mathbf{k} - \mathbf{k}')^2 \frac{f(\mathbf{k}) - f(\mathbf{k}')}{z + \epsilon_{\mathbf{k}} - \epsilon_{\mathbf{k}'}}. \quad (45)$$

On substituting the above equation in eqn. (25) and using eqn. (34), followed by analytic continuation, i.e. $z \rightarrow \omega + i\eta$, $\eta \rightarrow 0^+$, the imaginary part of the memory function becomes,

$$\begin{aligned} M''(\omega) &= \frac{2\pi}{3N^2} \frac{N_{\text{imp}}}{mN_e\omega} \sum_{\mathbf{k}, \mathbf{k}'} |(\mathbf{k}|U|\mathbf{k}')|^2 (\mathbf{k} - \mathbf{k}')^2 (f(\mathbf{k}) - f(\mathbf{k}')) \\ &\quad \times \delta(\omega + \epsilon_{\mathbf{k}} - \epsilon_{\mathbf{k}'}). \end{aligned} \quad (46)$$

Under the assumption that U is independent of momentum, i.e. for point like impurities [43,44] the expression further reduces to,

$$\begin{aligned} M''(\omega) &= \frac{2\pi}{3N^2} \frac{N_{\text{imp}} U^2}{mN_e\omega} \\ &\quad \times \sum_{\mathbf{k}, \mathbf{k}'} (\mathbf{k} - \mathbf{k}')^2 (f(\mathbf{k}) - f(\mathbf{k}')) \delta(\omega + \epsilon_{\mathbf{k}} - \epsilon_{\mathbf{k}'}). \end{aligned} \quad (47)$$

Converting the summation over momentum indices to the energy integrals and performing one integral involving the delta function, the equation further reduces to

$$\begin{aligned} M''(\omega) &= \frac{2}{3} \frac{N_{\text{imp}}}{N_e} \frac{U^2 m^3}{\pi^3 \omega} \\ &\quad \times \int_0^{\infty} d\epsilon \sqrt{\epsilon(\epsilon + \omega)} (2\epsilon + \omega) (f(\epsilon) - f(\epsilon')). \end{aligned}$$

This is an expression of imaginary part of the memory function or the scattering rate of the electronic quasiparticles due to the electron–impurity interactions. Here for simplicity we replace $\epsilon_{\mathbf{k}}$ and $\epsilon_{\mathbf{k}'}$ by ϵ and ϵ' respectively in the rest of the calculation. According to our proposed expansion, this result is equivalent to restrict eqn. (35) at $n = 1$ followed by a perturbative evaluation of the \dot{J} – \dot{J} correlation. In the next section we will perform a perturbative calculation at higher order and will show that this approximation has limited validity.

5. The MF with a higher order moment

The memory function with higher order moment can be calculated within the moment expansion proposed by us using eqn. (30). One can obtain more exact results by including higher order moments. Due to mathematical complexity, we restrict us to evaluate the memory function $M(z)$ defined in eqn. (35) at $n = 2$, i.e. by considering up-to the \dot{J} – \dot{J} correlation. We proceed as follows. We begin with the evaluation of $\langle\langle \dot{J}; \dot{J} \rangle\rangle_z$, which is defined as,

$$\begin{aligned} \langle\langle \dot{J}; \dot{J} \rangle\rangle_z &= -\langle\langle [J, H]; [J, H] \rangle\rangle_z \\ &= \langle\langle [[J, H], H]; [[J, H], H] \rangle\rangle_z. \end{aligned} \quad (48)$$

Now considering the non-interacting and the interacting parts of the Hamiltonian separately the above equation can be rewritten as,

$$\begin{aligned} \langle\langle \dot{J}; \dot{J} \rangle\rangle_z &= \langle\langle [[J, H_{\text{imp}}], H_0]; [[J, H_{\text{imp}}], H_0] \rangle\rangle_z \\ &\quad + \langle\langle [[J, H_{\text{imp}}], H_{\text{imp}}]; [[J, H_{\text{imp}}], H_0] \rangle\rangle_z \\ &\quad + \langle\langle [[J, H_{\text{imp}}], H_0]; [[J, H_{\text{imp}}], H_{\text{imp}}] \rangle\rangle_z \\ &\quad + \langle\langle [[J, H_{\text{imp}}], H_{\text{imp}}]; [[J, H_{\text{imp}}], H_{\text{imp}}] \rangle\rangle_z. \end{aligned} \quad (49)$$

The second term in the above expression is equal to the third term but with an opposite sign, due to the properties of the commutators. Hence they cancel each other and thus we obtain,

$$\langle\langle\dot{J}; \dot{J}\rangle\rangle_z = \langle\langle [J, H_{\text{imp}}], H_0 \rangle\rangle; [J, H_{\text{imp}}], H_0 \rangle\rangle_z + \langle\langle [J, H_{\text{imp}}], H_{\text{imp}} \rangle\rangle; [J, H_{\text{imp}}], H_{\text{imp}} \rangle\rangle_z. \quad (50)$$

To find the exact expression for the left hand side of the above equation, calculations can be performed in a way similar to that of the $\langle\langle\dot{J}; \dot{J}\rangle\rangle_z$ in section 4. The details of which are presented in Appendix B. After several algebraic manipulations, we obtain,

$$\begin{aligned} \langle\langle\dot{J}; \dot{J}\rangle\rangle_z &= \frac{2 N_{\text{imp}} U^2 m^2}{3 \pi^4} \\ &\times \int_0^\infty d\epsilon \int_0^\infty d\epsilon' \sqrt{\epsilon\epsilon'} (\epsilon + \epsilon') (\epsilon - \epsilon')^2 \frac{f(\epsilon) - f(\epsilon')}{z + \epsilon - \epsilon'} \\ &+ \frac{2 (N_{\text{imp}} U^2)^2 m^2}{3 \pi^4} \\ &\times \int_0^\infty d\epsilon \int_0^\infty d\epsilon' \sqrt{\epsilon\epsilon'} (\epsilon + \epsilon') \frac{f(\epsilon) - f(\epsilon')}{z + \epsilon - \epsilon'}. \end{aligned} \quad (51)$$

Using eqn. (51) and performing the energy integrals as done in the case of first moment (eqn. (45)), in eqn. (35), the expression for the memory function $M(z)$ becomes,

$$\begin{aligned} M(z) &= \frac{2 m^3}{3 \pi^4} \frac{1}{N_e} \left\{ -\frac{2}{z} N_{\text{imp}} U^2 \int_0^\infty d\epsilon \int_0^\infty d\epsilon' \epsilon \sqrt{\epsilon\epsilon'} \frac{f(\epsilon) - f(\epsilon')}{\epsilon - \epsilon'} \right. \\ &- \frac{1}{z^2} N_{\text{imp}} U^2 \int_0^\infty d\epsilon \int_0^\infty d\epsilon' \sqrt{\epsilon\epsilon'} (\epsilon + \epsilon') (\epsilon - \epsilon')^2 \\ &\times \frac{f(\epsilon) - f(\epsilon')}{(z + \epsilon - \epsilon')(\epsilon - \epsilon')} - \frac{1}{z^2} (N_{\text{imp}} U^2)^2 \int_0^\infty d\epsilon \\ &\left. \times \int_0^\infty d\epsilon' \sqrt{\epsilon\epsilon'} (\epsilon + \epsilon') \frac{f(\epsilon) - f(\epsilon')}{(z + \epsilon - \epsilon')(\epsilon - \epsilon')} \right\}. \end{aligned} \quad (52)$$

After further algebraic manipulations, the expression for the complex memory function $M(z)$ reduces to

$$\begin{aligned} M(z) &= \frac{2 m^3}{3 \pi^4} \frac{1}{N_e} \int_0^\infty d\epsilon \int_0^\infty d\epsilon' \sqrt{\epsilon\epsilon'} \frac{f(\epsilon) - f(\epsilon')}{\epsilon - \epsilon'} \\ &\times \left\{ -N_{\text{imp}} U^2 \frac{\epsilon + \epsilon'}{z + \epsilon - \epsilon'} \right. \\ &- (N_{\text{imp}} U^2)^2 \frac{\epsilon + \epsilon'}{(\epsilon - \epsilon')^2 (z + \epsilon - \epsilon')} \\ &\left. + \frac{2}{z} (N_{\text{imp}} U^2)^2 \frac{\epsilon}{(\epsilon - \epsilon')^2} \right\}. \end{aligned} \quad (53)$$

We are interested in the frequency dependent character of imaginary part of memory function $M''(\omega)$ as a function of real frequency. On performing analytic continuation, i.e. $z \rightarrow \omega + i\eta$, $\eta \rightarrow 0$, the expression for $M''(\omega)$ becomes,

$$\begin{aligned} M''(\omega) &= \frac{2 m^3}{3 \pi^3} \frac{1}{N_e} \int_0^\infty d\epsilon \int_0^\infty d\epsilon' \sqrt{\epsilon\epsilon'} \frac{f(\epsilon) - f(\epsilon')}{\epsilon - \epsilon'} \delta(\omega + \epsilon - \epsilon') \\ &\times \left\{ N_{\text{imp}} U^2 (\epsilon + \epsilon') + (N_{\text{imp}} U^2)^2 \frac{\epsilon + \epsilon'}{(\epsilon - \epsilon')^2} \right. \\ &\left. - 2 (N_{\text{imp}} U^2)^2 \frac{\epsilon}{(\epsilon - \epsilon')^2} \delta(\omega) \right\}. \end{aligned} \quad (54)$$

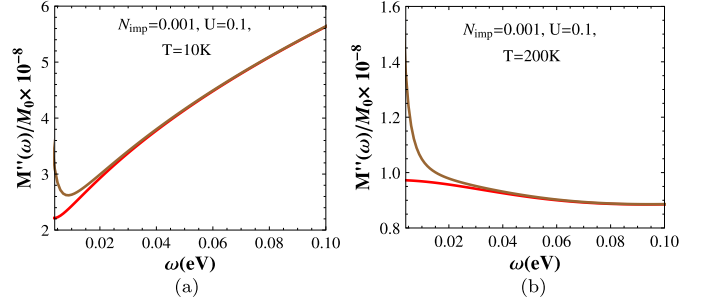


Fig. 1. Plots of the imaginary part of normalized memory functions at different temperatures: (a) at $T = 10$ K and (b) at $T = 200$ K. Here the red curve corresponds to the case with first moment only and the brown curve corresponds to the case where second moment is also considered within the present moment expansion of the memory function. In both cases, there is nice agreement between the results from the two different approaches at high frequency regimes. However they differ significantly in the low frequency regime. (For interpretation of the references to color in this figure legend, the reader is referred to the web version of this article.)

Now performing one of the energy integral, i.e. the integral over ϵ' , the above expression for the memory function at frequency $\omega > 0$ reduces to,

$$\begin{aligned} M''(\omega) &= \frac{2 m^3}{3 \pi^3} \frac{1}{N_e} \int_0^\infty d\epsilon \sqrt{\epsilon(\epsilon + \omega)} \frac{f(\epsilon) - f(\epsilon + \omega)}{\omega} (2\epsilon + \omega) \\ &\times \left\{ N_{\text{imp}} U^2 + (N_{\text{imp}} U^2)^2 \frac{1}{\omega^2} \right\}. \end{aligned} \quad (55)$$

This is an expression of imaginary part of the memory function for electrons in metal, within the second order truncation of our proposed moment expansion for correlation function. Here the first term within the braces corresponds to the contribution from the first moment [24] and the second term is the contribution from the second moment to the memory function. The frequency dependent behavior of the above expression for the imaginary part of the memory function or the scattering rate with different interaction strength U , impurity N_{imp} and T is discussed in the next section.

6. Results and comparison

Eqn. (55) describes the imaginary part of the memory function or the scattering rate as a function of ω , U , N_{imp} and T within a second order in moment expansion. We compare it with the imaginary part of the memory function obtained in eqn. (47), within a first order in moment expansion [24]. The validity of truncating such an expansion at the n -th order is valid when the n -th term in the expansion is smaller than the $(n - 1)$ -th term. In the present work we restrict us at the second order. In this case to check the validity of our results, we define an energy scale ω_0 above which the present high frequency expansion is valid. By taking the ratio of second order term to the first order term, the condition becomes $\frac{1}{\omega^2} \frac{\langle\langle\dot{J}; \dot{J}\rangle\rangle}{\langle\dot{J}; \dot{J}\rangle} \ll 1$. From eqn. (55), the above criterion translates to $\frac{N_{\text{imp}} U^2}{\omega^2} \ll 1$. This implies that our results are valid if the condition $\omega \geq (N_{\text{imp}} U^2)^{1/2} (= \omega_0)$ is satisfied.

In Fig. 1, we plot normalized imaginary part of MF $M''(\omega)/M_0$ as a function of frequency ω for both the cases (up-to the first moment and the second moment), keeping other parameters fixed.

In Fig. 1(a), the scattering rates are shown at temperature $T = 10$ K. It is observed that at high frequency regime, the result which includes the second moment contribution agrees well with the previous result (which includes only the first moment) [24]. But above the defined energy scale ω_0 (which is 0.004 in this figure), results deviate from each other. The second moment contributes more in the latter deviation thus increasing the magnitude

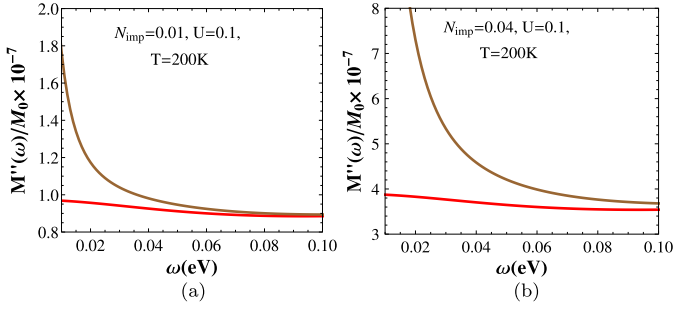


Fig. 2. Plots of the imaginary part of normalized memory functions at different impurity densities N_{imp} : (a) 0.01 and (b) 0.04. Here the red curve corresponds to the case with first moment only and the brown curve corresponds to the case where the second moment is also considered in the moment expansion. Here also a deviation occurs at low frequency regime as in the previous case. The increase in the impurity density enhances the magnitude of the memory function. (For interpretation of the references to color in this figure legend, the reader is referred to the web version of this article.)

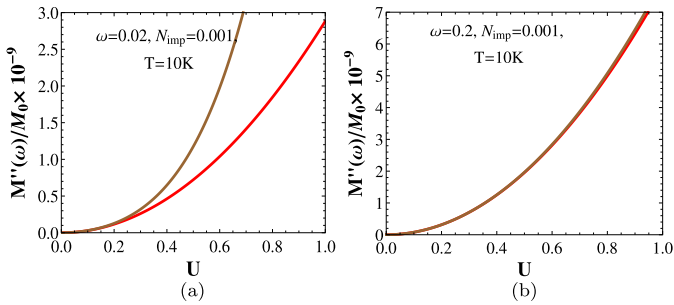


Fig. 3. Variation of the scattering rates with interaction strength U at different frequencies: (a) $\omega = 0.02$ eV and (b) 0.2 eV. Here the red curve represents the scattering rate with the first moment only and the brown curve is with the inclusion of the second moment. It is observed that the deviation is bigger for higher interaction strength in the low frequency regime. (For interpretation of the references to color in this figure legend, the reader is referred to the web version of this article.)

of the scattering rate compared to the case with only the first moment. We see that the magnitude of the scattering rate in this case is high as compared to the case with $n = 1$ term of $M''(\omega)$. Similarly, the scattering rates are plotted at a different temperature $T = 200$ K in Fig. 1(b). Here we observe the same behavior as in the previous figure, with temperature induced enhancement in the magnitude of the scattering rates.

In Fig. 2, again we plot the scattering rates fixing the temperature for different impurity densities $N_{\text{imp}} = 0.01$ and 0.04. We observe the same trend in both cases similar to the previous figure. Here the increase in the impurity density increases the scattering rates which leads to higher magnitude of the scattering rates. Also, here the results are valid for frequency greater than 0.01 and 0.02 in Figs. 2(a) and 2(b) respectively. From both Figs. 1 and 2 we find that the scattering rate with the first moment approximation is valid only for high frequency regime and the truncation becomes more severe as one increases the interaction strength.

To elaborate its dependence on the interaction strength U , the plot of the scattering rate with U at fixed frequency, N_{imp} and temperature is shown in Fig. 3. In Fig. 3(a), the scattering rate is shown at a small frequency $\omega = 0.02$ eV at which earlier we see that there is deviation in the results of memory function with different moment expansions. Here we find that the increase of U increases the scattering rate at low frequency due to the presence of the term $(N_{\text{imp}}U^2)^2$ in the moment expansion of the memory function. In Fig. 3(b) we observe that at a higher frequency ($\omega = 0.2$ eV), difference in $M''(\omega)$ with the increase of interaction strength, from two approximations becomes insignifi-

cant. More discussions on these results are presented in the next section.

7. Discussion

It is often convenient to express a frequency dependent response function in terms of a memory function or “multi-particle self-energy” [17]. In this work we propose a series expansion for the memory function for optical conductivity or the current-current correlation function. We show that many of the previous works [24,25,41,42], which address the optical conductivity of the metals within the memory function formalism, are equivalent to restricting at the lowest order in this expansion. We perform a higher order calculation for the same in the presence of electron-impurity interactions and compare our results with the results from one of the celebrated previous work [24]. In all these approaches, one needs to calculate the current-current correlation function ($\langle JJ \rangle$), a two particle correlator with some approximations. In summary, conventional Kubo approach [7] decouples $\langle JJ \rangle$ correlation into a product of single particle correlators whereas Götze and Wölfle [24] first write it in terms of $\langle \dot{J} \dot{J} \rangle$ and then use single particle decoupling. In the present approach, we extend the latter work further and write $\langle JJ \rangle$ in terms of $\langle \dot{J} \dot{J} \rangle$ and $\langle \ddot{J} \ddot{J} \rangle$ and use single particle decoupling of $\langle \dot{J} \dot{J} \rangle$. We see large discrepancy between the two results from the two approaches in the low frequency regime and also for higher impurity strengths.

These results are in accord with our proposal and also physically sensible. If we look at our expansion (eqn. (35)), we see that as we go to the higher frequencies, the contributions from the higher order moments become more and more irrelevant. On the other hand, higher time derivatives of the current operator involve the higher power of impurity strengths. Thus the inclusion of the higher moments is equivalent to including higher order contribution in the perturbation theory. Inclusion of the effects from higher moments is also manifested in Fig. 3 where variation of the scattering rates at a certain frequency with the impurity strengths is shown. In this figure we see that the scattering rate is increasing with impurity strength and the inclusion of higher order contribution leads to higher scattering rates. The results at very low frequency ($\omega \ll \omega_0$) should not be trusted much. As discussed earlier, in this regime the present approximation is not valid. In case when ω_0 is sufficiently small, result from the present method can be trusted even up-to lower frequency. But we see that the second moment contribution to the memory function is $M''_2 \sim \omega_0^2/\omega^2 M''_1$. This implies that the results for the memory function are in accord with the condition $|M(z)| \ll |z|$. This scenario can be clearly seen in Figs. 1 and 2 where the memory function $M''(\omega)$ is of very small magnitude as compared to the frequency ω .

To summarize, our proposal is mathematically simpler compared to the previous attempts [26,27] to calculate the memory function for the electronic conductivity beyond the lowest order perturbative calculations [24]. Within this systematic expansion, we can include interaction effects up-to required order depending on its strength. This method in principle can be applied for metals with other interactions as well as for non-metallic electronic systems [39,40] to estimate higher order perturbative corrections.

Appendix A. Calculation of $\langle J \dot{J} \rangle$

Consider that the ensemble average of current operators at the same time argument is represented by

$$\langle J \dot{J} \rangle = C \quad (\text{A.1})$$

where C is some constant.

Now, differentiate the above equation w.r.t. time

$$\begin{aligned} \langle \dot{J} | J \rangle + \langle J | \dot{J} \rangle &= 0 \\ \langle \dot{J} | J \rangle &= -\langle J | \dot{J} \rangle. \end{aligned} \quad (\text{A.2})$$

In another way, the ensemble average of J and \dot{J} can be expressed as

$$\begin{aligned} \langle \dot{J} | J \rangle &= \text{tr}(\rho [H, J] J) \\ &= \text{tr}(\rho H J J) - \text{tr}(\rho J H J) \\ &= \text{tr}(\rho J [H, J]) \\ &= \langle J | \dot{J} \rangle. \end{aligned} \quad (\text{A.3})$$

From equations (A.2) and (A.3), we conclude that $\langle J | \dot{J} \rangle = 0$.

Appendix B. Detailed calculation of the higher order contribution

To calculate $\langle \langle \dot{J}; \dot{J} \rangle \rangle_z$ we first calculate the first term of eqn. (50). For this we need $[[J, H_{\text{imp}}], H_0]$ which using eqns. (37) and (41) becomes,

$$\begin{aligned} [[J, H_{\text{imp}}], H_0] &= \frac{1}{N} \sum_{j, \mathbf{k}, \mathbf{k}'} \langle \mathbf{k} | U^j | \mathbf{k}' \rangle (v_x(\mathbf{k}) - v_x(\mathbf{k}')) (\epsilon_{\mathbf{k}'} - \epsilon_{\mathbf{k}}) c_{\mathbf{k}}^\dagger c_{\mathbf{k}'}. \end{aligned} \quad (\text{B.1})$$

Using the above expression, the first term of eqn. (50) becomes

$$\begin{aligned} &= \frac{1}{N^2} \sum_{j, \mathbf{k}, \mathbf{k}'} \sum_{i, \mathbf{p}, \mathbf{p}'} \langle \mathbf{k} | U^j | \mathbf{k}' \rangle \langle \mathbf{p} | U^i | \mathbf{p}' \rangle (v_x(\mathbf{k}) - v_x(\mathbf{k}')) \\ &\quad \times (v_x(\mathbf{p}) - v_x(\mathbf{p}')) (\epsilon_{\mathbf{k}'} - \epsilon_{\mathbf{k}}) (\epsilon_{\mathbf{p}'} - \epsilon_{\mathbf{p}}) \langle \langle c_{\mathbf{k}}^\dagger c_{\mathbf{k}'}; c_{\mathbf{p}}^\dagger c_{\mathbf{p}'} \rangle \rangle_z. \end{aligned} \quad (\text{B.2})$$

Here again we will consider the case of $i = j$ as considered in eqn. (44) and using eqn. (18) with performing time integration and ensemble average, the above equation reduces to

$$\begin{aligned} &= \frac{2N_{\text{imp}}}{N^2} \sum_{\mathbf{k}, \mathbf{k}'} |\langle \mathbf{k} | U | \mathbf{k}' \rangle|^2 (v_x(\mathbf{k}) - v_x(\mathbf{k}'))^2 (\epsilon_{\mathbf{k}} - \epsilon_{\mathbf{k}'})^2 \\ &\quad \times \frac{f(\mathbf{k}) - f(\mathbf{k}')}{z + \epsilon_{\mathbf{k}} - \epsilon_{\mathbf{k}'}}. \end{aligned} \quad (\text{B.3})$$

This expression is further simplified by converting summations into energy integrals and ignoring the momentum dependence of U as

$$= \frac{2}{3} N_{\text{imp}} \frac{U^2 m^2}{\pi^4} \int_0^\infty d\epsilon \int_0^\infty d\epsilon' \sqrt{\epsilon\epsilon'} (\epsilon + \epsilon') (\epsilon - \epsilon')^2 \frac{f(\epsilon) - f(\epsilon')}{z + \epsilon - \epsilon'}. \quad (\text{B.4})$$

Now we perform the calculations for the second term of eqn. (50).

First, $[[J, H_{\text{imp}}], H_{\text{imp}}]$ using eqns. (38) and (41) is written as

$$\begin{aligned} [[J, H_{\text{imp}}], H_{\text{imp}}] &= \frac{1}{N^2} \sum_{j, \mathbf{k}, \mathbf{k}'} \sum_{i, \mathbf{p}, \mathbf{p}'} \langle \mathbf{k} | U^j | \mathbf{k}' \rangle \langle \mathbf{p} | U^i | \mathbf{p}' \rangle (v_x(\mathbf{k}) - v_x(\mathbf{k}')) \\ &\quad \times [c_{\mathbf{k}}^\dagger c_{\mathbf{k}'}, c_{\mathbf{p}}^\dagger c_{\mathbf{p}'}] \\ &= \frac{N_{\text{imp}}}{N^2} \sum_{\mathbf{k}, \mathbf{k}', \mathbf{p}} \langle \mathbf{k} | U | \mathbf{k}' \rangle \langle \mathbf{k}' | U | \mathbf{p} \rangle (v_x(\mathbf{k}) - 2v_x(\mathbf{k}') + v_x(\mathbf{p})) c_{\mathbf{k}}^\dagger c_{\mathbf{p}}. \end{aligned} \quad (\text{B.5})$$

Using this, $\langle \langle [[J, H_{\text{imp}}], H_{\text{imp}}]; [[J, H_{\text{imp}}], H_{\text{imp}}] \rangle \rangle_z$ can be written as

$$\begin{aligned} &= 2 \frac{N_{\text{imp}}^2}{N^4} \sum_{\mathbf{k}, \mathbf{k}', \mathbf{p}, \mathbf{r}, \mathbf{r}', \mathbf{l}} \langle \mathbf{k} | U | \mathbf{k}' \rangle \langle \mathbf{k}' | U | \mathbf{p} \rangle \langle \mathbf{r} | U | \mathbf{r}' \rangle \langle \mathbf{r}' | U | \mathbf{l} \rangle \\ &\quad \times (v_x(\mathbf{k}) - 2v_x(\mathbf{k}') + v_x(\mathbf{p})) \\ &\quad \times (v_x(\mathbf{r}) - 2v_x(\mathbf{r}') + v_x(\mathbf{l})) \langle \langle c_{\mathbf{k}}^\dagger c_{\mathbf{p}}; c_{\mathbf{r}}^\dagger c_{\mathbf{l}} \rangle \rangle_z. \end{aligned} \quad (\text{B.6})$$

After calculating $\langle \langle c_{\mathbf{k}}^\dagger c_{\mathbf{p}}; c_{\mathbf{r}}^\dagger c_{\mathbf{l}} \rangle \rangle_z$ with help of eqn. (18) and substituting in eqn. (B.6) and taking U as independent of momentum, $\langle \langle [[J, H_{\text{imp}}], H_{\text{imp}}]; [[J, H_{\text{imp}}], H_{\text{imp}}] \rangle \rangle_z$ can be expressed as

$$\begin{aligned} &= 2 \frac{N_{\text{imp}}^2 U^4}{N^4 m^2} \sum_{\mathbf{k}, \mathbf{k}', \mathbf{p}, \mathbf{r}} \frac{1}{z + \epsilon_{\mathbf{k}} - \epsilon_{\mathbf{p}}} (k_x - 2k'_x + p_x) (p_x - 2r'_x + k_x) \\ &\quad \times (f_{\mathbf{k}} - f_{\mathbf{p}}). \end{aligned} \quad (\text{B.7})$$

After doing algebra, the above expression can be written as

$$= \frac{2}{3} \frac{N_{\text{imp}}^2 U^4 m^2}{\pi^4} \int_0^\infty d\epsilon \int_0^\infty d\epsilon' \sqrt{\epsilon\epsilon'} (\epsilon + \epsilon') \frac{f(\epsilon) - f(\epsilon')}{z + \epsilon - \epsilon'}. \quad (\text{B.8})$$

Substituting eqns. (B.4) and (B.8) in eqn. (50), we have

$$\begin{aligned} \langle \langle \dot{J}; \dot{J} \rangle \rangle_z &= \frac{2}{3} \frac{N_{\text{imp}} U^2 m^2}{\pi^4} \int_0^\infty d\epsilon \int_0^\infty d\epsilon' \sqrt{\epsilon\epsilon'} (\epsilon + \epsilon') (\epsilon - \epsilon')^2 \\ &\quad \times \frac{f(\epsilon) - f(\epsilon')}{z + \epsilon - \epsilon'} + \frac{2}{3} \frac{N_{\text{imp}}^2 U^4 m^2}{\pi^4} \\ &\quad \times \int_0^\infty d\epsilon \int_0^\infty d\epsilon' \sqrt{\epsilon\epsilon'} (\epsilon + \epsilon') \frac{f(\epsilon) - f(\epsilon')}{z + \epsilon - \epsilon'}. \end{aligned} \quad (\text{B.9})$$

References

- [1] D.N. Basov, T. Timusk, *Rev. Mod. Phys.* 77 (2005) 721.
- [2] D.N. Basov, R.D. Averitt, D. van der Marel, M. Dressel, K. Haule, *Rev. Mod. Phys.* 83 (2011) 471.
- [3] N.W. Ashcroft, N.D. Mermin, *Solid State Physics, Science: Physics*, Saunders College, 1976.
- [4] T. Timusk, *Solid State Commun.* 127 (2003) 337.
- [5] A.V. Puchkov, D.N. Basov, T. Timusk, *J. Phys. Condens. Matter* 8 (1996) 10049.
- [6] P. Bhalla, N. Singh, *Eur. Phys. J. B* 87 (2014) 213.
- [7] G.D. Mahan, *Many-Particle Physics*, 2nd ed., Plenum, New York, London, 1990.
- [8] H. Mori, *Prog. Theor. Phys.* 33 (1965) 423.
- [9] G.A. Baker, *Essentials of Padé Approximants*, Academic, London, 1975.
- [10] J. Wouters, V. Lucarini, *J. Stat. Phys.* 151 (2013) 850.
- [11] R. Haydock, V. Heine, M.J. Kelly, *J. Phys. C* 5 (1972) 2845.
- [12] M.H. Lee, J. Hong, *Phys. Rev. Lett.* 48 (1982) 634.
- [13] M.H. Lee, *Phys. Rev. B* 26 (1982) 2547.
- [14] J. Hong, *Phys. Rev. B* 26 (1982) 2227.
- [15] R. Zwanzig, *Phys. Rev.* 124 (1961) 983.
- [16] R. Zwanzig, in: W.E. Brittin, B.W. Downs, J. Downs (Eds.), *Lectures in Theoretical Physics*, vol. 3, Interscience, New York, 1961, p. 135.
- [17] N. Das, P. Bhalla, N. Singh, arXiv:1601.01127, 2016.
- [18] A.S.T. Pires, *Helv. Phys. Acta* 61 (1988) 988.
- [19] B.J. Berne, J.P. Boon, S.A. Rice, *J. Chem. Phys.* 45 (1966) 1086.
- [20] G.D. Harp, B.J. Berne, *Phys. Rev. A* 2 (1970) 975.
- [21] B.J. Berne, G.D. Harp, *Adv. Chem. Phys.* XVII (1970) 63.
- [22] W. Götze, P. Wölfle, *J. Low Temp. Phys.* 5 (1971) 575.
- [23] J.M. Ziman, *Electrons and Phonons*, Clarendon, Oxford, 1960.
- [24] W. Götze, P. Wölfle, *Phys. Rev. B* 6 (1972) 1226.
- [25] B. Arfi, *Phys. Rev. B* 45 (1992) 2352.
- [26] N. Plakida, *J. Phys. Soc. Jpn.* 65 (1996) 12.
- [27] N.M. Plakida, *Z. Phys. B* 103 (1997) 383.
- [28] A.A. Vladimirov, D. Ihle, N.M. Plakida, *Phys. Rev. B* 85 (2012) 224536.
- [29] D. Forster, *Hydrodynamic Fluctuations, Broken Symmetry and Correlation Functions*, Advanced Books Classics, 1995.

- [30] P. Fulde, *Correlated Electrons in Quantum Matter*, World Scientific, 2012.
- [31] I. Sega, P. Prelovšek, J. Bonča, *Phys. Rev. B* 68 (2003) 054524.
- [32] P. Prelovšek, I. Sega, J. Bonča, *Phys. Rev. Lett.* 92 (2004) 027002.
- [33] I. Sega, P. Prelovšek, *Phys. Rev. B* 73 (2006) 092516.
- [34] I. Sega, P. Prelovšek, *Phys. Rev. B* 79 (2009) 140504.
- [35] P. Prelovšek, I. Sega, *Phys. Rev. B* 74 (2006) 214501.
- [36] P.F. Maldague, *Phys. Rev. B* 16 (1977) 2437.
- [37] P. Grigolini, G. Grosso, G. Pastori Parravicini, *Phys. Rev. B* 27 (1983) 7342.
- [38] A. Lucas, *J. High Energy Phys.* 03 (2015) 071.
- [39] A. Lucas, S. Sachdev, *Phys. Rev. B* 91 (2015) 195122.
- [40] A.A. Patel, S. Sachdev, *Phys. Rev. B* 90 (2014) 165146.
- [41] N. Das, N. Singh, arXiv:1509.03418, 2015.
- [42] P. Bhalla, N. Singh, *Eur. Phys. J. B* 89 (2016) 49.
- [43] K.H. Bennemann, J.B. Ketterson, *Superconductivity*, vols. 1, 2, Springer, Heidelberg, 2008.
- [44] N. Das, N. Singh, *Phys. Lett. A* 380 (2015) 490.
- [45] M. Dupis, *Prog. Theor. Phys.* 37 (1967) 502.
- [46] L.P. Kadanoff, P.C. Martin, *Ann. Phys.* 24 (1963) 419.
- [47] R. Kubo, *J. Phys. Soc. Jpn.* 12 (1957) 570.
- [48] D.N. Zubarev, *Usp. Fiz. Nauk* 71 (1960) 71.